Tidal changes in the Lower Ems (1945-2005): reconstructing the effects of channel deepening and bottom roughness

BSc thesis

Marjolijn Schoemans

Utrecht University; Faculty of Geosciences; Department of Physical Geography

Student number: 9902996

November 2012 – April 2013 (Deltares, Unit Marine and Coastal Systems)

Supervisors: dr. Maarten van der Vegt and dr. ir. Thijs van Kessel

Supervisor (Deltares): dr. Bas van Maren

Index

List of figures

List of tables

1 INTRODUCTION

1.1. Background

This thesis was written as part of the graduation Bachelor of Sciences research at Utrecht University, Faculty of Geosciences, Department of Physical Geography. The research was carried out at Deltares, Unit Marine and Coastal Systems, Morphology and Sediment Dynamics Group. Deltares is a research institute with expertise covering projects related to water, soil and subsurface. The present research is part of the project 'Mud dynamics in the Ems-Dollard' which was initiated by Rijkswaterstaat Waterdienst following the Water Framework Directive (WFD). The WFD states that every EU member state has to achieve and maintain a good status of all water bodies by 2015. Measures and targets are laid out to improve the chemical and ecological quality of these water bodies (rivers, lakes, transitional and coastal waters). The focus is on three main themes: Clean water, Biotope and Connections. The goals of Clean water consist of reduction of chemical loads, reduction of eutrophication and improvement of water transparency / reduction of water turbidity. The project 'Mud dynamics in the Ems-Dollard' and this Bachelor of Science research focus on the latter and aim at identifying the hydrodynamic contribution to the increased turbidity in the Ems-Dollard estuary.

The Ems-Dollard estuary, including the Lower Ems river, has a long history of anthropogenic interventions. The on-going deepening of the Lower Ems is thought to have led to changes in hydrodynamics and suspended sediment concentration. Over the last 60 years, mean high water levels in the Lower Ems have increased and mean low water levels have decreased (Jensen et al., 2003; Vroom et al., 2012). At present, high water slack duration has increased near the mouth, promoting import of fine sediment. The system becomes more flood-dominant in the upstream direction, which contributes to the high trapping efficiency of the Lower Ems (Winterwerp, 2011; Vroom et al., 2012). It is thought that channel deepening has caused a change in tidal asymmetry and residual currents. Previous research suggests that the system has changed from flood-dominant to high water slack dominant (Herrling and Niemeyer, 2008c). This in turn has probably affected sediment-importing mechanisms, leading to a hyperconcentrated system and fluid mud formation (Talke and De Swart, 2006; Herrling and Niemeyer, 2008c; Vroom et al., 2012). Furthermore, bottom roughness is thought to have decreased over time. Fluid mud was first observed in the 1970's (Duinker et al., 1985) and occurred more frequently in the 1990's. Nowadays, fluid mud is permanently present and has become a problem for navigation (Winterwerp, 2011). The high suspended

sediment concentrations further affect tidal dynamics and enhance sediment import (Talke et al., 2009; Winterwerp, 2011).

1.2. Research objectives and structure of report

The main aim of this research is to investigate the effects on tidal dynamics of channel deepening and bottom roughness changes in the Lower Ems in the period 1945-2005. The focus is on changes in tidal asymmetry and estuarine circulation. The following sub-questions are defined:

- Is there a change in bottom roughness in the Lower Ems since 1945? How does this relate to changes in tidal characteristics?
- How do bathymetry changes modify the tidal characteristics (tidal range, flow velocity, tidal asymmetry)?
- What is the relative importance of deepening and bottom roughness for the tidal characteristics (tidal range, flow velocity, tidal asymmetry)?
- Is there a change in tidal asymmetry between 1945 and 2005? Can this explain the increased sediment import and high sediment trapping efficiency of the Lower Ems?
- Has estuarine dynamics (estuarine circulation, salt intrusion) changed over time?
- How do the changes in hydrodynamics relate to changes in sediment dynamics? Is there a shift in dominant sediment transport process since 1945?

This Bachelor of Science research consists of: a) literature study on the observed changes in tidal characteristics in the Lower Ems in the last 60 years, b) literature study on the effects of bottom roughness and high concentrations of suspended sediment on tidal characteristics, c) reconstruction of three historical bathymetries of the Lower Ems and Emden Fahrwasser: 1945, 1965 and 1985, d) 2D (depth-averaged) model runs to investigate changes in tidal characteristics in the period 1945-2005, using the reconstructed bathymetries and calibrated bottom roughness, e) 3D model runs to analyse the changes in estuarine circulation over time, f) 3D model runs using a simplified sediment-component to investigate the effect of the hydrodynamic changes on sediment import. Delft3D is used for the modelling. All model results are processed with MATLAB.

Chapter 2 consists of the theoretical background for this research. It gives an overview of the observed hydrodynamic changes in the Lower Ems since the 1960's. It also describes the effect of bottom roughness and high suspended sediment concentrations on tidal dynamics. Furthermore, hydrodynamics is linked with sediment dynamics. Chapter 3 (Materials &

Methods) covers of the model set-up in Delft3D. This chapter describes the available data and it explains the reconstruction of the historical bathymetries and the calibration of bottom roughness. It also gives an overview of all 2D and 3D model runs. Chapter 4 (Results) gives the model results and focusses on the changes over time of tidal characteristics in the Lower Ems, such as tidal range, tidal asymmetry and estuarine circulation. It briefly links the changes in hydrodynamics to changes in sediment import. A comparison between the model results of this study and the outcomes of previous research is given in chapter 5 (Discussion). Finally, the most important model outcomes are presented in chapter 6 (Conclusions), followed by a summary.

2 THEORETICAL BACKGROUND

This chapter provides basic knowledge about estuaries and tidal dynamics in general and about the Ems-Dollard estuary in particular. The characteristics of the Ems-Dollard estuary will be described in section 2.1. Because bottom roughness is an important factor in understanding the hydrodynamic changes in the Lower Ems, section 2.2 concentrates on bottom roughness in general. Section 2.3 summarizes the observed tidal changes in the Lower Ems since the 1960's and the effect of bottom roughness on tidal characteristics. Section 2.4 will deal with sediment transport and the role of tidal asymmetry, estuarine circulation and settling/scour lag in net sediment transport. Finally, sediment-fluid interactions are discussed in section 2.5.

2.1. Ems-Dollard estuary

An estuary is a partially enclosed coastal body of water. It has an open connection to the sea and receives fresh water input from rivers. (Potter et al., 2010). Estuaries can be seen as the transition zone between the coastal environment with its tidal and wave processes and the fluvial environment. This interaction results in a unique environment, with its own set of processes, e.g. estuarine circulation, turbidity maximum, flocculation, etc. (Dyer, 1994; Masselink et al., 2011).

The Ems-Dollard estuary (Fig. 2.1) is located on the Dutch-German border. It stretches from the island of Borkum to the tidal weir in Herbrum, the landward limit of the tidal influence since its construction in 1899. The total surface area of the Ems-Dollard estuary is ~500 km^2. The Ems-Dollard can be characterized as a partially-mixed, mesotidal estuary (Talke et al., 2009). The lower reaches, including the island of Borkum and the Eemshaven, are

influenced by the North Sea via a tidal inlet. The middle reaches, where Delfzijl is located, have a classic funnel-shape. The shallow Dollard bay consists of a large intertidal area, which has been significantly reduced in size due to land reclamations since the 16th century. The borders of the Ems-Dollard estuary have changed little since 1945 (Talke and De Swart, 2006).

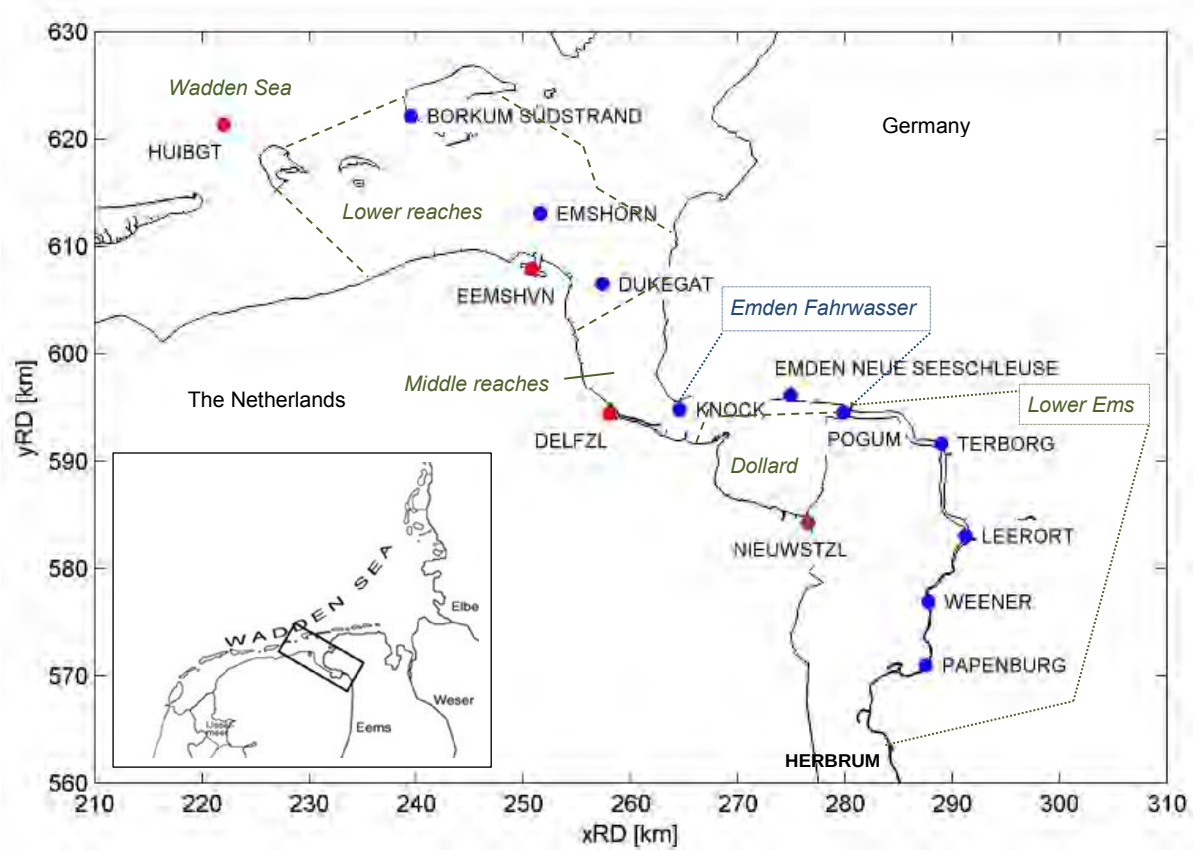

Fig. 2.1: Map of the Ems-Dollard estuary in NE Netherlands. The estuary is subdivided in lower reaches, middle reaches, Dollard and Lower Ems. An overview of Dutch (red) and German (blue) water level stations is given (adapted from Vroom et al., 2012).

The area of investigation is the upper part of the Ems-Dollard estuary: the Lower Ems tidal river (*Unterems*), which is the area between Pogum and the weir at Herbrum. Water level data from gauges in Knock, Emden, Pogum, Terborg, Leerort, Weener and Papenburg will be used and compared with modelled water levels for various time periods. Table 2.1 shows the distance to Knock of each water level station in the Lower Ems.

Table 2.1: Distance to Knock for each water level station in the Emden Fahrwasser and Lower Ems (based on Vroom et al., 2012).

Water level station in Lower Ems	*Distance to Knock [km]*
Emden NS	10
Pogum	16
Terborg	27
Leerort	37
Weener	45
Papenburg	51
weir Herbrum	67

The hydrodynamics in the Lower Ems are governed by a combination of tidal and fluvial processes. Wave processes do not play a role (Vroom et al., 2012). The Lower Ems is the dominant source of fresh water input and has a mean annual discharge of 100 m^3/s, varying between 20 m^3/s in summer and 400 m^3/s in winter. River width near Herbrum is about 60 m, widening in downstream direction to 600 m near Pogum (Herrling and Niemeyer, 2008a; Winterwerp, 2011). River depth is maintained at around -7 m for navigational purposes (Talke et al., 2009; Winterwerp, 2011).

The Ems-Dollard estuary has a long history of anthropogenic interventions (Talke and De Swart, 2006; Herrling and Niemeyer, 2008c; Vroom et al., 2012): land reclamations and diking since the 16th century, start of canalization of the Lower Ems in 1860, construction of groynes, artificial meander cut-offs and the construction of a weir at Herbrum in the late 19th century. Deepening of the Emden Fahrwasser, the stretch between Knock and Emden, began as early as 1901. Deepening activities in the Lower Ems commences at the beginning of the 20th century and continue until this day. The most recent anthropogenic intervention in the Ems-Dollard estuary is the construction of a storm surge barrier in 2001-2002, a few kilometres upstream of Emden. The 'Emsperrwerk' was constructed to protect the Lower Ems area from flooding, because on-going channel deepening in the Lower Ems river had resulted in increased water levels.

It is thought that the deepening of the Lower Ems has caused significant changes in the hydro- and sediment dynamics. Possibly, tidal asymmetry has changed, which has led to 'tidal pumping', an increased landward transport of fine sediment. The Lower Ems has become an efficient sediment trap and high concentrations of fine suspended sediment accumulate in this part of the estuary (Talke and De Swart, 2006; Vroom et al., 2012). Fine suspended sediment concentration increases in landward direction and is very high in the

Dollard and Lower Ems. With suspended sediment concentrations up to 30-40 g/l, the Lower Ems can be seen as a hyperconcentrated system. Hyperconcentrated conditionas are reached when the sediment concentration exceeds values of a 200-300 mg/l (Van Maren, 2009; Winterwerp, 2011). Nowadays, the Dollard and the Lower Ems have a muddy bed. Fluid mud was first observed in the 1970's (Duinker et al., 1985) and appeared periodically in the 1990's. At present, fluid mud with concentrations of 50-100 g/l is permanently present near the bottom of the Lower Ems. The average thickness is 1-2 m and it has become a serious problem for navigation (Winterwerp, 2011; Vroom et al., 2012). Fluid mud layers have a significant effect on the hydraulic roughness and therefore on tidal characteristics. Also complex sediment-fluid interactions play a role in the hydro- and sediment dynamics of the Lower Ems, which will be further discussed in section 2.5.

2.2. Bottom roughness

Bottom roughness is an important factor in understanding the hydrodynamic changes in the Lower Ems. The general idea is that the observed increase in tidal range in the Lower Ems river since the 1960's is at least partly related to a decrease in bottom roughness (Talke and De Swart, 2006; Vroom et al., 2012). It is also suggested that the deepening of the Ems and a reduction in hydraulic roughness have caused a change in tidal asymmetry towards a less flood-dominated system (Talke and De Swart, 2006; Herrling and Niemeyer, 2008c). This section concentrates on bottom roughness in general. The effects of bottom roughness on tidal characteristics will be further discussed in section 2.3.

Particle size (skin friction) and the presence of bedforms (form friction) determine the type of flow regime: hydraulically smooth versus hydraulically rough. This distinction is based on the ratio between the Nikuradse roughness length k_s and the thickness of the viscous sublayer, expressed by $\frac{v}{u*}$ (v is kinematic viscosity (m^2/s) and u_* is bed shear velocity (m/s)) (Van Rijn, 2011). Hydraulically smooth conditions exist when particles are much smaller than the thickness of the viscous sublayer ($\frac{u*k_s}{v} \leq 5$). Hydraulically rough conditions occur when larger sediment particles or bed forms protrude through the viscous sublayer and turbulence destroys the thin laminar layer ($\frac{u*k_s}{v} \geq 70$), so turbulence will affect the velocity profile (Van Rijn, 2011; Masselink et al., 2011).

Friction can be expressed by Chézy (C), Manning (n) or Darcy-Weisbach coefficient (f). The Delft3D Ems-Dollard model in this study uses the Manning coefficient n. This coefficient is

supposed to be independent of flow depth (however it varies slightly depending on water depth and hydraulic radius). *n* can be related to the Chézy coefficient *C* by equation 1. The formula to determine the Chézy coefficient *C* is given in equation 2. It follows that the friction term is non-linear and its influence is larger at low water. These friction relations show that Chézy coefficient *C* increases and Manning coefficient *n* decreases, when the bottom becomes smoother (roughness length k_s decreases) (Van Rijn, 2011). For example, a decrease in *n* from 0.02 to 0.01 $m/s^{1/3}$ indicates a change to hydraulically smoother flow conditions. A reduction in grain size and/or bed forms, e.g. ripples, dunes etc., will result in friction reduction, therefore less turbulence generation at the bed level and less energy loss from the flow. Deposition of fine sediment smoothens bed irregularities and therefore affects flow conditions and hence tidal characteristics.

$$C = \frac{R^{\frac{1}{6}}}{n} \qquad (1)$$

$$C = 18\log\left(\frac{12R}{k_s + 3.3\frac{\nu}{u_*}}\right) \qquad (2)$$

where *u* is the flow velocity (m/s), *R* is the hydraulic radius (m), *n* is the Manning coefficient ($m/s^{1/3}$), C is the Chézy coefficient ($m^{0.5}/s$), k_s is Nikuradse roughness length (m), *v* is kinematic viscosity (m^2/s) and u_* is bed shear velocity (m/s).

2.3. Tidal dynamics in the Ems river

This section describes tidal dynamics in general and of the Lower Ems in particular: tidal range, tidal asymmetry and estuarine circulation. A summary of the observed hydrodynamic changes in the Lower Ems in the last 60 years will be given. Also, the effect of bottom roughness on hydrodynamics will be discussed.

2.3.1. Tidal range

A tidal wave has a sinusoidal shape with amplitude of +*a* (high water) and –*a* (low water). The tidal range, the difference between high and low water levels, is influenced by the shallow and narrow nature of most estuaries. Effects include frictional damping, deformation of the tidal wave, shoaling and amplification due to width convergence. In addition, the tidal range varies according to the spring-neap tide cycle and according to a 18.6-year tidal cycle, which includes the lunar nodal tidal constituent (Masselink et al., 2011; Hoekstra, 2011).

Observations along the German coastline have revealed a strong increase in North Sea mean tidal range since 1965 (Fig. 2.2). Mean high water levels (MHW) have increased up to 40 cm/100 years, while mean low water levels (MLW) have decreased up to -10 cm/100 years, resulting in a 10% increase of mean tidal range along the North Sea coastline. This change is assumed to be related to global sea level rise (Jensen and Mudersbach, 2005).

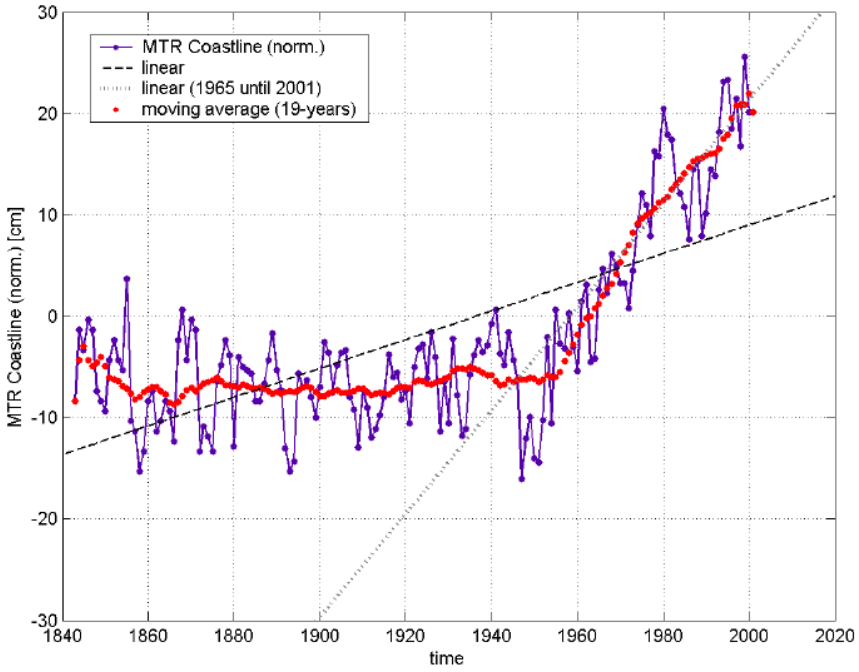

Fig. 2.2: Observed mean tidal range along the German coastline, combined data of twelve gauging stations at the German North Sea and four gauging stations at the German Baltic Sea coastline. 19-year average and linear trendlines are indicated (Jensen and Mudersbach, 2005).

Fig. 2.3 shows the tidal range in the Ems-Dollard estuary (lower and middle reaches, Dollard) The tidal range at the seaward entrance of the Ems-Dollard estuary, Borkum, increases ~10 cm since 1950, consistent with the increase along the North Sea coastline. The tidal range at Delfzijl, located in the middle reaches, increases with ~30 cm between 1950 and 1990 (Vroom et al., 2012). Present-day tidal range in the Lower Ems is ~3.5 m (Fig. 2.4). The tidal range near Papenburg has increased by 1.5 m since the 1960's. As a consequence, the location of the largest tidal range has shifted from Emden/Pogum to Papenburg (Jensen et al., 2003; Vroom et al., 2012).

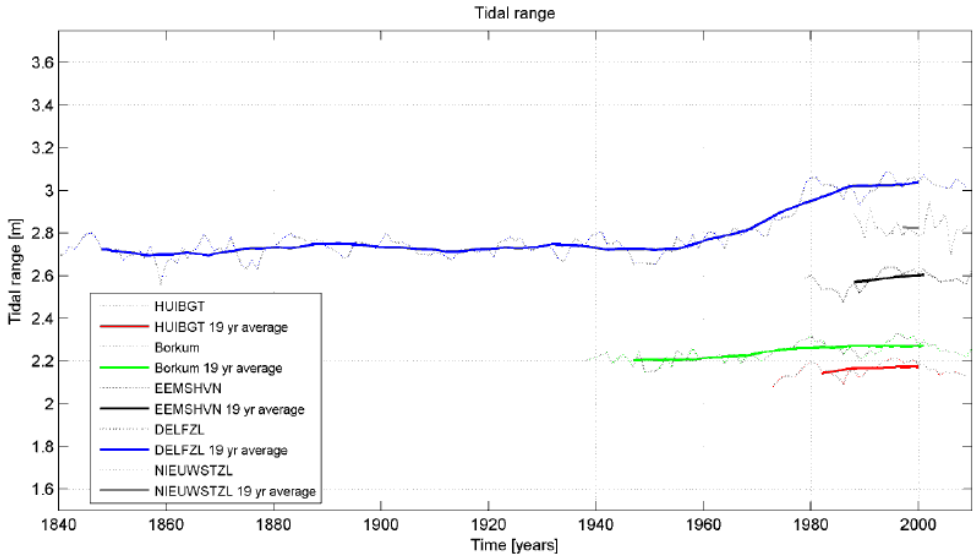

Fig. 2.3: Observed tidal range (= difference between yearly averaged HW and LW levels) in the lower and middle reaches of the estuary and in the Dollard. Yearly averaged tidal range (dotted) and 19-year averages (solid line) to account for the 18.6 year tidal cycle (Vroom et al., 2012).

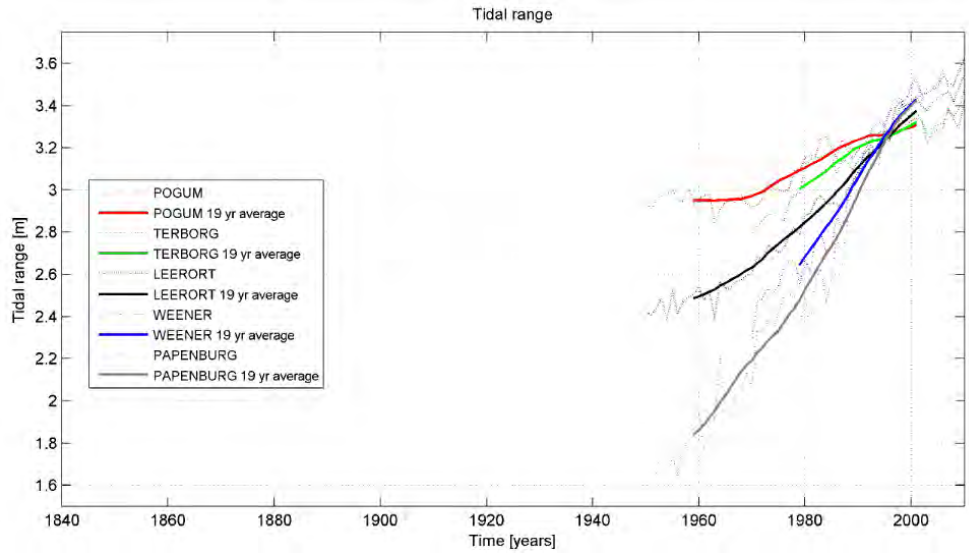

Fig. 2.4: Observed tidal range in the Lower Ems. Yearly averaged tidal range (dotted) and 19-year averages (solid line) to account for the 18.6 year tidal cycle (Vroom et al., 2012).

Mean high water levels in the Ems river show an overall gradual rise in the last 60 years (Fig. 2.5a) and also increase in the upstream direction (Vroom et al., 2012). MHW levels in the North Sea influence MHW levels in the Ems river: a 1 cm increase at Borkum causes a 1.7 cm increase in Papenburg (Jensen et al., 2003). Mean low water levels decrease significantly in the same period (Fig. 2.5b). North Sea MLW levels only have a small influence on the Ems-Dollard MLW levels (Jensen et al., 2003). The largest drop of MLW values since the 1960's in observed in Papenburg. At present, low water levels do not vary much for the different stations in the Lower Ems.

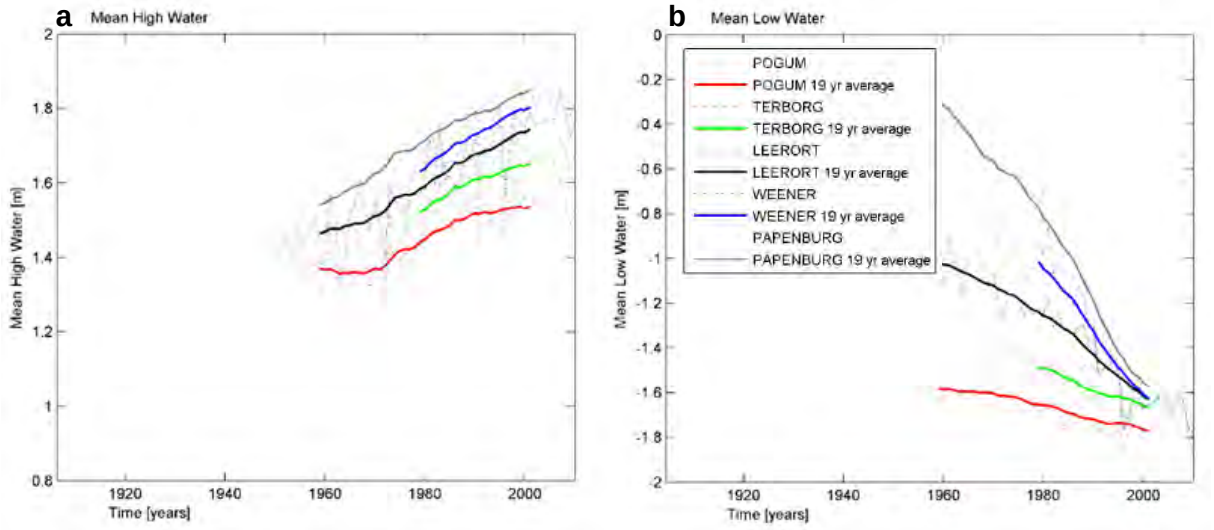

Fig. 2.5: Observed (a) MHW and (b) MLW levels in the Lower Ems. Yearly averaged values (dotted) and 19-year averages (solid line) (adapted from Vroom et al., 2012).

Comparison between observed and modelled 1937 and 2005 MHW/MLW levels between Knock and Herbrum further confirms that water levels have changed in time. It also reveals strong longitudinal differences. This is illustrated in Fig. 2.6. MHW levels have increased slightly, especially upstream of Leerort, while MLW levels have strongly decreased in this region (Herrling and Niemeyer, 2008c).

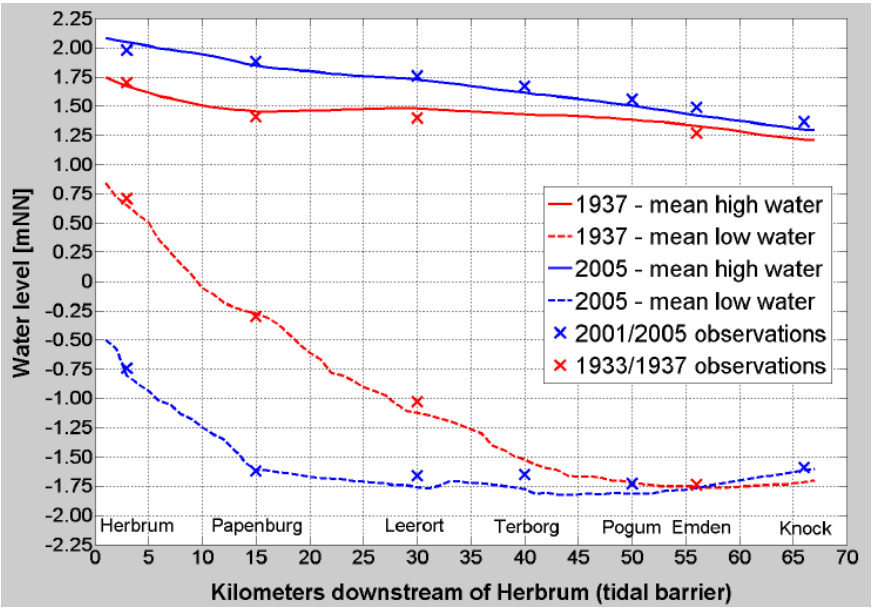

Fig. 2.6: Comparison of 1937 and 2005 observed MHW and MLW levels (crosses) and modelled MHW (solid line) and MLW levels (dashed) between Herbrum and Knock (Herrling and Niemeyer, 2008c).

2.3.2. Effect of bottom roughness on tidal range

When the tidal wave enters shallow coastal waters, it is deformed by bed friction, convergence and reflection at the estuary head. Friction leads to wave dampening and a decrease in tidal amplitude, while convergence leads to an increase in tidal amplitude (Hoekstra, 2011). The combination of frictional effects and convergence will cause an increase in the tidal amplitude and tidal range (convergence>friction) or a decrease (friction>convergence), depending on basin geometry and bottom roughness. This is illustrated in Fig. 2.7. Tide-dominated estuaries, like the Ems-Dollard estuary, are generally characterized by hypersynchronous conditions: the tidal range first increases from the estuary mouth in the upstream direction due to convergence, until friction eventually causes a decrease in tidal range. An increase in bottom friction will lead to a more landward decrease in tidal range and velocities (Dalrymple and Choi, 2007). Similarly, a smoother bed leads to an increase in tidal range. The hypothesis is that the observed increase in tidal range in the Lower Ems river since the 1960's is at least partly related to a smoothening of the bottom (Talke and De Swart, 2006; Vroom et al., 2012).

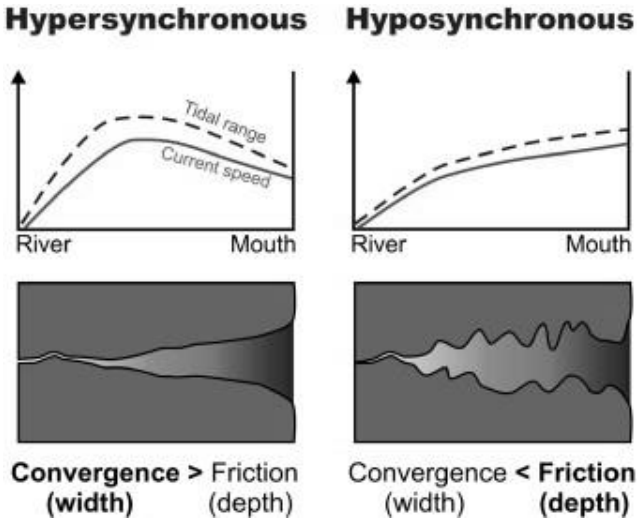

Fig. 2.7: The balance between convergence and friction leads to an increase or decrease in tidal amplitude (Dalrymple and Choi, 2007, after Salomon and Allen, 1983).

2.3.3. Tidal asymmetry and type of dominance

The tidal signal is the sum of a finite set of tidal constituents or sinusoids with different amplitude, period and phase (Masselink et al., 2011). The dominant tidal constituent in the North Sea and the Ems-Dollard estuary is M2, the Principal Lunar component with a period of 12.42 hours (Vroom et al., 2012). The tidal wave can be regarded as a shallow water wave with propagation velocity $c = \sqrt{gh}$. Since propagation velocity depends on water depth, the

tidal crest will move faster than the trough and tidal asymmetry will develop, even in a hypothetical frictionless estuary. So when the tidal wave enters shallow water, it shows deformation (Dronkers, 1986; Masselink et al., 2011). Since the North Sea is a shallow basin, the tidal wave is already distorted when it enters the even shallower Ems-Dollard estuary. The distortion results in the generation of higher harmonics or 'overtides'. The first overtide of M2 is M4. The distortion of tidal amplitude and velocity can be modelled with equations 3 and 4 (Friedrichs and Aubrey, 1988). For an undistorted tide, aM4:aM2=0, for a distorted tide aM4:aM2>0. The amplitude ratio is therefore a direct measure of the degree of distortion.

$$Amplitude = aM_2 \cos(\omega t - \theta_{M2}) + aM_4 \cos(2\omega t - \theta_{M4}) \quad (3)$$

$$Velocity = vM_2 \cos(\omega t - \varphi_{M2}) + vM_4 \cos(2\omega t - \varphi_{M4}) \quad (4)$$

where a is amplitude, v is tidal velocity, t is time, ω is tidal frequency, θ is phase of tidal amplitude, φ is phase of tidal velocity.

The overtides interact with the tidal constituents and may result in significant tidal asymmetry. Tidal asymmetry can be interpreted in several ways (Friedrichs and Aubrey, 1988; Maren and Winterwerp, 2012):

- Asymmetry in vertical tide (amplitude / water level elevation), when ebb duration is unequal to flood duration. If flood duration is shorter, the system is flood-dominant.
- Asymmetry in horizontal tide (flow velocity), in two ways:
    - Peak flow asymmetry, which is important for the net transport direction of coarse sediments and mixing into the water column. If flood velocity is higher, the system is flood-dominant. Peak flow asymmetry is related to asymmetry in ebb/flood duration: a shorter flood period usually means higher peak flood velocities.
    - Asymmetry in slack water duration, defined as the period of low velocity near the time of the turning of the tidal current. This affects the settling of fine sediments and the direction of fine sediment transport.

A phase difference between M2 and M4 can result in asymmetry in horizontal and vertical tide and cause a flood- or ebb-dominant system. When M2 and M4 amplitude are in phase (0° or 180°), ebb and flood duration are equal and the system is symmetrical. In theory, the velocity phase difference is ±90° and ebb/flood velocities are also equal. An amplitude phase difference between 0° and 180° results in a shorter rising tide. When the velocity phase difference is between -90° (270°) and 90°, this results in an asymmetrical tide and a flood-dominant system with higher flood velocities. Assuming the above described idealized relationship between amplitude and velocity phase difference, if the amplitude phase

difference is between 135°-225°, this means that high water slack duration is longer, hence settling time for sediments is longer, promoting import of fine sediments (Friedrichs and Aubrey, 1988; Vroom et al., 2012).

Table 2.2 summarizes the above described idealized relationship between M2 and M4 amplitude and velocity phase differences and ebb/flood dominance. It also gives an indication for the likely transport direction of coarse and fine sediments, based on ebb / flood / slack water duration. It is important to note that the presence of intertidal areas (V_s/V_c, ratio between tidal storage and volume of channels) and elevation (*a/h*, the ratio between offshore M2 amplitude and average water depth at mean sea level) influence this relationship. For example, estuaries with a large intertidal area usually are ebb-dominant (shorter ebb), since the limited water depth on the flats slows down the propagation of high water. In a highly flood-dominant system, an increase in channel depth generally leads to a less flood-dominant system, 2θM2-θM4 decreases away from 180° (Friedrichs and Aubrey, 1988). Therefore the relationship between amplitude and velocity phase difference, given in Table 2.2, is not always straightforward. It also depends on basin geometry, channel depth and intertidal storage.

Table 2.2: Tidal asymmetry: idealized relation between M2 and M4 amplitude and velocity phase difference (based on Friedrichs and Aubrey, 1988, and Vrooms et al., 2012).

aM4:aM2>0 (distorted tide)	*Amplitude phase difference (2θM2-θM4)*	*Velocity phase difference (2φM2-φM4)*	*Ebb / flood dominance and consequence for sediment transport*
Distorted, symmetrical tide	0° or 180°	270° or 90°	No dominance, equal ebb/flood duration and velocities
Distorted, asymmetrical tide	0°<θ<180 ° (max. 90°)	270°<φ<90° (max. 0°)	Flood-dominant, shorter flood with higher peak currents, import of coarse sediment
	135°<θ<225 ° (max. 180°)	45°<φ<135° (max. 90°)	Flood-dominant , longer high water slack, import of fine sediment
	180°<θ<360° (max. 270°)	90°<φ<270° (max. 180°)	Ebb-dominant, shorter ebb with higher peak currents, export of coarse sediment
	315°<θ<45 ° (max. 0°)	225°<φ<315° (max. 270°)	Ebb-dominant , longer low water slack, export of fine sediment

The phase difference between M2 and M4 amplitude and velocity can change in time and space, therefore the type of dominance can change. Fig. 2.8 shows the observed 2M2-M4 amplitude phase difference in the past decade in the Lower Ems. This period is too short to observe any temporal trends, but the spatial variation is obvious. Near Emden the amplitude phase difference is 180°, decreasing in the upstream direction, from 170° near Pogum to 105° near Papenburg. Assuming the idealized relationship between amplitude and velocity

phase difference (Table 2.2), this would mean that high water slack duration is longer near the mouth of the Lower Ems and fine sediments will have more time to settle, favouring the import of fine sediment. The system becomes more and more flood-dominant in the upstream direction (spatial change), with higher peak flood velocities. This flood-dominance is illustrated in Fig. 2.9, which shows the asymmetry in both ebb/flood duration and peak velocities in the upstream part of the Lower Ems. Flood duration is shorter and peak flood velocities are twice higher than peak ebb velocities. The historical development of the tidal asymmetry between 1945 and 2005 (temporal change) will be one of the subjects of this research.

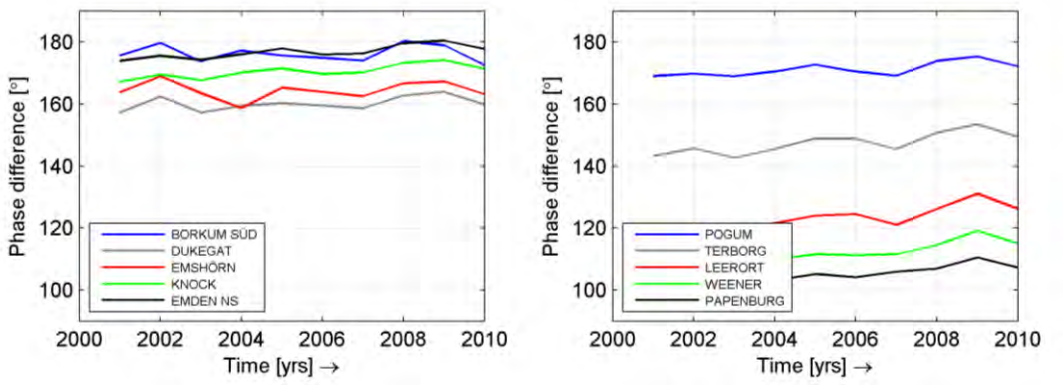

Fig. 2.8: Observed amplitude phase difference for all stations in the Ems-Dollard estuary (Vroom et al., 2012).

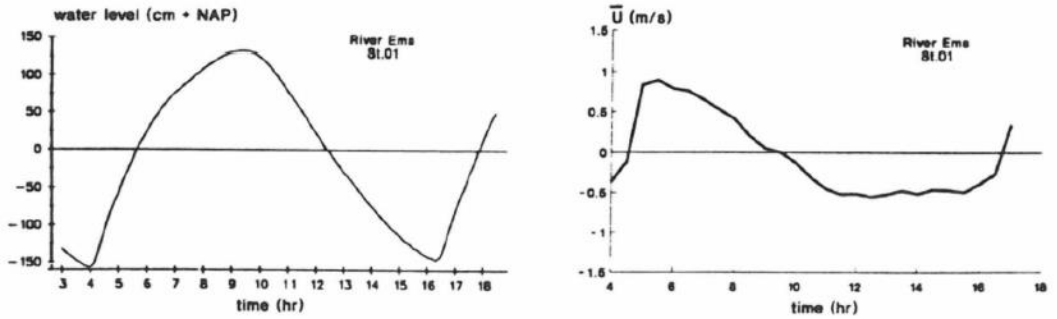

Fig. 2.9: Water level and flow velocity between Weener and Leerort, measured in 1990, showing an asymmetrical, flood-dominant system: shorter flood with higher peak flow velocity (Vroom et al., 2012, after Van Leussen, 1994).

2.3.4. Effect of bottom roughness on tidal asymmetry

Since the propagation speed of the wave is determined by water depth, the tidal trough is affected more than the tidal crest and asymmetry develops. Friction enhances the tidal asymmetry. It has more effect on the ebb tide and the time delay between low water at the estuary mouth and at the estuary head will increase, meaning ebb duration increases. Flood duration will become shorter with higher flood currents (Dronkers, 1986; Talke and De Swart,

2006; Hoekstra, 2011). A reduction in hydraulic roughness will reduce the effects of friction, especially on the ebb tide, and the propagation speed of the low water wave will increase. This will result in less tidal asymmetry. In the case of a flood-dominant estuary, the system will become less flood-dominant with reduced bottom roughness, although tidal amplitude will increase.

It is suggested that channel deepening and a reduction in bottom roughness over time has resulted in a less flood-dominant system in the Lower Ems (Talke and De Swart, 2006). Indeed, previous modelling experiments by Herrling and Niemeyer (2008c) show this trend between 1937 and 2005. Bottom roughness had to be calibrated to a smoother bottom in 2005 to match water level measurements. Comparison between model conditions shows an increase in flood duration upstream of Leerort since 1937, so the system has become less flood-dominant over time. For example at Papenburg, the duration of the flood phase has increased by ~45 min. Note that flood duration at each location is still shorter than the ebb period, both in 1937 and 2005 (Herrling and Niemeyer, 2008c). What part of this temporal change can be attributed to the increased water depth (deepening) and what part to a reduction in bottom roughness, is not investigated by Herrling and Niemeyer (2008c). This will be part of this present research.

2.3.5. Tidal phase lag / lead

In a straight, infinitely long and deep estuary without reflection, the tidal wave will be a progressive wave. This means that high or low tide will occur increasingly later along successive locations in the estuary. Maximum ebb/flood velocities will correspond with low/high tide. The moment of flow reversal, slack water, occurs mid-tide. The phase lag between vertical tide and horizontal tide is 0°. Bottom friction, shoaling and reflection at the basin margins and the resulting interference of the incoming and reflected tidal wave, can cause a standing wave pattern. In that case, the phase shift between the water level and the tidal currents is ±90°, approximately 3 hours. A phase lag occurs when the horizontal tide reverses later than the vertical tide (-90°<H-U<0°), a phase lead occurs when the horizontal tide reverses earlier (0°<H-U<90°) (Van Rijn, 2010; Masselink et al., 2011). In general, flow velocity will reverse earlier than the water level (H-U>0). This phase lead of the horizontal tide with respect to the vertical tide increases when bottom friction increases. Furthermore, friction also causes a phase shift between bottom and surface, causing the tide to reverse earlier near the bottom (Van Rijn, 2010). In general, strongly convergent estuaries have a

relative phase difference close to 90°, although the wave remains a progressive wave (Friedrichs and Aubrey, 1988).

2.3.6. Estuarine circulation

The general description of estuarine circulation is “subtidal currents that bring freshwater seaward in the upper portion of the water column, with an associated near-bed landward flow bringing salty water” (Burchard and Hetland, 2010). Both gravitational circulation and tidal straining (internal tidal asymmetry) contribute to this residual circulation pattern and show a similar residual flow profile.

Early studies assumed that gravitational circulation is the dominant contribution to estuarine circulation. Estuarine circulation was thought to be directly driven by the horizontal salinity gradient (Dyer, 1994). Interaction between less dense fresh water and denser seawater sets up a horizontal density gradient. In a mesotidal estuary, like the Ems-Dollard estuary, the tidal currents are strong enough to generate some turbulence at the river bed and induce vertical mixing. This causes the outflowing fresh water in the surface layer to have a higher salt content, which is being compensated by a landward flow in the more saline bottom layer. Fig. 2.10 illustrates this flow pattern with two-way mixing.

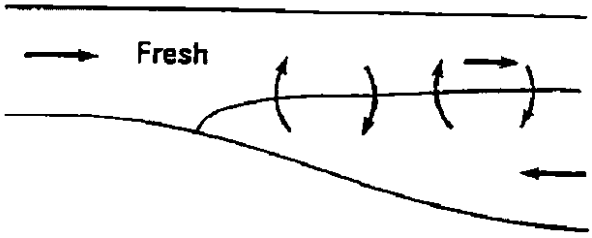

Fig. 2.10: Tidally averaged flow pattern in a partially-mixed estuary, with fresh water in the surface layer flowing seaward and a more saline landward flow in the bottom layer (gravitational circulation). Turbulence causes two-way mixing at the density interface (Dyer, 1994)

The strength of the gravitational circulation <u> is given in equation 5 (Van de Kreeke, 1991, based on field observations and the formula for gravitational circulation from Hansen and Rattray, 1965). From this equation follows that the strength of gravitational circulation scales linearly with the horizontal salinity gradient (*ds/dx*) and increases with increased *ds/dx*, but especially with water depth (h^3). The magnitude of the gravitational circulation will be small or even absent, when water depth is limited. Note that the Ems-Dollard estuary can be well-mixed (negligible vertical salinity differences) at low discharge or weakly stratified (vertical salinity gradient but poorly defined halocline) at high discharge. Therefore the horizontal

salinity gradient and thus the strength of the gravitational circulation varies depending on river discharge.

$$< u >= \frac{g\beta\frac{ds}{dx}}{48N_z} h^3 \left(1 - 9\left(\frac{z}{h}\right)^2 + 8\left(\frac{z}{h}\right)^3\right) \qquad (5)$$

where *ds/dx* is the horizontal salinity gradient (ppt/m), N_z is the diffusivity, *z* is the vertical position (m) and *h* is water depth (m)

Mixing/stratification can vary during a tidal cycle, depending on differences in ebb/flood velocities (and related bed shear stress). During one part of the tide, the development of turbulence may cause a well-mixed state, while stratified conditions exist during the other part (Lewis, 1997). This is illustrated in Fig. 2.11. The differential displacement of layers with a different density causes straining. Density straining during flood tide destabilizes the water column and the inflowing salt water substantially enhances small-scale turbulence and vertical mixing. However, stratification is enhanced during ebb and suppresses vertical mixing (Simpson et al., 1990). This internal tidal asymmetry affects the velocity profile and causes more downward transport of momentum during flood than during ebb. It may therefore enhance sediment trapping and the formation of an ETM (Jay and Musiak, 1994).

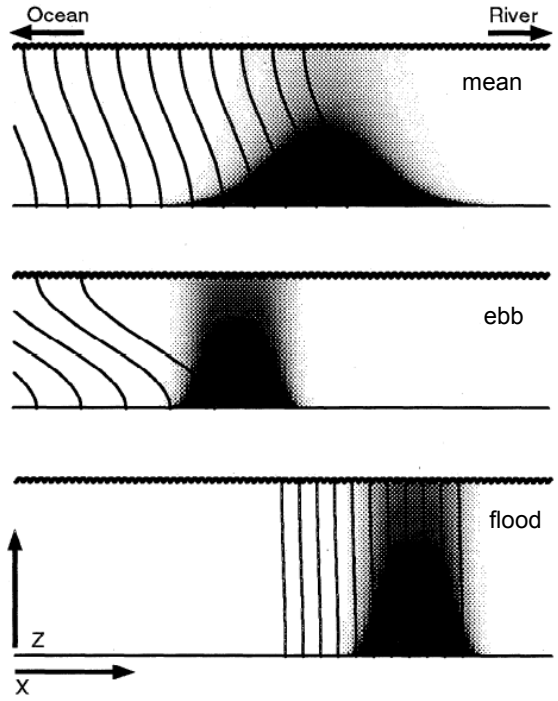

Fig. 2.11: Density contours and ETM for mean flow, ebb and flood in along-channel and vertical direction, illustrating tidal mixing asymmetry: stratified conditions during ebb and a well-mixed state during flood. Sediment concentration is affected by horizontal advection and vertical processes (erosion, deposition, settling, vertical mixing) (Jay and Musiak, 1994).

Burchard and Hetland (2010) found that gravitational circulation is only responsible for one-third of the estuarine circulation and internal tidal asymmetry (also called 'tidal straining' or 'strain-induced periodic stratification') contributes two-third, for situations without wind straining and residual runoff. Both processes (gravitational circulation and internal tidal asymmetry) result in a similar residual flow profile and scale linearly with the horizontal Richardson number Ri_x (a measure for the degree of stratification, equation 6), which depends on the horizontal buoyancy gradient and the squared water depth. The strength of estuarine circulation increases with increasing Ri_x. Tidal straining also exhibits a weak negative relation with the inverse Strouhal number St_i (a measure for the mixing associated with tidal flow, equation 7). The relative importance of gravitational circulation and tidal straining in each estuary is difficult to quantify (Burchard and Hetland, 2010), therefore in this study the term 'estuarine circulation' will be used for both processes.

$$Ri^{wt}{}_x = \frac{\partial_x b H^2}{(U^{wt})^2} \qquad (6)$$

$$St_i{}^{wt} = \frac{H}{TU^{wt}} \qquad (7)$$

where $Ri^{wt}{}_x$ is the modified horizontal Richardson number (-) and St_i^{wt} is the inverse Strouhal number (-), $\partial_x b$ is the constant horizontal buoyancy gradient, T is the tidal period (s), H is water depth (m) and U^{wt} is the flow velocity (m/s), composed of the contributions from wind w and tide t, instead of only the tidal velocity scale U_{max}.

Also density gradients due to high suspended sediment concentrations can contribute to the residual circulation pattern (Talke et al., 2009). This sediment-induced gravitational circulation will be further discussed in paragraph 2.5.2.

2.4. Sediment transport

Tidal dynamics determine flow characteristics, e.g. ebb/flood velocity, water level and direction of the residual current. This in turn influences sediment dynamics: erosion, transport, deposition and consolidation, which eventually may lead to morphological change. Paragraph 2.4.1 focusses on fine suspended sediment, since this is the present-day dominant sediment in the Lower Ems river. Paragraph 2.4.2 will further elaborate on the link between tidal dynamics and net sediment transport direction.

2.4.1. Erosion, suspension and deposition

Sediment particles are brought into suspension by the interaction between the flow and sediment bed. Sediment is eroded if bed shear stress exceeds shear strength. Bed shear stress τ depends on water depth and flow velocity (equation 8). The critical shear stress required to initiate sediment motion is non-dimensionalized in the Shields parameter θ and depends on grain size (equation 9) (Van Rijn, 2011). A higher critical shear stress is required to erode fine sediment particles (diameter < 63 µm). These particles do not protrude through the viscous sublayer and are therefore not exposed to the turbulent flow. Electrostatic forces also prevent easy entrainment (Masselink et al., 2011).

$$\tau = \rho g \frac{\bar{\bar{u}}^2}{C^2} \quad (8)$$

$$\theta = \frac{\tau}{(\rho_s - \rho) g D_{50}} \quad (9)$$

where τ is bed shear stress (N/m^2 or Pa), θ is the Shields parameter (-), ρ_s and ρ are sediment and fluid density respectively (kg/m^3), g is the gravitational acceleration (m/s^2), $\bar{\bar{u}}$ is cross-section averaged flow velocity (m/s), C is the Chézy-coefficient (m$^{0.5}$/s) and D_{50} is median grain size (m).

Sediment transport is governed by the balance between upward fluid forces (buoyancy due to turbulence) and downward gravitational forces. This balance determines the settling velocity and hence deposition. Particles will stay in suspension if bed shear velocity u_* exceeds settling velocity w_s (Masselink et al., 2011). Sediment transport q can generally be described by the relation $q \sim u^{3 \text{ to } 5}$ (Van Rijn, 2011). A small decrease in flow velocity will result in significantly smaller sediment transport. Coarse sediment responds quickly to changes in ebb/flood velocities and easily falls out of suspension, but since settling velocity for fine sediment is low, these particles need more time to settle. Therefore, peak flow asymmetry governs coarse sediment transport, while a difference in slack water duration is the most important factor for the net transport direction of fine sediment (Dronkers, 1986; De Swart and Zimmerman, 2009; Masselink et al., 2011), further discussed in paragraph 2.4.2.

Deposition is directly related to sediment characteristics. Cohesive sediment (silt and clay) behaves differently from non-cohesive sediment (sand). Cohesive particles tend to floc and form aggregates due to electrostatic forces. The combined mass of the flocs increases settling velocity and promotes deposition of fine sediments. Because salinity increases flocculation, this process is especially important in coastal and estuarine waters (Masselink et al., 2011). Winterwerp (2011) argues that peak flow asymmetry and asymmetry in slack

water duration result in flocculation asymmetry in the Lower Ems: the higher flood velocities form larger mud flocs, which settle rapidly during the longer high water slack, contributing to net landward sediment transport.

2.4.2. Net sediment transport

Tidal asymmetry, estuarine circulation and settling/scour lag may result in net sediment transport (e.g. Dyer, 1994; Masselink et al., 2011). These processes lead to a residual upstream-directed transport of fine sediments in the present-day Lower Ems river.

Tidal asymmetry is characterized by a difference in ebb and flood peak velocities, but also by a difference in high and low water slack duration (see paragraph 2.3.3). For non-cohesive material (e.g. sand), net sediment transport direction mostly depends on peak flow asymmetry. However for fine, cohesive material (mud), asymmetry in slack duration is the most important factor in governing net transport direction (Dronkers, 1986; De Swart and Zimmerman, 2009; Masselink et al., 2011). In the present-day Lower Ems, a sharp increase in sediment concentration is observed at the beginning of flood (Fig. 2.12), coinciding with a peak in flow velocity. During the following long high water slack, fine sediments have enough time to settle and sediment concentration is lowest. This will ultimately result in net landward sediment transport (Vroom et al., 2012). The Lower Ems becomes more flood-dominant in the upstream direction. The higher peak flood velocities (e.g. ~1 m/s in Leerort) are more effective in eroding and mixing the sediment over the water column than the lower ebb velocities (~0.5 m/s). Sediment availability is also high due to the presence of fluid mud layers. Combined with increased flocculation during flood, this asymmetry in peak flow velocities and vertical mixing leads to net sediment transport in landward direction and a trapping efficiency of the Lower Ems (Winterwerp, 2011).

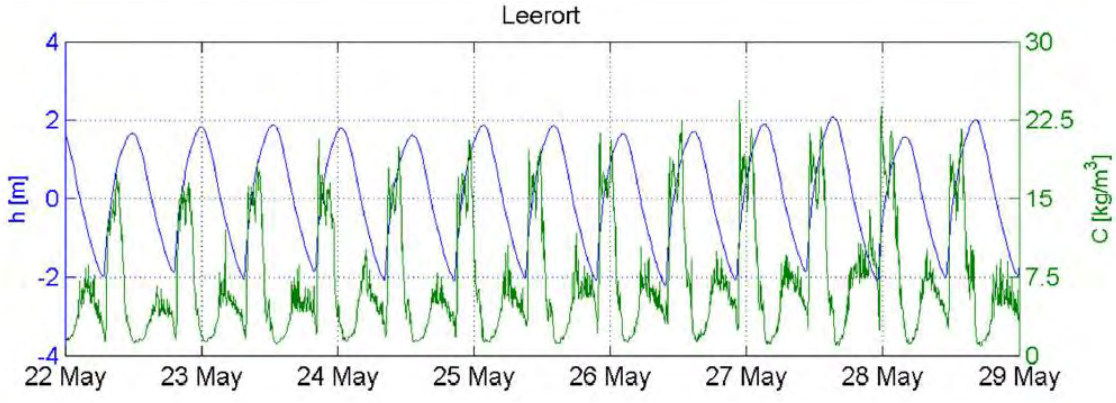

Fig. 2.12: Measured sediment concentrations and water levels at Leerort in May 2005 (Vroom et al., 2012).

Estuarine circulation causes additional upstream-directed transport, because the landward flow occurs in the bottom layer where the sediment concentration is highest, although sediment fluxes due to tidal asymmetry are generally much larger (Dyer, 1994).

Settling and scour lag can result in net landward movement within one tidal cycle in a flood-dominant system. Settling lag means that a sediment particle is deposited some period or distance from the point where the settling process started. When flow velocity decreases and turbulence is no longer capable of maintaining the particle in suspension, it starts to settle, but is carried further landward by the decreasing flood current. Scour lag means that sediment particles are not resuspended immediately after the turn of the tide: the threshold velocity of resuspension is higher than the threshold velocity of deposition, because particles can still be kept in suspension below the threshold for initial motion. The sediment particles will migrate landward until the maximum tidal velocity equals the threshold velocity (Dyer, 1994; Masselink et al, 2011). Peak flow asymmetry enhances this process, as the higher flood velocities are more effective in (re)suspending sediment particles and the subsequent high water slack time is longer. As a result, settling an scour lag cause net sediment transport in the direction of the peak current. (Dyer, 1994; De Swart and Zimmerman, 2009).

Spatial settling lag effects can result in additional landward transport, provided that there is a gradient in flow velocity. Sediment transport occurs in the direction of decreasing tidal current and/or decreasing depth, generally in up-estuary direction (De Swart and Zimmerman, 2009, after Postma, 1954, and Van Straaten and Kuenen, 1957).

When sediment availability is high, e.g. abundant sand/mud supply, net sediment transport depends directly on the hydrodynamic conditions (transport limitation). Morphological changes (sources/sinks) are the result of gradients in sediment transport. However, sediment scarcity can result in less sediment transport and net sediment transport depends directly on sediment supply (supply limitation). In this case, an increase in sediment supply will result in an increase in sediment transport. Also the morphological history is an important factor: the characteristics of the bottom (composition, layering, strength) are determined by historical conditions and influence sediment availability (Van Kessel, 2011).

2.5. Sediment-fluid interactions

Not only the hydraulic roughness of the river bed, but also high suspended sediment concentrations (ETM and fluid mud) influence hydrodynamics and cause hydraulic drag

reduction. This drag reduction has a similar effect on tidal dynamics as reduced bottom roughness. Sediment-fluid interactions affect the flow in multiple ways and the following processes each play a role in the Ems river (Winterwerp, 2006; Winterwerp et al, 2009; Van Maren et al, 2009a, 2009b, Talke et al., 2009):

- Damping of turbulence by vertical density gradients (stratification) and fluid mud formation. At high sediment concentrations, turbulence damping by stratification can lead to the collapse of the turbulent flow field and fluid mud formation, which will dampen turbulence even more.
- Sediment-induced gravitational circulation

2.5.1. Turbulence damping and fluid mud formation

Turbulence is damped by suspended sediment. In a stratified situation, with a low density water layer overlying a high density layer, the vertical transfer of mass and momentum results in energy loss and the damping of turbulence. This damping increases with stratification (Lewis, 1997) and is also referred to as 'sediment-induced buoyancy destruction' (Winterwerp et al. 2009, 2011).

Winterwerp (2001) showed that suspensions of non-cohesive and cohesive sediment behave differently. Flow velocity reduction in non-cohesive sediment suspensions results in the settling of part of the suspended load, which immediately forms a rigid bed on which turbulence generation remains possible, therefore keeping the rest of the particles in suspension. Gradual flow velocity reduction will therefore result in a gradual decrease in sediment carrying capacity and hence in a gradual decrease in sediment concentration. However flow velocity reduction in cohesive, muddy sediment suspensions with very high sediment concentration (near saturation concentration) will result in the collapse of the turbulent flow field (Winterwerp, 2001, 2006; Turner, 1973). When flow velocity decreases, the cohesive sediment starts to flocculate and form a layer of fluid mud. This leads to the creation of a two-layer flow with a sharp density gradient at the interface. At this interface the vertical turbulent mixing is significantly damped. This positive feedback results in the collapse of the turbulent flow field and a strong decrease in sediment carrying capacity. In nature, the collapse of the turbulent flow field will only happen at very high concentrations of cohesive sediment, when the fluid mud layer reaches sufficient thickness (>cm's) to smooth irregularities and hence also dampen turbulence production at the bed level (Winterwerp, 2001).

The present-day Lower Ems is characterized by hyperconcentrated sub-saturated conditions, and a 1-2 m thick fluid mud layer is present near the bottom. A relation for the saturation concentration is given in equation 10 (Winterwerp, 2006). When flow velocity decreases, the saturation concentration decreases with the cubed flow velocity and fluid mud formation can occur at even lower sediment concentrations than before.

$$C_s = \frac{1}{h}\int_0^h c_s dz = K_s \frac{\rho}{\Delta} \frac{U^3}{ghw_s} \qquad (10)$$

where C_s is saturation concentration, h is water depth, c_s is local saturation concentration, K_s is a proportionality factor, Δ is relative sediment excess density (= $(\rho_s-\rho_w)/\rho_s$), U is depth-averaged flow velocity and w_s is effective settling velocity, including hindered settling.

Winterwerp et al. (2009) quantified the drag reduction in estuaries that is caused by stratification and turbulence damping, depending on water depths and degree of stratification. In the Lower Ems, with a current average water depth of 6-7 m (Talke et al., 2009; Winterwerp, 2011), this means a possible drag reduction up to 15% due to stratification.

Fluid mud causes turbulence damping at the bed level, which results in a reduction of the effective hydraulic roughness. Since the propagation of the tidal wave depends on friction, this means that the presence of fluid mud will increase flow velocity and tidal amplitude. Indeed, reduction in hydraulic roughness and tidal amplification due to the presence of fluid mud has been shown for the Amazon shelf: the presence of fluid mud layers reduce effective bottom roughness by 50% (Beardsley et al., 1995) and bottom shear stress from 1-2 Pa to 0.75 Pa (Gabioux et al., 2005). Furthermore, a larger area of fluid mud could be correlated with more tidal amplification.

2.5.2. Sediment-induced gravitational circulation

The density difference caused by high suspended sediment concentrations not only dampens turbulence, but also affects the flow directly. Suspended sediment is an important factor for the residual circulation pattern and can cause additional upstream sediment transport (Talke et al., 2009).

Estuaries generally have a well-defined zone where suspended sediment concentration is higher than average. This so-called estuarine turbidity maximum (ETM) is typically located at the convergence zone of sediment and is influenced by the upstream-directed sediment

transport due to tidal asymmetry, estuarine circulation and settling/scour lag and the downstream-directed river discharge. In the Lower Ems, the turbidity peak is located near the transition from salt to fresh water, although it spreads out in the upstream direction. Concentrations near the surface can reach up to 1 g/l. Near the bottom, fluid mud concentrations can reach values of 10-80 g/l upstream of Terborg (Talke et. al, 2009). Fig. 2.13 shows that most suspended sediment is located in the fresh water region of the Lower Ems, where the effect of estuarine circulation is negligible. Salinity is well mixed over the entire water column, but large vertical sediment concentration gradients are present. Talke et al. (2009) argue that sediment-induced gravitational circulation, a density-driven current due to high concentrations of suspended sediment, contributes significantly to the direction of the residual flow and hence to net sediment transport. They suggest that upstream of the estuarine turbidity maximum (ETM) in the Lower Ems, gradients in suspended sediment concentration and salinity strengthen each other and result in a residual upstream-directed current. As the highest sediment concentrations are near the bottom, this causes upstream sediment transport. This turbidity-driven current can partly explain the longitudinal distribution of fine sediment upstream of the turbidity maximum (Talke et al., 2009).

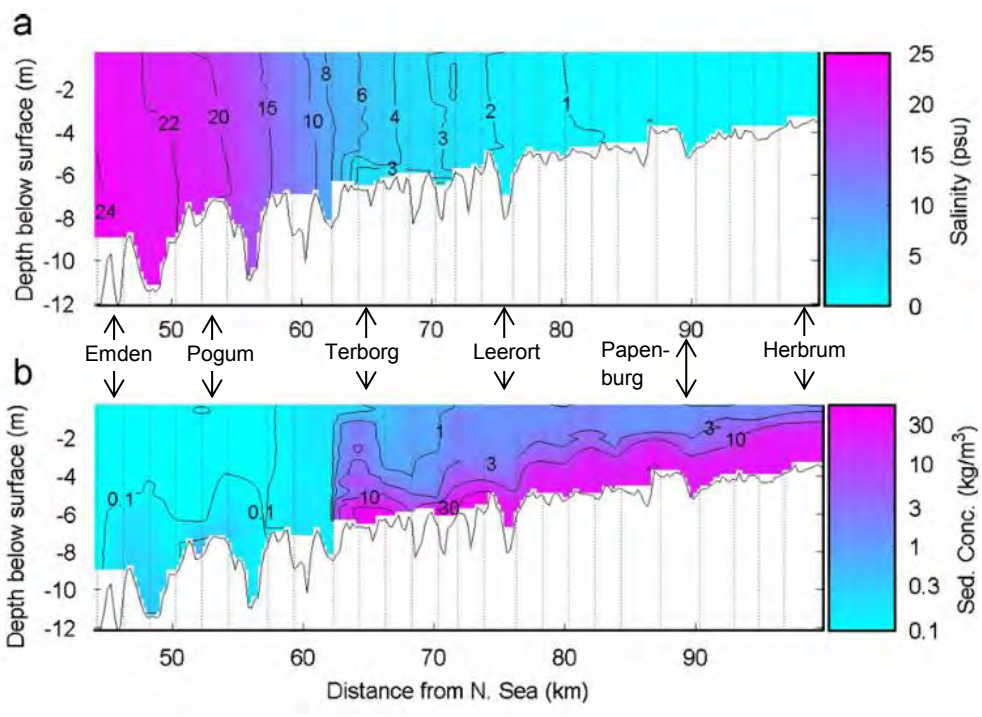

Fig. 2.13: Longitudinal distribution of (a) salinity and (b) suspended sediment concentration along the Lower Ems during ebb (adapted from Talke et al., 2009).

3 MATERIALS & METHODS

Two existing Delft3D models of the Ems-Dollard estuary are used: a depth-averaged 2-dimensional model and a 10-layer 3-dimensional model. This chapter discusses the set-up of these hydrodynamic models, focussing on the Emden Fahrwasser and the Lower Ems. Section 3.1 summarizes the general model set-up. This includes the computational grid, equations, historical bathymetries, hydraulic structures, boundary conditions and input parameters. An overview of all model runs is given in section 3.2. Three historical model conditions (1985, 1965 and 1945) with varying bottom roughness and the most recent situation (2005) are compared with each other and with available data from 2005.

3.1. General model set-up

The modelling software for this research is Delft3D (version 4.00.01). Delft3D is a multi-dimensional modelling program, capable of simulating hydrodynamics and sediment transport for unsteady flow in fluvial, estuarine and coastal environments. For this research, two existing models of the Ems-Dollard estuary are used: a depth-averaged (2D) and a 10-layer (3D) version. These models represent the 2005 situation. The set-up of the 2005 model and the calibration against present-day conditions is described in more detail in Van Maren et al. (2013). Both models (2D and 3D) use the measured 2005 bathymetry and measured water level time series at the up- and downstream boundaries. The 2D model is calibrated for bottom roughness. Existing hydraulic structures, like the Emssperrwerk and Geise training wall are also included. The general model set-up will be described below. When no specific model is mentioned, the set-up is applicable to both the 2D and 3D version.

3.1.1. Computational grid

The computational grid for the Ems-Dollard models was already available and is shown in Fig. 3.1. This fully curvilinear grid is generated with Delft3D RGF grid software. It consists of the Lower Ems, Dollard, the middle reaches and part of the lower reaches of the Ems-Dollard estuary. The resolution in the Lower Ems is about 80 m. The upstream boundary is located at weir Versen near Herbrum and at Leer Leda (a tributary, confluencing near Leerort). The downstream boundary is located in the Wadden Sea near Eemshaven. The 3D model includes 10 σ-layers with a relative layer thickness of 10% of the water depth.

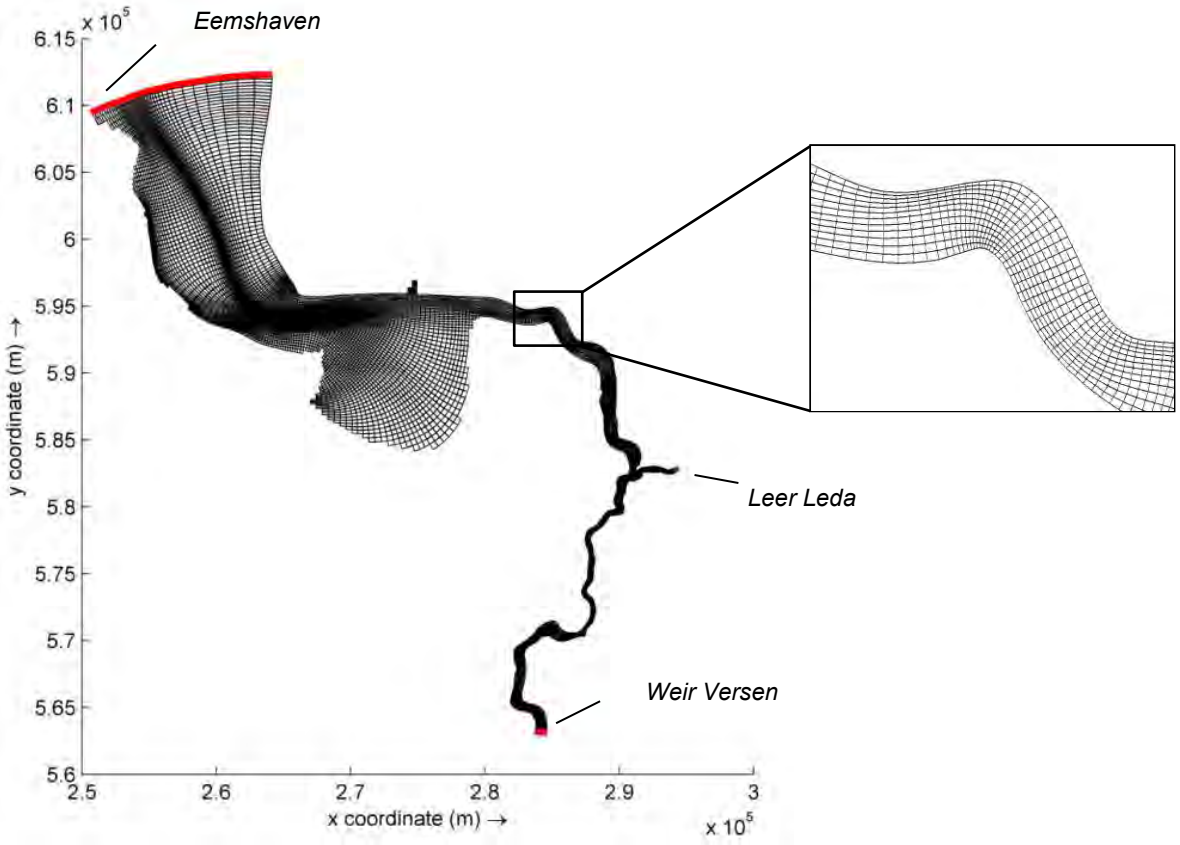

Fig. 3.1: Overview of the computational grid of the Ems-Dollard model. The downstream Wadden sea boundary and the two upstream boundaries, Leer Leda and weir Versen, are indicated.

3.1.2. Equations

Both Delft3D models solve the 2D (depth-averaged) or 3D non-linear shallow water equations. These are derived from the three dimensional Navier-Stokes equations for incompressible free surface flow. The models also include the continuity equations and momentum equations. The Delft3D models can be used to investigate hydrodynamic changes, e.g. changes in tidal amplitude, velocity, (relative) phase, tidal asymmetry (peak flow asymmetry, slack water duration) and estuarine circulation. The sediment transport module supports both suspended and bed load transport of (non-)cohesive sediments. The 10-layer 3D model allows for an analysis of (asymmetry in) mixing over the water column. Erosion and deposition of cohesive sediment fractions are calculated with the Partheniades-Krone formulations (Partheniades, 1965). Suspended sediment concentration is determined by solving a 3D advection-diffusion (mass-balance) equation and temporal settling/scour lag and spatial settling lag effects are taken into account. Hindered settling is accounted for by defining the settling velocity as a function of sediment concentration and non-hindered

settling velocity. Not included in the models are sediment-induced gravitational circulation, (asymmetry in) flocculation and fluid mud formation.

A detailed description of the governing equations can be found in the Delft3D-FLOW user manual (Deltares, 2012). All equations are formulated in orthogonal curvilinear coordinates, components are perpendicular to the cell faces of the computational grid. The equations are solved for a finite grid area in combination with initial model parameters and specific boundary conditions.

3.1.3. Bathymetries

The initial 2D and 3D models include the measured 2005 bathymetry. Channel deepening was carried out as a function of various chart datums: mean high water levels in the Lower Ems and average spring low water (SKN) in the Emden Fahrwasser. These water levels vary in time and space as a result of changing tidal characteristics. Determining these values (relative to mean sea level, m +NAP) is the first step in reconstructing historical bathymetries. In this way, channel deepening as a function of MHW or SKN is converted to a historical bathymetry relative to mean sea level (m +NAP). The bathymetry adaptations were implemented in the 2005 bathymetry according to these historical water levels and information about channel deepening. The historical bathymetries for three periods were reconstructed, using the 2005 bathymetry as a basis: 1985, 1965 and 1945. This interval was taken to approximate tidal variations due to the 18.6-year tidal cycle.

Measured bathymetry (2005)
The initial 2D and 3D models include the bathymetry that was obtained with echo soundings (Fig. 3.2). Low frequency echo sounding was used in the Lower Ems. The bathymetric data was projected onto the computational grid using QUICKIN software.

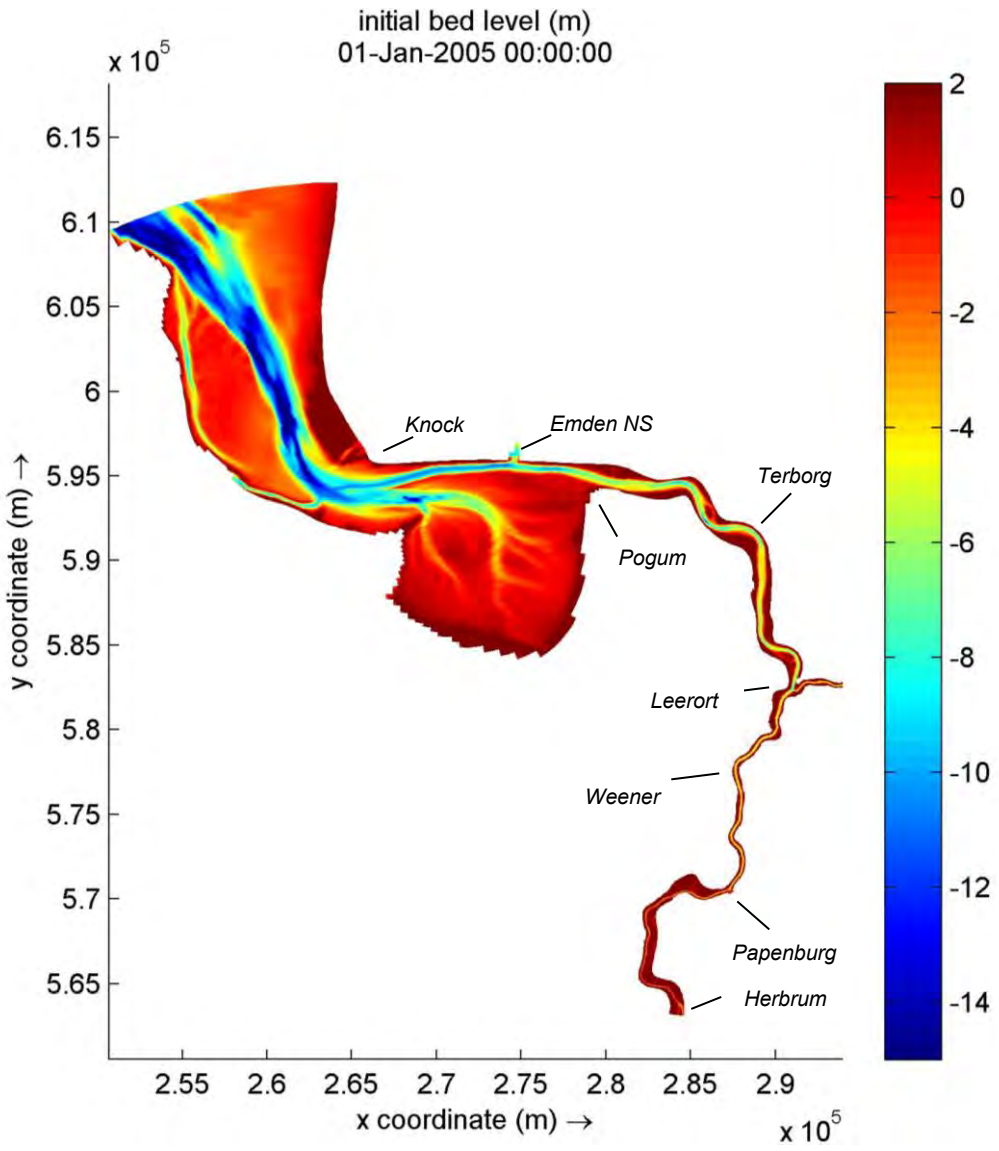

Fig. 3.2: Measured 2005 bed level (m NAP) of the Ems-Dollard estuary.

MHW and SKN values

All deepening activities are relative to mean high water levels or average spring low water levels, therefore these values have to be determined. Water level measurements were available from the federal waterway agency of Emden (*Wasser- und Schifffahrtsamt Emden*) for 1985 and 1965. These measurements consist of the exact time and height of each high and low water. Mean high water (MHW) values were determined from this data. MHW is defined as the average height of all high waters recorded at a given place over a 19-year period. For example, for the 1985 model state, the 19-year averages for each gauge are calculated using the high water levels in the period 01-01-1976 till 31-12-1994 (9 years before and after 1985). In this way, 19-year averaged MHW values were determined for all water level stations in the Emden Fahrwasser (Knock and Emden NS) and along the Lower Ems (Pogum, Terborg, Leerort, Weener and Papenburg). Because Knock, Terborg and

Weener are recent stations, the 19-year averages for these stations could only be determined for the 1985 model condition. Unfortunately, no water level data prior to 1949 was available (the existing German data was not available to Deltares), Instead, the 19-year averaged MHW values were estimated from a graph by Herrling and Niemeyer (2008c), showing the historical trend of yearly MHW for stations along the Lower Ems. This was done by fitting a trend line by hand. The error margin for this method is approximately 5 cm. Fig. 3.3 shows the thus obtained 19-averaged MHW values for all gauges. High water levels increase linearly in the upstream direction, from Knock to Papenburg, and MHW levels also increase in time.

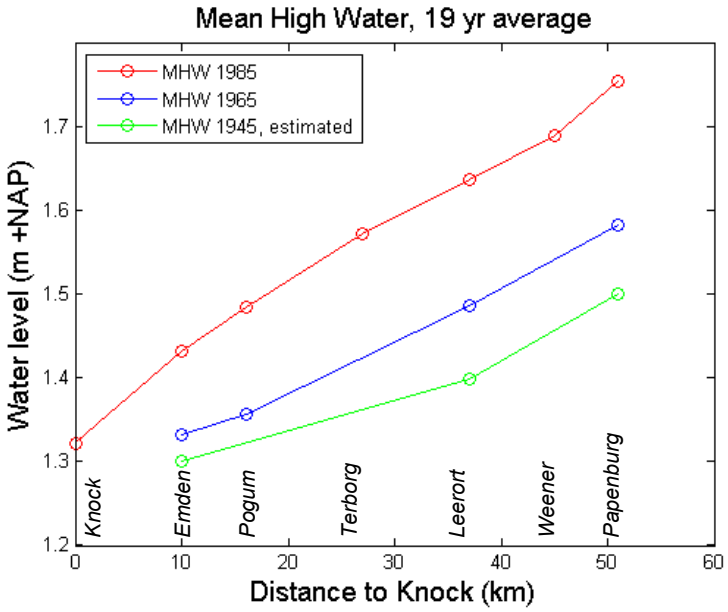

Fig. 3.3: Measured (1985 and 1965) and estimated (1945) mean high water levels (19-year averaged values) for water level stations in the Emden Fahrwasser and along the Lower Ems, including trend lines.

Channel deepening in the Emden Fahrwasser was carried out as a function of SKN (*Seekartennull* or chart datum, CD). For the German North Sea coastline and the Ems-Dollard estuary, SKN is defined as the average spring low water levels or Lowest Astronomical Tide (Bundesamt für Seeschifffahrt und Hydrographie). The available water level data did not include SKN values. Instead, for 1985 and 1965 the dates of full and new moon are used. Since spring tide generally lags behind in coastal areas (Van Rijn, 2010), SKN values are obtained by averaging the low water levels that are measured 1-3 days after full/new moon. The 1945 SKN value for Emden was again based on another graph by Herrling and Niemeyer (2008c) showing the historical trend of yearly MLW levels. Low water levels are fairly constant in Emden, therefore it was assumed that SKN levels are also

constant. MLW levels in 1945 seems slightly higher than in 1965, so SKN water level at this location was estimated slightly above the 1965 SKN value.

Reconstruction of historical bathymetries

Table 3.1 summarizes the anthropogenic interventions (channel deepening, streamlining, constructions) in the Lower Ems and the Emden Fahrwasser. Which interventions are included in the 1985, 1965 and 1945 reconstructed bathymetries respectively, is also indicated.

Table 3.1: Chronology of fairway deepening and other interventions in the Lower Ems (after Vroom et al., 2012 and personal communication with M. Krebs, jan. 2013).

Included in model situation:				*Year*	*Intervention in Lower Ems*
2005	*1985*	*1965*	*1945*		
				Before 1939	Emden Fahrwasser at -6 m SKN
				1932 - 1939	Waterway depth: 5.5m m below MHW between Pogum and Leerort; 4.1m m below MHW between Leerort and Papenburg
				1939 - 1942	Maintaining Emden Fahrwasser at -7 m SKN.
				1942 - 1948	No maintenance between 1942 and 1945. After 1945 natural depth Emden Fahrwasser between - 5.8 and -6 m SKN.
				1957	Deepening Emden Fahrwasser to -8 m SKN
				1958 - 1961	Construction of 2.2 km training dam 'Seedeich', 12 km Geise training wall from Pogum to Geisesteerwert and 17 new groynes.
				1961 - 1962	Deepening of Leerort-Papenburg to 5 m below MHW. Narrowing of river between Herbrum - Papenburg by extension of groynes.
				1965	Emden Fahrwasser at -8.5 m SKN
				1983 - 1986	Deepening Lower Ems on trajectory Emden-Papenburg to 5.7 m below MHW
				1984 - 1985	Streamlining of river near Weekeborg and Stapelmoor (increase of radius), reduced river length with 1 km
				1991 - 1994	On-going deepening of Lower Ems on trajectory Emden - Papenburg to 6.3 m, 6.8 m and 7.3 m below MHW
				2001-2002	Construction of storm surge barrier Emssperrwerk

All deepening activities are relative to mean high water levels (19-year averages) or average spring low water levels. The resulting historical waterway depth is shown in Fig. 3.4. The 1985, 1965 and 1945 bathymetries are reconstructed based on this waterway depth. In appendix A, two representative areas of each reconstructed bathymetry are shown in more detail (Emden Fahrwasser and the stretch around Leerort).

The largest bathymetry change in de Emden Fahrwasser (between Knock and Emden NS) took place between 1945 and 1965, when the approach to Emden harbour was deepened from ~ -9 m NAP to ~ -10,5 m NAP. This depth has been maintained since then, which is confirmed by the measured 2005 bathymetry. For the 1965 and 1985 model situation, the 2005 depth of the Emden Fahrwasser was used. For the 1945 model situation the depth of this stretch was reduced to ~ -9 m NAP.

As can be seen in Fig. 3.4, the stretch between Pogum and Leerort has remained at a constant depth of approximately -4 m NAP between 1945 and 1985. However, the on-going deepening in the uppermost stretch of the Lower Ems (between Leerort and Papenburg) has lowered the waterway depth from ~ -2.7 m NAP in 1945, to ~ -3.5 m in 1965, to a depth of ~ -4 m in 1985. These depth changes have been included in the model conditions of 1945, 1965 and 1985 respectively. In the 1990's the entire river stretch from Emden to Papenburg was deepened to its present depth of approximately -5.5 to -7 m NAP (with deeper parts in outer bends). No information about deepening measures was available upstream of Papenburg and east of Leerort (river Leda), therefore these river parts were not modified in the model.

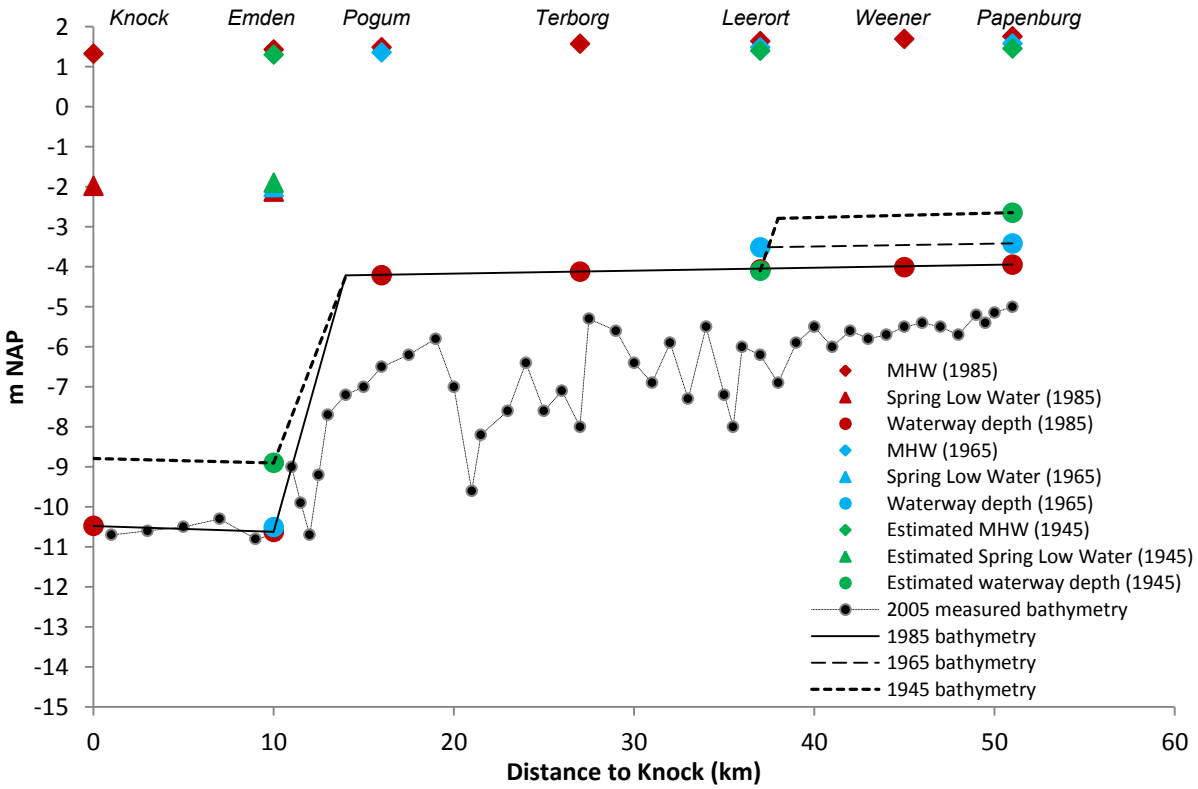

Fig. 3.4: Reconstructed bathymetries of 1985, 1965 and 1945, based on channel deepening activities, mean high water levels and average spring low water levels. An impression of the measured 2005 bathymetry is given. All values are given in m +NAP (=m +NN).

Depth was modified from the available 2005 bathymetry using QUICKIN software. Individual depth points were adjusted to the historical condition by decreasing the individual depth points that exceed the reconstructed waterway depth of Fig. 3.4. From Papenburg to Pogum, waterway depth was slightly increased in downstream (along-channel) direction with steps of 0.01 m between grid cells. This allows for a gradual transition. The steep transition between the Emden Fahrwasser and the Lower Ems (between Emden and Pogum) was done with steps of 0.3 m between grid cells. Fig. 3.5 gives an example of a cross-section near Weener, showing the subsequent modification of the 2005 bathymetry to the historical bathymetries.

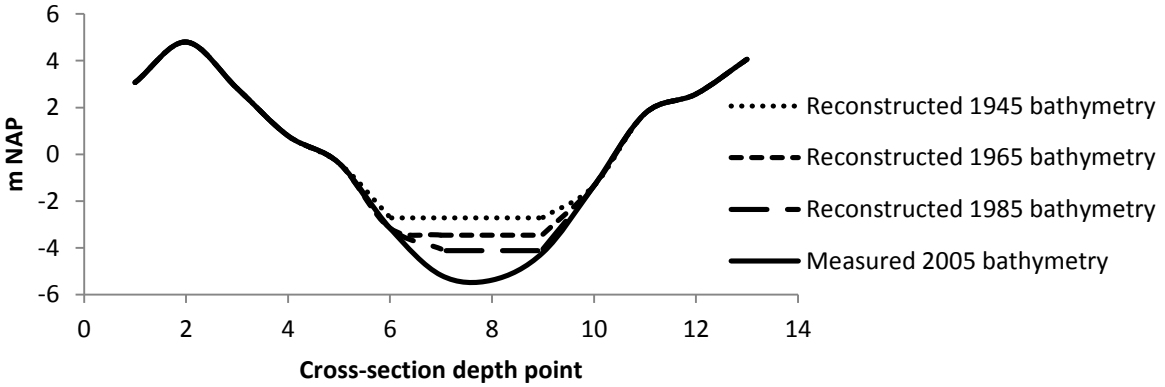

Fig. 3.5: Cross-section of the Lower Ems near Weener, showing a comparison between the measured 2005 bathymetry and the reconstructed 1985, 1965 and 1945 bathymetries.

In addition to deepening activities, the Lower Ems has a history of man-induced changes to river bends. Artificial meander cut-offs between 1892 and 1929 shortened the river by 1.8 km (Krebs, 2012). The latest streamlining measure was the increase in bend radius at Weekeborg and Stapelmoor in 1984-1985 (Fig. 3.6), making it easier for ships to navigate. These streamlined curves are present in the 2005 and 1985 model situation. For the 1965 and 1945 model situation, a reconstruction of the Weekeburg curve prior to streamlining was made by shifting the main river channel to its previous position in the outer meander bend, which was still visible in the outline of the river (Fig. 3.7). The original position of the main channel at Stapelmoor was not clear and could therefore not be reconstructed. However, this is not expected to significantly influence model outcomes.

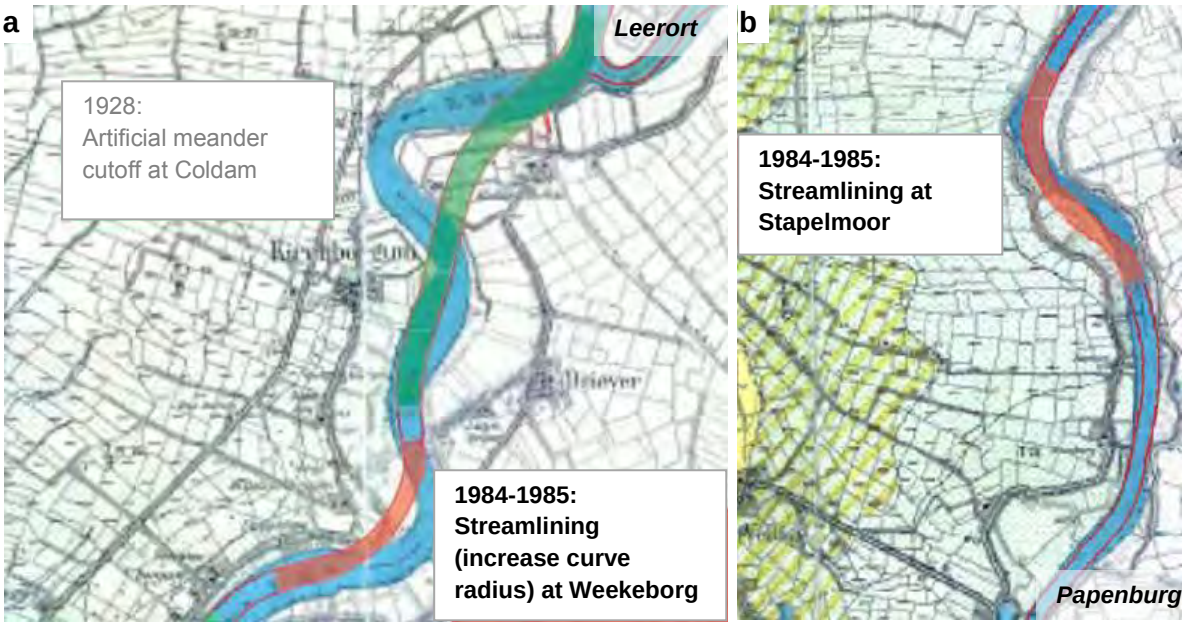

Fig. 3.6: Streamlining of meander bends at (a) Weekeborg and (b) Stapelmoor (adapted from Krebs, 2012).

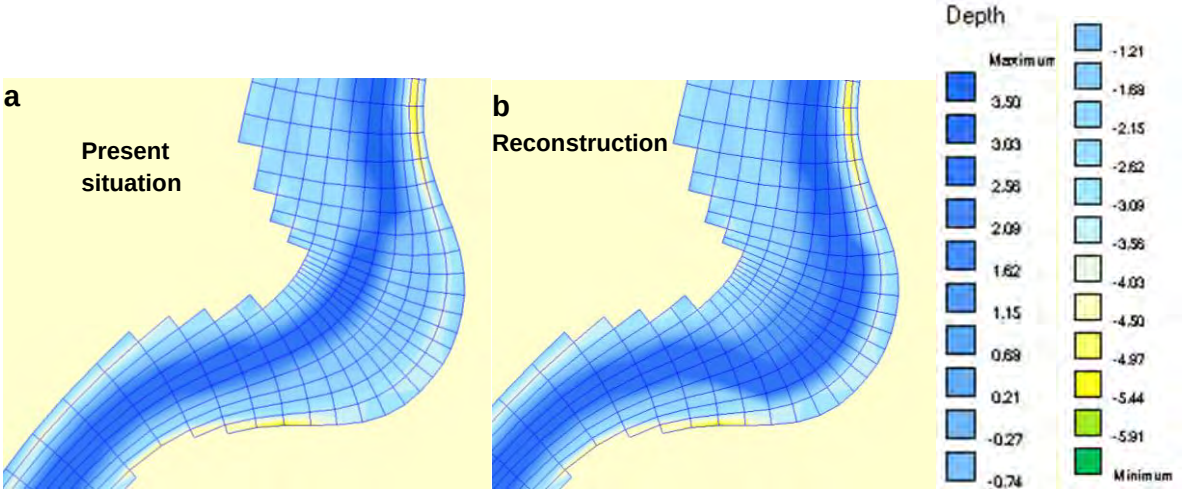

Fig. 3.7: Man-induced changes at the Weekeborger curve. (a) present situation (2005 / 1985), (b) reconstruction of the situation before streamlining (1965 / 1945).

3.1.4. Schematization of hydraulic structures

Fixed hydraulic structures like dams, groynes and weirs affect the flow. These hydraulic structures are represented in the Ems-Dollard models in two ways: hydraulic structures that block the flow between grid cells (e.g. thin dams) and structures that cause energy loss (e.g. weirs). The Emssperrwerk (Fig. 3.8 and Fig. 3.9) is a storm surge barrier that was constructed in 2001-2002. The largest part of the Emssperrwerk consists of pillars and is not included in the model, as the pillars only have a local effect on the flow. Only part the Emssperrwerk blocks the flow near the mouth of the Lower Ems and is included as a thin dam.

Fig. 3.8: Photograph of the Emssperrwerk, the recently constructed storm surge barrier near Pogum (Krebs, 2012).

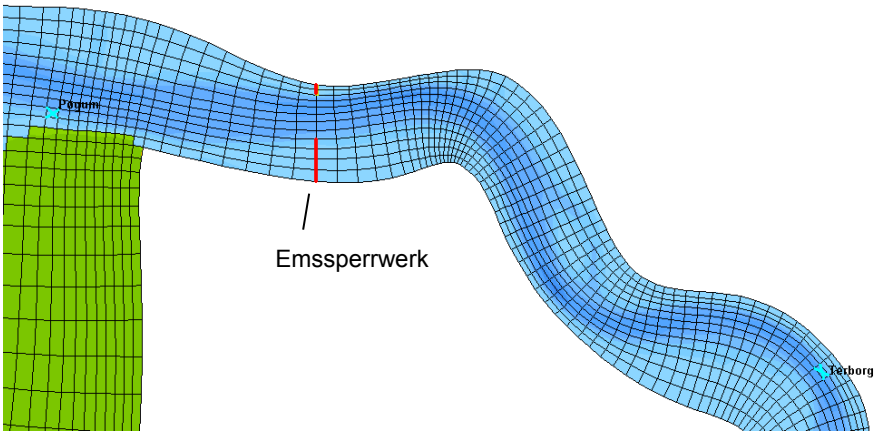

Fig. 3.9: Location of Emssperrwerk in the Delft3D models (in red). Dry points are indicated in green.

The Geise training wall (*Geise-Leitdamm,* Fig. 3.10) was constructed between 1958-1961 and borders the Emden Fahrwasser. It is modelled as a weir with crest heights of 0.4-1.1 m NAP. Water exchange over the dam is possible at high water conditions, but the dam causes energy losses. This effect is modelled with a quadratic energy loss term that is added to the momentum equation. The mathematical formulation and implementation of these hydraulic structures is described in the Delft3D-FLOW user manual (Deltares, 2012).

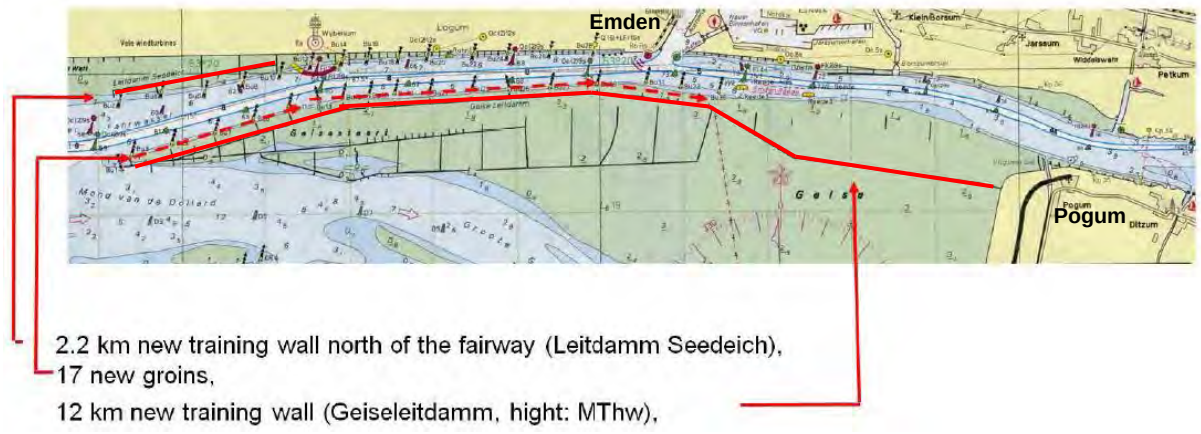

Fig. 3.10: Location of the 12 km long Geise training wall (Geiseleitdamm) and other structures, built between 1958-1961 (adapted from Krebs, 2012).

Several 2D model runs with and without the Emssperrwerk and Geise training wall were done for the historical situations, to investigate the effect of these constructions on the tidal characteristics (see section 3.2).

3.1.5. Boundary conditions

A distinction should be made between closed and open boundaries. The contours of the Ems-Dollard estuary are closed or natural boundaries. Flow velocity normal to these land-water boundaries is set to zero. The Wadden Sea boundary and the two upstream boundaries, Leer Leda and Weir Versen, are open or artificial boundaries. These water-water boundaries do not hinder the flow and only exist to restrict the computational area. Open boundary conditions have to be specified, in this case water level and salinity time series at the downstream end and river discharge at the upstream end.

Downstream boundary conditions

The 2005 model situation uses a measured water level time series at Eemshaven as the downstream boundary condition. This time series has a resolution of 10 minutes (Fig. 3.11). The water level station at Eemshaven started measuring from 1978 onwards and 19-year averaged high water levels, low water levels and tidal range have remained fairly constant since then. No data is available prior to 1978, so the 2005 water level series has also been used as the Wadden Sea boundary condition for the 1985, 1965 and 1945 model situation. This is also preferable for comparison reasons.

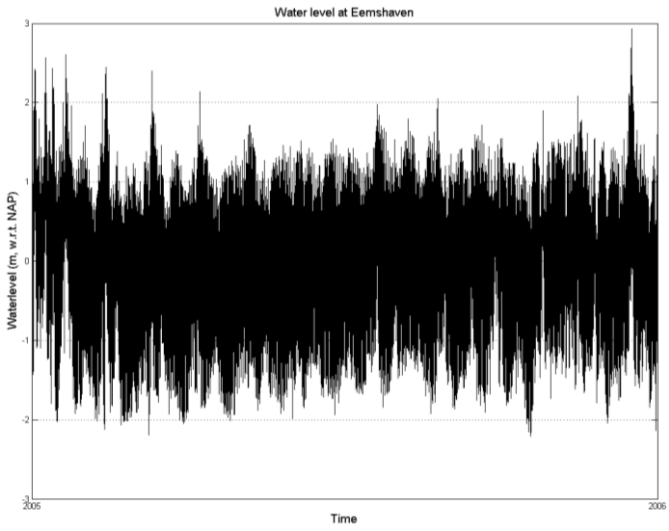

Fig. 3.11: Downstream boundary condition: water level time series of 2005 at Eemshaven (m NAP), resolution is 10 minutes (Waterbase database, Rijkswaterstaat).

In addition to water level, a salinity time series is specified at the Wadden Sea boundary. As there are no continuous salinity measurements, this was derived from a previous model in combination with 2005 measurements at Knock. The salinity time series was generated based on a linear relation between salinity at the boundary and at Knock (Fig. 3.12).

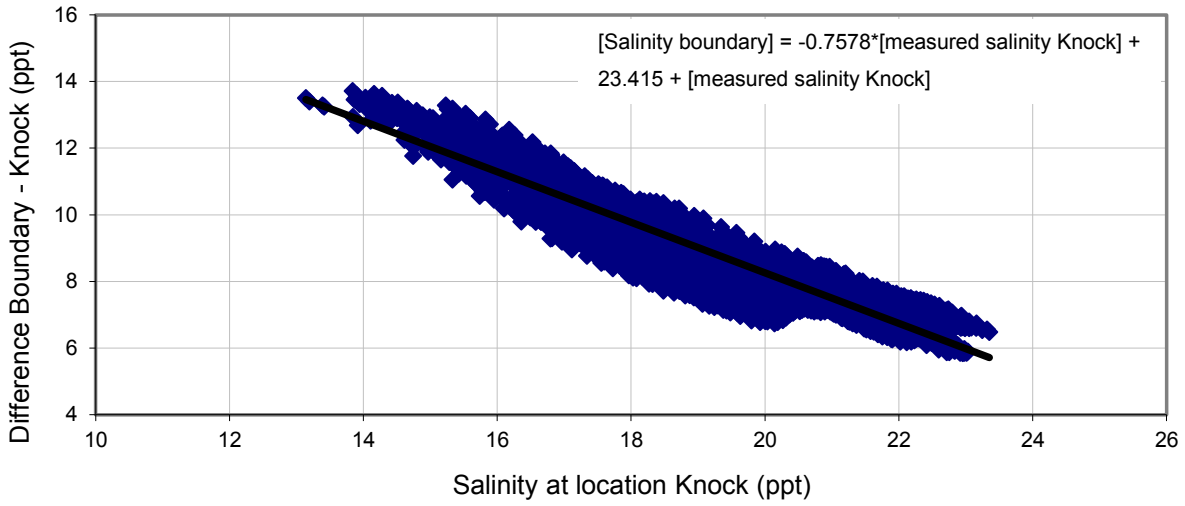

Fig. 3.12: Linear relation between the difference in salinity at the seaward boundary and Knock, based on a previous model, and the measured salinity at Knock (internal report T. Vijverberg).

Upstream boundary conditions

At the two upstream boundaries, Leer Leda near Leerort and weir Versen near Herbrum, measured discharge time series served as input for the 2005 models. The data of Leer Leda has a resolution of 15 minutes (Fig. 3.13a), at weir Versen daily discharge data is used (Fig. 3.13b). The discharge at weir Versen is 2-5 times higher than at Leer Leda. No discharge data was available for the historical situations, so the 2005 discharge data was also used as input in all model conditions. Salinity is set to zero near the upstream boundaries.

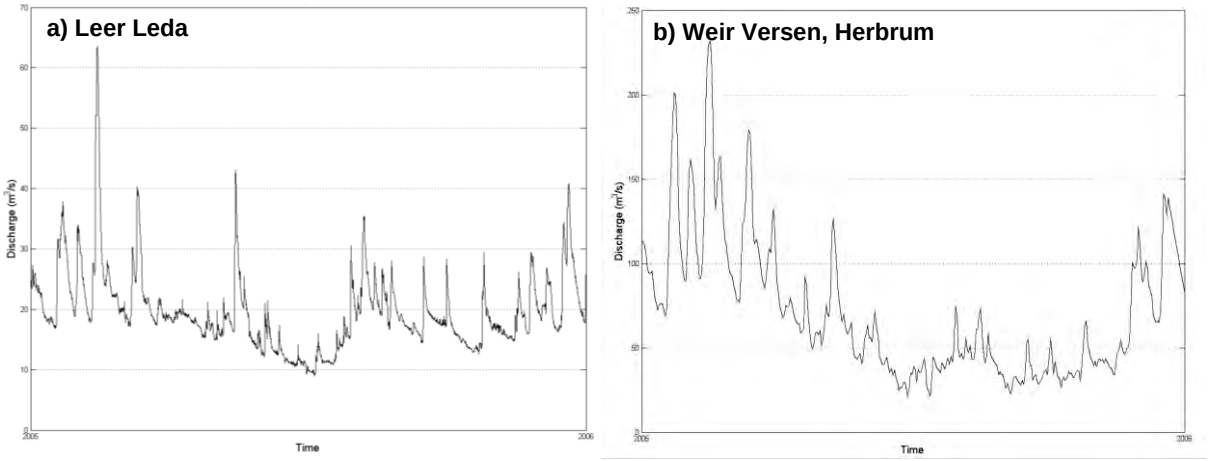

Fig. 3.13: Upstream boundary discharge time series (m^3/s) at (a) Leer Leda, resolution is 15 minutes, and (b) weir Versen, daily discharge. Data from the German Niedersächsischer Landesbetrieb für Wasserwirtschaft, Küsten- und Naturschutz.

3.1.6. Model parameters

The 2005 model set-up includes various physical and numerical parameters. These parameters are summarized in Table 3.2 and are also used for the 1985, 1965 and 1945 model set-up. Only bottom roughness is varied between model runs (further described in section 3.2).

Table 3.2: Physical and numerical parameters in the initial 2005 model set-up of the 2D and 3D version. These parameters are also used in the 1985, 1965 and 1945 model conditions.

General		
2D / 3D	Latitude	53.2° N
2D / 3D	Water density	1020 kg/m³
2D / 3D	Water temperature	15°C
2D / 3D	Gravitational acceleration	9.81 m/s²
2D / 3D	Horizontal eddy viscosity	1 m^2/s
2D	Vertical eddy diffusivity	10 m^2/s
3D	Vertical eddy diffusivity	1 m^2/s
Time		
2D	Time step	1 minute
3D	Time step	0.5 minutes
2D / 3D	Simulation start time	01 01 2005 00:00:00 (dd mm yyyy HH:MM:SS)
2D	Simulation stop time	01 01 2006 00:00:00
3D	Simulation stop time excl. sediment	01 09 2005 00:00:00
3D	Simulation stop time incl. sediment	01 04 2005 00:00:00
3D specific parameters		
3D	Number of σ-layers	10 with equidistance of 10%
3D	Model for 3D Turbulence	k-ε model
Sediment		
3D	Reference density for hindered settling	1600 kg/m^3
3D	Specific density of sediment	2600 kg/m^3
3D	Thatcher-Harleman time lag[1]	30 min.
3D	*Sediment fraction 1* Dry bed density Median grain size (D50) Initial sediment layer thickness	(sand) 1560 kg/m^3 300 μm 0.05 m
3D	*Sediment fraction 2* Dry bed density Settling velocity Boundary concentration Critical shear stress for erosion Erosion parameter	(mud) 500 kg/m^3 1 mm/s 0.05 kg/m^3 (Wadden Sea and Leda) 0.2 Pa 0.01 kg/m^2/s
3D	*Sediment fraction 3* Dry bed density Settling velocity Boundary concentration Critical shear stress for erosion Erosion parameter	(mud) 500 kg/m^3 0.125 mm/s 0.05 kg/m^3 (Wadden Sea and Leda) 0.2 Pa 0.01 kg/m^2/s

[1] This is a 'memory effect' at the open boundary. It solves the discontinuity that can occur at the turn of the tide if the outflow concentration differs from the inflow concentration (boundary condition). The transition/return time from the outflow value to the inflow value is described mathematically by the Thatcher-Harleman time lag. During this interval, the concentration will gradually return to the prescribed boundary condition. See the Delft3D-FLOW user manual (Deltares, 2012) for more details.

Although the 2D model does not include a vertical density gradient or estuarine circulation, salinity does create a longitudinal density gradient which affects the flow. The 3D model has 10 σ-layers, which allows for vertical exchange of flow energy and salinity between layers. For the 3D model runs including sediment, a global initial concentration for each sediment fraction was imposed at the Wadden Sea boundary and at Leer Leda. There is no initial sediment concentration in the Lower Ems and sediment-fluid interactions are turned off. For the clay fractions, typical values for non-consolidated / loosely consolidated clay are used.

3.2. Calibration and model runs

Calibrated bottom roughness for the 2005 model condition is shown in Fig. 3.14. Manning coefficient *n* is 0.01 s/m$^{1/3}$ uniform in the Lower Ems (upstream of Pogum), ~0.015 s/m$^{1/3}$ in the Emden Fahrwasser and Dollard and ~0.02 s/m$^{1/3}$ in the rest of the Ems-Dollard estuary. These values serve as a basis for the set-up of the historical conditions.

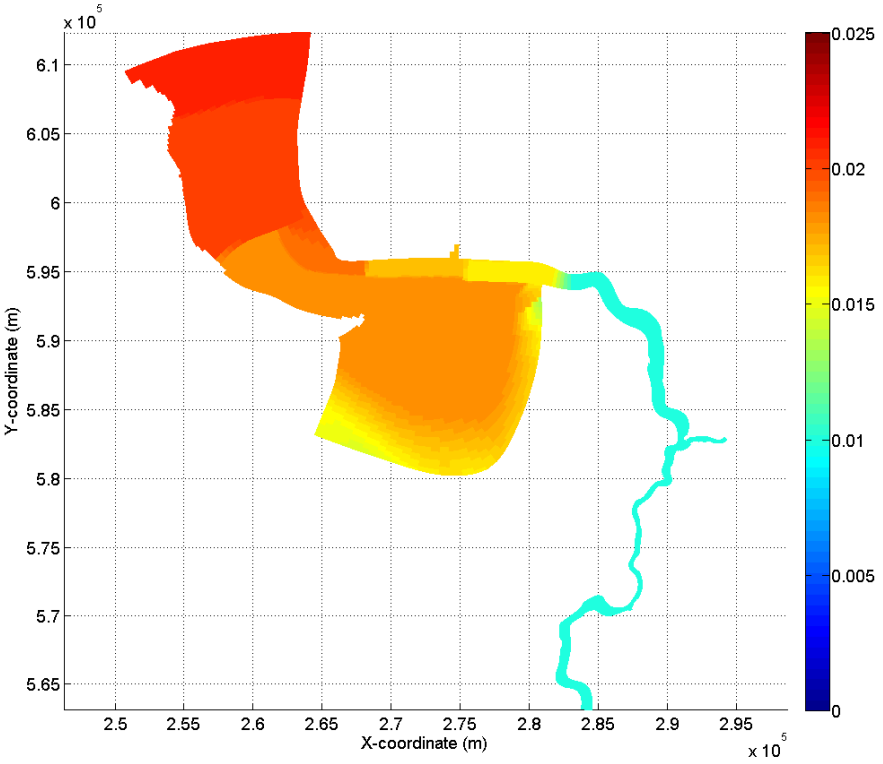

Fig. 3.14: Calibrated bottom roughness (Manning coefficient) in the 2005 model.

Calibration of the historical model situations consists of varying bottom roughness in the Lower Ems from the present-day Manning coefficient of 0.01 s/m$^{1/3}$ (very smooth bottom, typical for a muddy system) to a slightly rougher bottom of 0.015 and 0.02 s/m$^{1/3}$ (0.02 s/m$^{1/3}$ is typical for a sandy system). This calibration process is carried out in order to achieve

global agreement between the measured and modelled mean high/low water levels. For each time period (1985, 1965 and 1945) several 2D model runs with varying Manning coefficient are carried out. All runs include the reconstructed bathymetry, as described in paragraph 3.1.3. Also the Emssperrwerk (ESW) and Geise training wall are removed in several model runs. In this way, the contribution of bathymetry, bottom roughness and hydraulic structures to the changes in the tidal characteristics, as well as the relative importance –if any– of these variables can be determined. Table 3.3 gives an overview of all 2D model runs.

Table 3.3: Overview of 2D model runs, with reconstructed bathymetry, calibrated bottom roughness and presence/absence of hydraulic structures. Simulation period is one year.

	Bathymetry	*Manning coefficient (s/m$^{1/3}$)*	*Included hydraulic structures*		*Model run nr.*
			ESW	*Geise*	
2005 (reference situation)	2005 depth, measured	n=0.01 in Ems, ~0.015 in Emden Fahrwasser and ~0.02 in rest of Ems-Dollard estuary (see Fig. 3.14)	Yes	Yes	*1*
1985	1985 depth	n from 2005 model	Yes	Yes	*2*
	1985 depth	n=0.02 s/m$^{1/3}$ uniform	Yes	Yes	*3*
	1985 depth	n from 2005 model	No	Yes	*4*
1965	1965 depth	n from 2005 model	Yes	Yes	*5*
	1965 depth	n=0.015 s/m$^{1/3}$ in Lower Ems (upstream of Pogum), rest of estuary from 2005 model	Yes	Yes	*6*
	1965 depth	n=0.02 s/m$^{1/3}$ uniform	Yes	Yes	*7*
1945	1945 depth	n from 2005 model	Yes	Yes	*8*
	1945 depth	n=0.02 s/m$^{1/3}$ uniform	Yes	Yes	*9*
	1945 depth	n=0.02 s/m$^{1/3}$ uniform	No	Yes	*10*
	1945 depth	n=0.02 s/m$^{1/3}$ uniform	No	No	*11*

The most representative model conditions for each period are used for the 3D model runs, based on the outcomes of the 2D model runs. These model runs are summarized in Table 3.4 (next page). No additional calibration is performed for the 3D model. The Emssperrwerk and Geise training wall are not removed in any period. The simulation period was shortened from one year to a few months for practical reasons (computation time).

Table 3.4: Overview of 3D model runs, with reconstructed bathymetry, bottom roughness, sediment input at boundary and simulation period. All model runs include the Emssperrwerk and Geise traning wall.

	Bathymetry	*Manning coefficient*	*Sediment input at boundaries*	*Simulation period*
2005 (reference situation)	2005 depth, measured	n=0.01 in Ems, ~0.015 in Emden Fahrwasser and ~0.02 in rest of Ems-Dollard estuary (see Fig. 3.14)	No	01/01 – 01/04, 01/04 – 01/09
			Yes	01/01 – 01/04
1985	1985 depth	n from 2005 model	No	01/01 – 01/04, 01/04 – 01/09
			Yes	01/01 – 01/04
1965	1965 depth	n=0.015 s/m$^{1/3}$ in Lower Ems (upstream of Pogum), rest of estuary from 2005 model	No	01/01 – 01/04, 01/04 – 01/09
			Yes	01/01 – 01/04
1945	1945 depth	n=0.02 s/m$^{1/3}$ uniform	No	01/01 – 01/04, 01/04 – 01/09
			Yes	01/01 – 01/04

4 RESULTS

Sections 4.1 to 4.3 describe the 2D model results, section 4.4 deals with the 3D model runs without sediment and section 4.5 describes the results of the 3D model runs with a fixed sediment concentration at the boundaries (see Table 3.2, paragraph 3.1.6). All model results are processed with MATLAB.

4.1. Bottom roughness (2D)

Fig. 4.1, Fig. 4.2 and Fig. 4.3 (p. 50-51) show a comparison between measured and modelled MHW and MLW levels for three representative stations: Papenburg, Leerort and Emden. A complete comparison for all seven water level stations (Papenburg, Weener, Leerort, Terborg, Pogum, Emden and Knock) can be found in appendix B.

The model is able to reproduce the increase in MHW and decrease in MLW levels with only bathymetry and bottom roughness changes. In general, the largest change since 1945 is observed in Papenburg, at the upstream end of the Lower Ems: the tidal range has increased from ~1,5 m (1945), ~2 m (1965), ~2,5 m (1985), to ~3,5 m (2005). Leerort shows the same trend of increasing tidal range, but to a lesser degree. Water levels in Emden have remained fairly constant since 1945. This increase in tidal range in the Lower Ems agrees with observations (see paragraph 2.3.1).

The modelled 2005 water levels fit the data well. This is to be expected, since it represents the best calibrated model situation.

For 1985, the first model run with the reconstructed 1985 bathymetry and present-day Manning coefficient agrees best with the data. The second model run with a rougher bottom (n=0.02 uniform) causes MLW levels to be significantly underestimated at Papenburg (Fig. 4.1), Weener, Leerort (Fig. 4.2) and Terborg. The difference between these two model runs is much less at high water, because friction is non-linear and its effect is largest at low water. No significant difference due to bottom roughness was seen in Emden (Fig. 4.3) and Knock, since bottom roughness in the 2005 model was already calibrated to n≈0.018-0.02 $s/m^{1/3}$. Bottom roughness in Pogum was n≈0.015 $s/m^{1/3}$ in 2005 and a change to n=0.02 $s/m^{1/3}$ does not significantly influence water levels. The influence of the Emssperrwerk on the water level is negligible: comparison of the model runs with and without Emssperrwerk (*n* from 2005 model) does not show any difference in MHW or MLW levels. This is in agreement with Talke and de Swart (2006), who state that the storm surge barrier, when open, does not affect the tides. The 2D model runs suggest that bottom roughness has not changed since 1985. It is therefore likely that the present-day fluid mud layers, already occurred in 1985. The observed changes in water level can be solely attributed to the changes in bathymetry between 1985 and 2005: the deepening activities in the 1980's and 1990's have led to a depth change of approximately 2 m in the entire Lower Ems (see Table 3.1, paragraph 3.1.3), which has significantly influenced mean high and low water levels.

In the 1965 model run with only the reconstructed bathymetry, MHW and MLW levels for Papenburg (Fig. 4.1) and Leerort (Fig. 4.2) are overestimated. When bottom roughness is adjusted to a slightly rougher bottom, model results show better agreement with the data. In Papenburg, the model runs with n=0.02 $s/m^{1/3}$ (uniform) and n=0.015 $s/m^{1/3}$ (in the Ems) both agree reasonably well with the water level data. In Leerort, the model run with n=0.015 $s/m^{1/3}$ corresponds best with the observed low water levels. Overall, a Manning coefficient of 0.015 $s/m^{1/3}$ performs best for all stations. This suggests that the bottom has become smoother between 1965 and 1985. This period corresponds with the first observations of fluid mud in the Lower Ems. Duinker et al. (1985) describes the presence of a fluid mud layer at neap tide in 1976. The periodical occurrence of these fluid mud layers reduces the effective hydraulic roughness, hereby causing an increase in mean high and low water levels. The observed increase in tidal range between 1965 and 1985 cannot be explained based only on bathymetry changes. However, when roughness changes are included, the increase in MHW and MLW in the Lower can be explained, with the smoothening of the bottom between 1965

and 1985 as the most important factor. This is most likely due to the first appearance of fluid mud layers in that period.

For 1945, the model run with only the reconstructed bathymetry (and n=0.01 s/m$^{1/3}$) overestimates both MHW and MLW levels. The model run with increased bottom roughness (n=0.02 s/m$^{1/3}$) shows better agreement with the data. This suggests that the bottom was even rougher in 1945, compared to 1965, with a roughness similar to the present-day sandy bottom of the lower reaches of the Ems-Dollard estuary. In Papenburg (Fig. 4.1) and Leerort (Fig. 4.2) both bathymetry and bottom roughness changes are responsible for the observed changes in water level. This part of the river was deepened between 1945 and 1965. Downstream, in Knock, Emden (Fig. 4.3) and Pogum, no significant difference between model runs is seen and water levels have remained fairly constant between 1945 and 1965. The Geise training wall, which was built in the late 1950's, has had no influence on mean high and mean low water levels. The dam probably only causes energy losses when water is exchanged between the Emden Fahrwasser and the Dollard. It has no effect in the main ebb/flood flow direction.

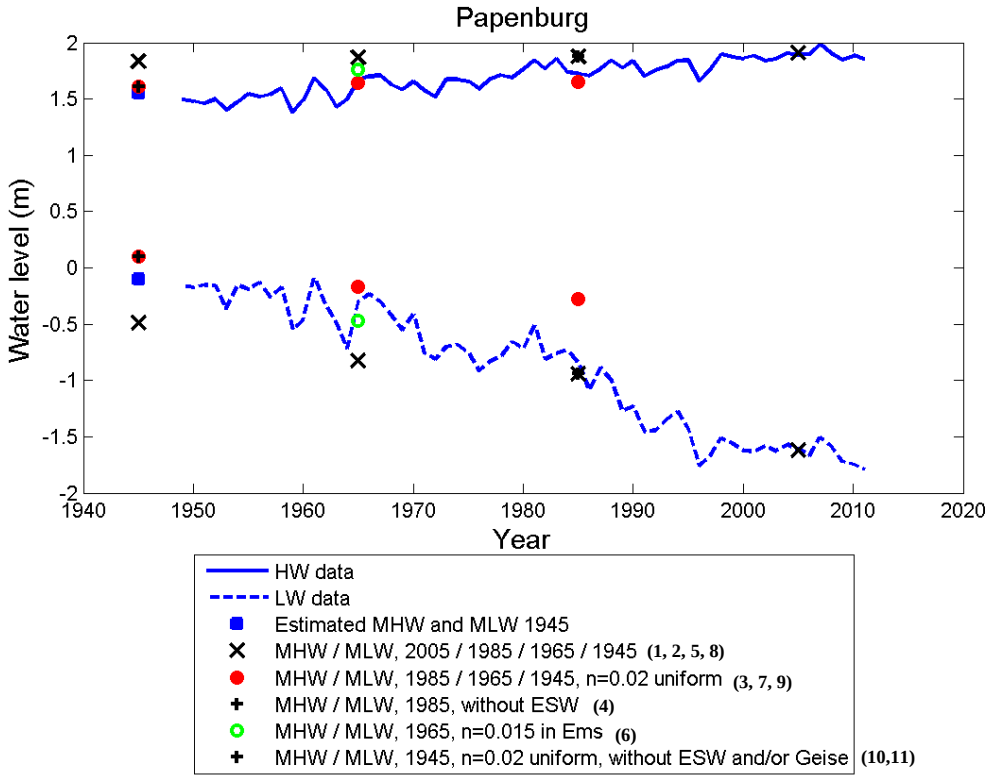

Fig. 4.1: Comparison of measured and modelled mean high / low water levels at Papenburg, model run nr. is indicated, see Table 3.3. Manning coefficient *n* in s/m$^{1/3}$. When no *n* is indicated, *n* from the 2005 model is used. *ESW* is Emssperrwerk and *Geise* is Geise training wall. 1945 estimated values are based on Herrling and Niemeyer (2008c). See Table 3.3 for an overview of model runs.

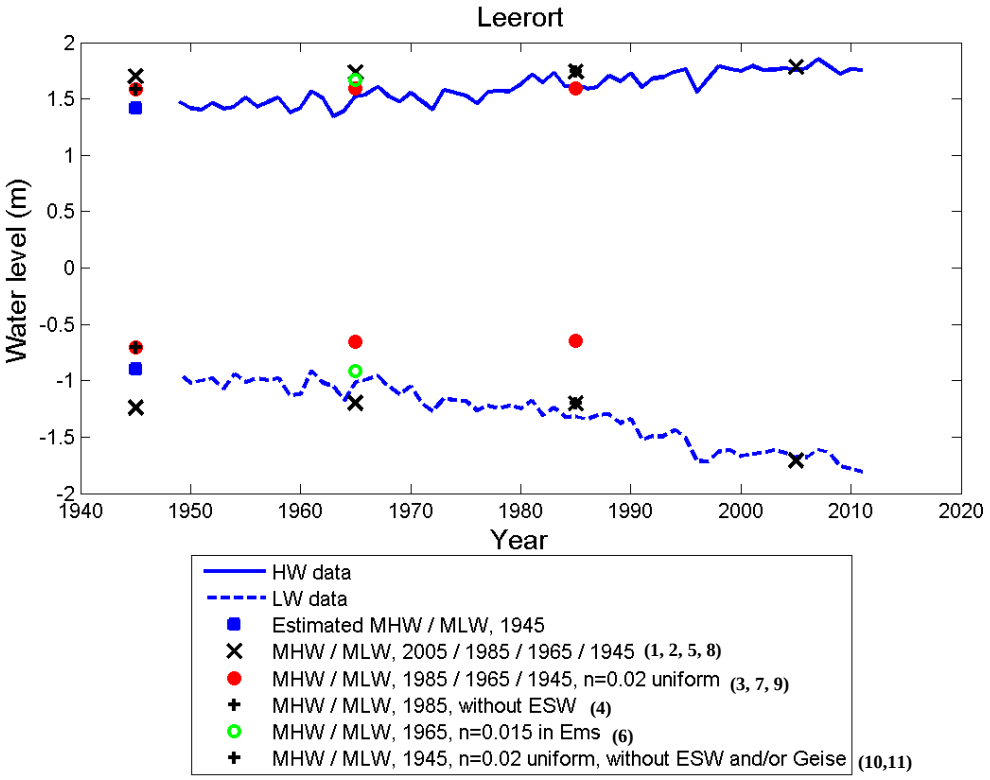

Fig. 4.2: Comparison of measured and modelled mean high / low water levels at Leerort.

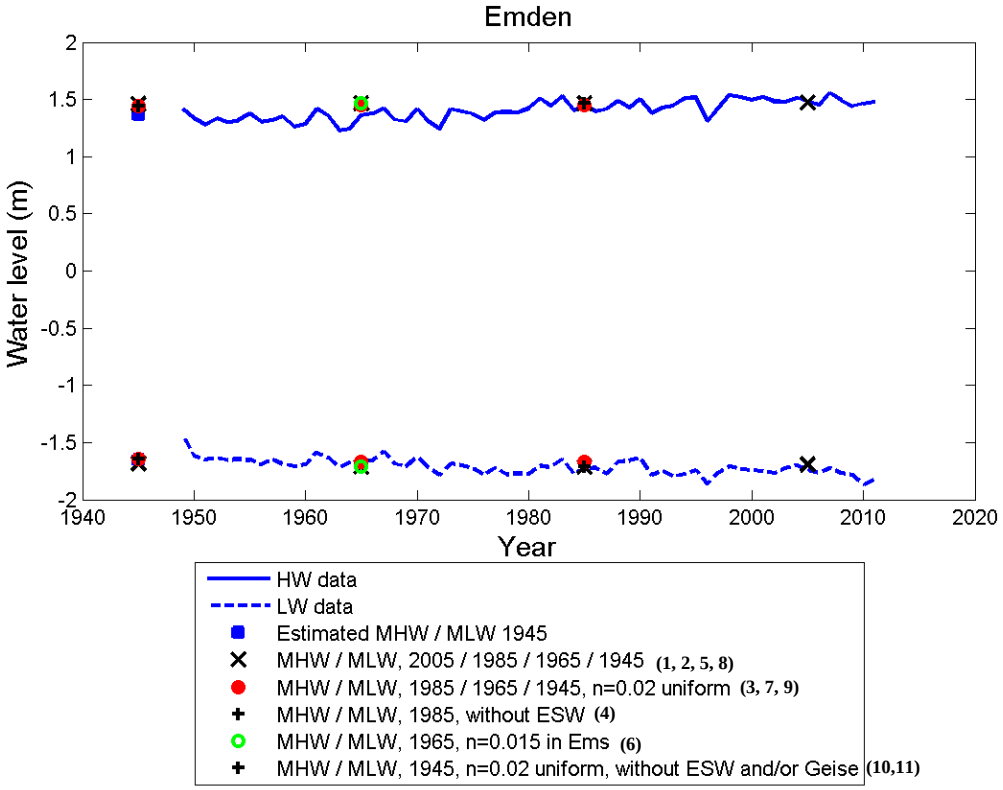

Fig. 4.3: Comparison of measured and modelled mean high / low water levels at Emden.

In short, the most representative model situation for each period are: 1945 bathymetry with n=0.02 uniform; 1965 bathymetry with n=0.015 in the Ems; 1985 bathymetry with n=0.01 in the Ems. The above comparison shows that the 2D model is able to reproduce the changes in tidal range by adjusting bathymetry and bottom roughness. It also shows that bottom roughness has indeed decreased since 1945. Between 1945 and 1965, both bathymetry and roughness changes contribute to the observed water level changes. Between 1965 and 1985, the smoothening of the bottom in the Lower Ems is largely responsible for the observed changes in water level. Most likely, the first periodic appearance of fluid mud is responsible for this. Between 1985 and 2005, extensive channel deepening in the entire Lower Ems has resulted in a significant increase in MHW and MLW levels. Bottom roughness has not changed in that period.

4.2. Water level and velocity (2D)

Comparison between modelled water levels and flow velocities shows an asymmetrical, flood-dominant system at the upstream end of the Lower Ems. Flood-dominance decreases both in downstream direction and in time. Appendix C lists the modelled water levels and corresponding flow velocities for all water level stations. Extra observation points are added in between stations.

From Papenburg to Terborg, the tide is asymmetrical and characterized by a shorter flood period with higher peak flow velocities. This is illustrated in Fig. 4.4 (p.53), showing one tidal cycle and corresponding velocities at an observation point between Papenburg and Weener. Flood duration increases in downstream direction. Near Emden (Fig. 4.5, p.53), the tide becomes almost symmetrical with equal ebb/flood duration, but slightly higher ebb velocities.

Differences in tidal asymmetry and peak velocities between model runs are primarily caused by the smoothening of the bottom. In the period 1945-2005, flood duration and flow velocities increase at the upstream river end. For example, flood duration increases with ~35 minutes in Papenburg (Fig. 4.4a). The system becomes less flood-dominant in time, as expected when bottom roughness decreases (also see paragraph 2.3.4): a reduction in hydraulic roughness enhances the propagation speed of the tidal trough. Overall, the smoothening of the bottom appears to be the most important factor for the reduced asymmetry and increased velocity between 1945 and 1985. The reduced bottom roughness also significantly shortens the time between peak ebb velocities and peak flow velocities upstream of Leerort in this period. Between 1985 and 2005, deepening causes a significant increase in ebb amplitude

due to the larger water depth and the non-linearity of the friction factor. The same trend is observed elsewhere in the Lower Ems. At Emden (Fig. 4.5), the vertical tide remains symmetrical between 1945 and 2005 and the decrease in bottom roughness only influences peak flow velocities. Ebb/flood dominance will be further discussed in paragraphs 4.3.3 and 4.3.4, based on the 2M2-M4 amplitude and velocity phase difference.

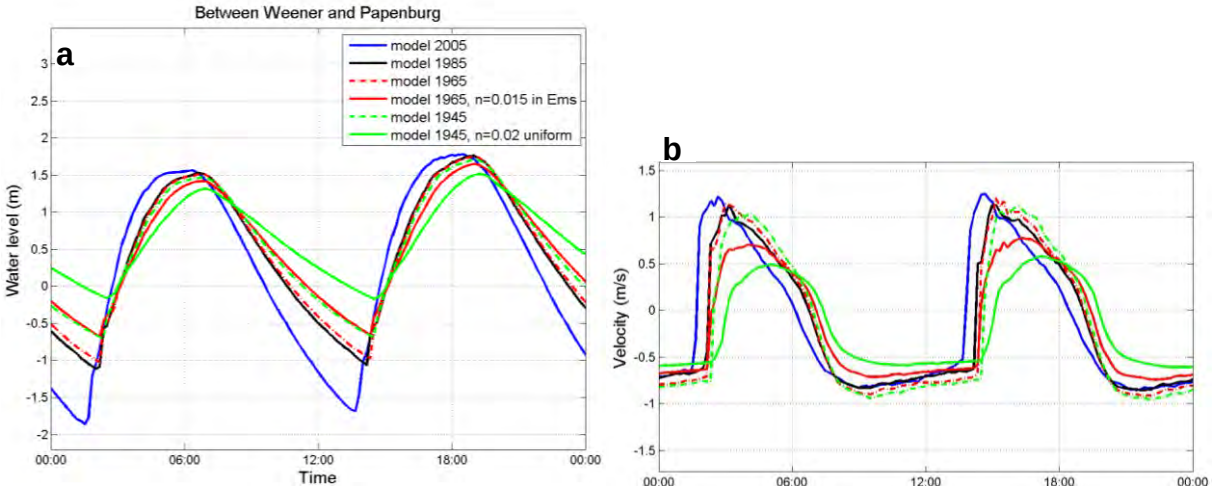

Fig. 4.4: (a) Water level and (b) flow velocity between Weener and Papenburg for different model situations: 2005, 1985 (n from 2005 model), 1965 (n from 2005 model and n=0.015 in Ems) and 1945 (n from 2005 model and n=0.02 uniform). Rising water level and positive velocities indicate flood.

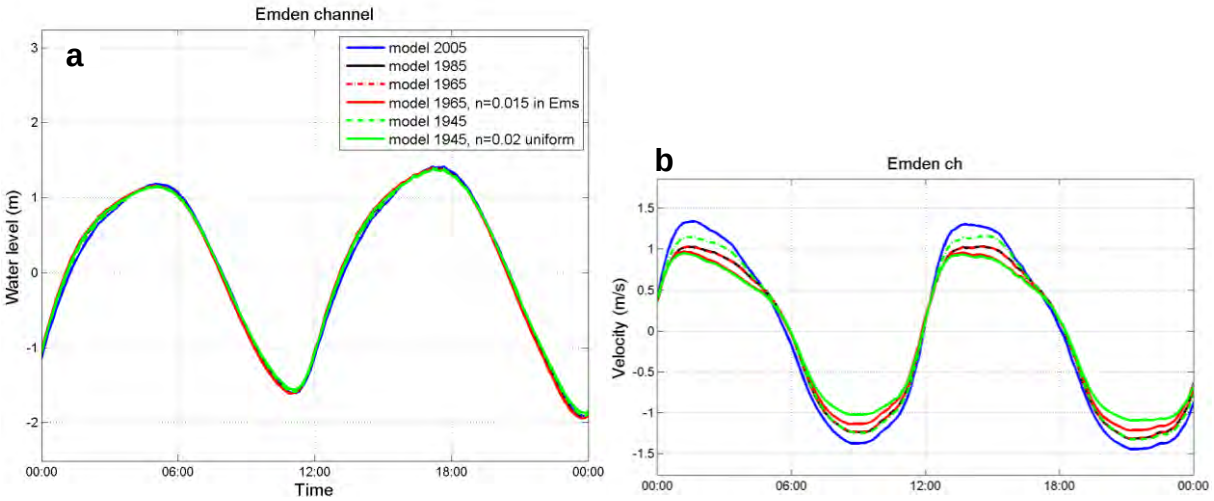

Fig. 4.5: (a) Water level and (b) flow velocity at Emden for different model situations: 2005, 1985 (n from 2005 model), 1965 (n from 2005 model and n=0.015 in Ems) and 1945 (n from 2005 model and n=0.02 uniform). Rising water level and positive velocities indicate flood.

The propagation speed of the tidal wave through the Ems river has increased between 1945 and 2005. Comparison between modelled and observed 2005 water levels shows that the modelled propagation speed of the tidal wave is somewhat underestimated for the most upstream stations. This is probably due to the limited river width at the upstream river end, hence model resolution becomes important. It is not expected to significantly influence

general model outcomes. Based on the modelled water level data, the time delay between high water in Pogum and high water in Papenburg is ~2 hours in the 1945 model situation. In comparison, this time delay is ~1 hour in 2005. The measured time delay between HW in Pogum and Papenburg is closer to 1:45 hours in 1945 (as measured in 1949) and ~30 minutes in 2005. The model results indicate that tidal propagation speed has increased over time.

4.3. M2 and M4 characteristics (2D)

This section will examine the effects of deepening and reduced bottom roughness on M2 and M4 amplitude (4.3.1), velocity (4.3.2), amplitude phase (4.3.3), velocity phase (4.3.4) and relative phase between horizontal and vertical tide (4.3.5).

4.3.1. Amplitude

Both M2 amplitude and M4 amplitude have increased since 1945 in the entire Lower Ems, in particular in the most upstream stations. Fig. 4.6 and Fig. 4.7 (p.55) show the changes in M2 amplitude. Values correspond well with measured 2005 and 1980 values as presented by Chernetsky et al. (2010). While M2 amplitude used to be maximum in Emden/Pogum, nowadays M2 amplitude increases up to Papenburg, where the amplitude has more than doubled since 1945. This trend of increasing tidal amplification at the upstream river end is already occurring from 1945 onwards, but only after 1985 does M2 amplitude in Papenburg exceed M2 amplitude in Emden, the tide is amplified all the way in the upstream direction. A comparison between model runs shows the same trend as described in paragraph 2.3.1. Between 1945 and 1965, bathymetry and especially roughness changes contribute to the observed M2 amplification. In the period 1965-1985, the smoothening of the bottom is the most important factor for M2 amplification: less energy is lost due to bottom friction and therefore the amplitude is less damped (also see paragraph 2.3.2). In that period, channel deepening in the Lower Ems was limited to the stretch between Leerort and Papenburg and only at those locations does the increase in water depth have any effect on M2 amplitude. In the period 1985-2005, the entire Lower Ems was deepened. This has caused a significant amplification of the tide as a direct response to the increased water depth and reduction of effective hydraulic roughness.

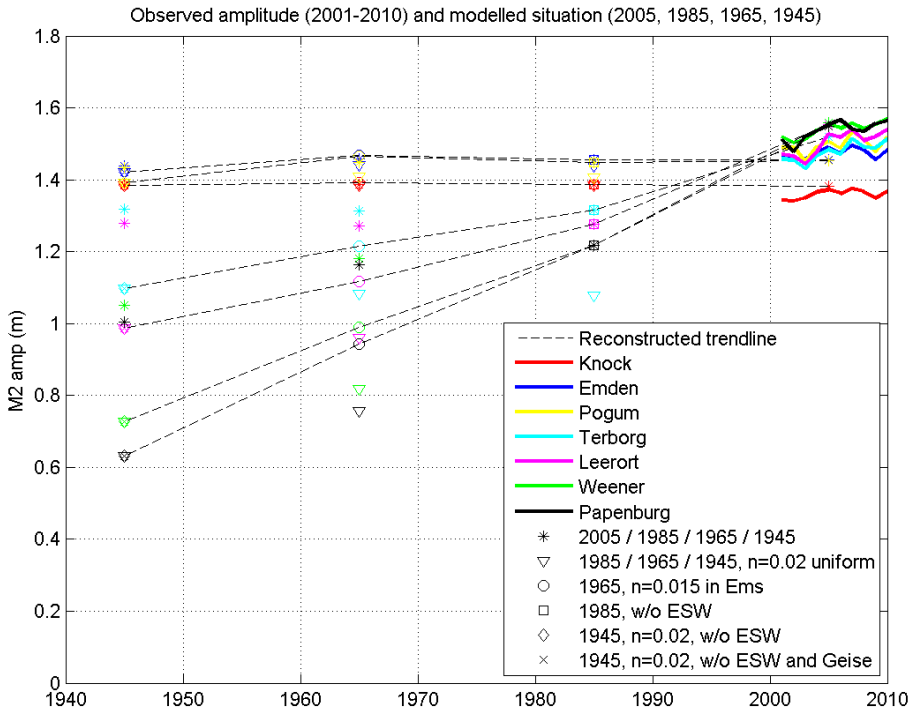

Fig. 4.6: Observed (2001-2010) and modelled (2005, 1985, 1965, 1945) M2 amplitude. Colours indicate different water level stations. Symbols indicate different model runs. The trend line connects the following model situations: 1945 with n=0.02 uniform; 1965 with n=0.015 in Ems; 1985 and 2005 with n=0.01 in Ems (=calibrated roughness in the 2005 model).

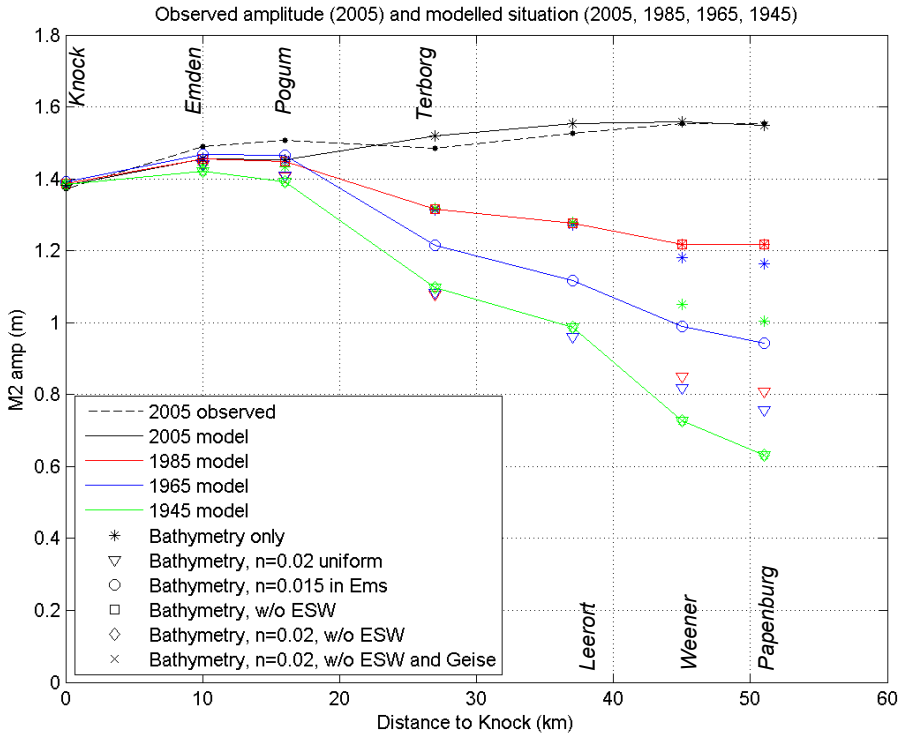

Fig. 4.7: Observed (2005) and modelled (2005, 1985, 1965, 1945) M2 amplitude, longitudinal.

The M4 amplitude is shown in Fig. 4.8 (chronological) and Fig. 4.9 (longitudinal). This shows the same trend of amplification between 1945 and 2005 as the M2 amplitude. However, model performance for the M4 component is less accurate. The amplitudes (and phases) of the higher harmonics upstream of Terborg are overestimated in the 2005 model and therefore most likely also in the historical model situations. The error margin is approximately 25% for the M4 amplitude. Various test simulations using a closed boundary at weir Versen did not improve model results (internal communication T. Vijverberg). Because of the error margin between modelled and observed M4 amplitude, only the modelled situations are considered when comparing model runs.

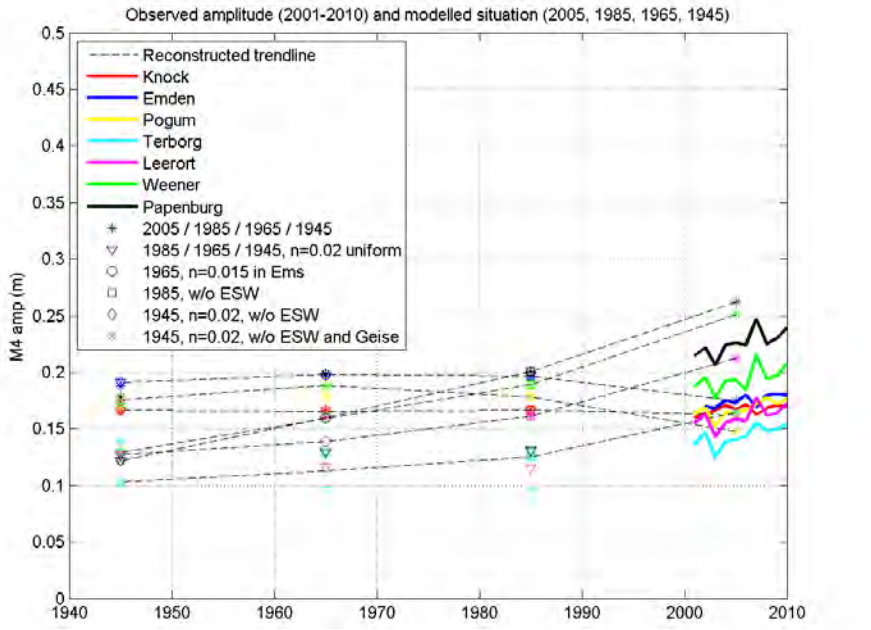

Fig. 4.8: Observed (2001-2010) and modelled (2005, 1985, 1965, 1945) M4 amplitude.

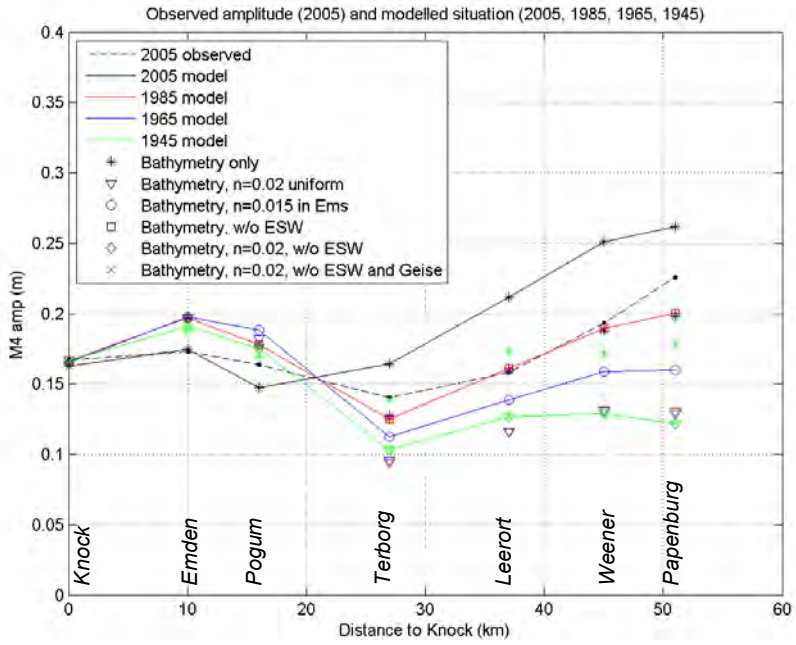

Fig. 4.9: Observed (2005) and modelled (2005, 1985, 1965, 1945) M4 amplitude, longitudinal.

The ratio between M4 and M2 amplitude is depicted in Fig. 4.10 (chronological) and Fig. 4.11 (longitudinal). This ratio is a direct measure of the degree of distortion (see paragraph 2.3.3): a larger M4:M2 amplitude ratio means more distortion. Because of the lack of intertidal storage area (flats, marshes) in the part of the Ems-Dollard estuary, the amplitude M4:M2 ratio is directly related to the water depth (or *a/h*, the ratio between offshore M2 amplitude and water depth). The distortion of the tidal wave is largest in Papenburg, where water depth is smallest. The ratio decreases in downstream direction. Between 1945 and 2005, M4:M2 ratio decreases slightly in the Emden Fahrwasser.

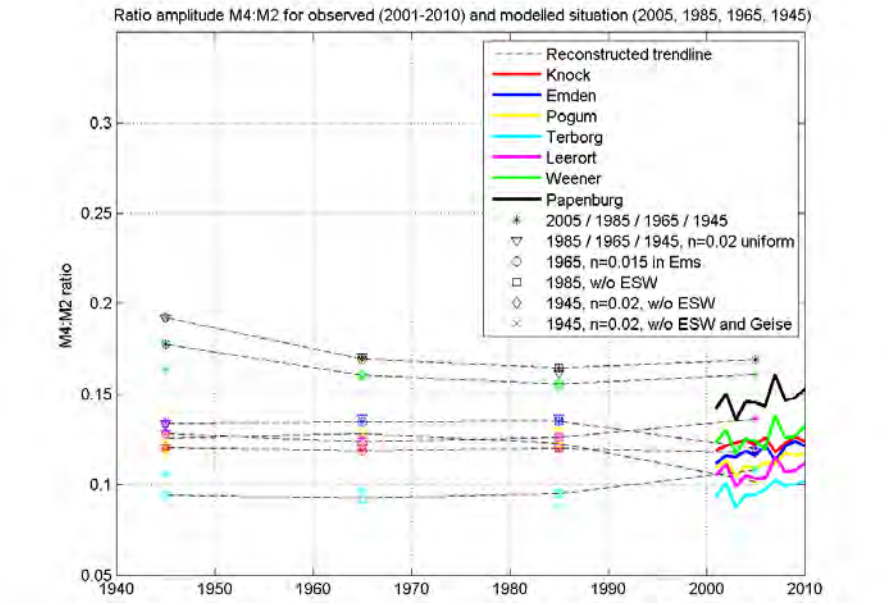

Fig. 4.10: M4:M2 amplitude ratio for observed (2001-2010) and modelled (2005, 1985, 1965, 1945) conditions.

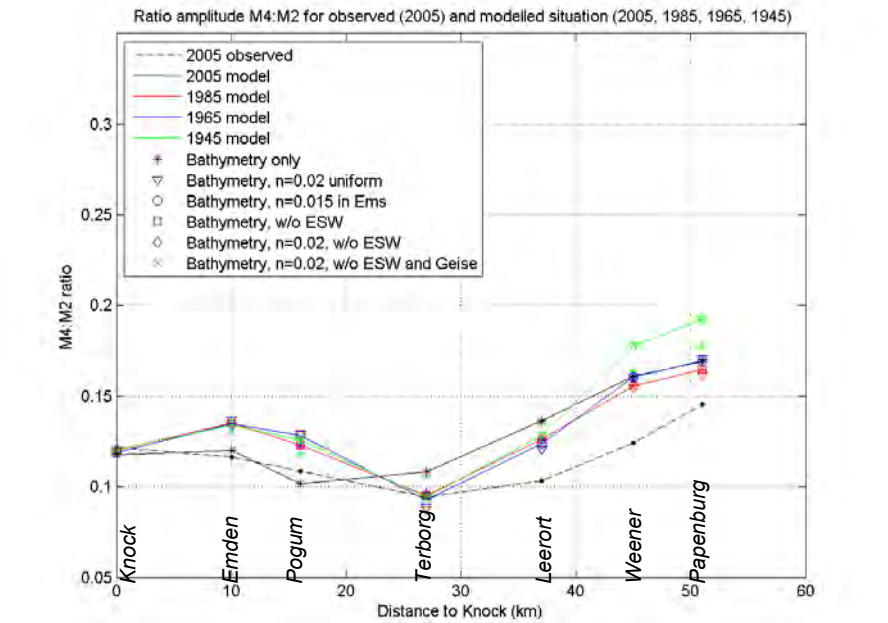

Fig. 4.11: M4:M2 amplitude ratio for observed (2005) and modelled (2005, 1985, 1965, 1945) conditions, longitudinal.

4.3.2. Velocity

Depth-averaged M2 and M4 velocities are shown in Fig. 4.12 and Fig. 4.13 (p.59) respectively. Since flow velocity is much more dependent on location than water level, all observation points are located within the main channel. Between 1945 and 1985, the behaviour of the M2 and M4 velocities does not change, except for an overall increase in magnitude of ~40%. Comparison between model runs shows that this amplification is primarily caused by the smoothening of the bottom, resulting in less energy loss from the flow. Interestingly, the behaviour of M2 and M4 velocities changes between 1985 and 2005: M2 velocity increases in Emden, but decreases in Pogum, Terborg and Leerort. Velocity in Terborg decreases most: ~20%.

The decrease in flow velocity between 1985 and 2005 between Pogum and Leerort has to be the result of channel deepening in the Lower Ems, since bottom roughness did not change in this period and no depth changes were made in the Emden Fahrwasser. It can be explained by the fact that peak discharge did not increase as much as water depth, therefore flow velocity decreases (assuming $Q = UA = Ubh$). Channel depth change in % is taken as an indication for the change in cross-sectional area. This is a valid assumption, since the channel was deepened over approximately the entire width (or made shallower when reconstructing the bathymetries, see paragraph 3.1.3). A rough estimation of the relative increase in depth h versus instantaneous peak discharge Q was made for Pogum and Terborg for the period 1985-2005. In Pogum, channel depth increases ~25%, peak flood discharge increases ~30% (Fig. 4.14a, p.60) and peak ebb discharge ~15% (Fig. 4.14b, p.60). This explains the model observations which show increasing flood velocities and decreasing ebb velocities in Pogum after 1985, illustrated in Fig. 4.15a (p.60). This difference in increase of ebb and flood discharge is also supported by previous research (Herrling and Niemeyer, 2008c), which shows that peak flood discharge between Pogum and Leerort increases more than peak ebb discharge between 1937 and 2005. It is unclear how this difference in discharge increase can be explained. In Terborg, water depth increases ~40% between 1985 and 2005, but peak ebb/flood discharge only increases ~25/35% and the larger cross-sectional area compared to the discharge results in flow reduction. This is illustrated in Fig. 4.15b (p.60).

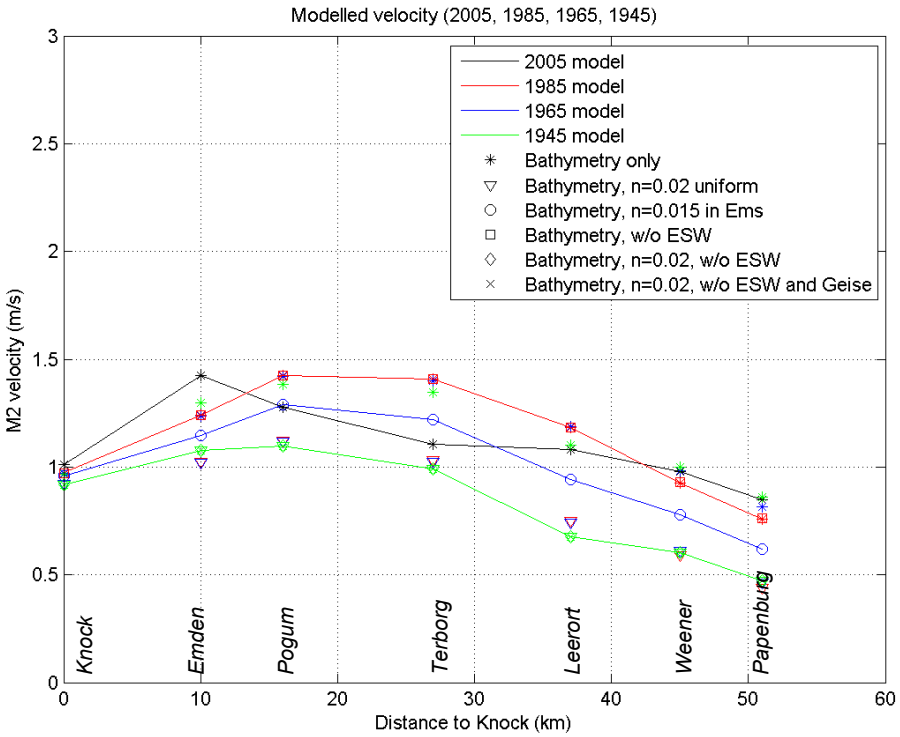

Fig. 4.12: Modelled M2 velocity (2005, 1985, 1965 and 1945 situation), longitudinal.

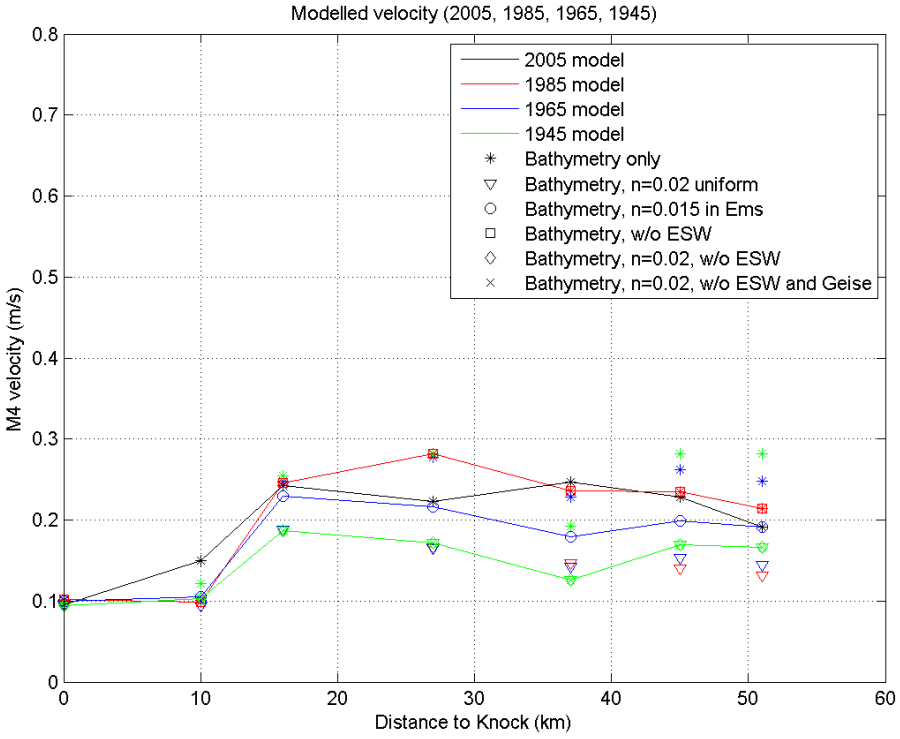

Fig. 4.13: Modelled M4 velocity (2005, 1985, 1965 and 1945 situation), longitudinal.

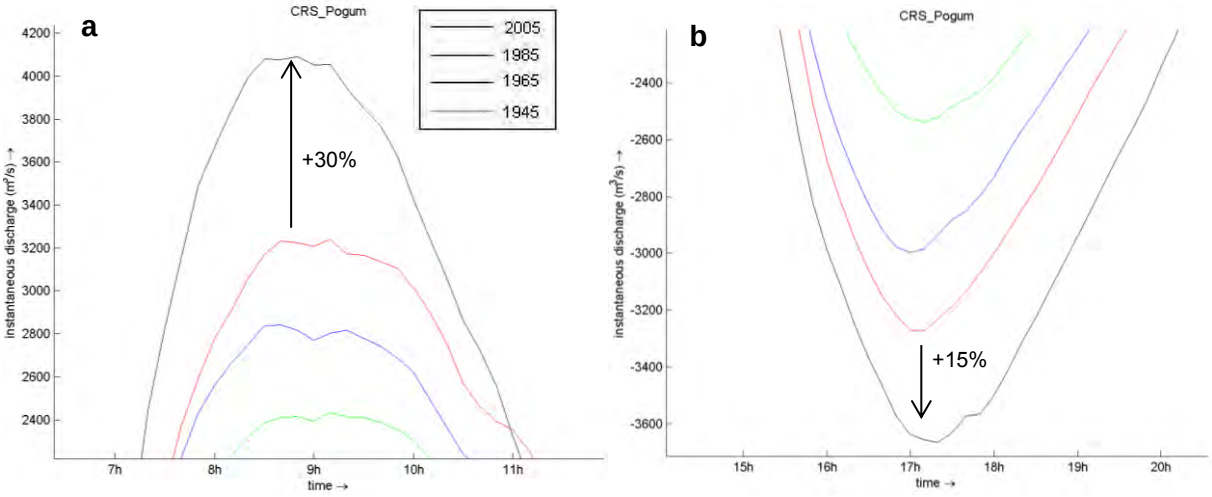

Fig. 4.14: Example of the changes in instantaneous peak discharge (m^3/s) between 1985 and 2005 in Pogum. (a) ~30% increase in flood discharge and (b) ~15% increase in ebb discharge.

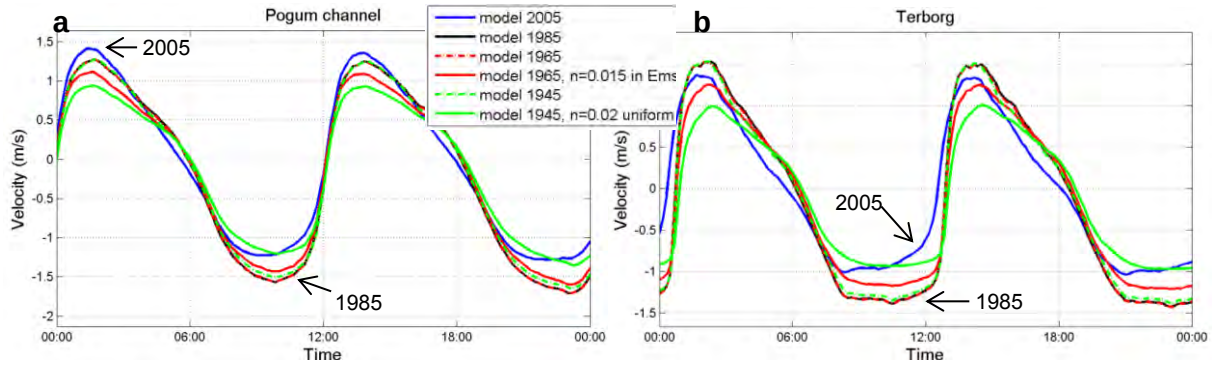

Fig. 4.15: Modelled flow velocity (2005, 1985, 1965 and 1945 situation) in (a) Pogum, showing the increase in flood velocities, but decrease in ebb velocities between 1985 and 2005 and (b) Terborg, showing the decrease in both ebb and flood velocities between 1985 and 2005. High water slack duration is longer at both stations.

In paragraph 2.5.1, the effect of flow velocity reduction in highly concentrated (cohesive) sediment suspensions was discussed. It was shown that a reduction of flow velocity will lead to a collapse of the turbulent flow field. Fluid mud layers were already occasionally observed between 1965 and 1985 (Duinker et al., 1985) and this is evidence that sediment concentration was already near-saturation. It is likely that a decrease in ebb/flood flow velocities in the period 1985-2005 has significantly decreased the saturation concentration C_s, since this depends on u^3 (see equation 10, paragraph 2.5.1). This means that the collapse of the turbulent flow field and fluid mud formation will occur at lower sediment concentrations than before flow reduction. The sediment carrying capacity of the flow will be significantly reduced. This could explain the permanent presence of fluid mud layers nowadays.

The ratio of M4:M2 velocity is shown in Fig. 4.16 (chronological) and Fig. 4.17 (longitudinal). The velocity M4:M2 ratio is about 2 times higher than the amplitude ratio. The ratio increases in the upstream direction where water depth decreases. The 1985 and 2005 ratio match the observations, as presented by Chernetsky et al. (2010). Contrary to model results of Chernetsky et al. (2010), no decrease in M4:M2 velocity ratio was found between 1985 and 2005 in the first 20 km from Knock. Furthermore, the ratio is found to decrease upstream of Leerort in this period, instead of increase. No significant change over time is found for the other stations.

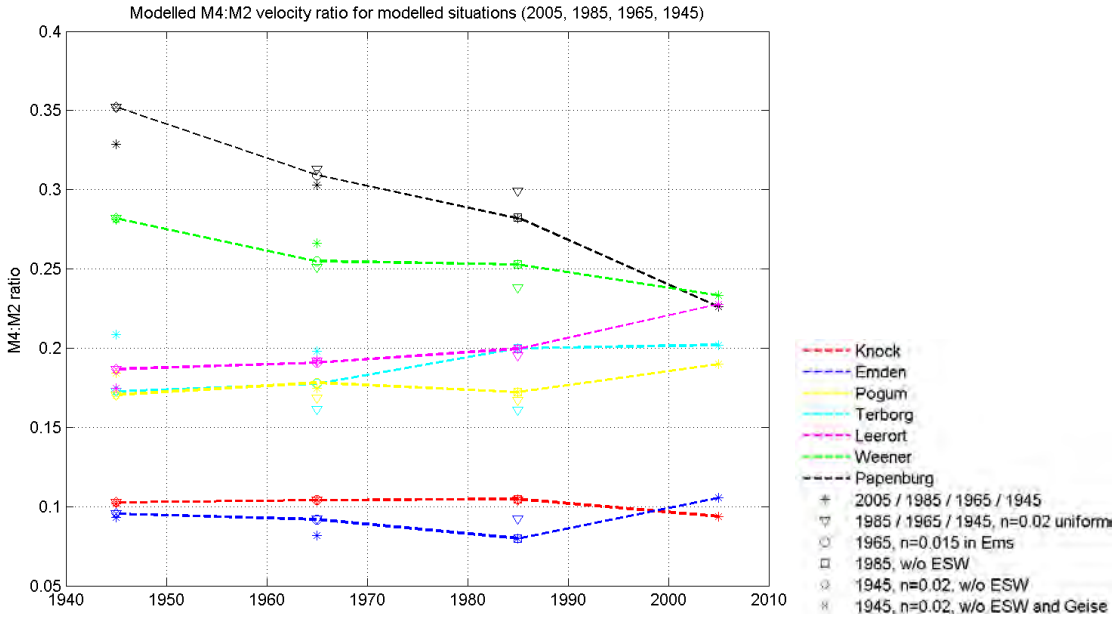

Fig. 4.16: Modelled M4:M2 velocity ratio (2005, 1985, 1965 and 1945 situation), chronological.

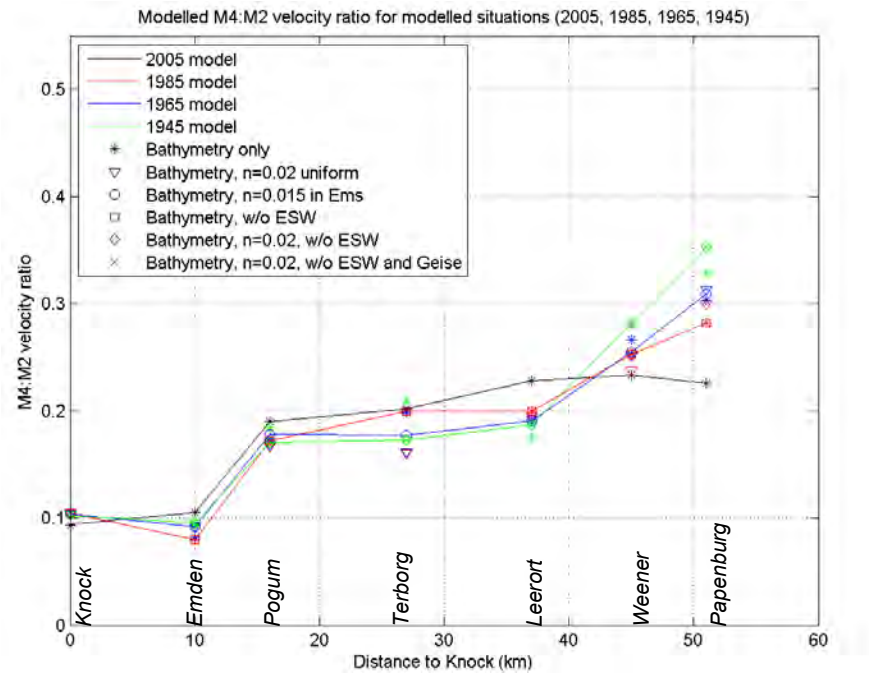

Fig. 4.17: Modelled M4:M2 velocity ratio (2005, 1985, 1965 and 1945 situation), longitudinal.

4.3.3. Amplitude phase

The changes in M2 amplitude phase (Fig. 4.18, chronological, and Fig. 4.19, longitudinal) and M4 amplitude phase (Fig. 4.20 and Fig. 4.21, p.63) are shown below. M2 and M4 phases in Knock, Emden and Pogum have remained constant in time, meaning that the characteristics of the vertical tidal (water level elevation/duration) have not changed. M2 and M4 phases have decreased for all other stations in the Lower Ems. For example, the relative difference between M2 phase in Knock and M2 phase in Papenburg has decreased from ~100° in 1945 to ~55° in the 2005 model. This indicates that nowadays the tidal wave propagates faster through the Lower Ems, as was already illustrated in section 4.2. However, as noted earlier, there is an error margin between the observed and modelled M2 and M4 phases. This error margin is approximately 10% in the entire Lower Ems.

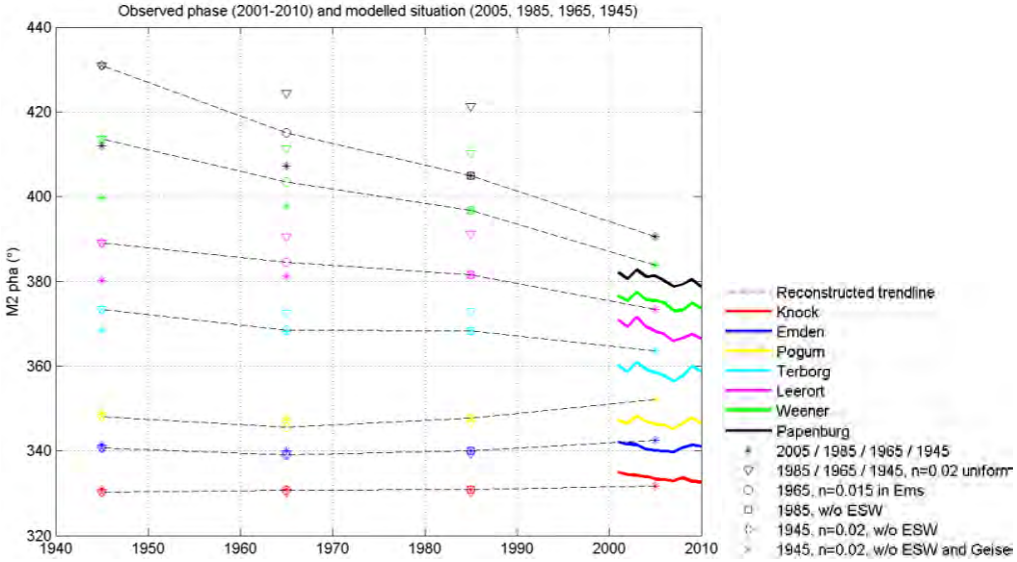

Fig. 4.18: Observed (2001-2010) and modelled (2005, 1985, 1965, 1945) M2 amplitude phase.

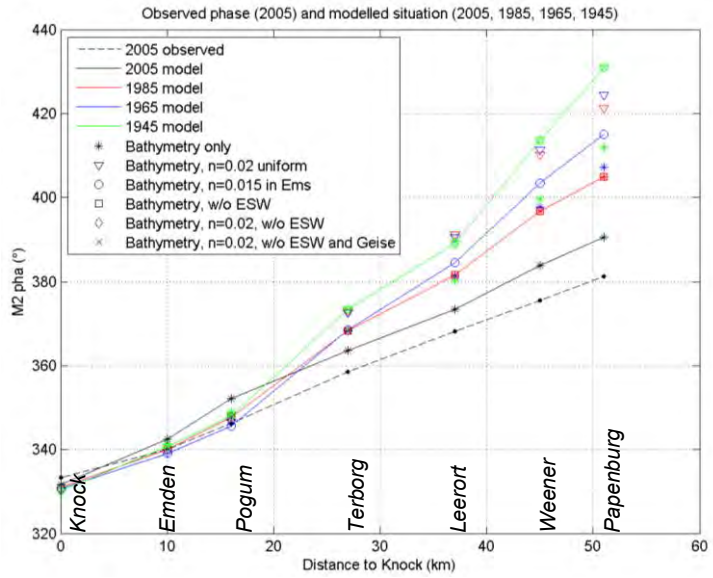

Fig. 4.19: Observed (2005) and modelled (2005, 1985, 1965, 1945) M2 amplitude phase, longitudinal.

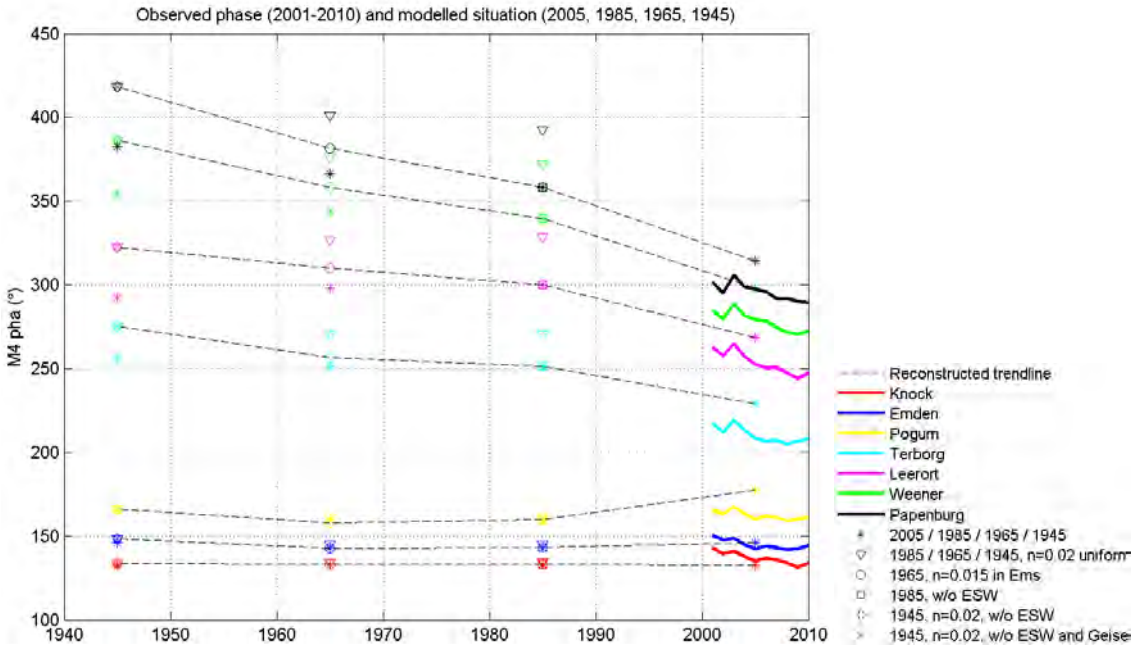

Fig. 4.20: Observed (2001-2010) and modelled (2005, 1985, 1965, 1945) M4 amplitude phase. 360°=0°.

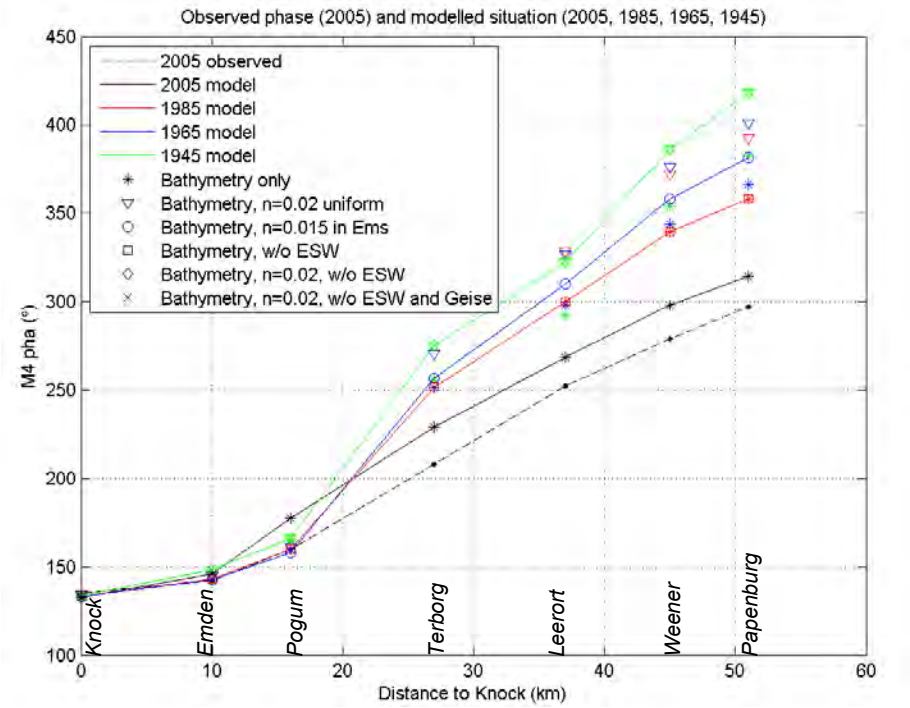

Fig. 4.21: Observed (2005) and modelled (2005, 1985, 1965, 1945) M4 amplitude phase, longitudinal. 360°=0°.

The amplitude phase difference between M2 and M4 (2M2-M4) is shown in Fig. 4.22 and Fig. 4.23 (p.65). The amplitude phase differences in Knock, Emden and Pogum have not changed since 1945. The amplitude phase difference of 170°-180° at these locations results in an almost symmetrical tide with equal ebb/flood duration. Assuming the idealized relationship between horizontal and vertical tide (Table 2.2 in paragraph 2.3.3), ebb/flood flow velocities should be equal and high water slack duration is longer. In that case, import of fine suspended sediment is expected to be maximum at these locations for the entire period. However, the symmetry in Knock, Emden and Pogum is only true for the duration of ebb/flood water levels. Ebb/flood flow velocities are not symmetrical at these locations. In fact, based on the velocity phase difference, Knock is ebb-dominant. Emden and Pogum change from being ebb-dominant to flood-dominant between 1985 and 2005, which could explain the increased import of fine sediment and the present-day high trapping efficiency of the Lower Ems. This will be further discussed in paragraph 4.3.4. 2M2-M4 amplitude phase difference increases for all other stations in the Lower Ems. For example, the phase difference at Terborg increases from 110° in 1945, to 140°/150° in 2005. This would indicate that the system becomes less flood-dominant over time and high water slack duration becomes an increasingly more important factor for the import of fine suspended sediment.

Comparison between model runs for stations in the Lower Ems shows that flood duration was already increasing in the period 1945-1985 as a result of a decrease in bottom roughness. Less bottom roughness reduces the frictional effects especially at low tide, causing the time delay between low water at the mouth and head to decrease, hence tidal asymmetry is reduced (also see paragraph 2.3.4). This trend was enhanced after 1985 as a direct response to channel deepening in the entire Lower Ems, which has caused an increase in water depth, leading to a reduction in effective bottom roughness.

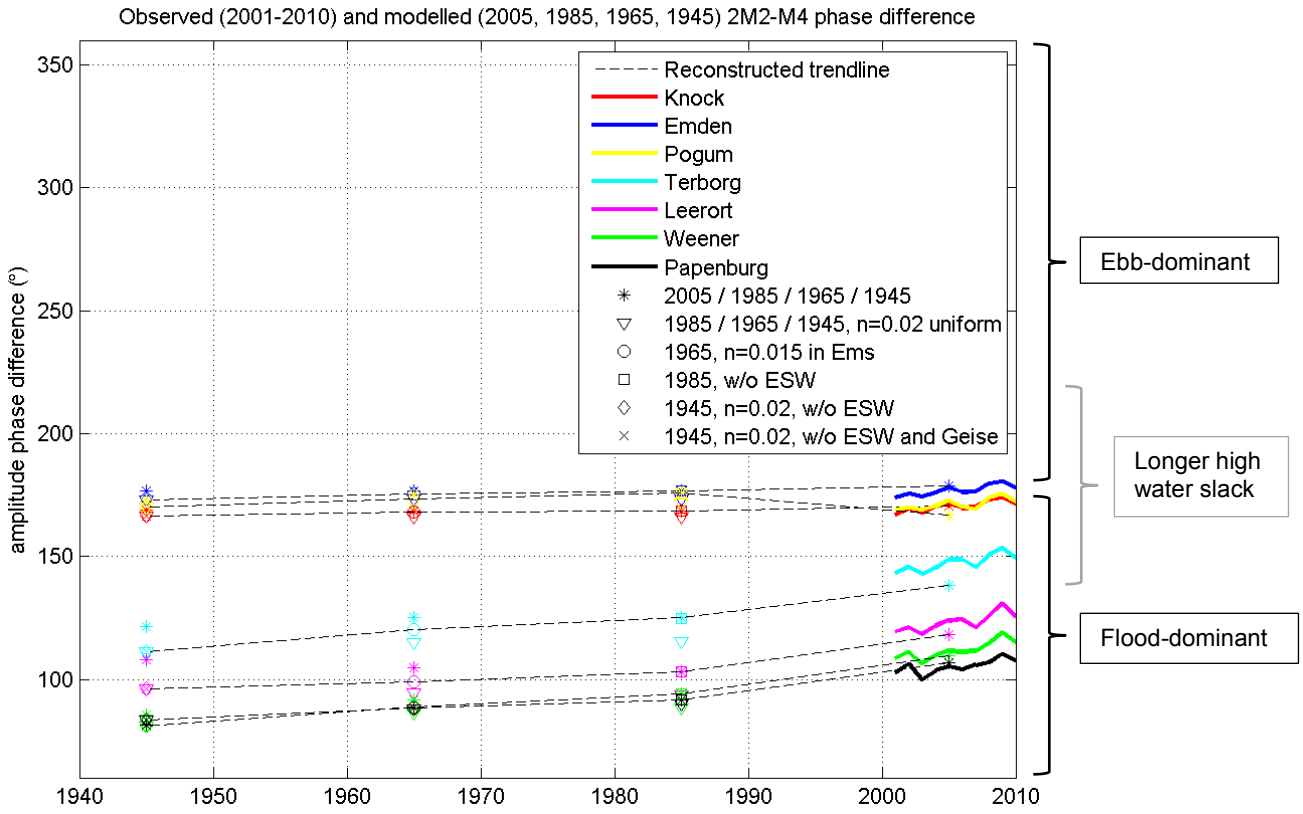

Fig. 4.22: Observed (2001-2010) and modelled (2005, 1985, 1965, 1945) amplitude phase difference, defined as 2M2-M4. Ebb/flood dominance is indicated, assuming the relationship between horizontal and vertical tide of Table 2.2.

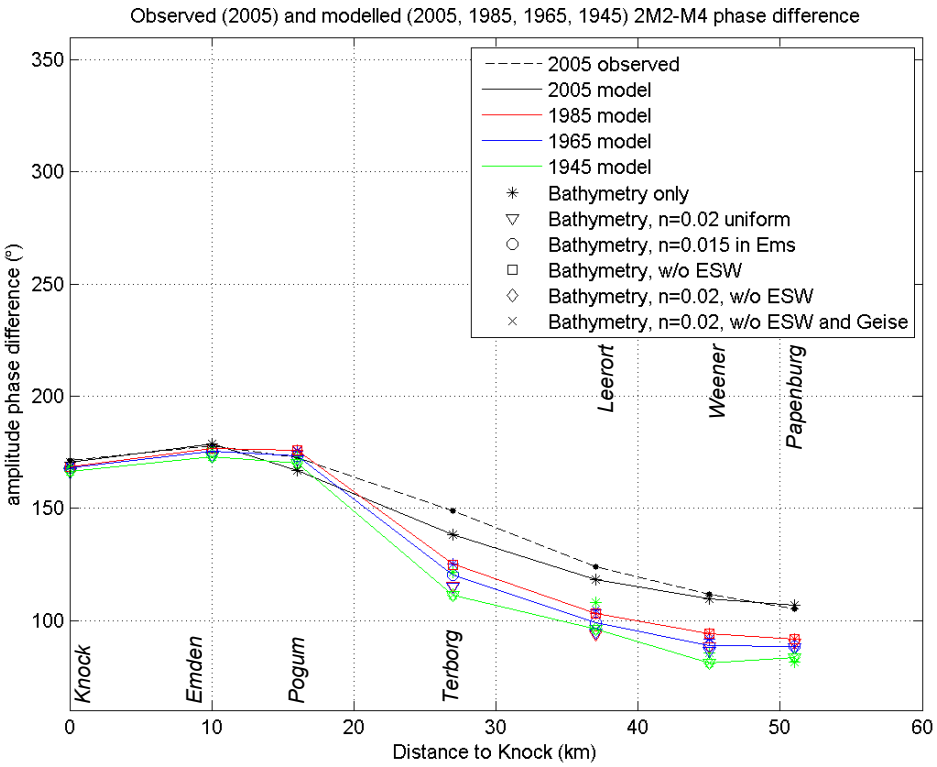

Fig. 4.23: Observed (2005) and modelled (2005, 1985, 1965, 1945) amplitude phase difference, longitudinal.

4.3.4. Velocity phase

The changes in M2 velocity phase (Fig. 4.24 and Fig. 4.25, p.67) and M4 velocity phase (Fig. 4.26 and Fig. 4.27, p.68) show a similar trend as the amplitude phase. The character of the M2 velocity phase shows similar behaviour, except for a general decrease over time in the Lower Ems, especially between 1985 and 2005. The character of the M4 velocity phase near the river mouth (Emden and Pogum) has also changed in this period. The interaction between M2 and M4 has resulted in the change from an ebb-dominant to a flood-dominant system near the entrance, as will be illustrated by the 2M2-M4 velocity phase difference.

Velocity phase at Knock remains constant, suggesting that ebb/flood-dominance has not changed over time at this location. Upstream of Terborg, M2 and M4 velocity phases show a similar trend: both decrease over time due to reduced bottom roughness (1945-1985) and bathymetry changes (1945-1985: only between Leerort and Papenburg, 1985-2005: in entire Lower Ems). No change in ebb/flood-dominance is expected here. The two most interesting stations are Emden and Pogum. In 1985, M2 and M4 velocity phase is larger in Pogum compared to Emden. In 2005, M2 and M4 velocity phases are similar at both locations and flow reversal is at the same time. This is most likely caused by the increase in water depth in the entire Lower Ems (but not Emden), resulting in a decrease of effective hydraulic roughness and hence a decrease in M2 velocity phase in Pogum, but not in Emden. This has consequences for the type of dominance at these two locations (2M2-M4 velocity phase difference), as will be discussed below.

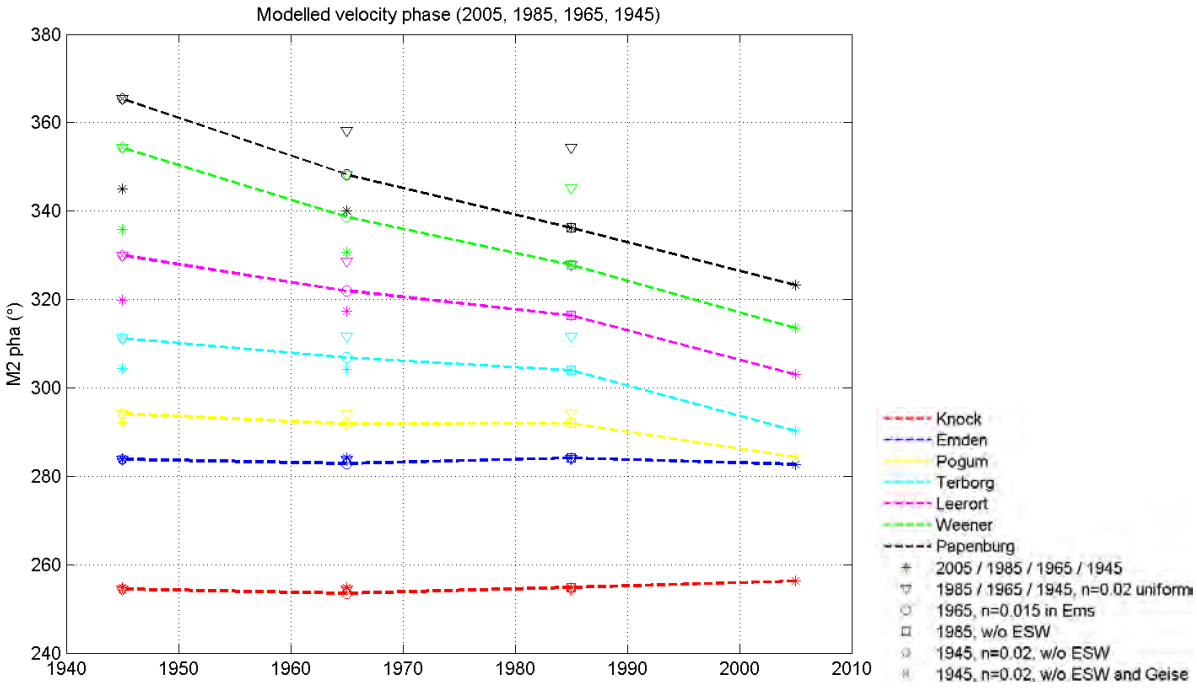

Fig. 4.24: Modelled M2 velocity phase (2005, 1985, 1965 and 1945 situation). 360°=0°.

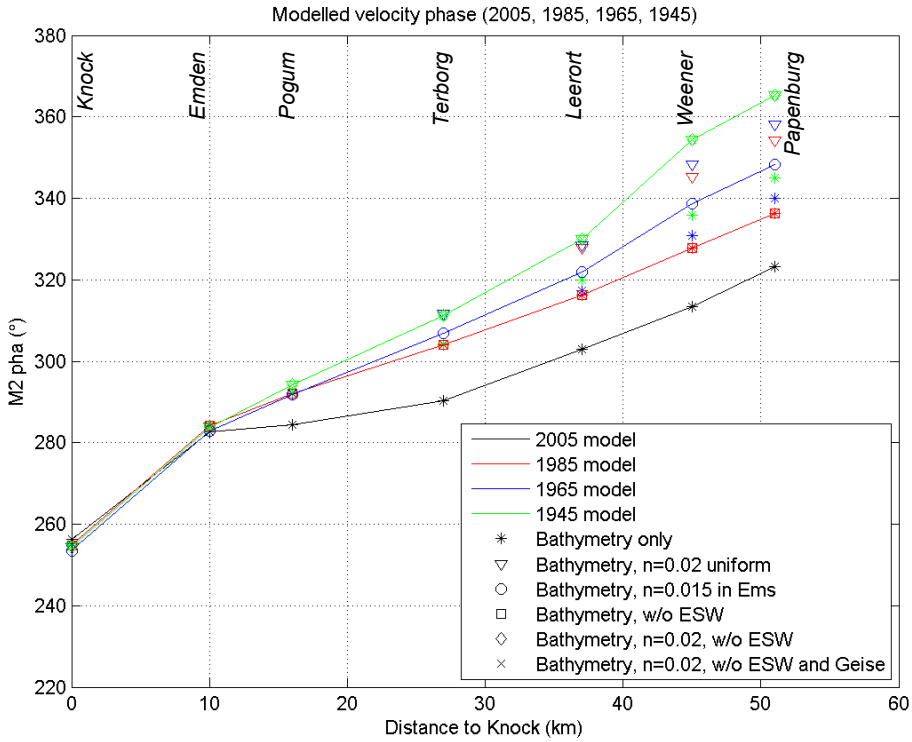

Fig. 4.25: Modelled M2 velocity phase (2005, 1985, 1965 and 1945 situation), longitudinal. 360°=0°.

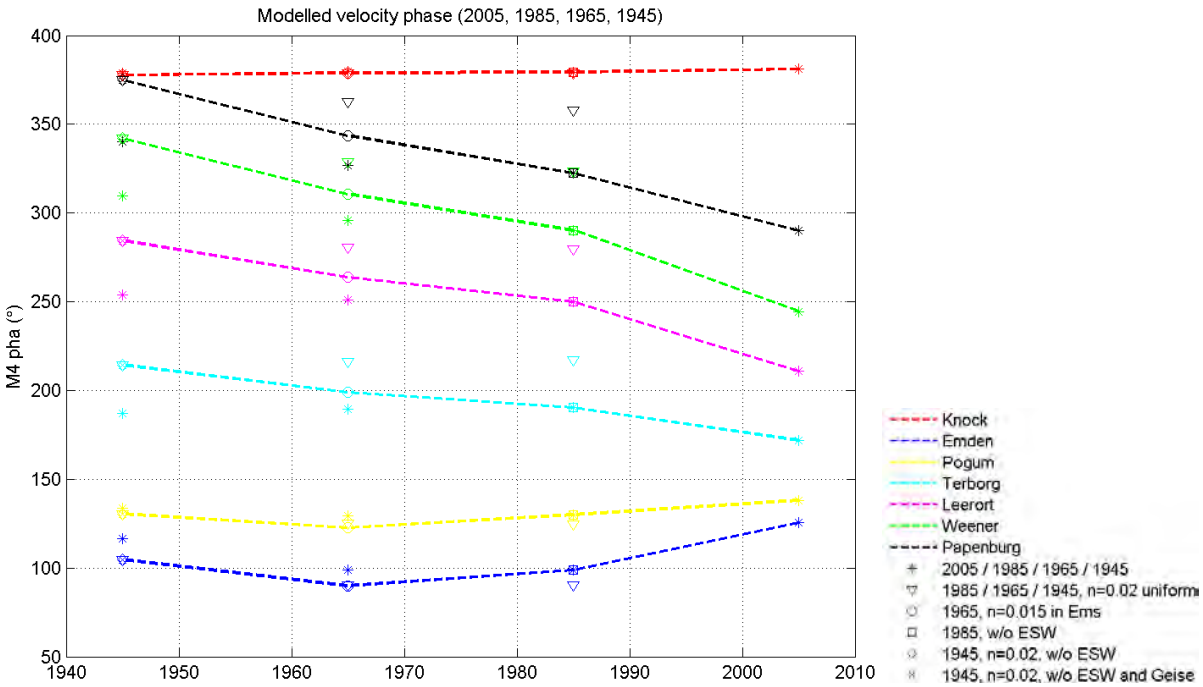

Fig. 4.26: Modelled M4 velocity phase (2005, 1985, 1965 and 1945 situation). 360°=0°.

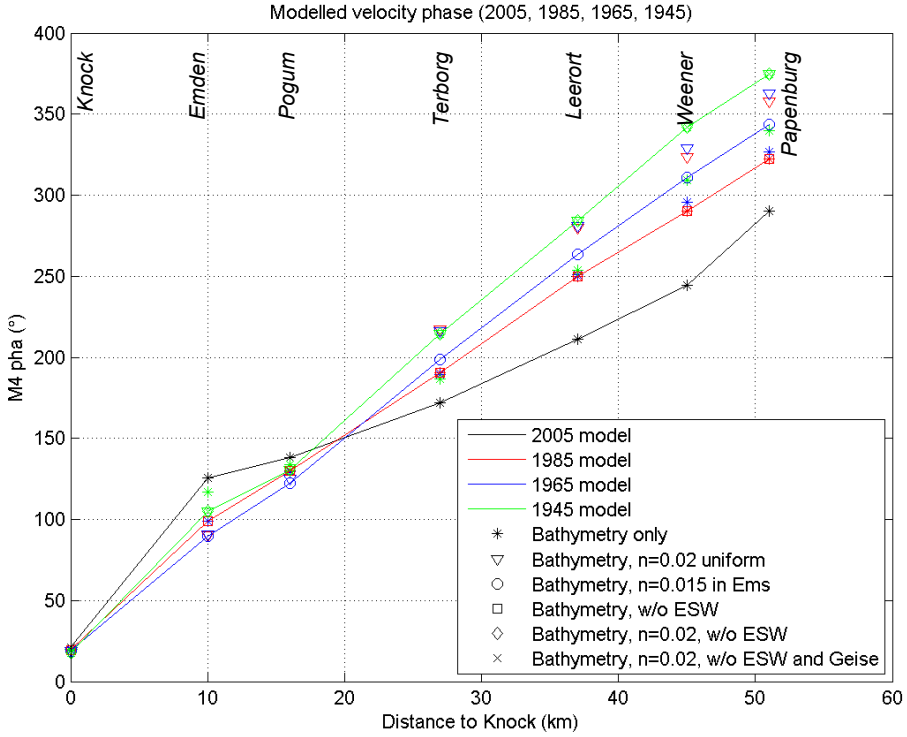

Fig. 4.27: Modelled M4 velocity phase (2005, 1985, 1965 and 1945 situation), longitudinal. 360°=0°.

While the amplitude phase difference gives a first indication of the ebb/flood dominance of the system, this is only true for an idealized relationship between water level and flow velocity phase. The type of dominance also depends on basin geometry, channel depth and intertidal storage. Ultimately, the velocity phase difference is the most important indication for the type of dominance, as it determines the direction of sediment transport and the morphological development of the estuary.

Fig. 4.28 and Fig. 4.29 (p.70) show the velocity phase difference between M2 and M4 (2M2-M4). As Friedrichs and Aubrey (1988) already noticed, the velocity phase difference in a highly flood-dominant system is within 20 degrees of a maximum asymmetric tide (0°). This is true for the upstream part of the Ems (Leerort, Weener and Papenburg), which are highly flood-dominant in the period 1945-1985. In the same period, the three most downstream stations (Knock, Emden and Pogum) are ebb-dominant, indicating that ebb flow velocities are higher, even though the tide is symmetrical with respect to water level (also see Fig. 4.22, paragraph 4.3.3). High water slack duration is longer at these three locations. Previous research by Chernetsky et al. (2010) also found 'a pronounced flood-dominance in the last 30 km of the estuary with a small ebb dominated region at the entrance' in 1980.

However, in 2005 the type of dominance near the river mouth has changed: Emden and Pogum shift from being ebb-dominant to flood-dominant between 1985 and 2005, as the result of changes in the M2 and M4 phases. This shift from higher ebb velocities to higher flood velocities in Pogum is also illustrated in Fig. 4.30 (p.71). Only Knock remains ebb-dominant in 2005, with longer high water slack. The Lower Ems is flood-dominant, but moves into the direction of a high water slack dominant system. The 2005 model results are validated by observations in 2005, as presented by Chernetsky et al. (2010). The modeled phase differences are within a 10-20° range of the observed values. They also show ebb-dominance in Knock (~125°) and increasing flood-dominance in the upstream direction.

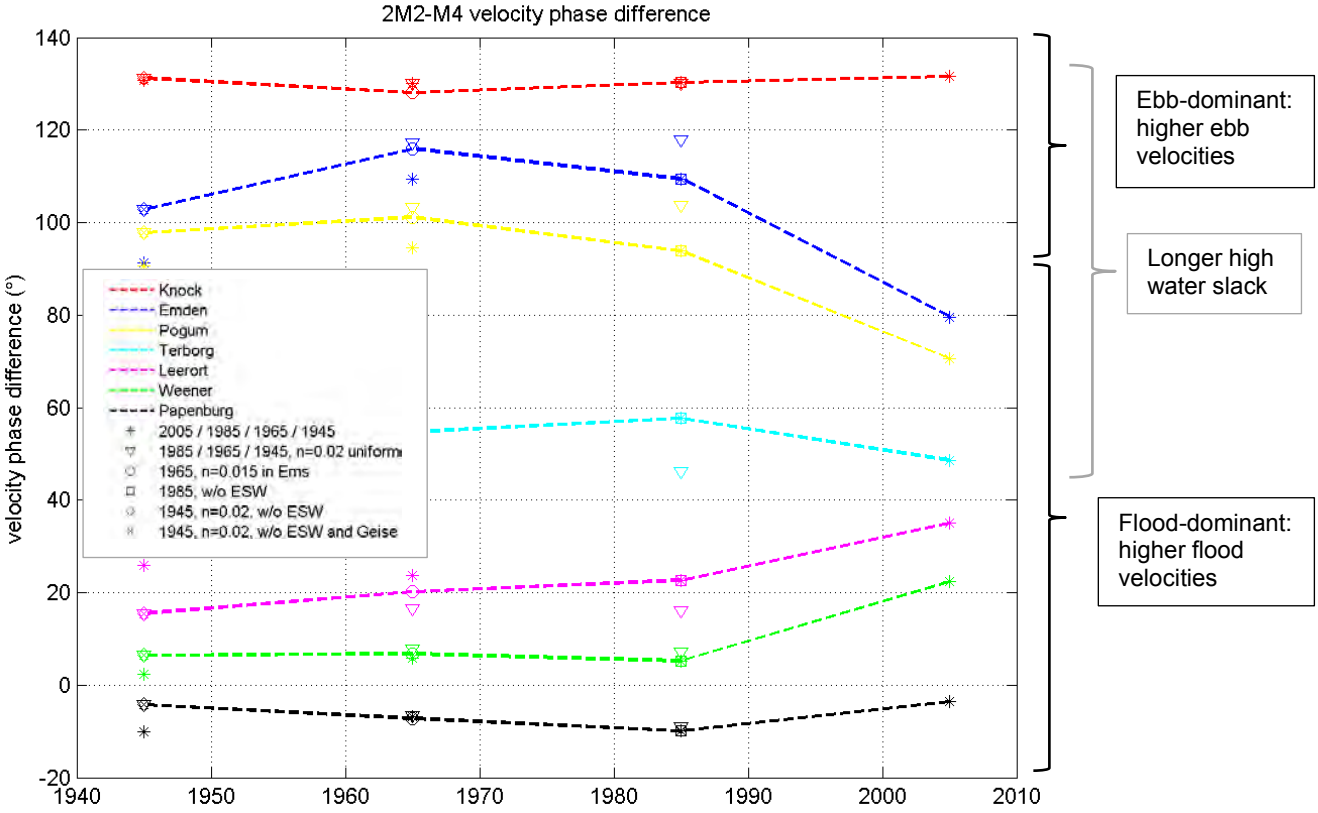

Fig. 4.28: Modelled velocity phase difference (2005, 1985, 1965 and 1945 situation), defined as 2M2-M4. 360°=0°. Ebb/flood dominance is indicated.

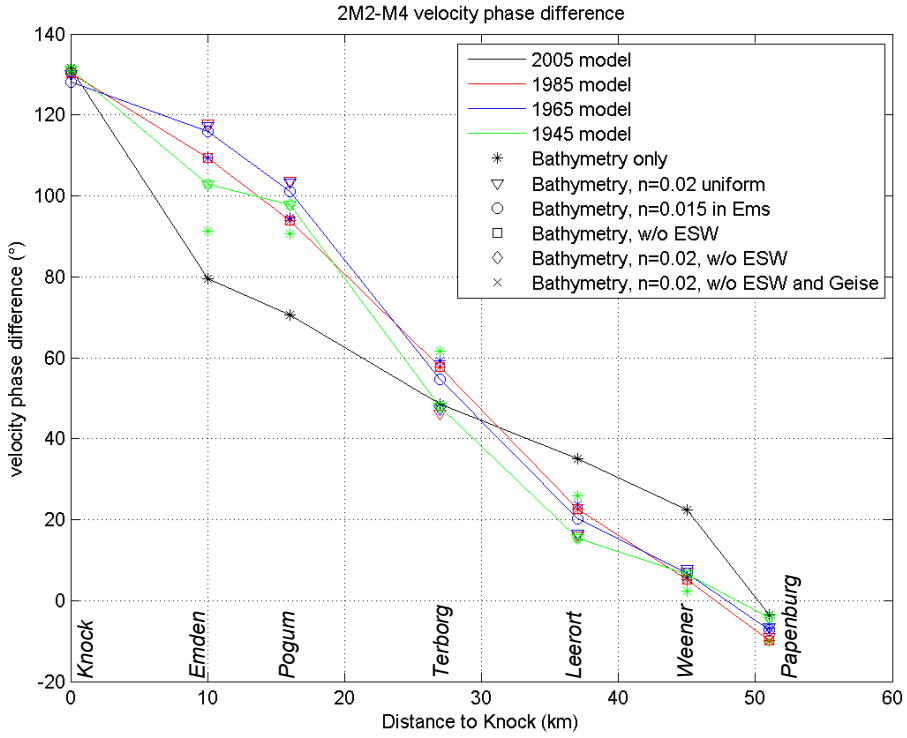

Fig. 4.29: Modelled velocity phase difference (2005, 1985, 1965 and 1945 situation), longitudinal.

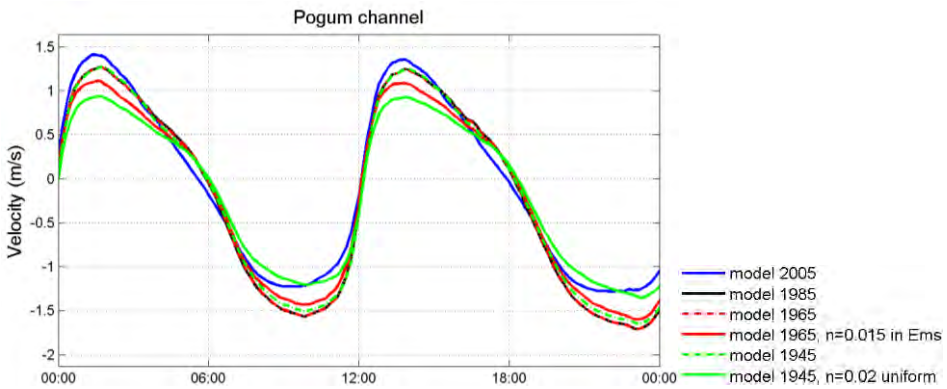

Fig. 4.30: Modelled flow velocity (2005, 1985, 1965 and 1945 situation) in Pogum, showing the change from higher ebb velocities in the period 1945-1985 to higher flood velocities in 2005. High water slack duration remains longer.

This change from ebb- to flood-dominance near the river mouth is expected to have serious consequences for sediment import. It is possible that this is the cause of the present-day high sediment concentrations in the Lower Ems. High water slack duration near the mouth (Emden and Pogum) remains longer for the entire period 1945-2005. This contributes to landward sediment transport, as more fine sediment will settle after flood. Before 1985, the higher ebb velocities in Emden and Pogum stir up more fine sediment into the water column and transport it seaward, therefore balancing the sediment import. But after 1985, flood velocities increase and ebb velocities decrease, resulting in more effective entrainment, vertical mixing and flocculation during flood and rapid settling during the longer high water slack (also see section 2.4). This ultimately results in net landward sediment transport and a high trapping efficiency of the Ems nowadays. Upstream, the flood-dominance leads to further landward sediment transport. Sediment availability is high due to a permanent fluid mud layer. Further research is needed to confirm this.

4.3.5. Relative phase difference H-U

The relative phase difference between vertical tide (H) and horizontal tide (U) is shown in Fig. 4.31 (M2) and Fig. 4.32 (M4). The relative phase difference determines if the tide behaves as a standing (H-U=90°) or progressive wave (H-U=0°) (also see paragraph 2.3.5). The relative phase difference increases between 1945 and 2005. This indicates that the system becomes closer to resonance. Both channel deepening, especially after 1985, and the smoothening of the bottom between 1945-1985, contribute to the shift in the direction of a standing wave pattern in the Lower Ems.

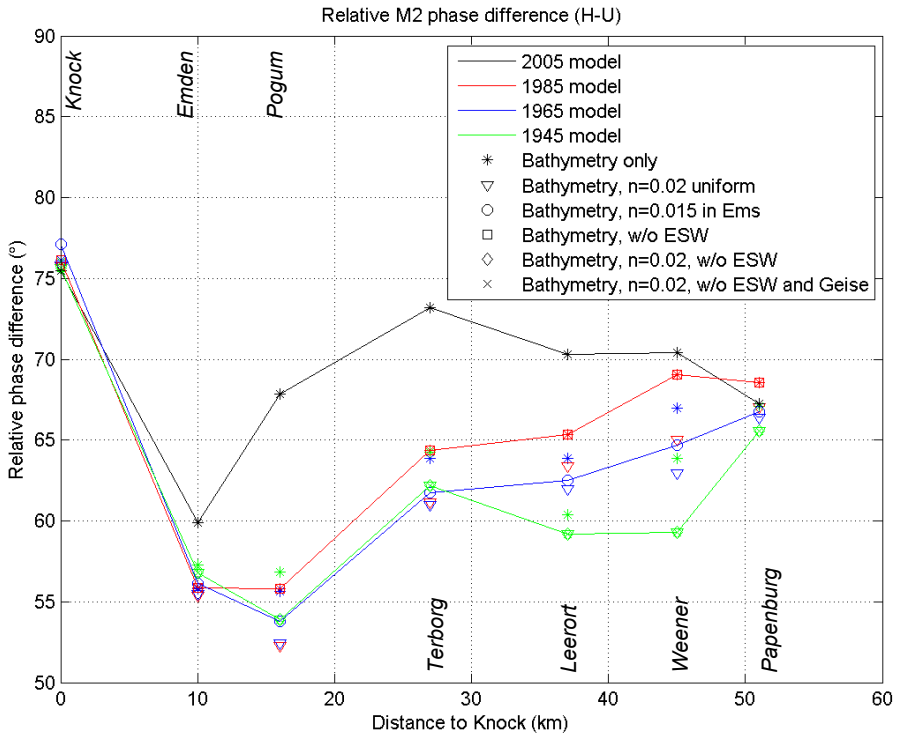

Fig. 4.31: Modelled relative M2 phase difference between vertical tide (water level) and horizontal tide (velocity) for the 2005, 1985, 1965 and 1945 model situation, longitudinal.

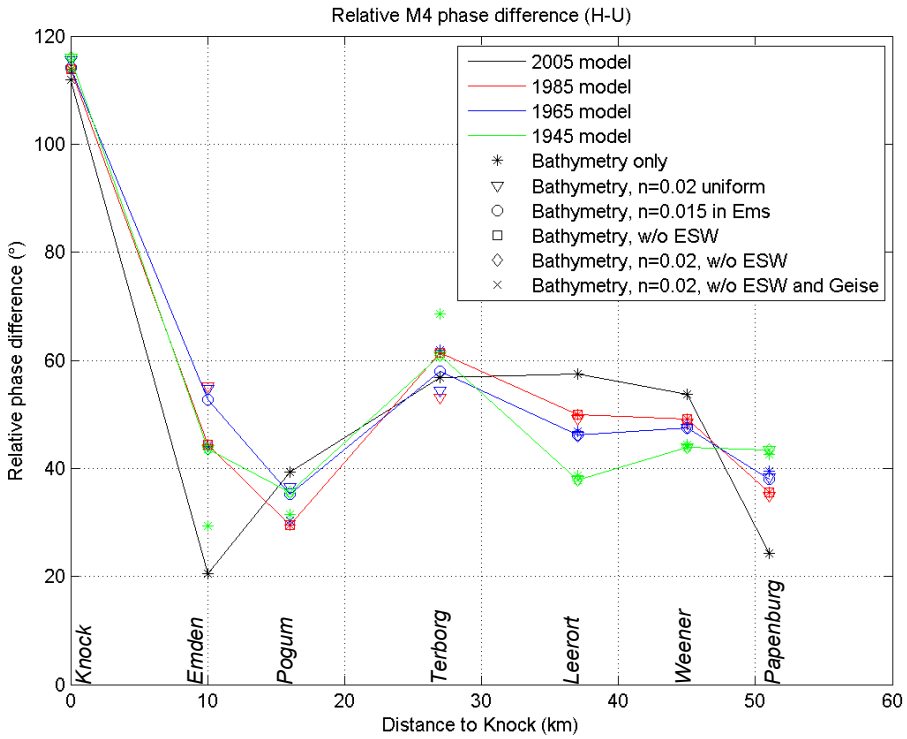

Fig. 4.32: Modelled relative M4 phase difference between vertical tide (water level) and horizontal tide (velocity) for the 2005, 1985, 1965 and 1945 model situation, longitudinal.

4.4. Salinity and residual circulation (3D)

Salinity distribution and the direction of the residual current are investigated with the 3D model, which consists of 10 σ-layers. The focus is on the occurrence of estuarine circulation and the changes in time. Only the four most representative model situations are compared, therefore the relative importance of bathymetry versus roughness changes cannot be determined. These model situations are: 2005 and 1985 with n=0.01 s/m$^{1/3}$ in the Ems, 1965 with n=0.015 s/m$^{1/3}$ in the Ems, 1945 with n=0.02 s/m$^{1/3}$ uniform. Salinity and residual current for three spring-neap cycles with different river discharge are compared: high discharge (winter, 100-225 m^3/s), intermediate discharge (winter, 70-115 m^3/s) and low discharge (summer, 30-60 m^3/s). The residual current is superimposed on the tidal cycle and can be determined by averaging over the tidal cycle. Variations in the residual current within the tidal cycle or within the spring-neap cycle are not investigated. The figures with the residual current and salinity at high / low discharge for all stations and extra observation points in between can be found in appendix D.

Fig. 4.33 shows mean bottom salinity, averaged over one spring-neap cycle with high/intermediate river discharge (Fig. 4.33a) and low discharge (Fig. 4.33b). As expected, salinity decreases in the upstream direction and salinity in the Lower Ems is higher when river discharge is low. Salt intrusion at most stations in the Lower Ems has increased between 1945 and 1985. It decreases slightly between 1985 and 2005 upstream of Terborg. This decrease after 1985 is not yet fully understood, but it may be related to the decreasing peak flood velocities in this period.

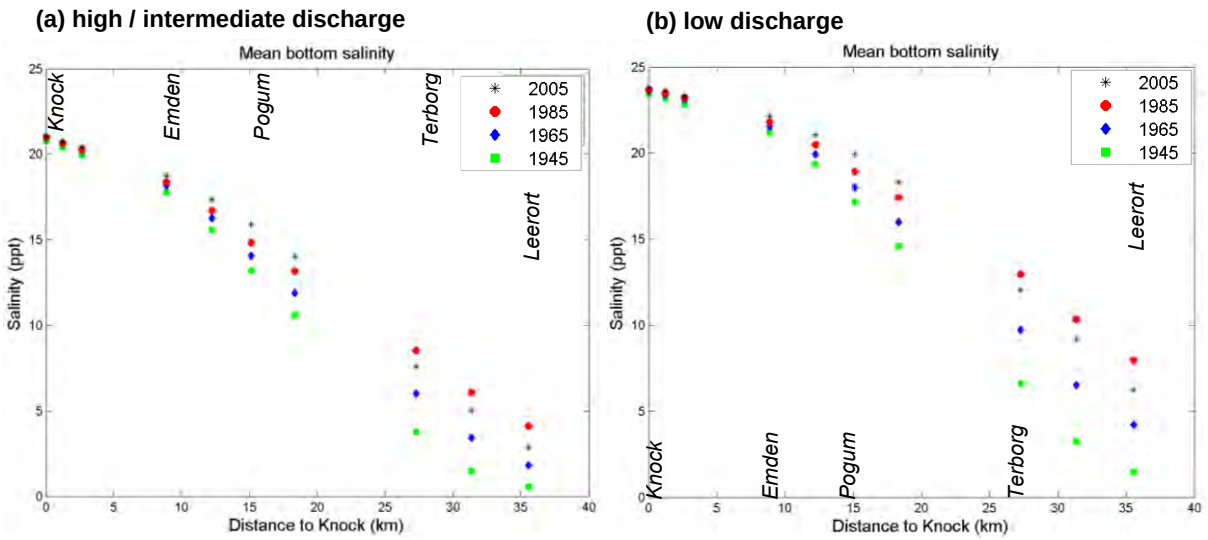

Fig. 4.33: Mean bottom salinity from Knock to Leerort, (a) at high / intermediate discharge (~100-225 m^3/s and 70-115 m^3/s, no difference in salinity for these two conditions) and (b) at low discharge (~30-60 m^3/s). All values are averaged over one spring-neap cycle.

In general, salinity is well-mixed over the water column and is highest at the end of flood and lowest at the end of ebb. The degree of stratification is approximated by the difference between bottom and surface salinity. Stratification is highest at high or low water, when flood/ebb velocities are decreasing, and is destroyed when the flow reverses. Fig. 4.34 illustrates the salinity difference between the surface and bottom for four observation points. Salinity around Knock (Fig. 4.34a) is ~18-22 ppt (parts per thousand or ‰, ≈ gram salt per kg water). Salinity decreases in the upstream direction and is ~15-20 ppt in Emden (Fig. 4.34b). For most part of the tide, salinity is well mixed over the water column. Weakly stratified conditions only exist at high tide with high river discharge, when surface salinity drops. At Pogum, the mouth of the Lower Ems, bottom salinity is ~10-20 ppt and drops to ~5-15 ppt in Terborg (Fig. 4.34c) and ~2-8 ppt in Leerort (Fig. 4.34d). Salinity and degree of stratification are fairly constant between 1945 and 2005 from Knock to Emden. However, upstream of Emden mean bottom salinity increases over time, while stratification does not change. The combination of channel deepening and reduced bottom roughness has led to more salt intrusion, further up the river.

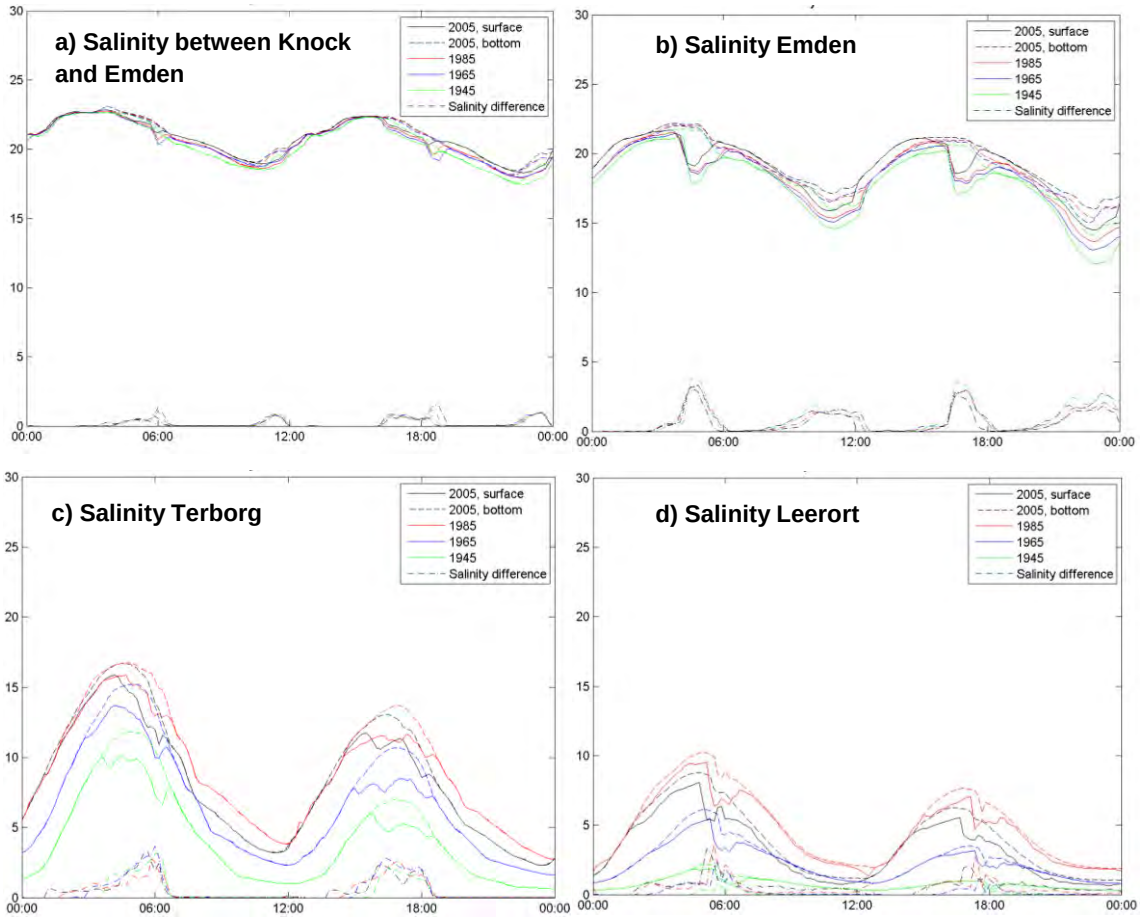

Fig. 4.34: Salinity in ppt (a) between Knock and Emden, (b) Emden, (c) Terborg and (d) Leerort. Surface / bottom salinity and vertical salinity difference (bottom-surface) are shown for one tidal cycle with high discharge (~100-225 m^3/s) during spring tide.

The horizontal salinity gradient of the bottom layer has been determined based on the mean bottom salinity and the along-channel distance between the observation points. The longitudinal salinity gradient is the average bottom salinity difference (in ppt per km) between two subsequent observation points, for one spring-neap cycle with high / intermediate / low river discharge. The resulting salinity gradient between Knock and Leerort is shown in Fig. 4.35. At high or intermediate discharge, the salinity gradient is largest between Emden and Terborg. At low discharge, the area of the largest salinity gradient is located further upstream. Between 1945 and 2005 salinity gradient decreases downstream of Pogum and increases upstream of Terborg, for all discharge conditions. Furthermore, the area with the highest salinity gradient moves in the upstream direction over time: at high discharge conditions this area shifts from Pogum to Terborg and at low discharge conditions it shifts from Terborg to Leerort.

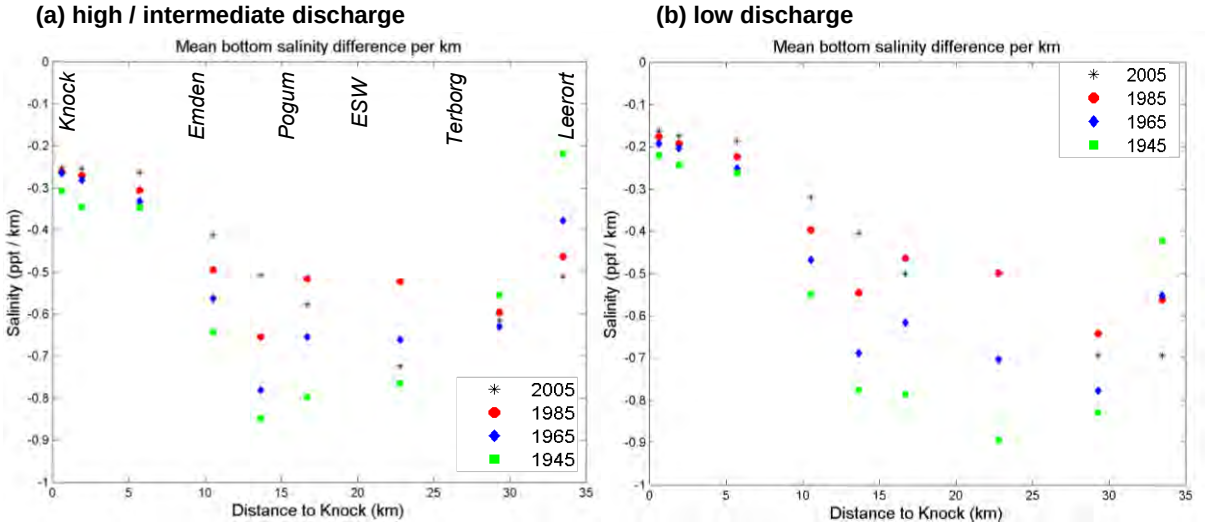

Fig. 4.35: Salinity gradient (in ppt per km) (a) at high and intermediate discharge (~100-225 m^3/s and 70-115 m^3/s, no difference in salinity for these two conditions) and (b) at low discharge (~30-60 m^3/s). All values are averaged over one spring-neap cycle.

Because gravitational circulation scales linearly with the salinity gradient *ds/dx* (or with the horizontal buoyancy gradient $\partial_x b$, see paragraph 2.3.6), it is expected that this salinity-driven current is stronger between Emden and Terborg, compared to upstream of Terborg. Indeed, no estuarine circulation is observed in Knock, downstream of Emden, where the salinity gradient is lower. The residual current is directed downstream for all discharge conditions and does not change direction between 1945 and 2005. This is illustrated in Fig. 4.36. To account for ebb/flood water level differences, normalized depth *z/h* is used.

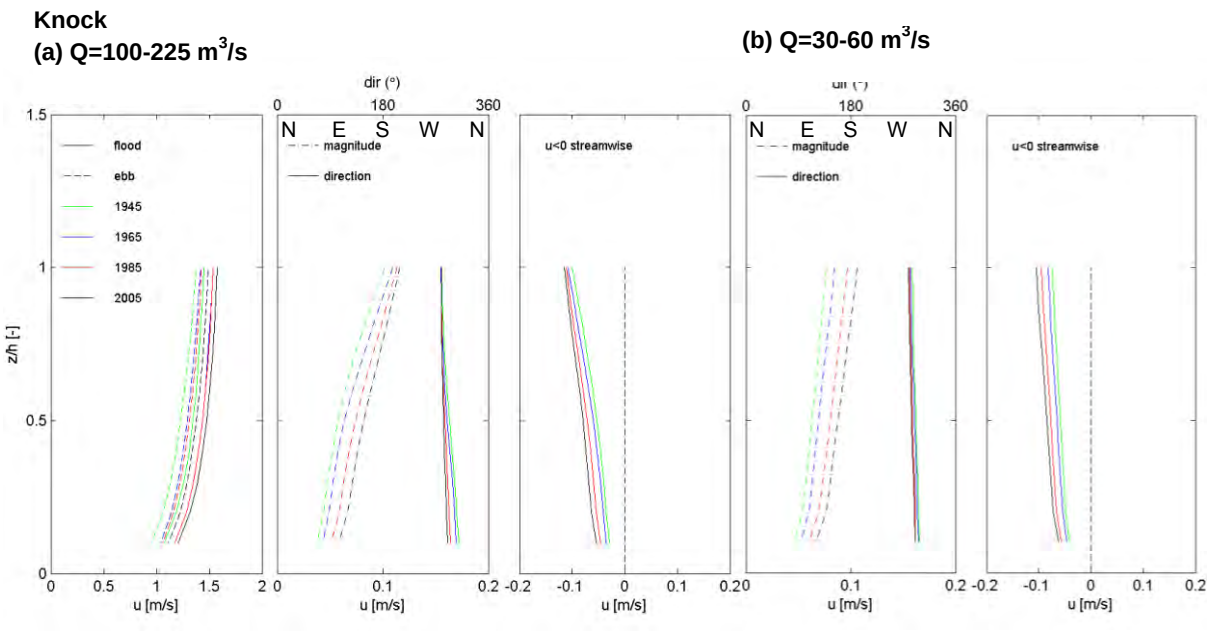

Fig. 4.36: Residual current at Knock. The residual current is always in downstream direction, ~ 270° (west), no estuarine circulation is observed. (a) Ebb/flood velocities, magnitude and direction of residual current, streamwise component of residual current, at high discharge (100-225 m^3/s) and (b) at low discharge (30-60 m^3/s. All values are averaged over one spring-neap cycle.

Estuarine circulation is observed around Emden at high and intermediate discharge, but not at low discharge (Fig. 4.37, p.77). The near-bottom current is more pronounced from 1965 onwards and it extends higher up the water column. This suggests that the estuarine circulation has intensified over time. Although the horizontal salinity gradient has decreased over time (see Fig. 4.35), water depth in the Emden Fahrwasser has increased between 1945 and 1965 from ~-9 m to ~-10.5 m NAP, and the strength of estuarine circulation scales with water depth (h^3 or h^2, paragraph 2.3.6). Discharge also is an important factor for the occurrence of estuarine circulation: the circulation near Emden disappears at low river discharge. This can be explained by the decrease of the salinity gradient at low discharge, which affects the strength of the salinity-driven current. These model results are supported by observations by Van de Kreeke (1991), who finds that the contribution of salinity-driven residual flow is very low during low discharge events (30 m^3/s), <1cm/s.

Similarly, discharge conditions influence the occurrence of estuarine circulation a few kilometres upstream, between Emden and Pogum (Fig. 4.38, p.78). Here, estuarine circulation is only observed at intermediate discharge in 1965 and 2005, but not at high and low discharge. The occurrence of estuarine circulation can be partly explained by the fact that salinity gradient and water depth (due to deepening of Emden Fahrwasser after 1945) were sufficiently large in 1965. Since then, the salinity gradient decreases, causing the

disappearance of the salinity-driven current near the bottom. It is not fully understood why the estuarine circulation reappears between 1985 and 2005 at intermediate discharge conditions, since water depth in the Emden Fahrwasser did not change and the salinity gradient has decreased even more. Probably this is caused by the more pronounced estuarine circulation near Emden.

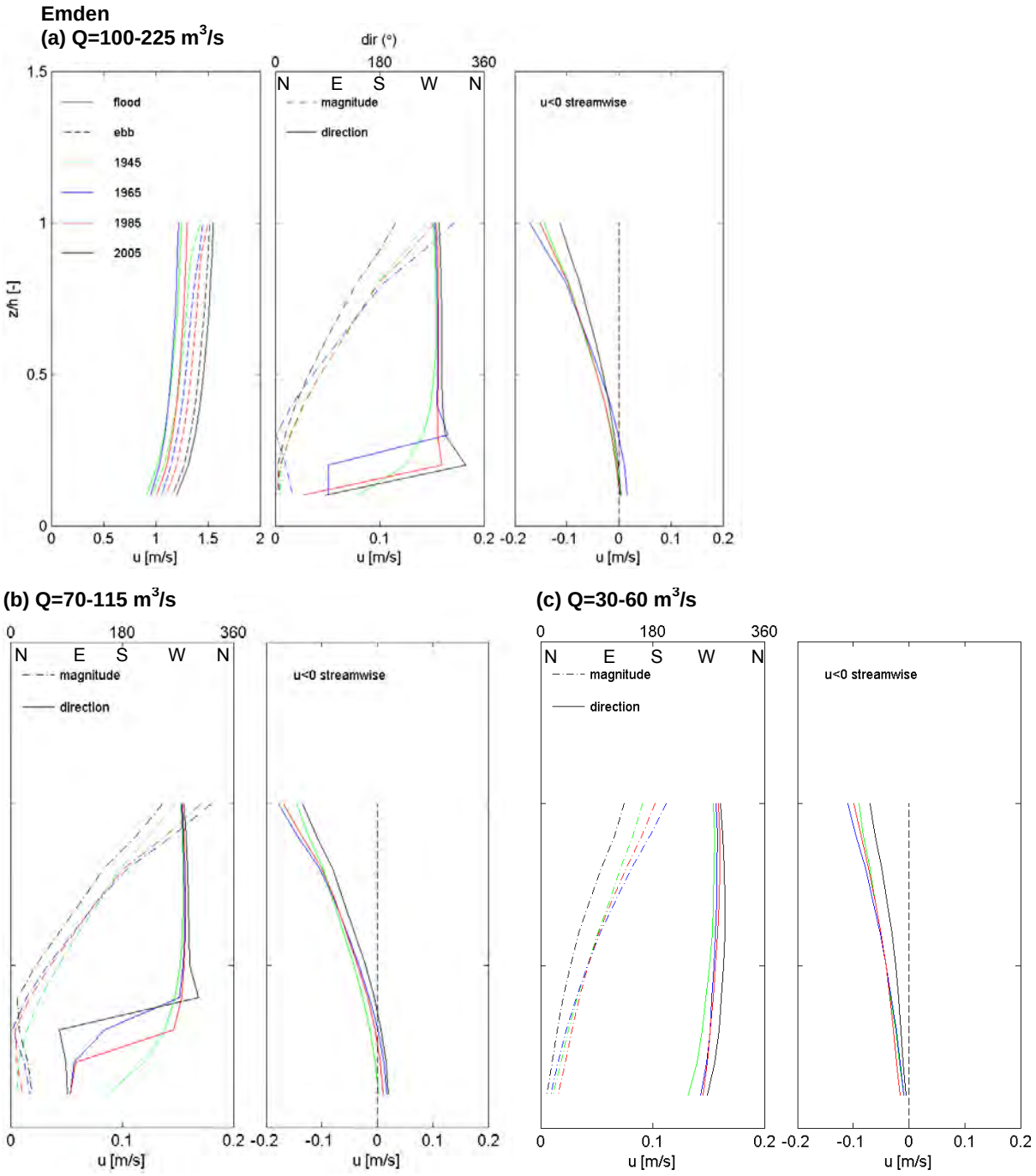

Fig. 4.37: Residual current at Emden, showing estuarine circulation at high and intermediate discharge, but not at low discharge. (a) Ebb/flood velocities, magnitude and direction of residual current, streamwise component of residual current, at high discharge (100-225 m^3/s), (b) at intermediate discharge (70-115 m^3/s) and (c) at low discharge (30-60 m^3/s. All values are averaged over one spring-neap cycle. Streamwise direction for this station is ~ 270° (west).

Between Emden and Pogum

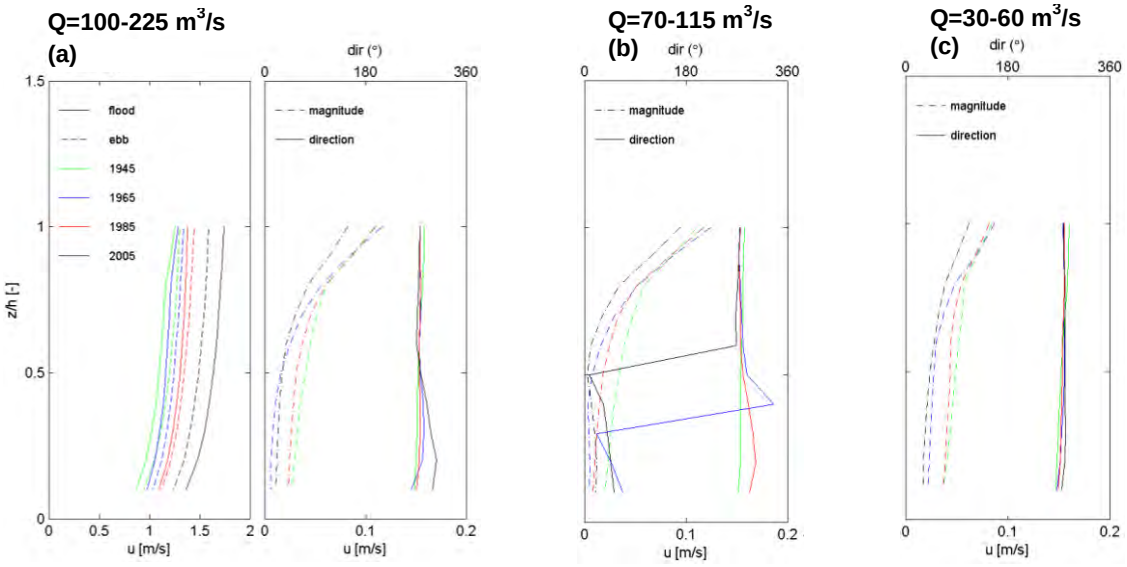

Fig. 4.38: Residual current between Emden and Pogum, showing estuarine circulation at intermediate discharge. (a) Ebb/flood velocities, magnitude and direction of residual current at high discharge, (b) at intermediate discharge and (c) at low discharge. All values are averaged over one spring-neap cycle. Streamwise direction for this station is ~ 270° (west).

Since the strength of the estuarine circulation scales with water depth, the shallow channel upstream of Pogum likely is an important limiting factor for the occurrence of estuarine circulation. Indeed, estuarine circulation is absent in Pogum and the residual current is always in downstream direction (Fig. 4.39, p.79). No difference in residual current for spring-neap cycles at high, intermediate or low discharge is seen. Although the salinity gradient is high at this location (see Fig. 4.35), it is likely that the limited water depth (~5-6 m) prevents the occurrence of a near-bottom upstream-directed current. The magnitude of the residual current decreases significantly between 1985 and 2005, which is in line with the decrease in ebb/flood velocities in this period (see paragraph 4.3.2). The 3D model results also suggest that Pogum shifts from higher ebb velocities to higher flood velocities after 1985, which is consistent with the 2D model results (see paragraph 4.3.4).

Further upstream, the residual current is always in downstream direction. No estuarine circulation is observed in the Lower Ems at either high, intermediate or low river discharge. Only near Emssperrwerk, a few kilometres upstream of Pogum, a change in the direction of the residual current is observed between 1985 and 2005: the near-bottom residual current shifts from westward (downstream direction) to southward and the magnitude decreases (Fig. 4.40, p.79). This is likely the result of local bathymetry changes and an increase in salinity gradient between 1985 and 2005. No difference was observed between high or low discharge conditions. Note that the Emssperrwerk was not removed in the historical 3D model runs.

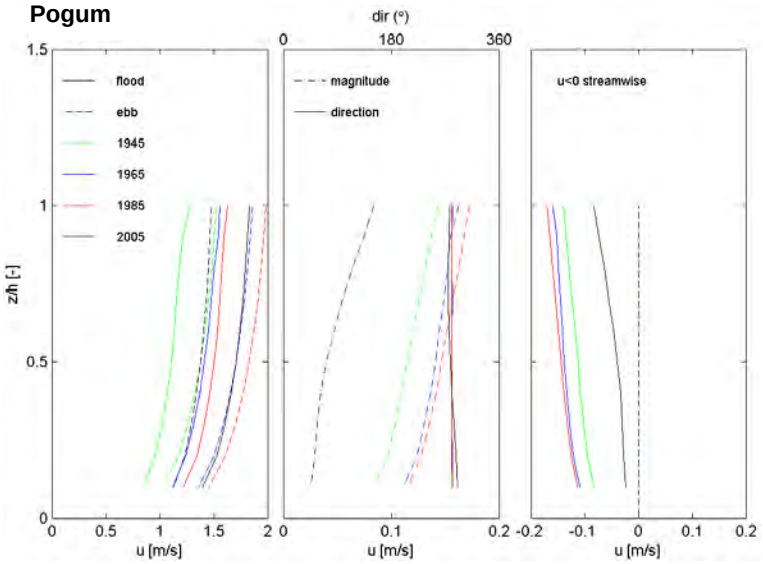

Fig. 4.39: Residual current in Pogum, showing no estuarine circulation and a decrease in magnitude of the residual current between 1985 and 2005 at intermediate discharge. All values are averaged over one spring-neap cycle at high discharge. Streamwise direction for this station is ~ 270° (west).

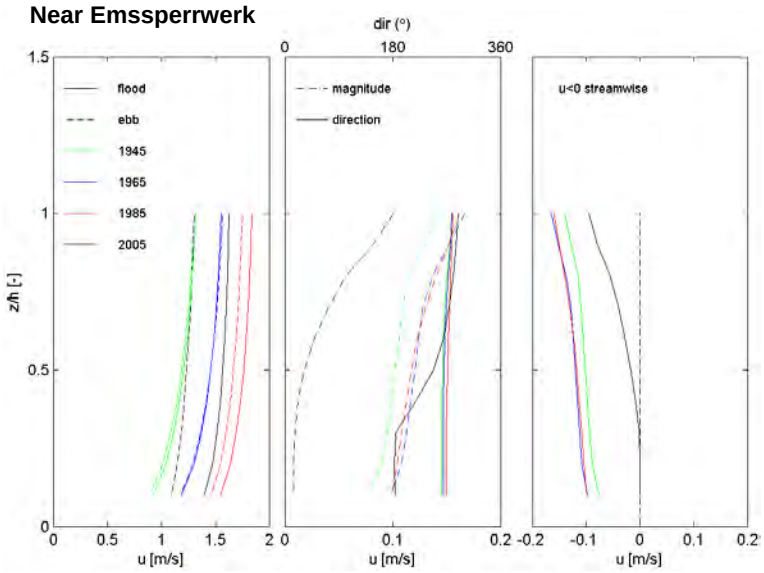

Fig. 4.40: Residual current near Emssperrwerk, showing a decrease in magnitude and a shift in direction of the near-bottom current between 1985 and 2005 at high discharge. All values are averaged over one spring-neap cycle at high discharge. Streamwise direction for this station is ~ 270° (west).

To summarize, both water depth and the horizontal salinity gradient (or horizontal buoyancy gradient) influence the occurrence of estuarine circulation in the Lower Ems. It seems that the limited water depth in the Lower Ems prevents the occurrence of estuarine circulation, despite the higher longitudinal salinity gradient. A near-bottom upstream-directed current is only observed around Emden, where both water depth and salinity gradient are sufficient. The occurrence of estuarine circulation at this location is also influenced by river discharge:

the salinity gradient in the Emden Fahrwasser decreases at low discharge conditions, causing the estuarine circulation to disappear. The salinity-driven current in Emden seems to have intensified slightly over time. Other changes over time are an overall salinity increase in the Lower Ems since 1945 and a decrease in salinity gradient in the Emden Fahrwasser and downstream parts of the Lower Ems, hereby shifting the area of the highest salinity gradient further upstream, where water depth is limited. Stratification has not changed over time. Note that only one observation point within the channel is used to study the residual flow pattern, cross-sectional differences are not examined. The residual flow pattern is averaged over one spring-neap cycle. Variations within the tidal cycle (differences in estuarine circulation during ebb or flood) are not investigated.

4.5. Sediment (3D)

The focus of this research is whether hydrodynamics in the Lower Ems have changed due to channel deepening and reduced bottom roughness and if this can explain the present-day high sediment trapping. The previous sections have focused on the hydrodynamic changes since 1945 due to channel deepening and reduced bottom roughness. Paragraph 4.5.1 will link the hydrodynamic changes to changes in sediment dynamics. Paragraph 4.5.2 focusses on the consequences for sediment transport and will provide some preliminary results of the changes in sediment concentration and transport in the Lower Ems.

4.5.1. From hydrodynamics to sediment dynamics

For the entire period 1945-2005, the hydrodynamic characteristics that are important for sediment transport are:

- A flood-dominant system with higher peak flood velocities in the Lower Ems, which are more effective in eroding and mixing the sediment over the water column than the lower peak ebb velocities, resulting in net sediment import.
- Longer high water slack duration in the Emden Farhwasser (Knock, Emden) and near the mouth of the Lower Ems (Pogum, Terborg), which means that fines have more time to settle after flood, resulting in net landward sediment transport.
- Estuarine circulation in the Emden Fahrwasser, but not in the Lower Ems.
- Temporal scour/settling lag and spatial settling lag effects further cause a net landward sediment transport.

Since 1945, water depth has increased and bottom roughness has decreased. This has affected hydrodynamics and sediment dynamics. The most important changes are:

- Overall M2 velocity increase between 1945-2005, resulting in increased ebb/flood flow velocities. However, M2 velocity decreases between Pogum and Leerort in the period 1985-2005. This results in a local decrease of ebb and/or flood velocities (depending on relative increase of water depth versus discharge), affecting the saturation concentration and fluid mud formation.
- Shift from ebb-dominance (higher ebb velocities) to flood-dominance (higher flood velocities) near the mouth of the Lower Ems between 1985 and 2005. While sediment was mostly exported before 1985, it is imported into the Lower Ems after 1985.
- Slow change from a flood-dominant system to a more high water slack dominant system in the Lower Ems, increasing the import of fines.
- More pronounced estuarine circulation from Emden to Pogum (but: depending on river discharge). This likely enhances upstream-directed sediment transport.
- Decrease in magnitude of the downstream-directed residual current for most stations in the Lower Ems.

4.5.2. Sediment transport

To investigate the combined effects of these hydrodynamic characteristics and changes between 1945-2005, the 3D model was extended with a sediment transport model, containing simple equations for erosion and deposition. A fixed sediment concentration (sediment source) was imposed at the Wadden Sea and Leda boundaries, not at weir Versen. No initial sediment concentration was prescribed in the Ems-Dollard estuary. The model set-up and specification of the sediment fractions are described in paragraph 3.1.6. No calibration against observations was carried out and the model outcomes should therefore be interpreted qualitatively, not quantitatively. The results give an indication for the changes in sediment-importing mechanisms in time and their consequences for the sediment dynamics in the Lower Ems.

Sediment-fluid interactions (turbulence damping, sediment-induced gravitational circulation) and flocculation are not included in the present 3D model. This means that only ebb/flood flow velocities, tidal asymmetry (peak flow asymmetry, slack water duration), mixing over the water column, temporal settling/scour lag and spatial settling lag effects are important for the net sediment transport in these 3D model simulations. An improved transport module is currently being developed within the project ‘Mud dynamics in the Ems-Dollard’, which is

better calibrated (e.g. settling velocity, erosion parameter) and includes improved model formulations for turbulence damping and sand-mud buffering.

The sediment concentration for all stations is shown in Fig. 4.41 (p.84). This is the sediment concentration for all layers after a model simulation of 3 months (01/01–01/04), which includes several high discharge peaks (see Fig. 3.13). Most change is seen in Pogum and in the upper part of the Lower Ems: the sediment concentration in Pogum is lower in 2005 compared to the earlier model situation, but the sediment concentration in Weener and Papenburg increases between subsequent model situations, especially after 1965. The zone with the highest suspended sediment concentration shifts from the mouth of the Lower Ems to the upstream reaches of the river.

The cumulative suspended load transport through a cross-section is given in Fig. 4.42 (p.85). Cross-section Dukegat, in the lower reaches of the estuary near Eemshaven, is indicative for the total suspended load transport. Cumulative suspended load transport at Knock and GeiserN do not change much over time. [Note that sediment import at Knock is determined for the whole cross-section, which divides into a north branch (GeiseN, leading to the Emden Fahrwasser) and south branch (leading to the Dollard). The ebb-dominance at Knock (paragraph 4.3.4) is only determined for one observation point.] Cumulative transport is negative for Pogum between 1945-1985, indicating sediment export. This is consistent with the hydrodynamic conditions (ebb-dominance). In 2005, Pogum starts importing sediment into the Lower Ems, which is expected based on the shift from ebb- to flood-dominant conditions in this period. Sediment transport through all cross-sections in the Lower Ems increases in the period 1945-2005, but especially in Terborg and Weener in 1985 and 2005. This provides further evidence that sediment import into the Lower Ems has increased over time.

Fig. 4.43 (p.86) illustrates the available mass of sediment at the bed. This is the sum of all sediment fractions. In 1945 and 1965, most sediment accumulates at the bed in Emden and Knock. In 1985, the available sediment mass in Emden Fahrwasser is less and more sediment settles in the upstream part of the Lower Ems, near Papenburg. A significant change is seen in the 2005 model situation: available sediment mass at the bed is dramatically higher in the entire Lower Ems, from Terborg to Papenburg. This indicates a significant increase in the sediment-importing mechanisms in 2005, compared to earlier model situation. Most sediment now accumulates in Terborg, which could be an indication for the location of the estuarine turbidity maximum, which is typically located at the convergence

zone of sediment. It is likely that no equilibrium situation has been established yet after this 3-month model simulation, therefore the ETM is not further investigated in this research.

These preliminary 3D model results indicate that the sediment-importing mechanisms have become stronger over time. The suspended sediment concentration used to be highest in Pogum, but has shifted to the upstream part of the river. Sediment import (transport through cross-section) in the Emden Fahrwasser has not changed over time, but sediment import into the Lower Ems has increased after 1985 due to the dominance-shift in Pogum. While the main sediment deposition zone used to be the Emden Fahrwasser (before 1985), the incoming sediment is now being transported further upstream and eventually settles in the Lower Ems (Terborg, Leerort, Weener, Papenburg). This is consistent with the hyper-concentrated conditions and the high trapping efficiency of the present-day Lower Ems.

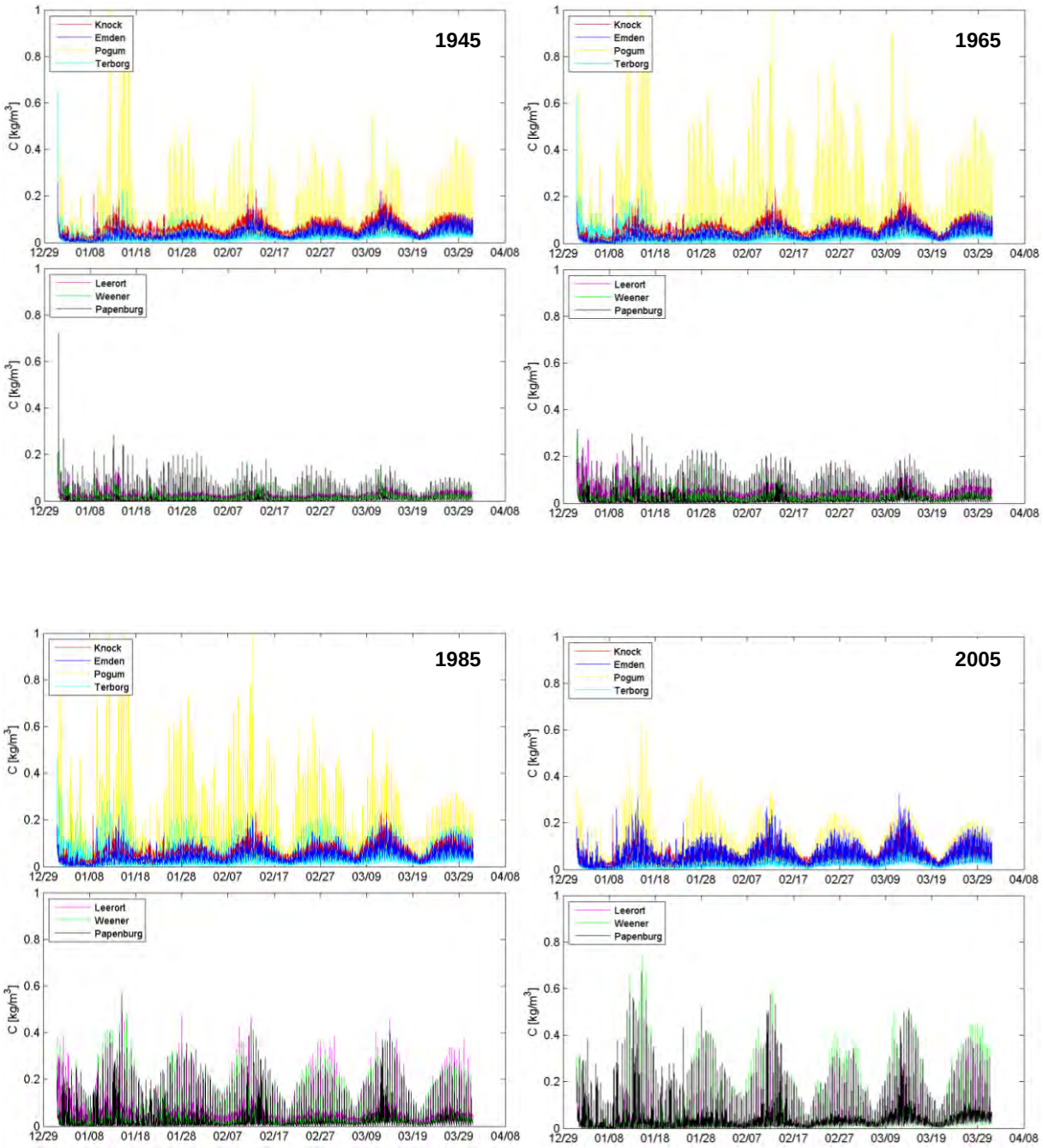

Fig. 4.41: Sediment concentration (sum of all layers, kg/m^3) at stations in the Emden Fahrwasser and Lower Ems. Simulation time is 3 months.

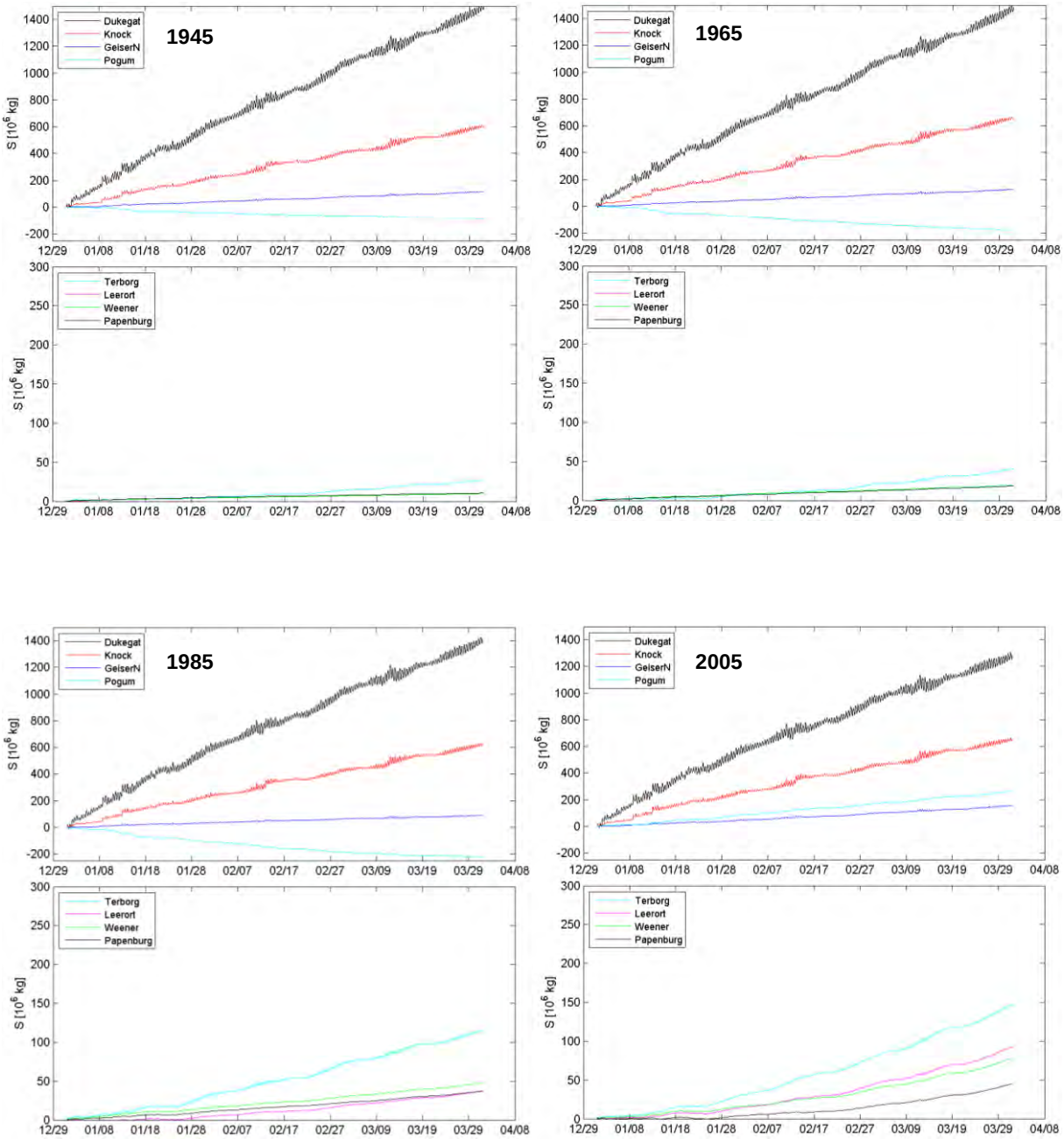

Fig. 4.42: Cumulative suspended load transport (entrained in the water column) through cross-section. Positive values mean sediment import into the Lower Ems. Dukegat is indicative for the total suspended load transport. GeiserN is located between Knock and Emden. Simulation time is 3 months. Note the scale difference between the top and bottom figure of each period.

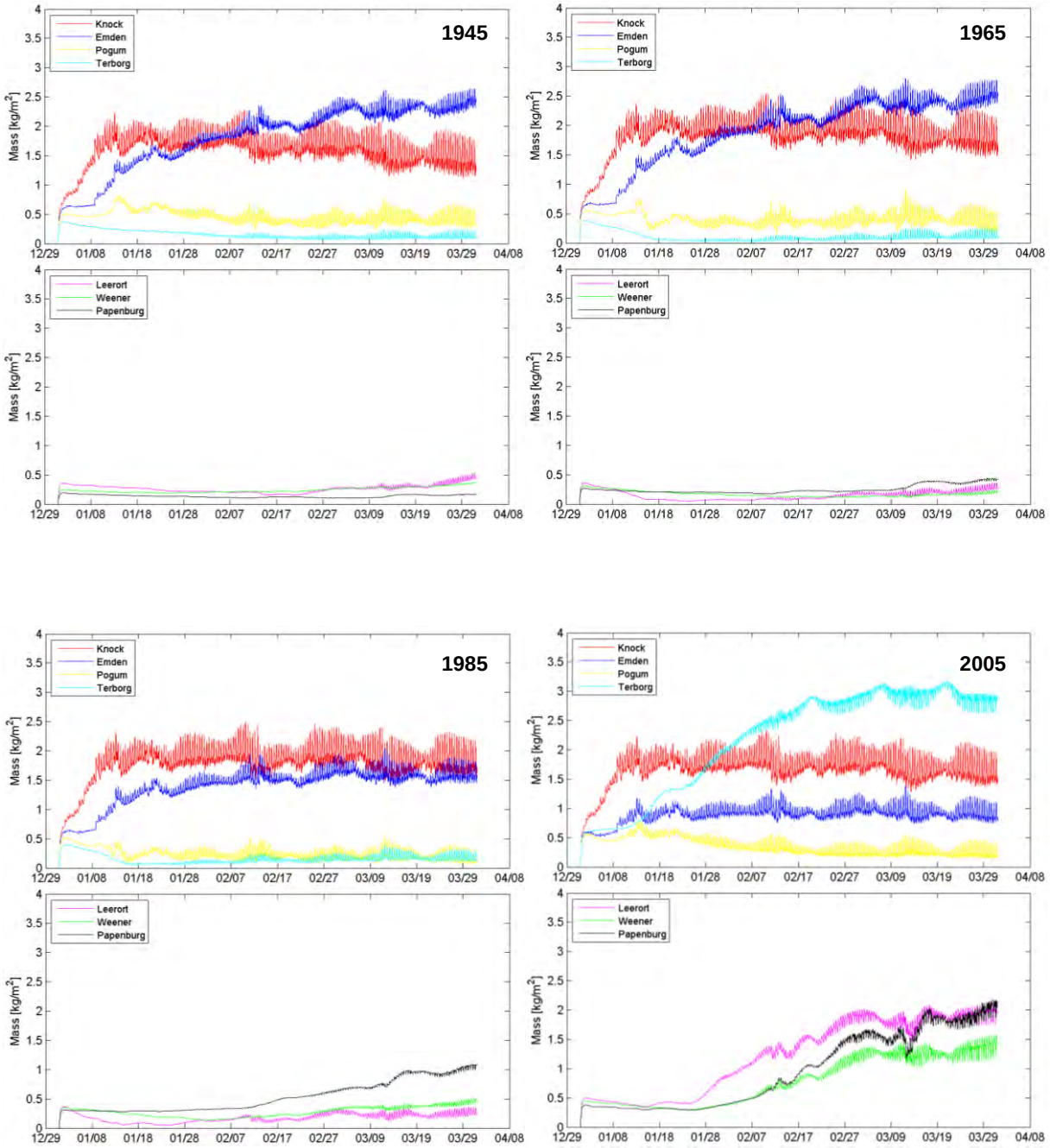

Fig. 4.43: Available mass of sediment (kg/m^2) at bed of water level stations in the Emden Fahrwasser and Lower Ems. Simulation time is 3 months.

5 DISCUSSION

This chapter compares the model results with previous research. Similarities and differences will be pointed out. The Delft3D models that were used in this study are well suited for reproducing the tidal characteristics in the Lower Ems and the changes over time. Because multiple model runs were carried out, which differed only in bathymetry or bottom roughness, the relative effects of both could be determined separately. The 2D model is able to reproduce the changes in tidal range by only adjusting bathymetry and bottom roughness. The model results agree well with previous research and they confirm existing ideas (e.g. reduced bottom roughness and changes in tidal asymmetry). This research improves our understanding of the causes of the tidal changes in the Lower Ems in the period 1945-2005 and its consequences for sediment import.

The outcomes of this present research show that bottom roughness has decreased between 1945 and 1985 in the Lower Ems and that channel deepening (decrease in effective hydraulic roughness) is responsible for the tidal changes after 1985. Previous research indeed suggests that bottom roughness has decreased over time in the Lower Ems. Herrling and Niemeyer (2008c) had to reduce bottom roughness between 1937 and 2005 to be able to reproduce the measured water levels. Chernetsky et al. (2010) and Schuttelaars et al. (2012) found a decrease in the stress parameter and vertical eddy viscosity between 1980 and 2005, based on necessary calibrations to match their model with observations. However, no decrease in bottom roughness between 1985 and 2005 was necessary in this present research to reproduce the water level observations. Jensen et al. (2003) agree that bottom roughness has decreased in the Lower Ems since the 1940's. However, they only attribute this to the large increase in water depth due to channel deepening and therefore the decrease in effective hydraulic roughness. This is found to be valid for the period 1985-2005.
Evidence for the decrease in bottom roughness over time comes from fluid mud observations. Fluid mud was first observed in the 1970's by Duinker et al. (1985) and became persistent after channel deepening in the 1990's. Nowadays, fluid mud layers are permanently present in the Lower Ems (Winterwerp, 2011; Vroom et al., 2012). The present research suggests that bottom roughness has not changed between 1985 and 2005. This implicates that fluid mud already occurred frequently before 1985.

Flow velocities in the Lower Ems show an overall increase in magnitude over time. This is similar to findings of Herrling and Niemeyer (2008c) in the period 1937-2005. However, between 1985 and 2005, model results indicate that velocities have decreased locally in river stretch between Pogum and Leerort. This is possibly related to a relatively smaller increase

in discharge compared to the increase in water depth at these stations. This velocity reduction can cause a significant decrease in the saturation concentration. Therefore the collapse of the turbulent flow field and fluid mud formation can occur at lower sediment concentrations. It could therefore explain the fast deterioration of the conditions in the Lower Ems in the past decades and the permanent presence of fluid mud layers nowadays. This local velocity decrease between 1985 and 2005 is not found in previous studies. It is possible that this is caused by differences in the model set-up and/or reconstructed bathymetry. Chernetsky et al. (2010) use a 2DV model with the measured 1980 and 2005 bathymetry and assume an exponentially converging estuary. Actual basin geometry and width changes in the Lower Ems are therefore not modelled. Herrling and Niemeyer (2008c) only compare the hydrodynamic changes at one location (5 km upstream of Terborg) between 1937 and 2005, not for time steps in-between. They find an overall increase in ebb and flood velocity. This is in agreement with the results of this study when only 1945 and 2005 are compared. The local decrease in flow velocity between 1985 and 2005 is an interesting finding, which requires more research.

It is suggested that the Lower Ems has become a less flood-dominant system over time (Talke and De Swart, 2006), where flood-dominance is defined as the relative longer duration of flood compared to ebb (2M2-M4 amplitude phase difference). Herrling and Niemeyer (2008c) have already shown an increase in flood duration since 1937 (~45 min. in Papenburg). The present research also shows that flood duration has increased over time (~35 min. in Papenburg) and that the system has become slightly more high water slack dominant. The relative importance of a smoothening of the bottom versus channel deepening differs between periods.

The amplitude phase difference near the mouth of the Lower Ems indicates a symmetrical tide with equal ebb/flood duration. It is then expected that ebb/flood flow velocities should also be equal. However, model results suggest that they are not symmetrical. In fact, the type of dominance at Emden and Pogum shifts from ebb- to flood-dominance (2M2-M4 velocity phase difference) between 1985 and 2005. This is supported by model results from Chernetsky et al. (2010), who also find an ebb-dominant region near the mouth of the Lower Ems in 1980, but not in 2005. The present model indicates that Knock remains ebb-dominant in 2005, which is consistent with the observations presented by Chernetsky et al. (2010), but is not reproduced in their model.

Chernetsky et al. (2010) find an intensified estuarine circulation between Knock and Pogum in the period 1980-2005 due to increased water depth and a decrease in vertical mixing. Vroom et al. (2012) state that a strong salinity gradient exists between Knock and Emden,

which generates a pronounced estuarine circulation. However, the present model outcomes indicate that estuarine circulation is only observed around Emden, where both water depth and salinity gradient are sufficient. The salinity gradient is too small between Knock and Emden and water depth is too limited upstream of Pogum for the occurrence of estuarine circulation. The model outcomes indicate that estuarine circulation in Emden has intensified from 1965 onwards. This can be related to the deepening of the Emden Fahrwasser between the 1945 and 1965. Also, the circulation is absent at low river discharge, when the salinity gradient in the Emden Fahrwasser decreases. It is important to note that no extra calibration was performed on the 3D model. Model results would likely be improved by calibrating the model using salinity information. In this study, only one observation point within the channel is used to investigate the residual flow pattern. Huijts et al. (2009) show that across-channel density gradients can influence the transverse distribution of the residual flow and a horizontal circulation pattern can occur, with in- and outflow at different sides of the channel. Also channel curvature in the Lower Ems can lead to an asymmetric across-channel distribution of the residual flow pattern. The apparent absence of estuarine circulation at one observation point does therefore not exclude its occurrence elsewhere in the cross-section.

Model results indicate that the sediment-importing mechanisms have become stronger over time. Although sediment import into the Emden Fahrwasser has not changed over time, the import into the Lower Ems has increased significantly after 1985 due to the dominance-shift in Pogum. Incoming sediment is no longer mainly deposited in the Emden Fahrwasser, but is being transported up-river. The area of the highest suspended sediment concentration shifts to the upstream part of the river. This is consistent with the present-day observations in the Lower Ems (Talke et al., 2009; Winterwerp, 2011).
The development of a hyperconcentrated system is a long-term process and the Lower Ems was already flood-dominant in 1945. It would therefore be interesting to investigate the effects of the land reclamations (loss of intertidal area) in the past centuries on tidal asymmetry and type of dominance. There are plans to recreate intertidal areas along the Lower Ems to reduce the high turbidity (BAW, German Federal Waterways Engineering and Research Institute). Apart from the hydrodynamic effects of these new retention basins depending on their location (Alebregtse, 2013), also hysteresis must be taken into account.

The Ems-Dollard 2D and 3D models are able to quantitatively reproduce the present-day hydrodynamic observations. The historical conditions should be interpreted in a more qualitative way, since parameters and boundary conditions may differ from historical conditions. Model assumptions can greatly influence model outcomes. Schuttelaars et al. (2012) found that increasing the estuary length by relocating the weir at Herbrum significantly

reduces sediment import into the Lower Ems. They therefore plead for a ‘synergetic use’ between observations, idealized models (to quickly assess model sensitivity and provide qualitative insights) and state-of-the-art numerical models (to quantitatively assess the effects of interventions).

6 CONCLUSIONS

The aim of this research was to investigated the effects of channel deepening and bottom roughness on the tidal characteristics in the Lower Ems. The Ems-Dollard Delft3D model is well able to reproduce the changes in tidal range by adjusting bathymetry and bottom roughness. Because multiple model runs are carried out, a distinction between the effects of deepening versus reduced bottom roughness can be made. The most representative model situation for each period are: 1945 with n=0.02 uniform; 1965 with n=0.015 in the Ems; 1985 and 2005 with n=0.01 in the Ems.

Model results suggest that bottom roughness has decreased between 1945 and 1985. This coincides with the first observations of fluid mud in the Lower Ems. The smoothening of the bottom is largely responsible for the observed changes in water level (MHW, MLW, tidal range), although channel deepening also leads to a reduction of effective hydraulic roughness. M2 and M4 amplitude have increased since 1945 in the entire Lower Ems, in particular in the most upstream stations. Similarly, the smoothening of the bottom is the most important factor for the increased tidal velocity and reduced flood-dominance between 1945 and 1985. Bottom roughness does not change between 1985 and 2005. This suggests that fluid mud already occurred frequently in 1985. The observed water level increase in the period 1985-2005 is caused by extensive channel deepening in the entire Lower Ems.
Flow velocity decreases locally (between Pogum and Leerort) after 1985, which is likely caused by the fact that discharge did not increase as much as water depth. This velocity reduction may lead to fluid mud formation at lower sediment concentrations than before. This could explain the permanent presence of fluid mud layers nowadays.

The amplitude and velocity phase differences in the Lower Ems shows a slow shift from a flood-dominant system (longer flood with higher peak flow velocities) to a high water slack dominant system. Flood duration increases over time due to reduced bottom roughness, the system becomes less flood-dominant. This trend is enhanced after 1985 as a direct response to channel deepening. The amplitude phase difference near the river mouth suggests an

almost symmetrical tide and does not change over time. However, the velocity phase difference shows that Emden and Pogum change from being ebb-dominant to flood-dominant between 1985 and 2005. This has resulted in significantly more sediment import.

The 3D model shows that salinity has increased for most stations in the Lower Ems between 1945 and 1985. The zone with the highest salinity gradient has moved in the upstream direction over time, but the limited water depth in the Lower Ems prevents the occurrence of estuarine circulation. Estuarine circulation is only observed around Emden, where both water depth and salinity gradient are sufficient. The deepening of the Emden Fahrwasser between 1945 and 1965 has led to a more pronounced estuarine circulation, although the near-bottom upstream-directed current disappears at low river discharge.

The hydrodynamic changes in the period 1945-2005 indeed result in more sediment import into the Lower Ems. This is an indication that the sediment-importing mechanisms have become stronger over time. The zone with the highest suspended sediment concentration shifts from the river mouth to the upstream reaches of the Lower Ems. Cumulative suspended load transport indicates that Pogum was exporting sediment before 1985, but is importing sediment after 1985, which is expected because of the shift from ebb- to flood-dominance. Incoming sediment is now being transported further upstream. This is consistent with the present-day observations.

The outcomes of this study can provide useful information about the future development of similar estuaries, such as the Scheldt estuary on the border between the Netherlands and Belgium. It improves our understanding of estuaries where anthropogenic interventions cause a change in tidal processes.

Summary

The Ems-Dollard estuary, located on the Dutch-German border, has a long history of anthropogenic interventions. Channel deepening in the past decades has influenced tidal and sediment dynamics. Major present-day ecological and economic problems are the hyperconcentrated conditions and fluid mud formation in the Lower Ems river. This research is part of the project 'Mud dynamics in the Ems-Dollard' which was initiated by Rijkswaterstaat Waterdienst following the Water Framework Directive and it was carried out at Deltares, Delft. It investigates the effects of channel deepening and bottom roughness changes in the Lower Ems in the period 1945-2005, to provide insight into the hydrodynamic contribution to the increased turbidity. The focus is on changes in tidal range, asymmetry and estuarine circulation and their implications for sediment dynamics. Two existing Delft3D models of the Ems-Dollard estuary are used: a depth-averaged (2D) model and a 10-layer (3D) model, both representing the 2005 situation. Three historical bathymetries are reconstructed, using the measured 2005 bathymetry as a basis: 1985, 1965 and 1945. Bathymetry reconstructions are done based on (a) historical mean high water and average spring low water levels, and (b) information about channel deepening. Bottom roughness is calibrated to achieve global agreement with observed mean high/low water levels. Results suggest that bottom roughness has decreased between 1945 and 1985. Both channel deepening and a reduction in bottom roughness have the same effect: a decrease in (effective) hydraulic roughness in the period 1945-2005. The relative importance differs between periods. This has caused (a) an increase in tidal range and peak flow velocities in the Lower Ems, resulting in higher suspended sediment concentrations, and (b) a decrease in M2 and M4 amplitude phase and velocity phase, resulting in a slow change from a flood-dominant system towards a more high water slack dominant system. Channel deepening after 1985 has accelerated this development. Flow velocities have decreased locally, which is related to the balance between the increase in discharge versus the increase in water depth. This may have enhanced fluid mud formation through a reduction of the saturation concentration. Furthermore, channel deepening after 1985 is responsible for a shift from ebb- to flood-dominant conditions near the river mouth, hence a significant increase in sediment import. Estuarine circulation is only observed around Emden, where both water depth and salinity gradient are sufficient. The deepening of the Emden Fahrwasser between 1945 and 1965 has led to a more pronounced near-bottom upstream-directed current at this location.

Keywords: Delft3D; Modeling; Ems-Dollard estuary; Netherlands; Estuaries; Deepening; Bottom roughness; Tides; Hydrodynamics; Tidal asymmetry; Flood-dominance; Tidal pumping; Estuarine circulation; Sediment transport

References

Alebregtse, N.C. (2013). Effect of retention basins on tidal characteristics in the Ems. Presentation Ems-Scheldt Workshop 2013, Delmenhorst, Germany.

Beardsley, R.C., Candela, J., Limeburner, R., Geyer, R.W., Lentz, J., Castro, B.M., Cacchione, D. and Carneiro, N. (1995). The M_2 tide on the Amazon shelf. Journal of Geophysical Research, Vol. 100, No. C2, 2283-2319.

Burchard, H. and Hetland, R.D. (2010). Quantifying the Contributions of Tidal Straining and Gravitational Circulation to Residual Circulation in Periodically Stratified Tidal Estuaries. Journal of Physical Oceanography, 40: 1243-1262. DOI: 10.1175/2010JPO4270.1

Chernetsky, A.S., Schuttelaars, H.M. and Talke, S.A. (2010). The effect of tidal asymmetry and temporal settling lag on sediment trapping in tidal estuaries. Ocean Dynamics, 60:1219-1241. DOI 10.1007/s10236-010-0329-8

Dalrymple, R.W. and Choi, K. (2007). Morphologic and facies trends through the fluvial-marine transition in tide-dominated depositional systems: A schematic framework for environmental and sequence-stratigraphic interpretation. Earth-Science Reviews, Vol. 81, Issues 3-4, p. 135-174.

Deltares (2012). Delft3D-FLOW: Simulation of multi-dimensional hydrodynamic flows and transport phenomena, including sediments. User Manual, Hydro-Morphodynamics, Version: 3.15.25157

DHI-WASY GmbH (2012). Perspektive Lebendige Ems. Teilprojekt Wasserbau. Endbericht juni 2012. Syke, Germany

Dronkers, J. (1986). Tidal asymmetry and estuarine morphology. Netherlands Journal of Sea Research, 20 (2/3): 117-131

Duinker, J.C., Hillebrand, M.T.J, Nolting, R.F. and Wellershaus, S. (1985). The river Ems: Processes affecting the behaviour of metals and organochlorines during estuarine mixing. Netherlands Journal of Sea Research, 19 (1): 19-29.

Dyer, K.R. (1994). Estuarine sediment transport and deposition. In: Sediment Transport and Depositional Processes, Pye, K. (ed), Blackwell Scientific Publications, Oxford, p. 193-218.

Friedrichs, C.T. and Aubrey, D.G. (1988). Non-linear tidal distortion in shallow well-mixed estuaries: a synthesis. Estuarine, Coastal and Shelf Science, 27: 521-545.

Gabioux, M., Vinzon, S.B. and Paiva, A.M. (2005). Tidal propagation over fluid mud layers on the Amazon shelf. Continental Shelf Research, 25:113–125

Hansen, D.V. and Rattray Jr., M.(1965). Gravitational Circulation in Straits and Estuaries. Journal of Marine Research, vol. 23, 2.

Herrling, G. and Niemeyer, H.D. (2008a). Set-up of a hydrodynamic model for the Ems-Dollard estuary. Harbasins Report.

Herrling, G. and Niemeyer, H.D. (2008b). Reconstruction of the historical tidal regime of the Ems-Dollard estuary prior to significant human changes by applying mathematical modelling. Harbasins Report.

Herrling, G. and Niemeyer, H.D. (2008c). Comparison of the hydrodynamic regime of 1937 and 2005 in the Ems-Dollard estuary by applying mathematical modelling. Harbasins Report.

Hoekstra, P. (2011). Coastal Morphodynamics: Processes, landforms and sedimentary products. Course guide GEO3-4306, Utrecht University.

Huijts, K.M.H., Schuttelaars, H.M., Swart, H.E. de, and Friedrichs, C.T. (2009). Analytical study of the transverse distribution of along-channel and transverse residual flows in tidal estuaries. Continental Shelf Research, 29: 89–100

Jay, D.A. and Musiak, J.D. (1994). Particle trapping in estuarine tidal flows. Journal of Geophysical Research, vol. 99, No. C10, 20445-20461.

Jensen, J., Mudersbach, C. and Blasi, C. (2003). Hydrological changes in tidal estuaries due to natural and anthropogenic effects. 6th International MEDCOAST Conference, Ravenna, Italy.

Jensen, J. and Mudersbach, C. (2005). Recent sea level variations at the North Sea and Baltic Sea coastlines. ICEST, USA.

Kessel, T. van (2011). Abundance or scarcity? Stirring up sediments and discussion. Presentation NCK 2011.

Krebs, M. (2012). Historical developments in the Ems estuary and its area. Overview of morphological hunman-induced changes to the Ems river and estuary. WSA Emden, Germany. NCK presentation.

Van de Kreeke, J. (1991). Longterm measurements of physical parameters in the Ems Estuary: a descriptive analysis of current velocity and salinity. Hydrest Inc report, Miami, Florida, 22 p.

Lewis, R. (1997). Dispersion in Estuaries and Coastal Waters. Wiley & Sons, Chichester, UK. 312 p.

Masselink, G., Hughes, M. and Knight, J. (2011). Introduction to Coastal Processes & Geomorphology. Second edition. Hodder Education, London, UK. 416 p.

Maren, D.S. van, Winterwerp, J.C. (2012). The role of flow asymmetry and mud properties on tidal flat sedimentation. Continental Shelf Research. DOI:10.1016/j.csr.2012.07.010. In press.

Maren, D.S. van, Winterwerp, J.C., Wang, Z.Y. and Pu, Q. (2009a). Suspended sediment dynamics and morphodynamics in the Yellow River, China. Sedimentology: 56, 785–806

Maren, D.S. van, Winterwerp, J.C., Wu, B.S. and Zhou, J.J. (2009b). Modelling hyperconcentrated flow in the Yellow River. Earth Surface Processes and Landforms. Published online in Wiley InterScience, DOI: 10.1002/esp.1760

Maren, D.S. van, Vroom, J., Vijverberg, T., Schoemans, M., and Rooijen, A. van (2013). Mud dynamics in the Ems-Dollard, phase 2: Setup hydrodynamic models. Deltares report, project 120511-001.

Partheniades, E. (1965). Erosion and Deposition of Cohesive Soils. Journal of the Hydraulics Division, ASCE 91 (HY 1): 105–139.

Potter, I.C., Chuwen, B.M., Hoeksema, S.D. and Elliott, M. (2010). The concept of an estuary: A definition that incorporates systems which can become closed to the ocean and hypersaline. Estuarine, Coastal and Shelf Science, 87: 497–500

Rijn, L.C., van (2010). Tidal phenomena in the Scheldt Estuary. LTV Zandhuishouding Schelde Estuarium. Deltares report, project 1202016, 99 p.

Rijn, L.C. van (2011). Principles of fluid flow and surface waves in rivers, estuaries, seas and oceans (edition 2011). Aqua Publications, 900 p.

Schuttelaars, H.M., De Jonge, V.N. and Chernetsky, A. (2012). Improving the predictive power when modelling physical effects of human interventions in estuarine systems. Ocean & Coastal Management. doi:10.1016/j.ocecoaman.2012.05.009. In press.

Simpson, J.H., Brown, J., Matthews J. and Allen, G. (1990). Tidal straining, density currents, and stirring in the control of estuarine stratification. Estuaries, 26, 1579–1590.

Swart, H.E. de, and Zimmerman, J.T.F. (2009). Morphodynamics of Tidal Inlet Systems. Supplemental Material. Annual Review of Fluid Mechanics, 41:203-229. doi: 10.1146/annurev.fluid.010908.165159

Talke, S.A. and Swart, H.E. de (2006). Hydrodynamics and Morphology in the Ems/Dollard Estuary: Review of Models, Measurements, Scientific Literature, and the Effects of Changing Conditions. IMAU Report # R06-01. University of Utrecht, Institute for Marine and Atmospheric Research Utrecht (IMAU)

Talke, S.A. , Swart, H.E. de, and Schuttelaars H.M. (2009). Feedback between residual circulations and sediment distribution in highly turbid estuaries: An analytical model. Continental Shelf Research, 29: 119–135

Turner, J. S. (1973). Buoyancy Effects in Fluids, Cambridge Univ. Press, New York.

Vroom, J., Boogaard, H. van den, and Maren, D.S. van (2012). Mud dynamics in the Ems-Dollard, research phase 2: Analysis existing data. Deltares report, project 120511-001.

Winterwerp, J. C. (2001). Stratification effects by cohesive and noncohesive sediment. Journal of Geophysical Research. Vol . 106, no. C10, p.22.559-22.574

Winterwerp, J.C. (2006). Stratification effects by fine suspended sediment at low, medium, and very high concentrations. Journal of Geophysical Research, Vol. 111, C05012, doi:10.1029/2005JC003019

Winterwerp, J.C., Lely, M. and He, Q. (2009) Sediment-induced buoyancy destruction and drag reduction in estuaries. Ocean Dynamics, 59: 781-791. DOI:10.1007/s10236-009-0237-y

Winterwerp, J.C. (2011). Fine sediment transport by tidal asymmetry in the high-concentrated Ems River: indications for a regime shift in response to channel deepening. Ocean Dynamics, 61: 203-215. DOI: 10.1007/s1023-010-0332-0.

Appendix A: Historical bathymetries (reconstructed)

Two representative areas of each reconstructed bathymetry (1985, 1965 and 1945): the river stretch around Leerort and the Emden Fahrwasser.

1985 Lower Ems:

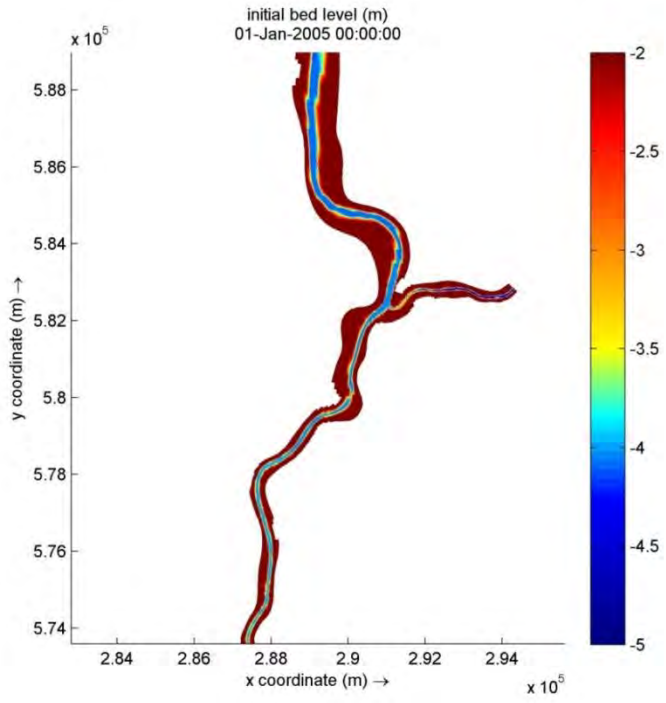

1985 Emden Fahrwasser:

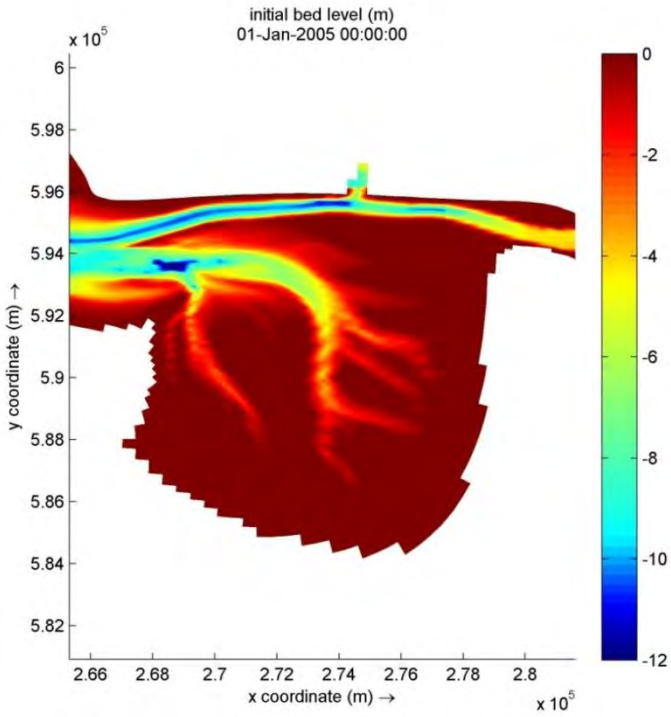

1965 Lower Ems:

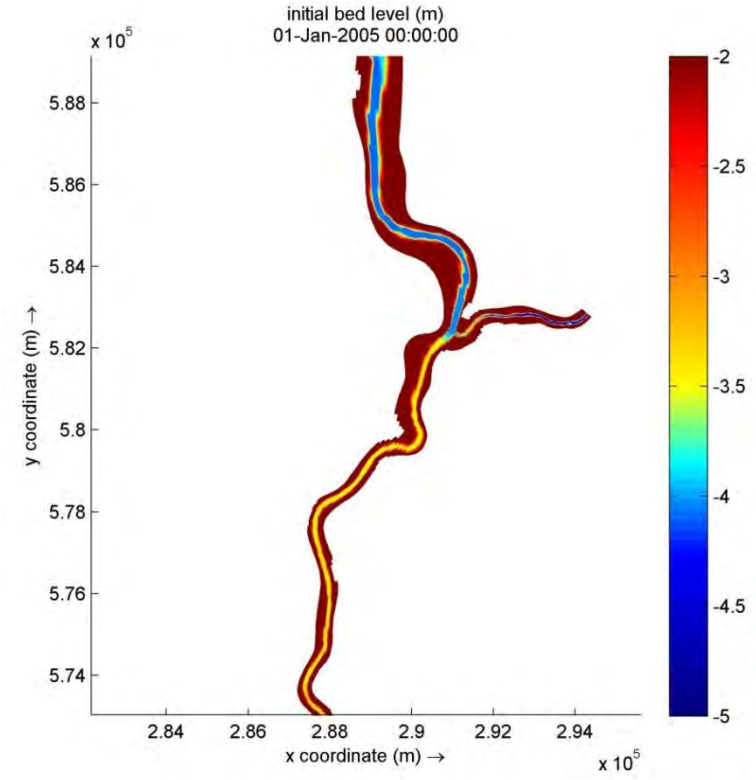

1965 Emden Fahrwasser:

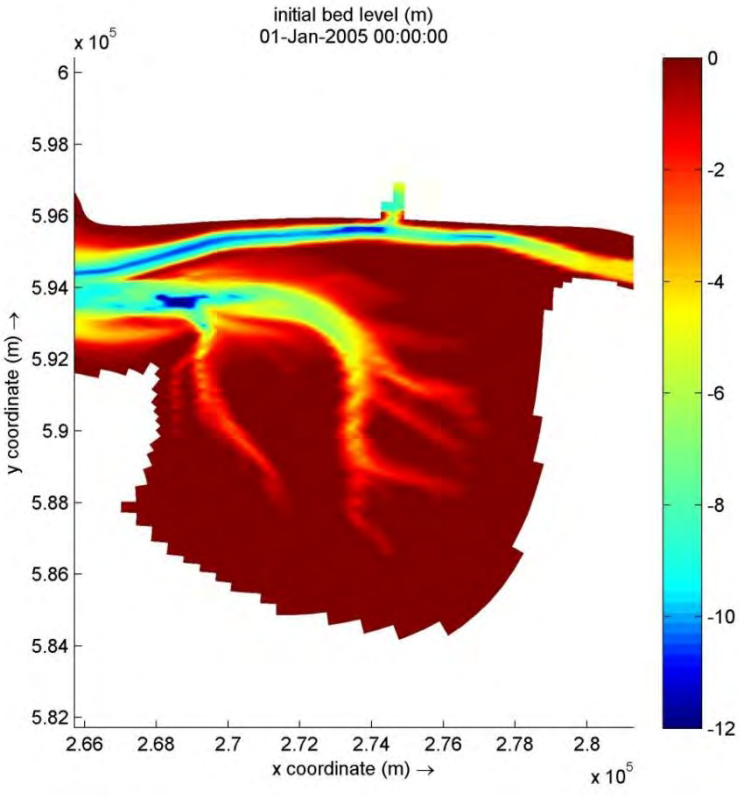

1945 Lower Ems:

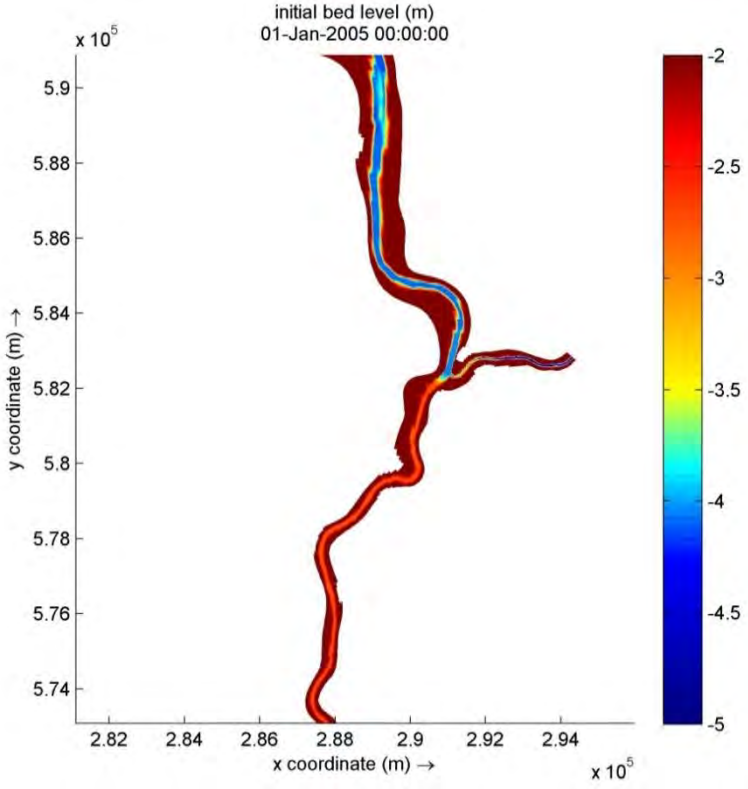

1945 Emden Fahrwasser:

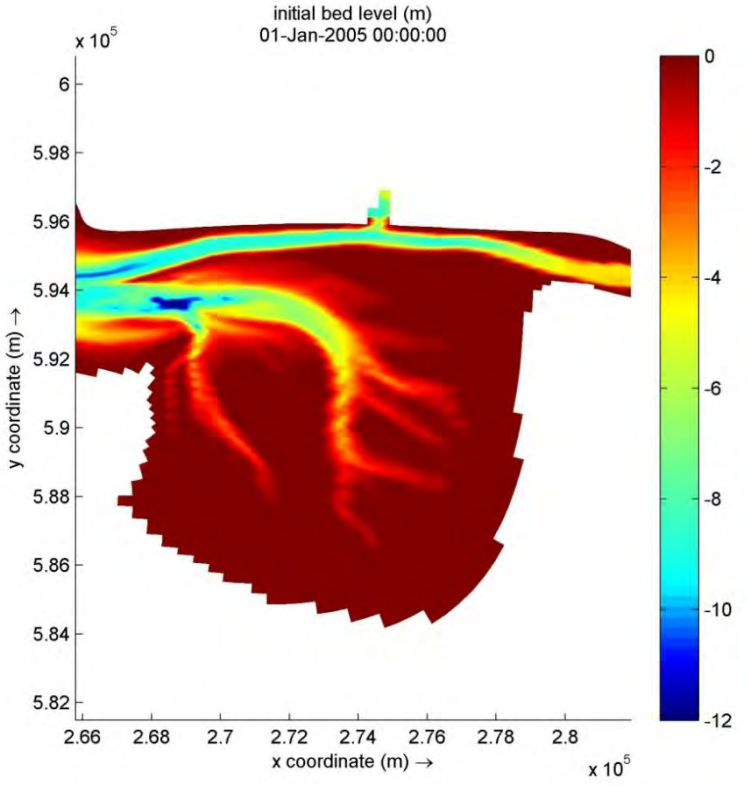

Appendix B: Measured and modelled MHW and MWL values

Comparison of measured and modelled mean high / low water levels for all water level stations. From Knock to Papenburg (in upstream direction):

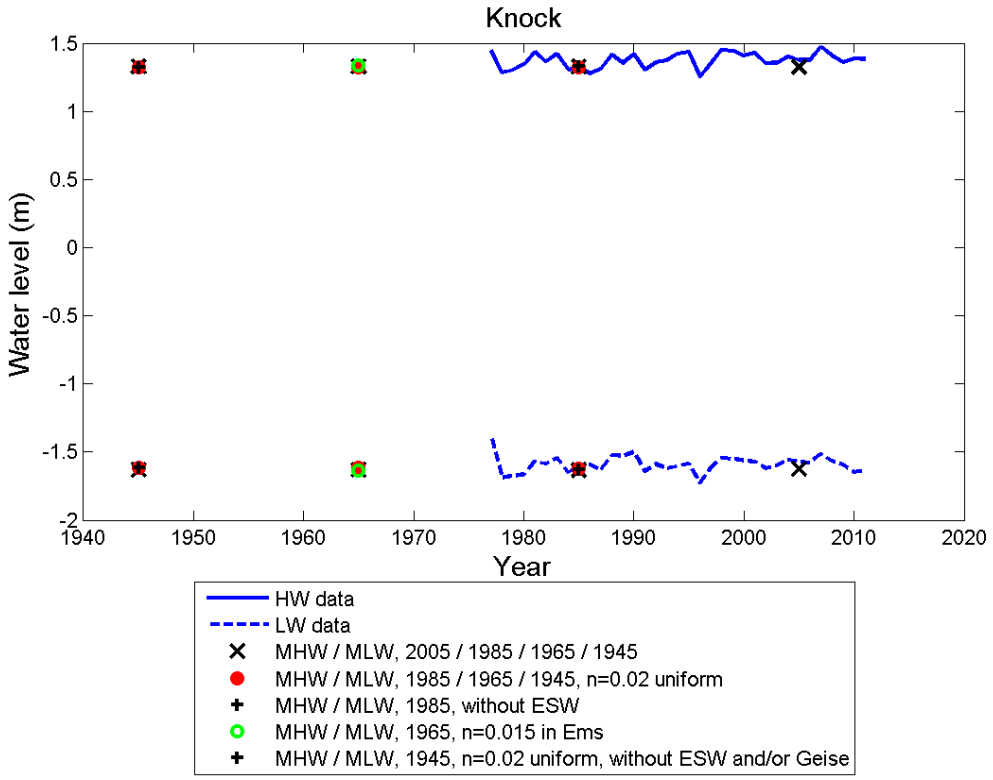

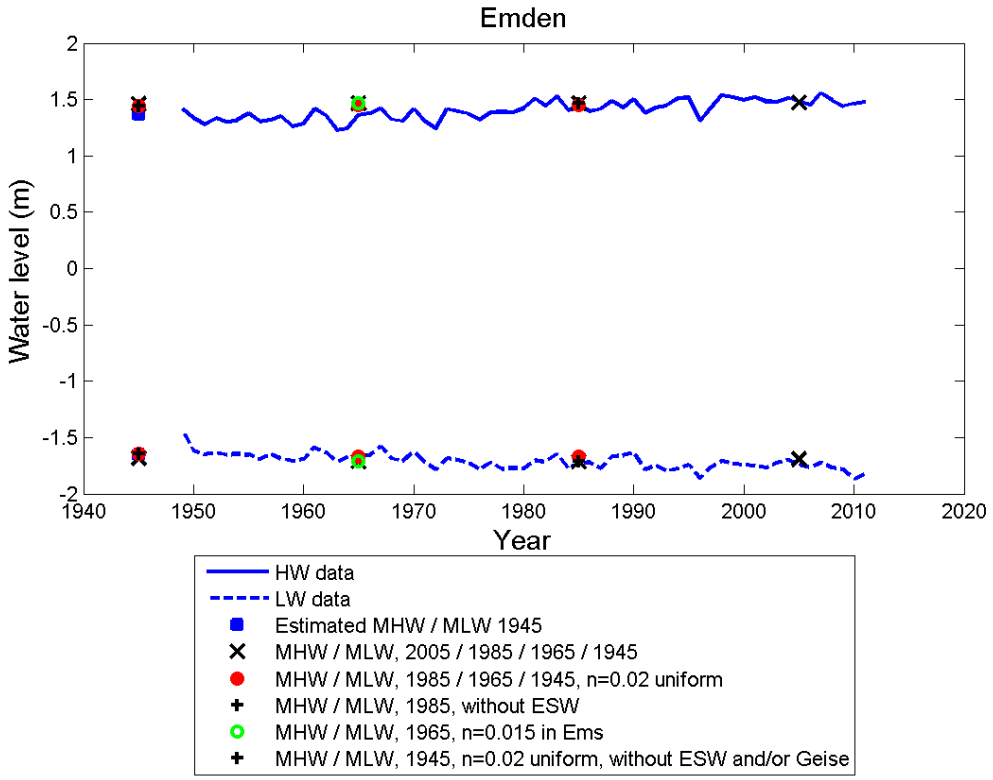

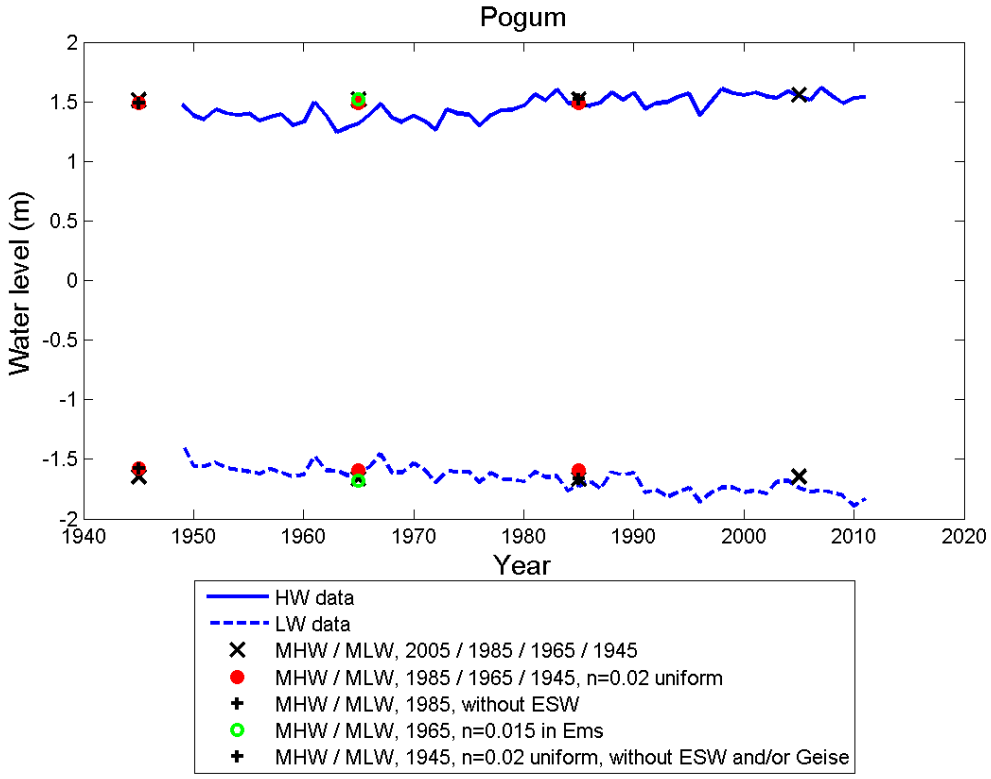
Pogum
Water level (m)
Year
HW data
LW data
MHW / MLW, 2005 / 1985 / 1965 / 1945
MHW / MLW, 1985 / 1965 / 1945, n=0.02 uniform
MHW / MLW, 1985, without ESW
MHW / MLW, 1965, n=0.015 in Ems
MHW / MLW, 1945, n=0.02 uniform, without ESW and/or Geise

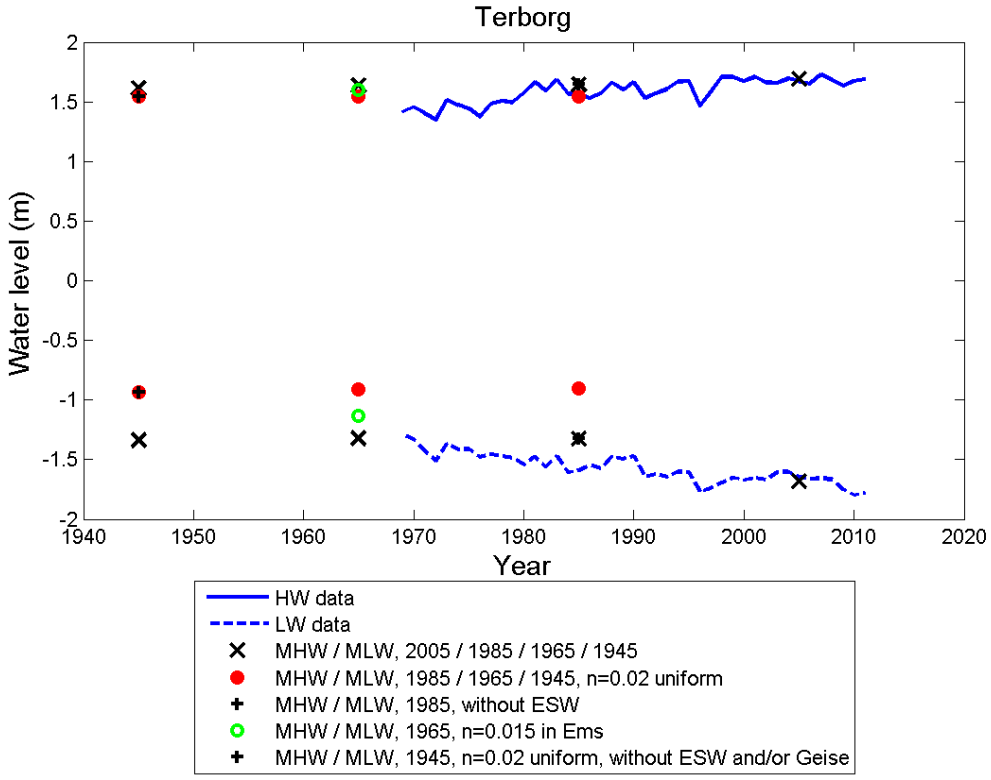
Terborg
Water level (m)
Year
HW data
LW data
MHW / MLW, 2005 / 1985 / 1965 / 1945
MHW / MLW, 1985 / 1965 / 1945, n=0.02 uniform
MHW / MLW, 1985, without ESW
MHW / MLW, 1965, n=0.015 in Ems
MHW / MLW, 1945, n=0.02 uniform, without ESW and/or Geise

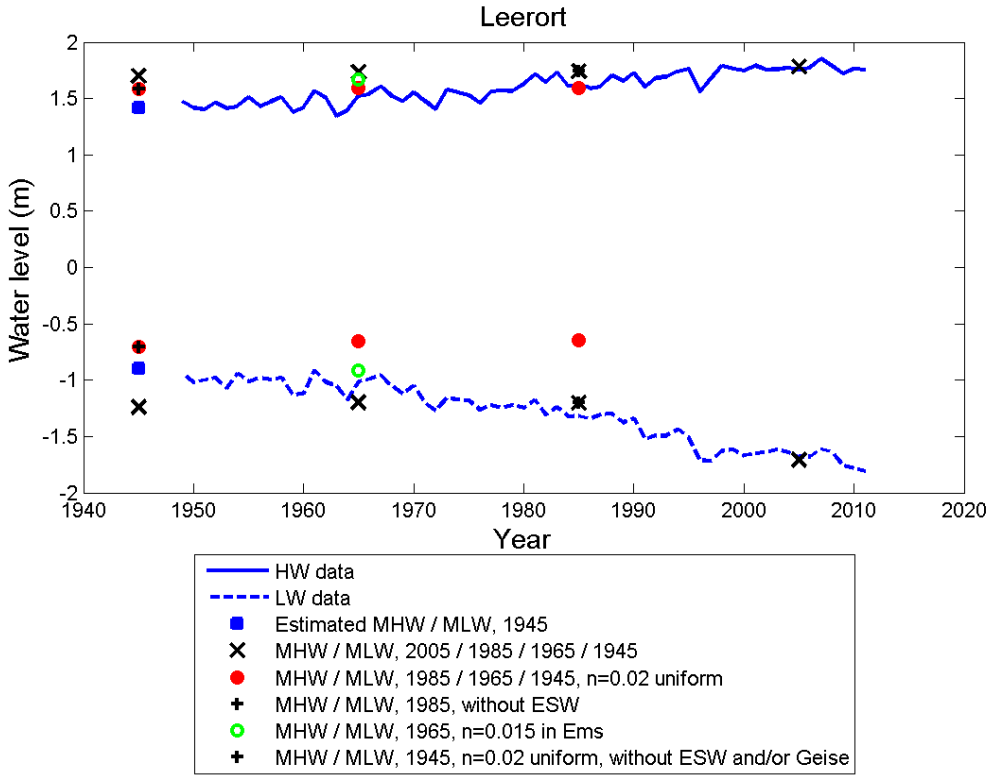
Leerort
Water level (m)
Year
HW data
LW data
Estimated MHW / MLW, 1945
MHW / MLW, 2005 / 1985 / 1965 / 1945
MHW / MLW, 1985 / 1965 / 1945, n=0.02 uniform
MHW / MLW, 1985, without ESW
MHW / MLW, 1965, n=0.015 in Ems
MHW / MLW, 1945, n=0.02 uniform, without ESW and/or Geise

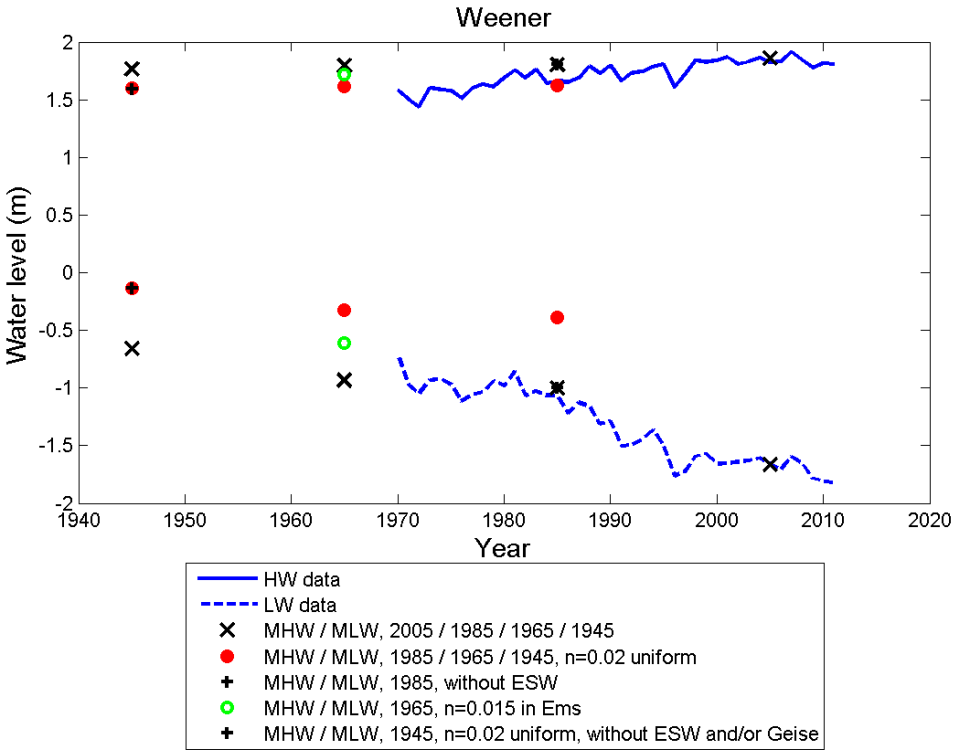
Weener
Water level (m)
Year
HW data
LW data
MHW / MLW, 2005 / 1985 / 1965 / 1945
MHW / MLW, 1985 / 1965 / 1945, n=0.02 uniform
MHW / MLW, 1985, without ESW
MHW / MLW, 1965, n=0.015 in Ems
MHW / MLW, 1945, n=0.02 uniform, without ESW and/or Geise

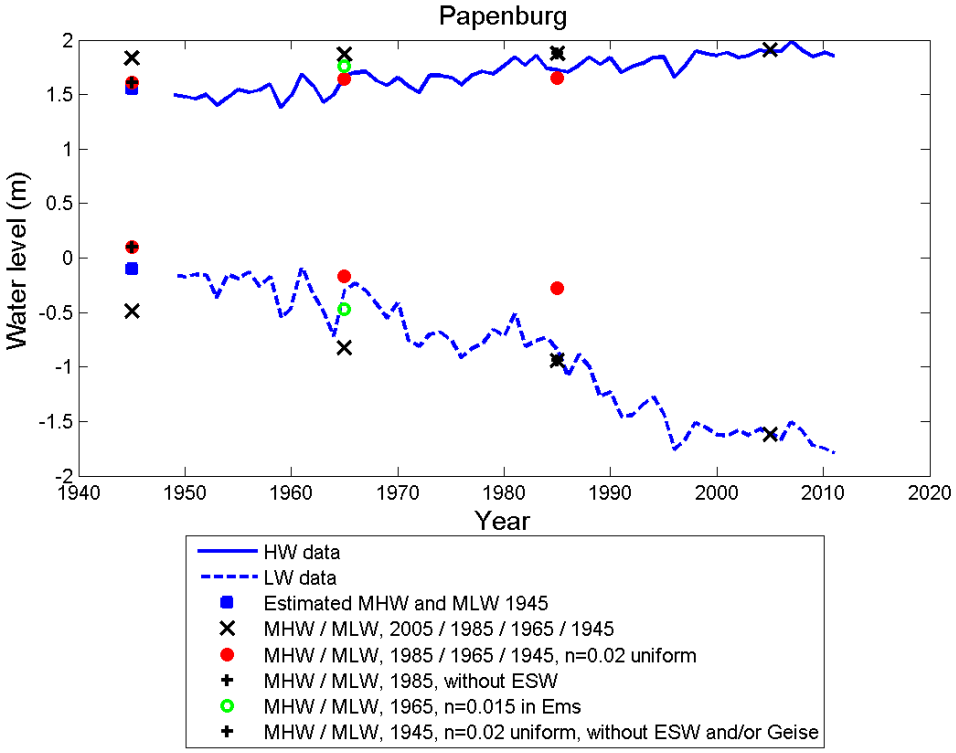
Papenburg
Water level (m)
Year
2
1.5
1
0.5
0
-0.5
-1
-1.5
-2
1940
1950
1960
1970
1980
1990
2000
2010
2020
HW data
LW data
Estimated MHW and MLW 1945
MHW / MLW, 2005 / 1985 / 1965 / 1945
MHW / MLW, 1985 / 1965 / 1945, n=0.02 uniform
MHW / MLW, 1985, without ESW
MHW / MLW, 1965, n=0.015 in Ems
MHW / MLW, 1945, n=0.02 uniform, without ESW and/or Geise

Appendix C: Water level and velocity

Comparison of water level (top) and velocity (bottom) between model situations for 2005, 1985, 1965 and 1945. 2005 water level observations are included when available. From Knock to Papenburg (in upstream direction):

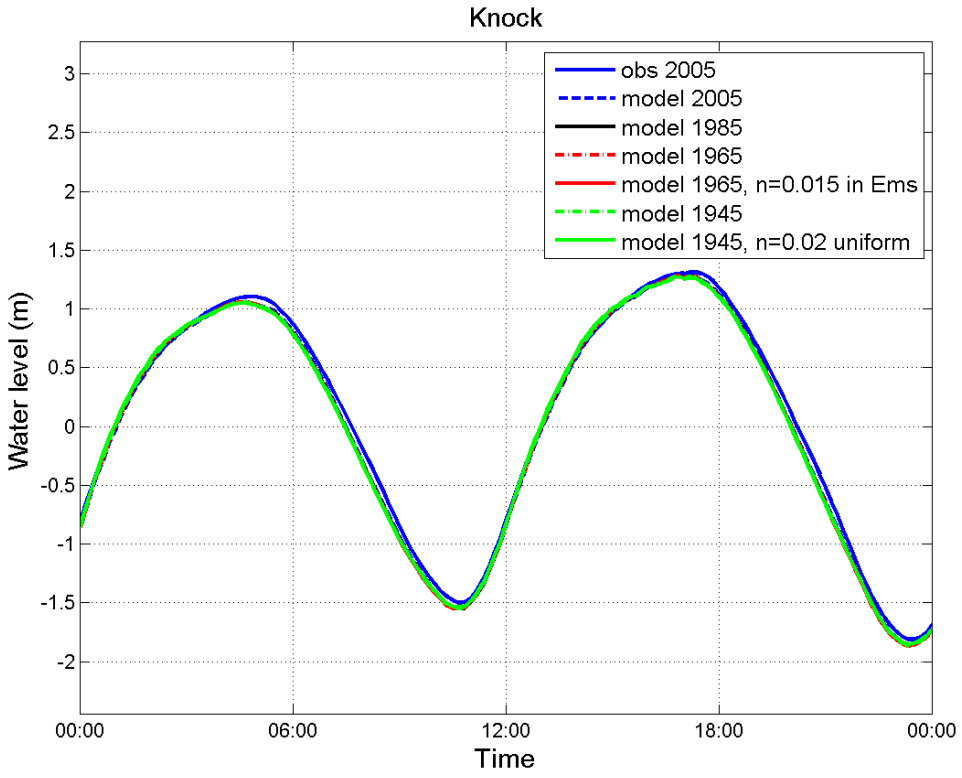

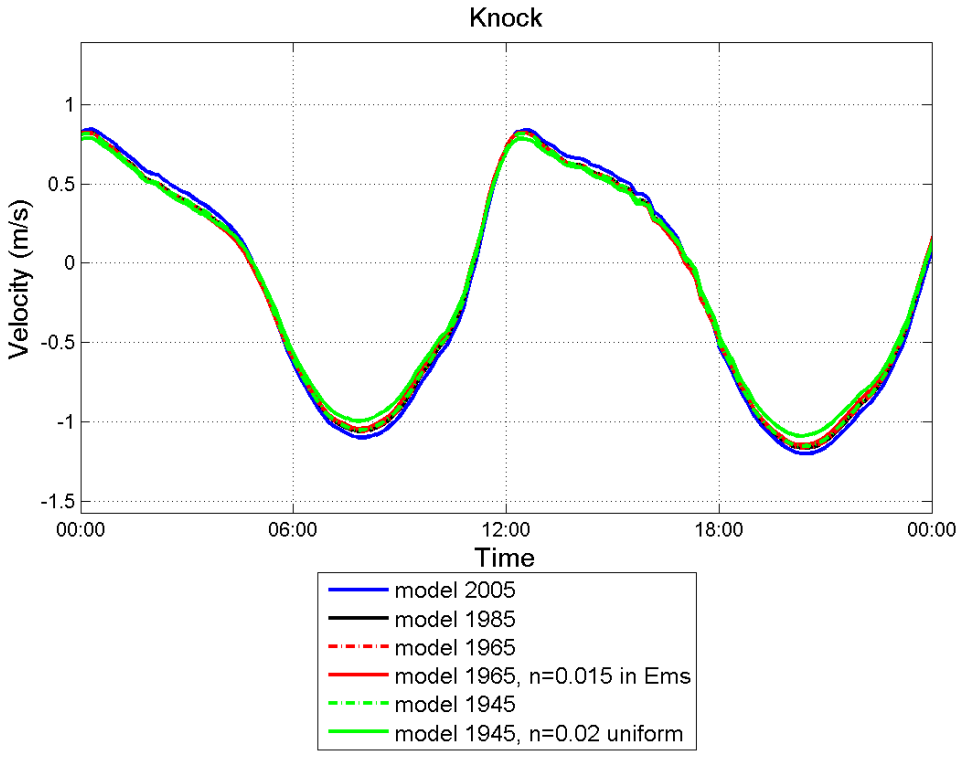

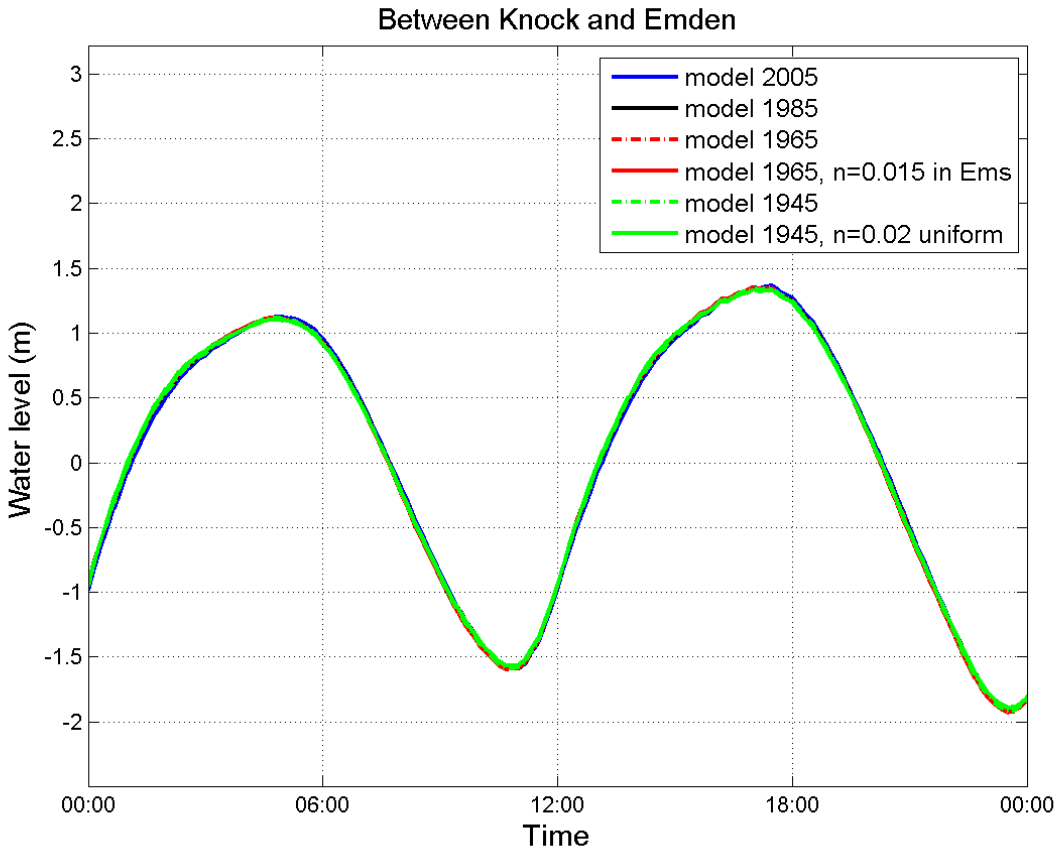
Between Knock and Emden
model 2005
model 1985
model 1965
model 1965, n=0.015 in Ems
model 1945
model 1945, n=0.02 uniform
Water level (m)
3
2.5
2
1.5
1
0.5
0
-0.5
-1
-1.5
-2
00:00
06:00
12:00
18:00
00:00
Time

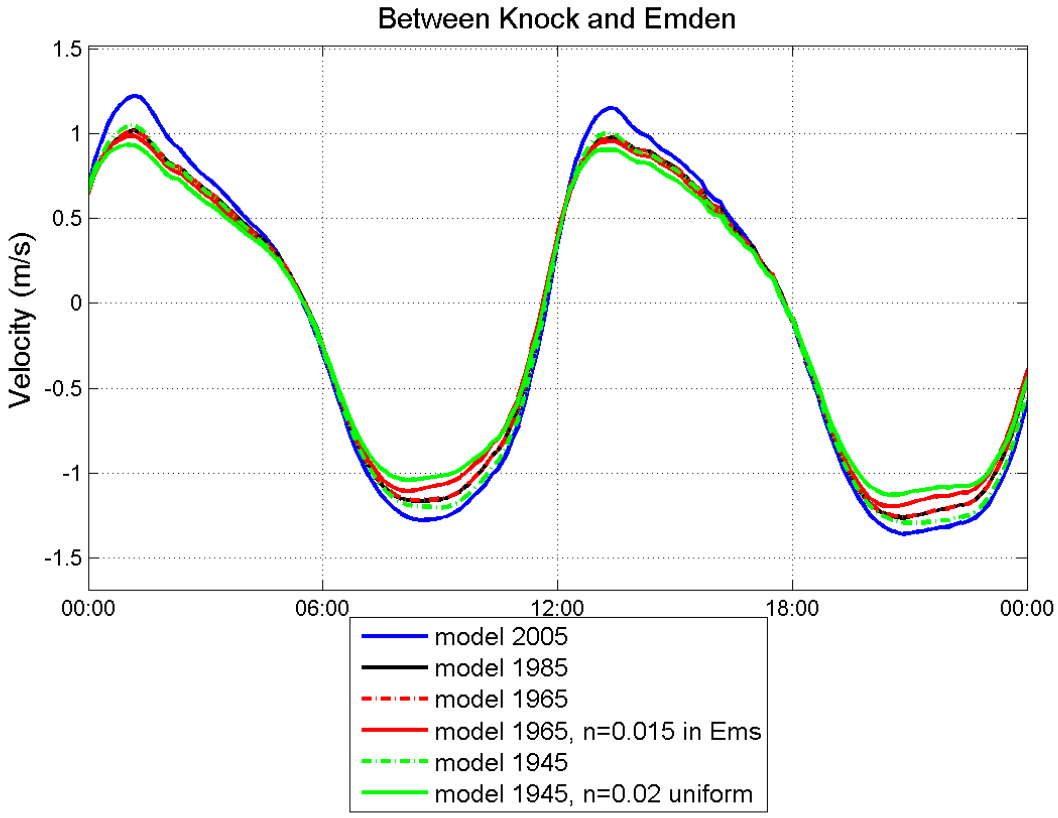
Between Knock and Emden
Velocity (m/s)
1.5
1
0.5
0
-0.5
-1
-1.5
00:00
06:00
12:00
18:00
00:00
model 2005
model 1985
model 1965
model 1965, n=0.015 in Ems
model 1945
model 1945, n=0.02 uniform

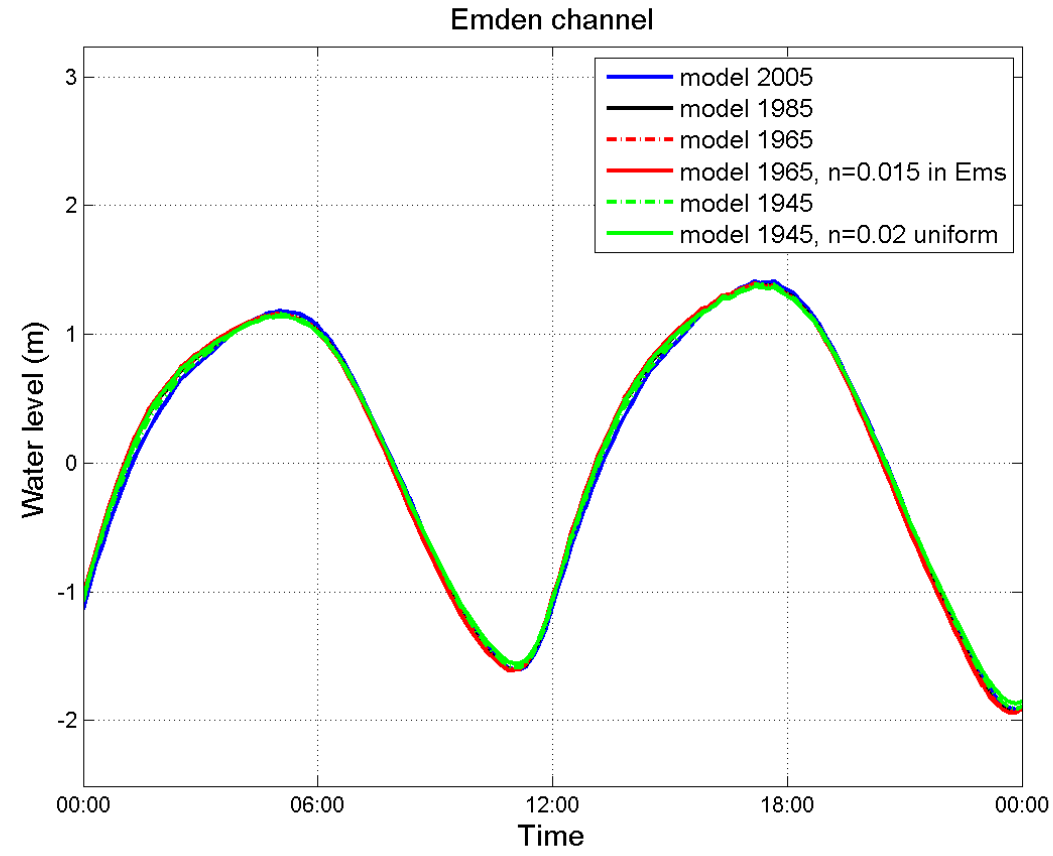
Emden channel
model 2005
model 1985
model 1965
model 1965, n=0.015 in Ems
model 1945
model 1945, n=0.02 uniform
Water level (m)
3
2
1
0
-1
-2
00:00
06:00
12:00
18:00
00:00
Time

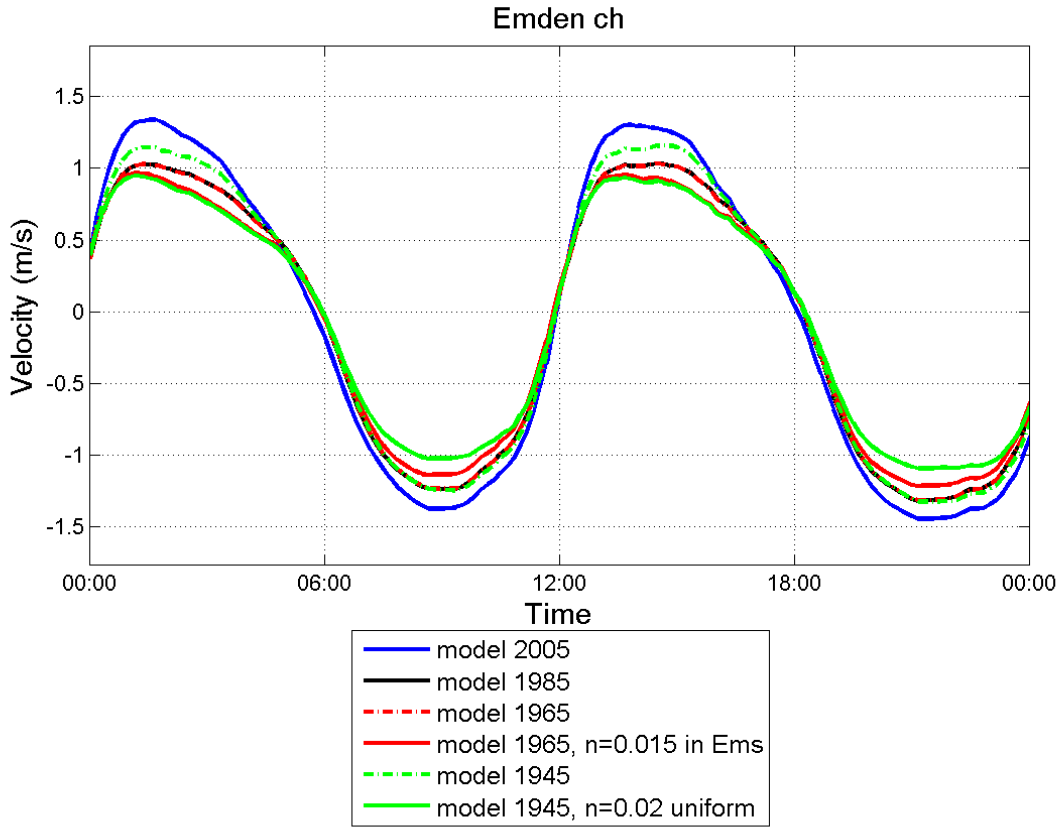
Emden ch
Velocity (m/s)
1.5
1
0.5
0
-0.5
-1
-1.5
00:00
06:00
12:00
18:00
00:00
Time
model 2005
model 1985
model 1965
model 1965, n=0.015 in Ems
model 1945
model 1945, n=0.02 uniform

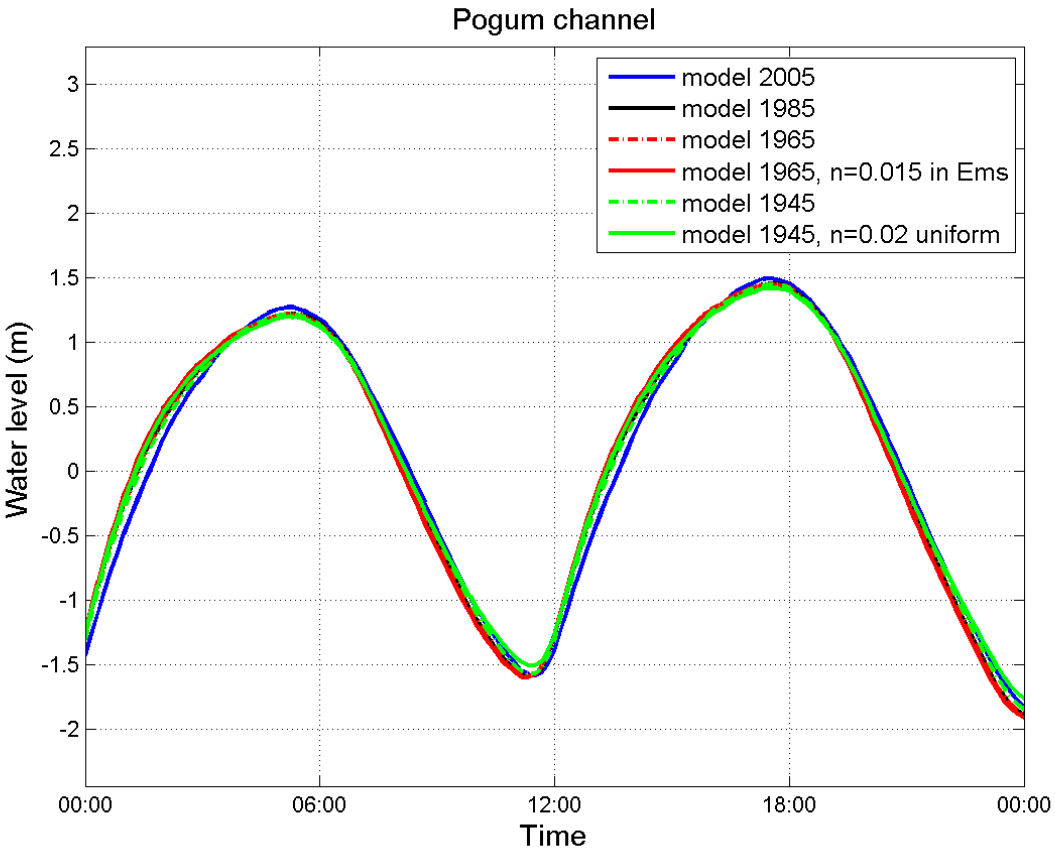
Pogum channel
model 2005
model 1985
model 1965
model 1965, n=0.015 in Ems
model 1945
model 1945, n=0.02 uniform
Water level (m)
3
2.5
2
1.5
1
0.5
0
-0.5
-1
-1.5
-2
00:00
06:00
12:00
18:00
00:00
Time

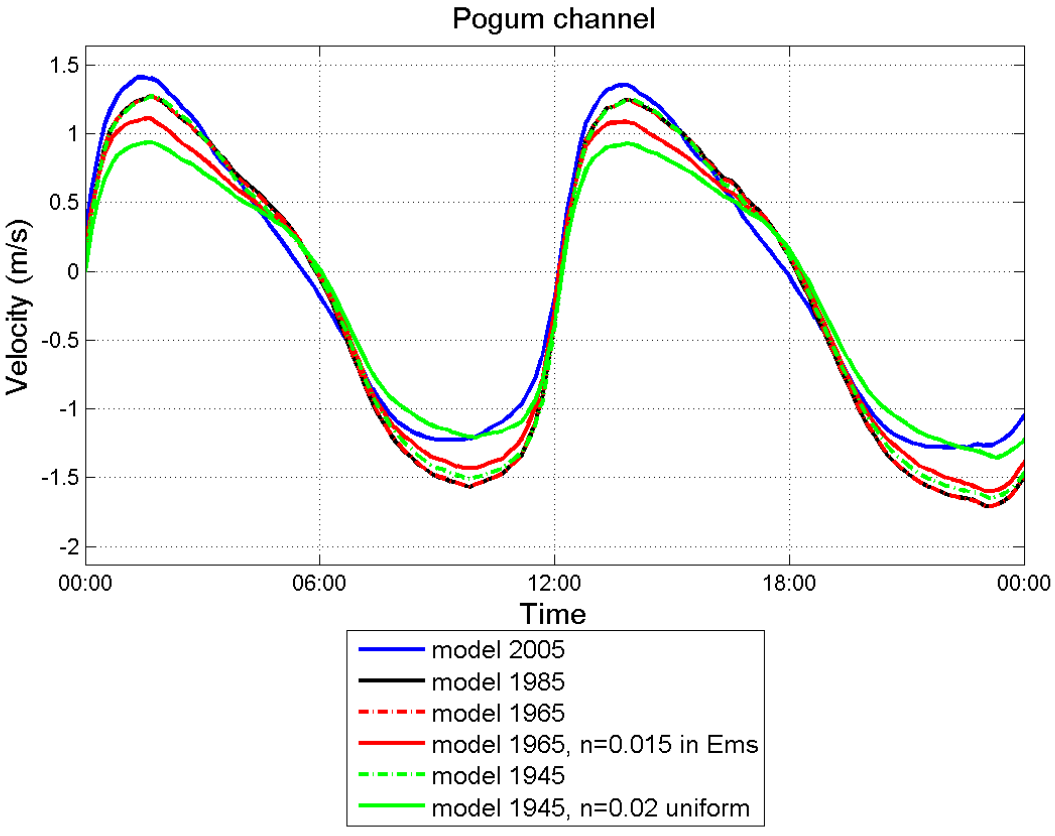
Pogum channel
Velocity (m/s)
1.5
1
0.5
0
-0.5
-1
-1.5
-2
00:00
06:00
12:00
18:00
00:00
Time
model 2005
model 1985
model 1965
model 1965, n=0.015 in Ems
model 1945
model 1945, n=0.02 uniform

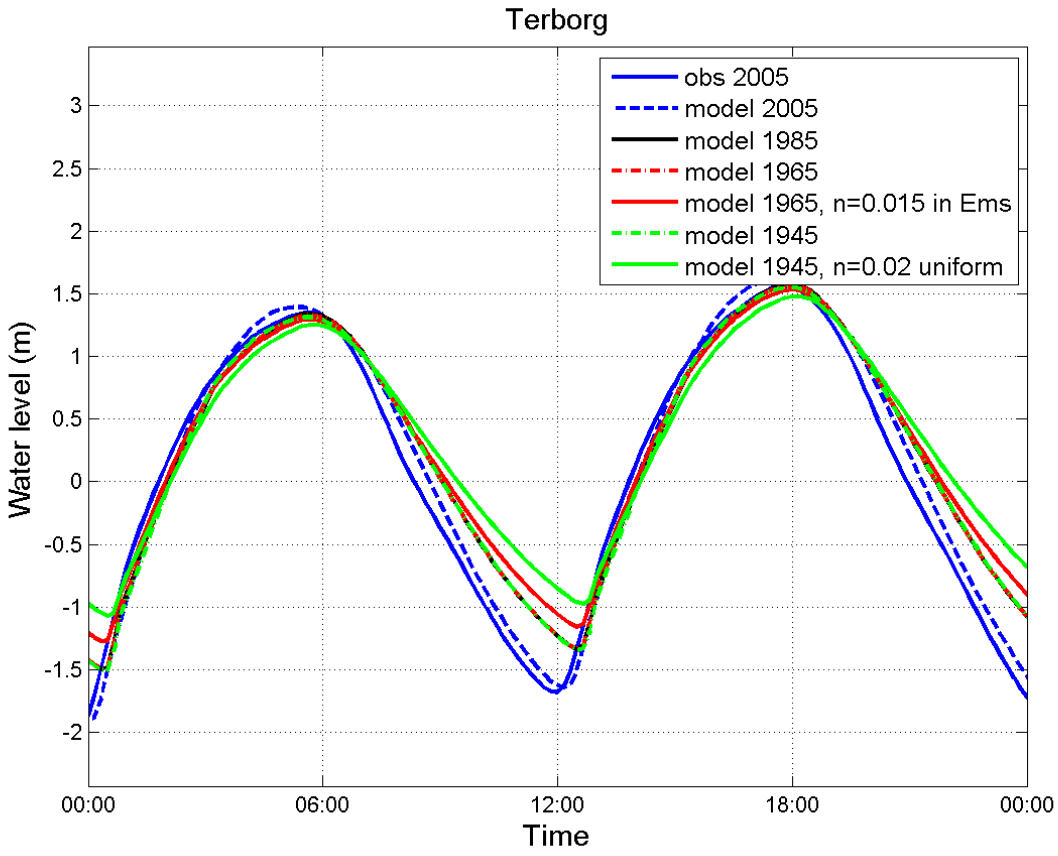
Terborg
obs 2005
model 2005
model 1985
model 1965
model 1965, n=0.015 in Ems
model 1945
model 1945, n=0.02 uniform
Water level (m)
3
2.5
2
1.5
1
0.5
0
-0.5
-1
-1.5
-2
00:00
06:00
12:00
18:00
00:00
Time

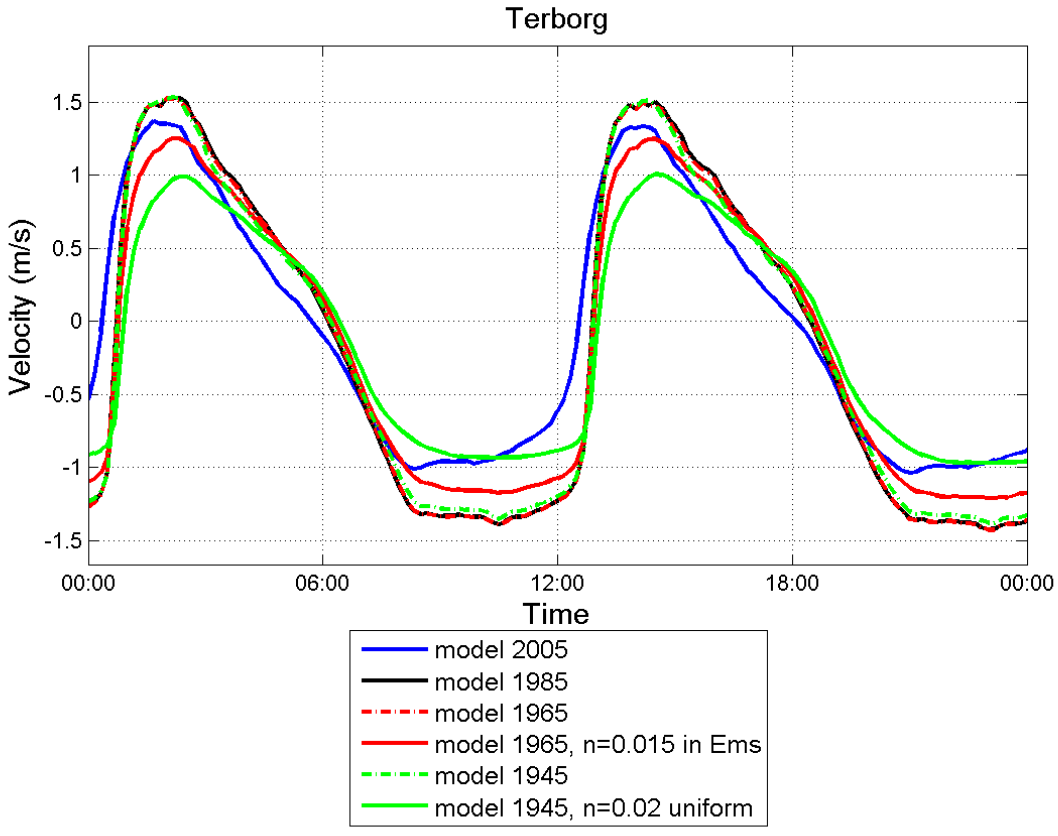
Terborg
Velocity (m/s)
1.5
1
0.5
0
-0.5
-1
-1.5
00:00
06:00
12:00
18:00
00:00
Time
model 2005
model 1985
model 1965
model 1965, n=0.015 in Ems
model 1945
model 1945, n=0.02 uniform

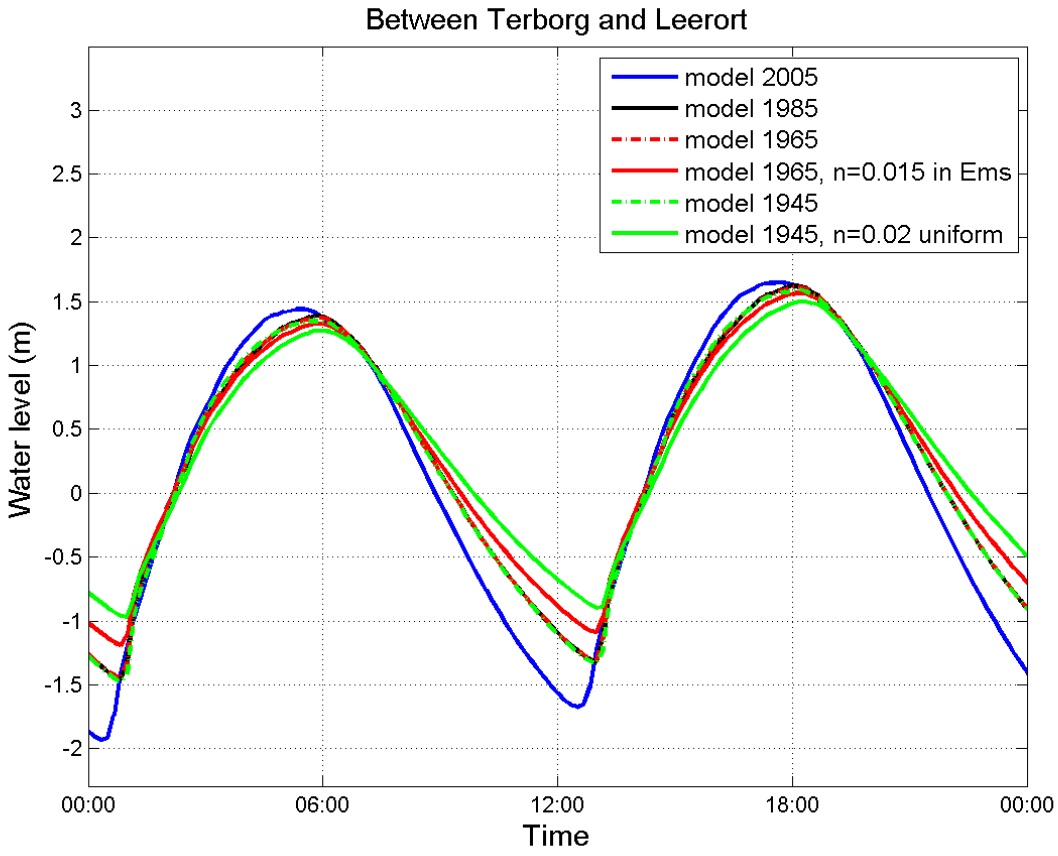
Between Terborg and Leerort
model 2005
model 1985
model 1965
model 1965, n=0.015 in Ems
model 1945
model 1945, n=0.02 uniform
Water level (m)
3
2.5
2
1.5
1
0.5
0
-0.5
-1
-1.5
-2
00:00
06:00
12:00
18:00
00:00
Time

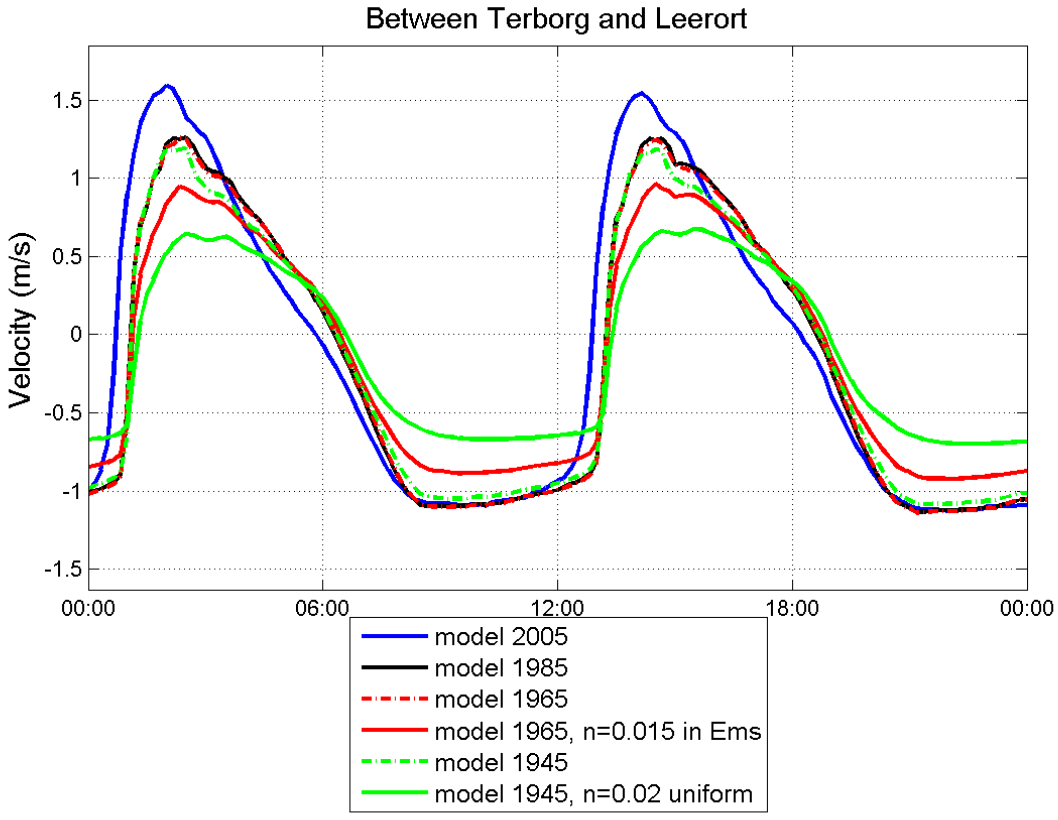
Between Terborg and Leerort
Velocity (m/s)
1.5
1
0.5
0
-0.5
-1
-1.5
00:00
06:00
12:00
18:00
00:00
model 2005
model 1985
model 1965
model 1965, n=0.015 in Ems
model 1945
model 1945, n=0.02 uniform

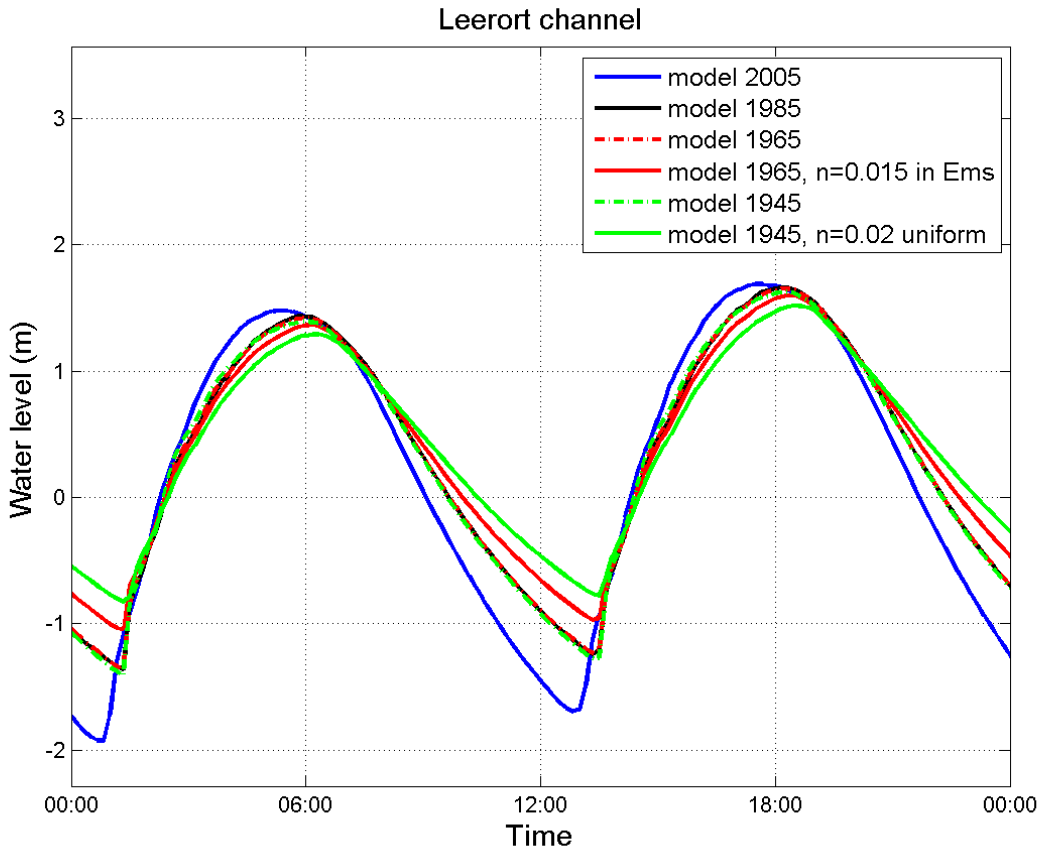
Leerort channel
model 2005
model 1985
model 1965
model 1965, n=0.015 in Ems
model 1945
model 1945, n=0.02 uniform
Water level (m)
3
2
1
0
-1
-2
00:00
06:00
12:00
18:00
00:00
Time

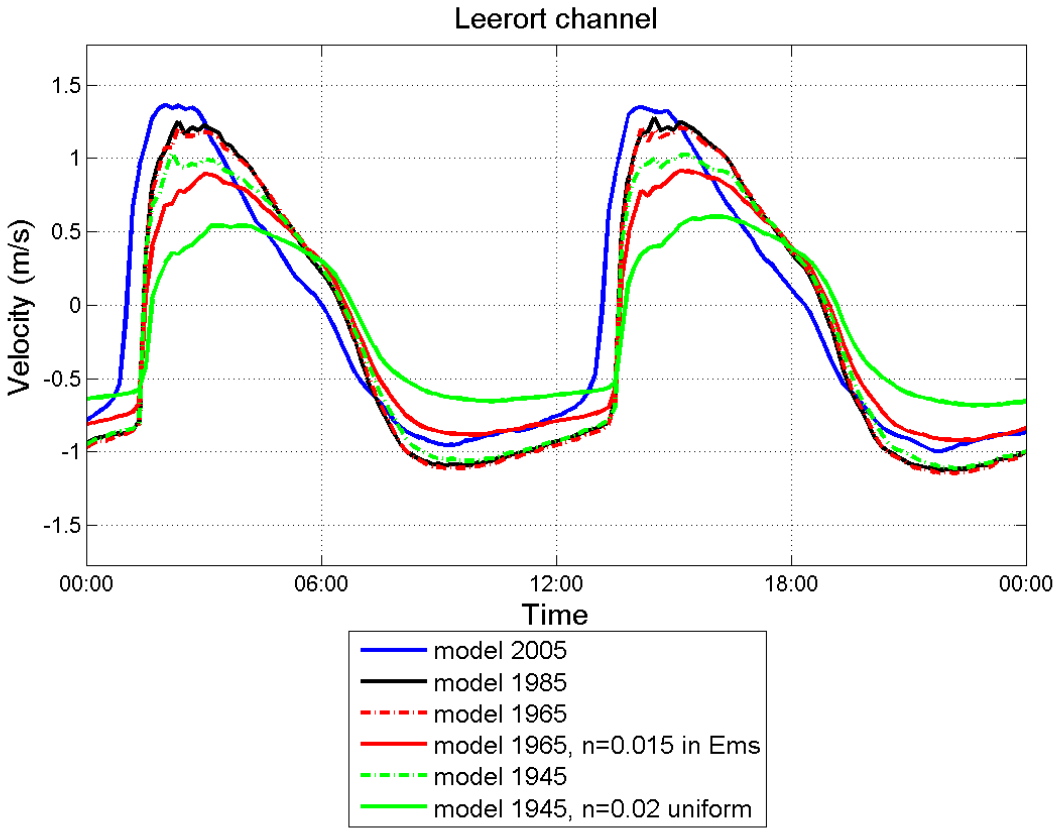
Leerort channel
Velocity (m/s)
1.5
1
0.5
0
-0.5
-1
-1.5
00:00
06:00
12:00
18:00
00:00
Time
model 2005
model 1985
model 1965
model 1965, n=0.015 in Ems
model 1945
model 1945, n=0.02 uniform

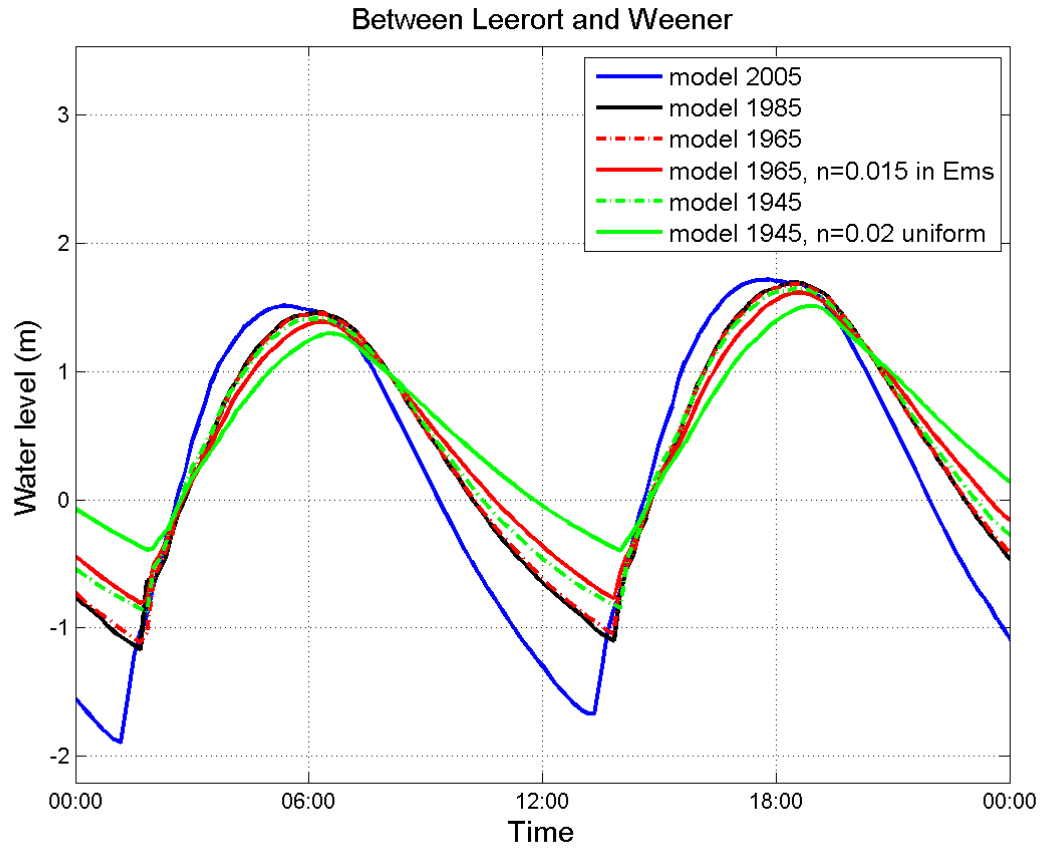
Between Leerort and Weener
model 2005
model 1985
model 1965
model 1965, n=0.015 in Ems
model 1945
model 1945, n=0.02 uniform
Water level (m)
3
2
1
0
-1
-2
00:00
06:00
12:00
18:00
00:00
Time

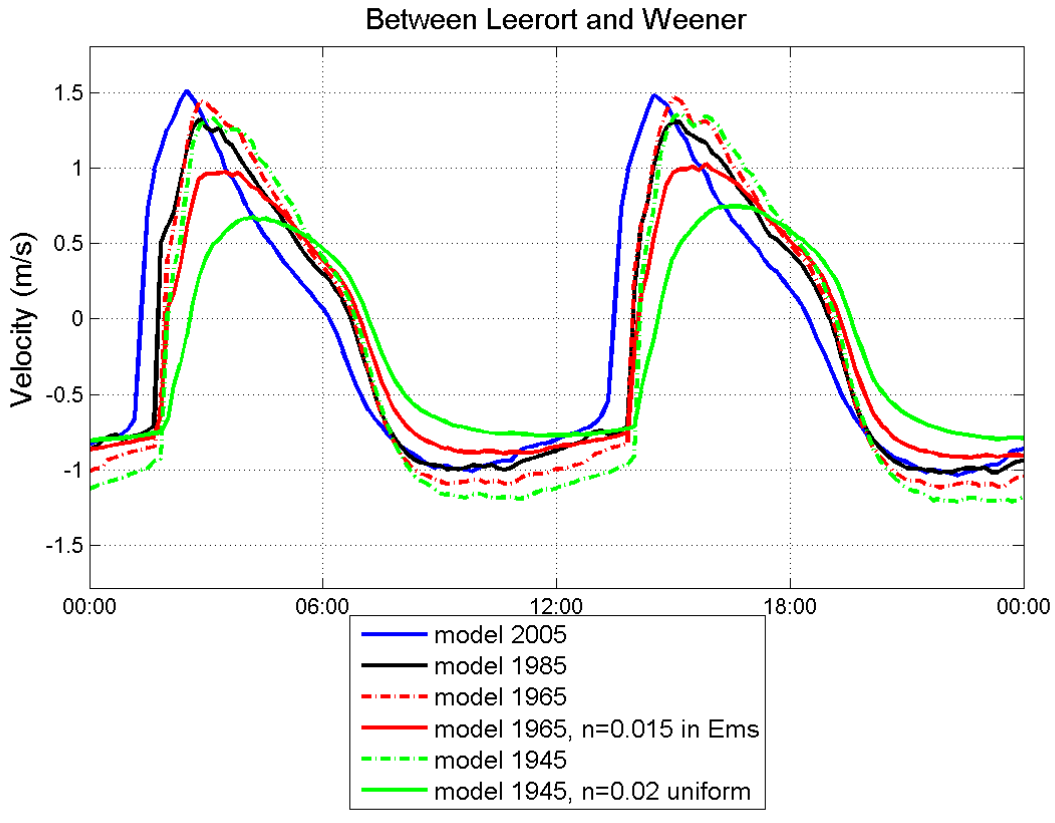
Between Leerort and Weener
Velocity (m/s)
1.5
1
0.5
0
-0.5
-1
-1.5
00:00
06:00
12:00
18:00
00:00
model 2005
model 1985
model 1965
model 1965, n=0.015 in Ems
model 1945
model 1945, n=0.02 uniform

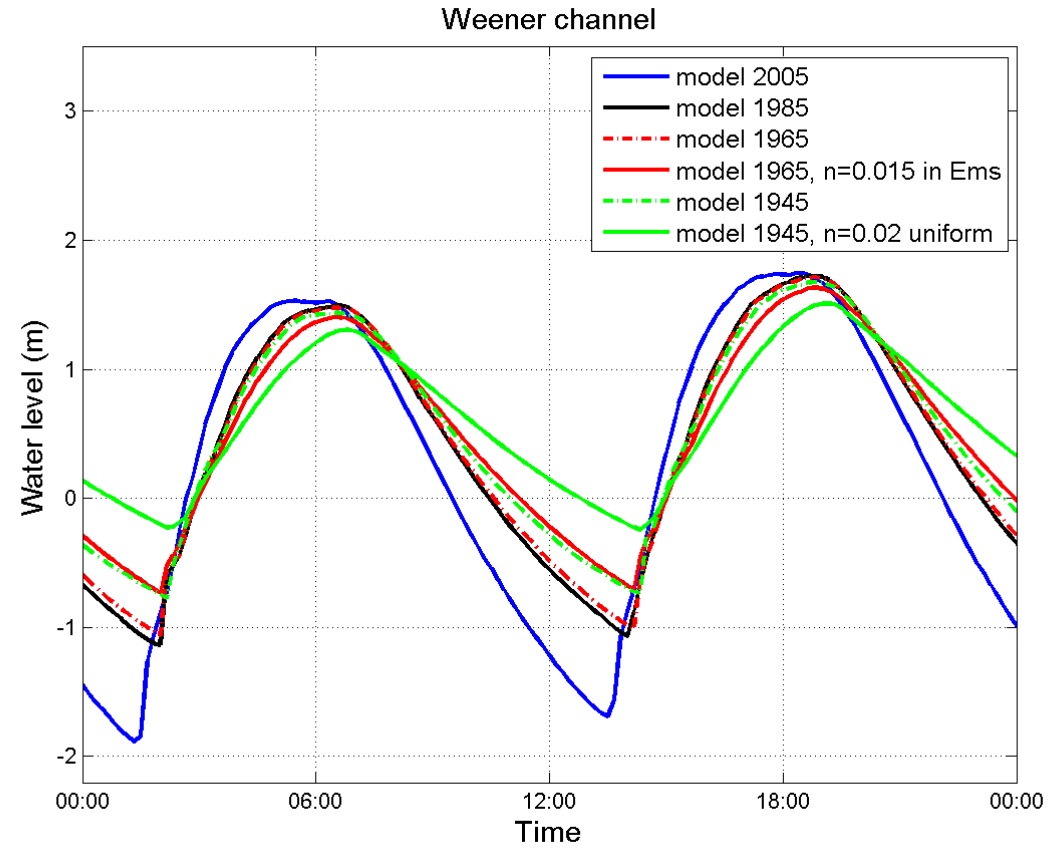
Weener channel
model 2005
model 1985
model 1965
model 1965, n=0.015 in Ems
model 1945
model 1945, n=0.02 uniform
Water level (m)
3
2
1
0
-1
-2
00:00
06:00
12:00
18:00
00:00
Time

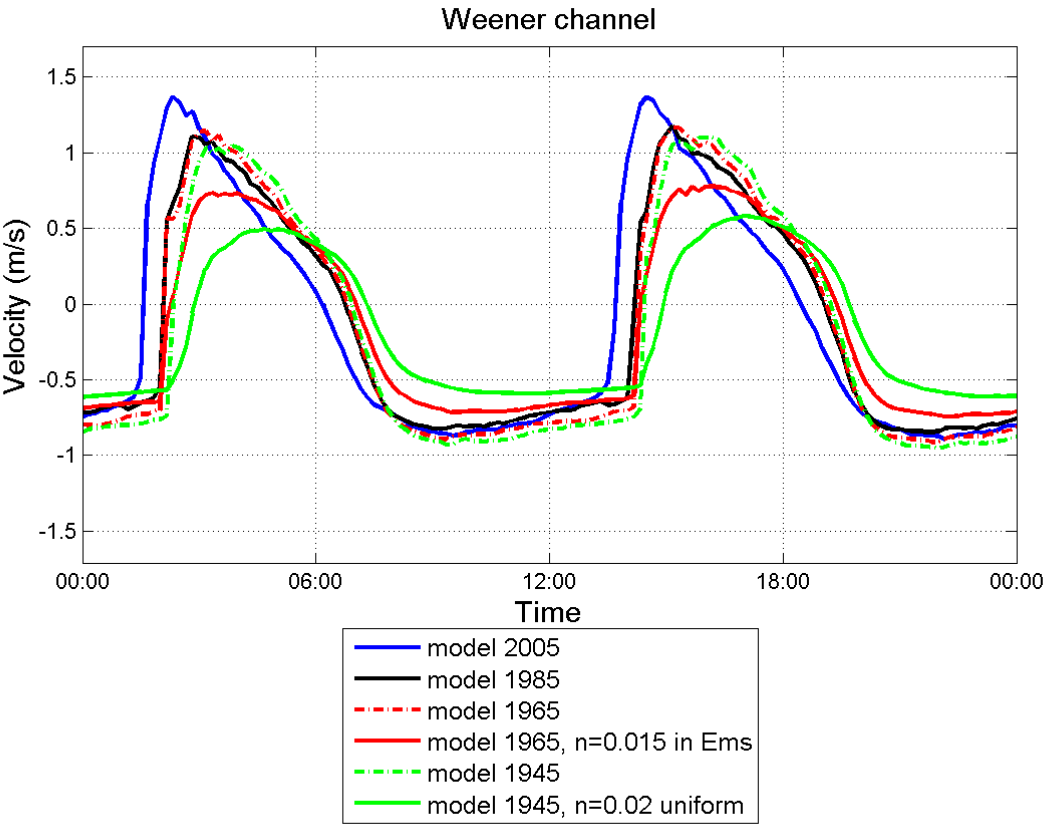
Weener channel
Velocity (m/s)
1.5
1
0.5
0
-0.5
-1
-1.5
00:00
06:00
12:00
18:00
00:00
Time
model 2005
model 1985
model 1965
model 1965, n=0.015 in Ems
model 1945
model 1945, n=0.02 uniform

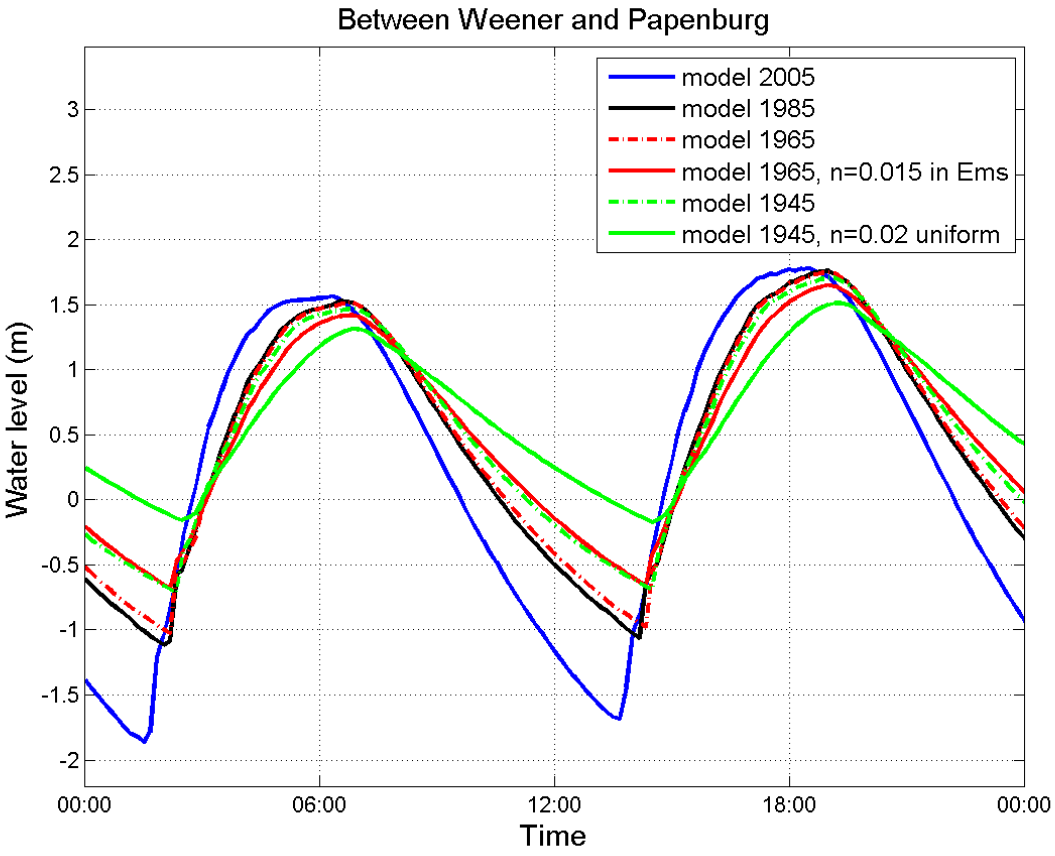
Between Weener and Papenburg
model 2005
model 1985
model 1965
model 1965, n=0.015 in Ems
model 1945
model 1945, n=0.02 uniform
Water level (m)
3
2.5
2
1.5
1
0.5
0
-0.5
-1
-1.5
-2
00:00
06:00
12:00
18:00
00:00
Time

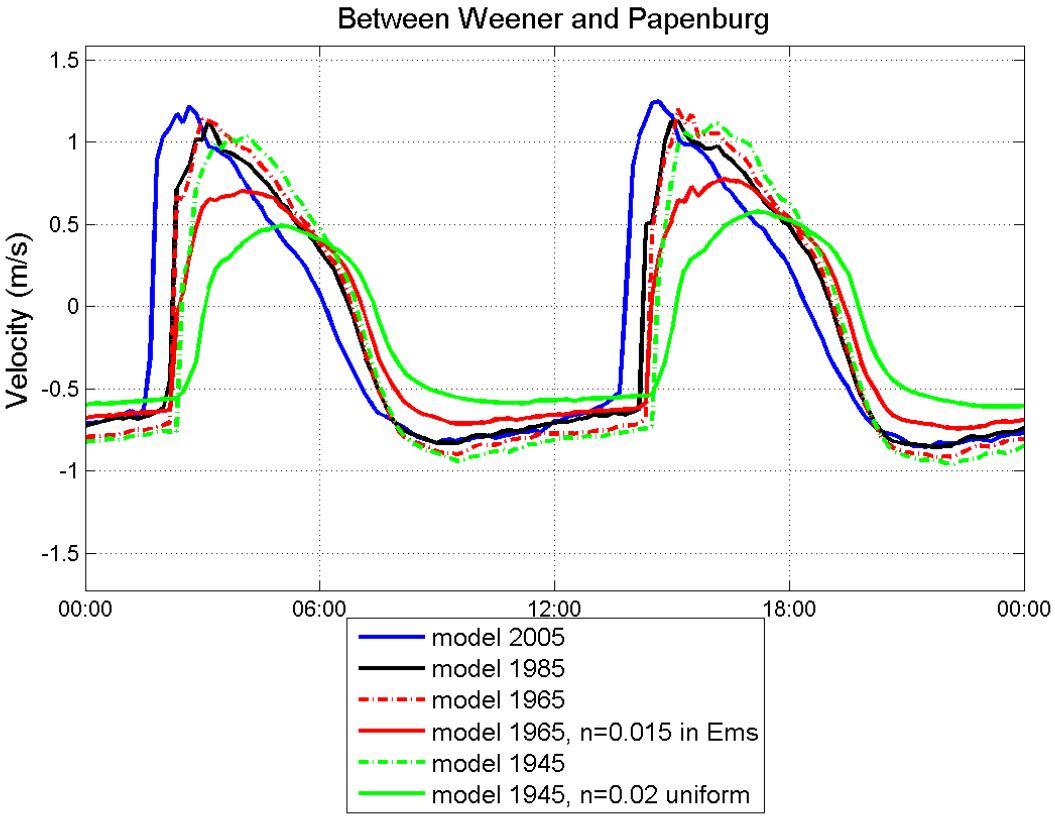
Between Weener and Papenburg
Velocity (m/s)
1.5
1
0.5
0
-0.5
-1
-1.5
00:00
06:00
12:00
18:00
00:00
model 2005
model 1985
model 1965
model 1965, n=0.015 in Ems
model 1945
model 1945, n=0.02 uniform

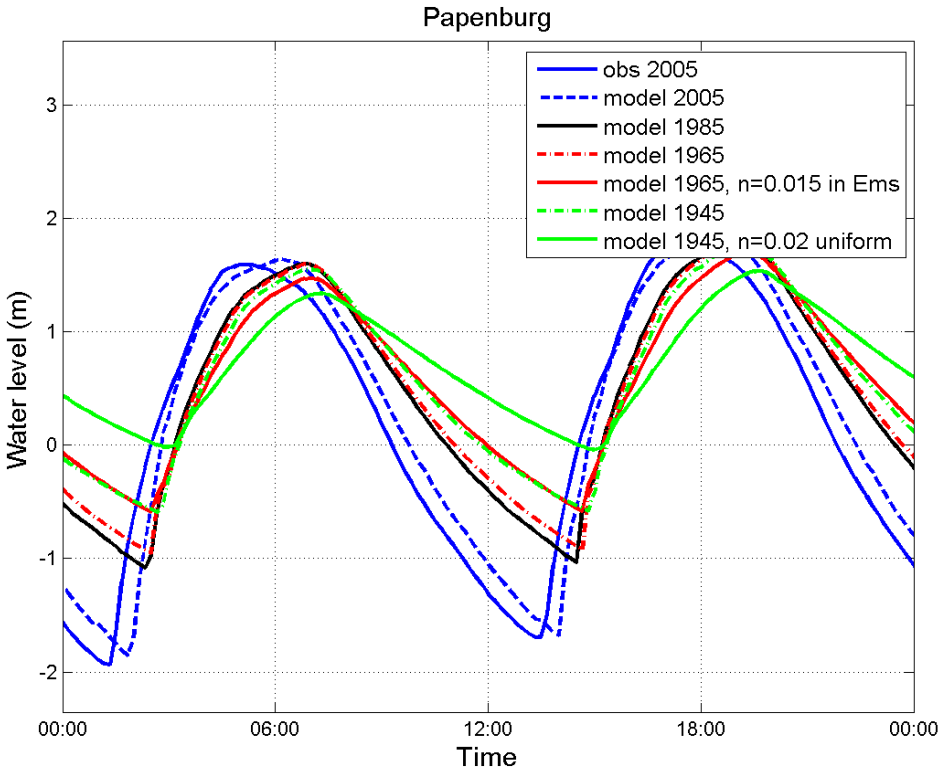
Papenburg
obs 2005
model 2005
model 1985
model 1965
model 1965, n=0.015 in Ems
model 1945
model 1945, n=0.02 uniform
Water level (m)
3
2
1
0
-1
-2
00:00
06:00
12:00
18:00
00:00
Time

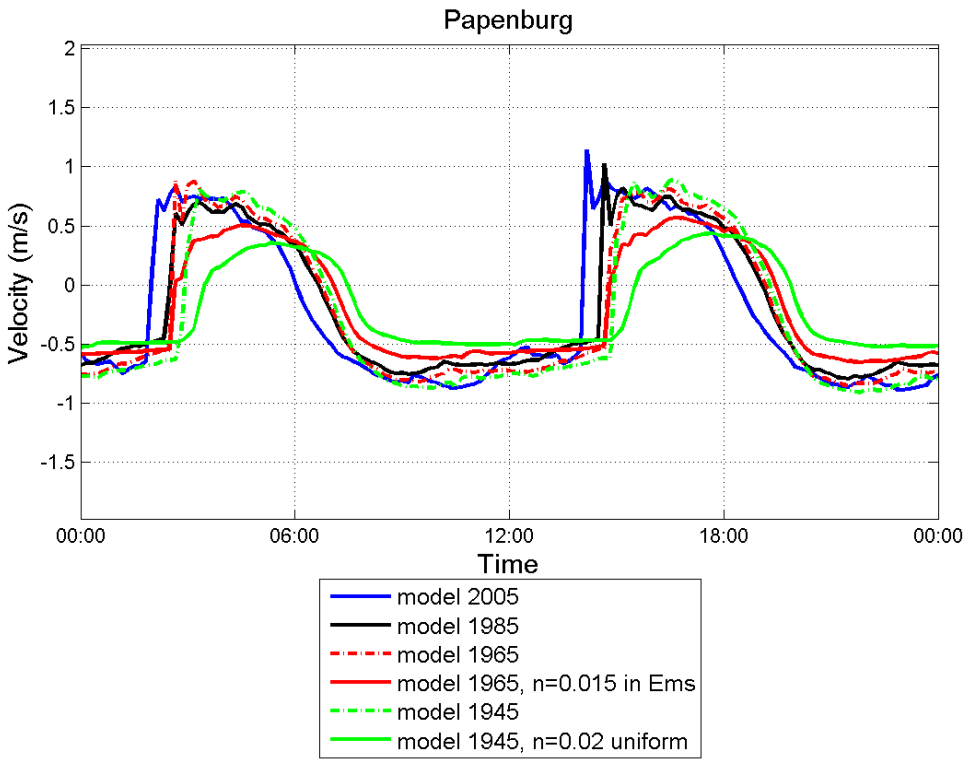
Papenburg
Velocity (m/s)
2
1.5
1
0.5
0
-0.5
-1
-1.5
00:00
06:00
12:00
18:00
00:00
Time
model 2005
model 1985
model 1965
model 1965, n=0.015 in Ems
model 1945
model 1945, n=0.02 uniform

Appendix D: Residual circulation and salinity

(next pages)

From Knock to Papenburg, in upstream direction.

- Magnitude and direction of residual circulation averaged over one spring-neap cycle: (discharges are measured values from 2005 at weir Versen near Herbrum)
    - High discharge, spring-neap cycle: 100-225 m^3/s 9 feb - 23 feb
    - Low discharge, spring-neap cycle: 30-60 m^3/s 20 jun - 4 jul
- Salinity in ppt. Salinity difference is determined by bottom layer – surface layer.

Residual current, high Q (spring-neap cycle):

Residual current, low Q (spring-neap cycle):

KNOCK

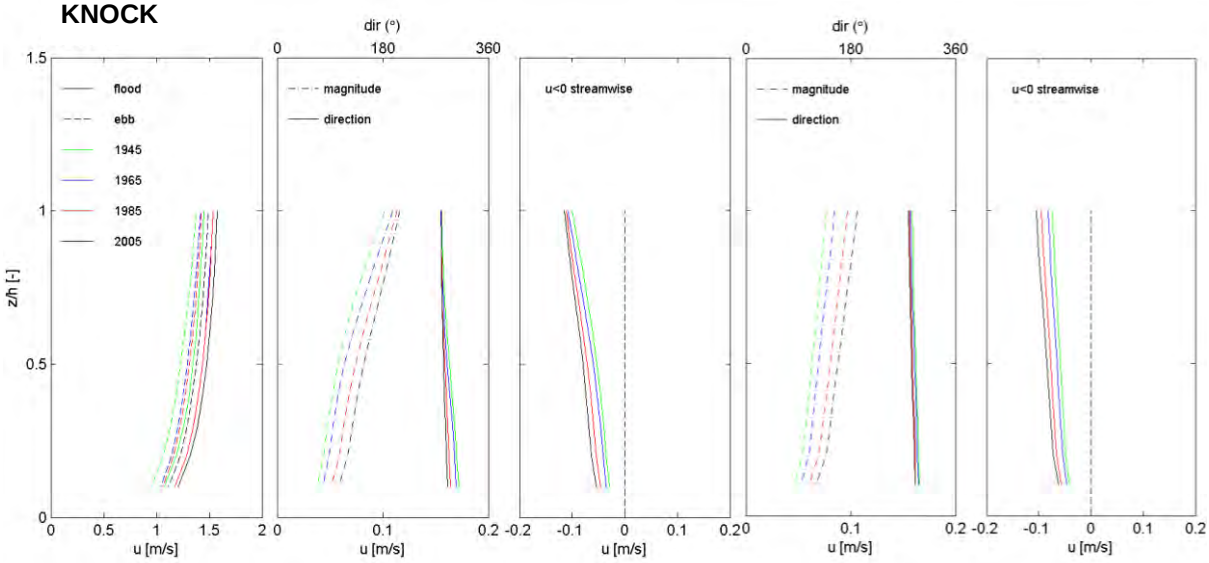

Salinity, high Q (spring-neap cycle):

Salinity, high Q (1 day):

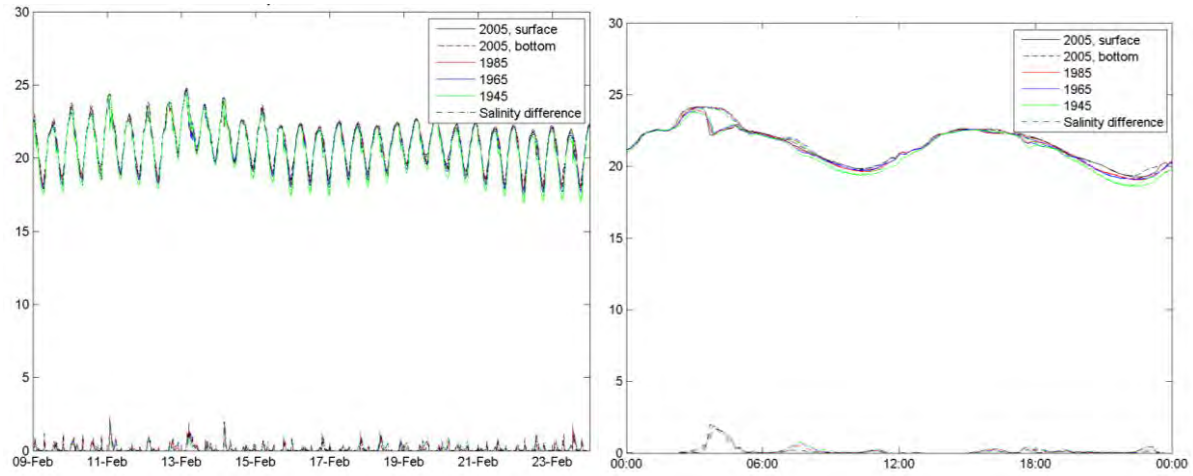

Salinity, low Q (spring-neap cycle):

Salinity, low Q (1 day):

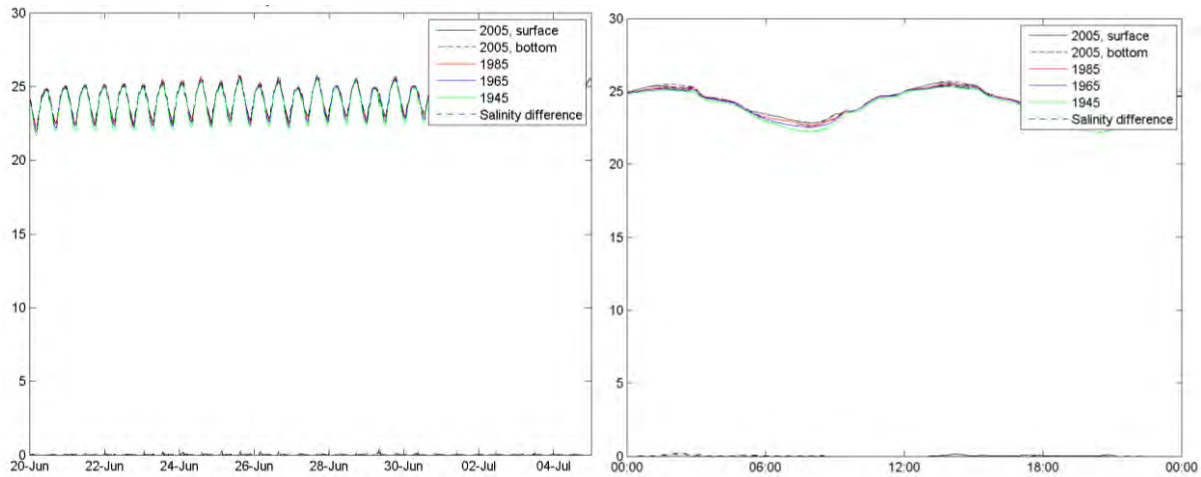

GEISE TRAINING WALL NEAR KNOCK

Residual current, high Q (spring-neap cycle):

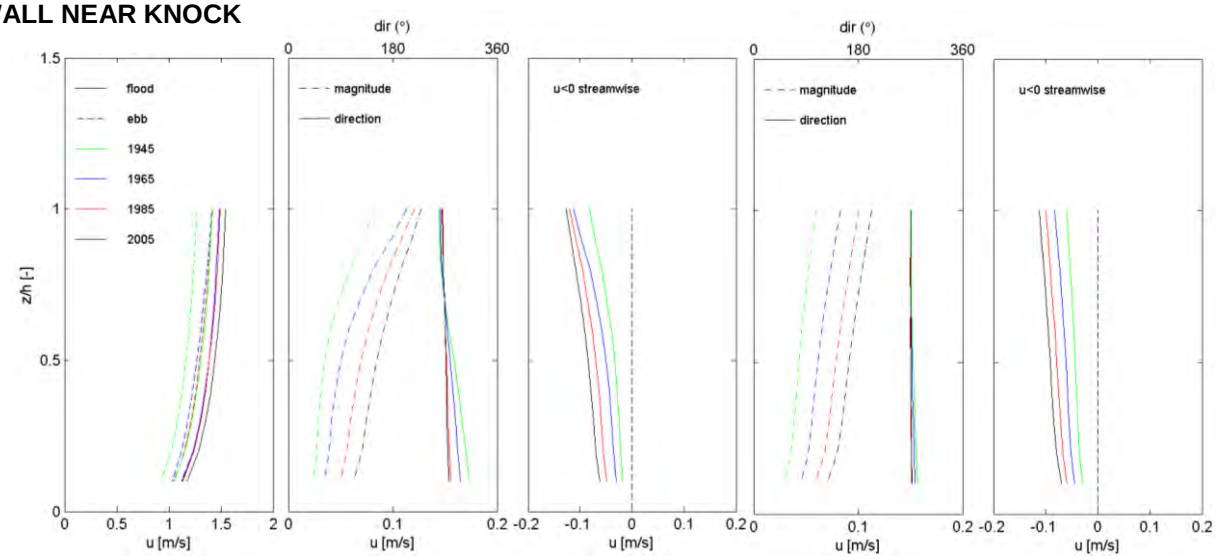

Residual current, low Q (spring-neap cycle):

Salinity, high Q (spring-neap cycle):

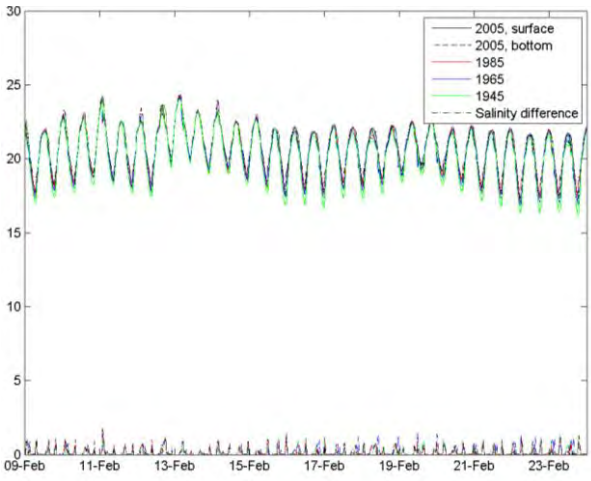

Salinity, high Q (1 day):

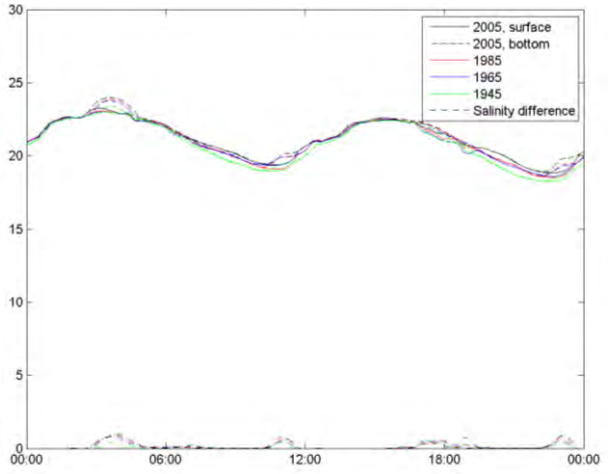

Salinity, low Q (spring-neap cycle):

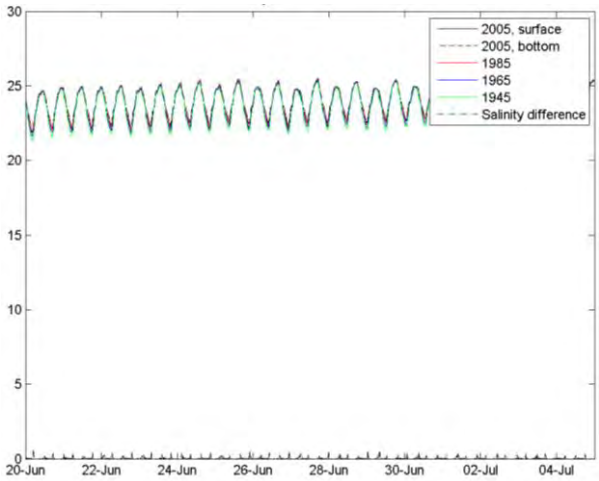

Salinity, low Q (1 day):

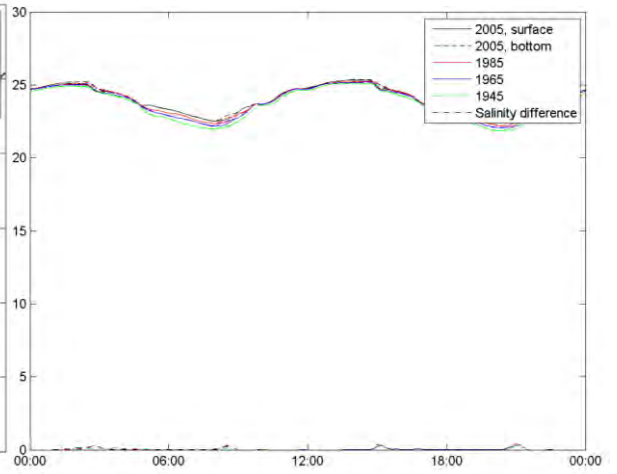

BETWEEN KNOCK AND EMDEN

Residual current, high Q (spring-neap cycle):

Residual current, low Q (spring-neap cycle):

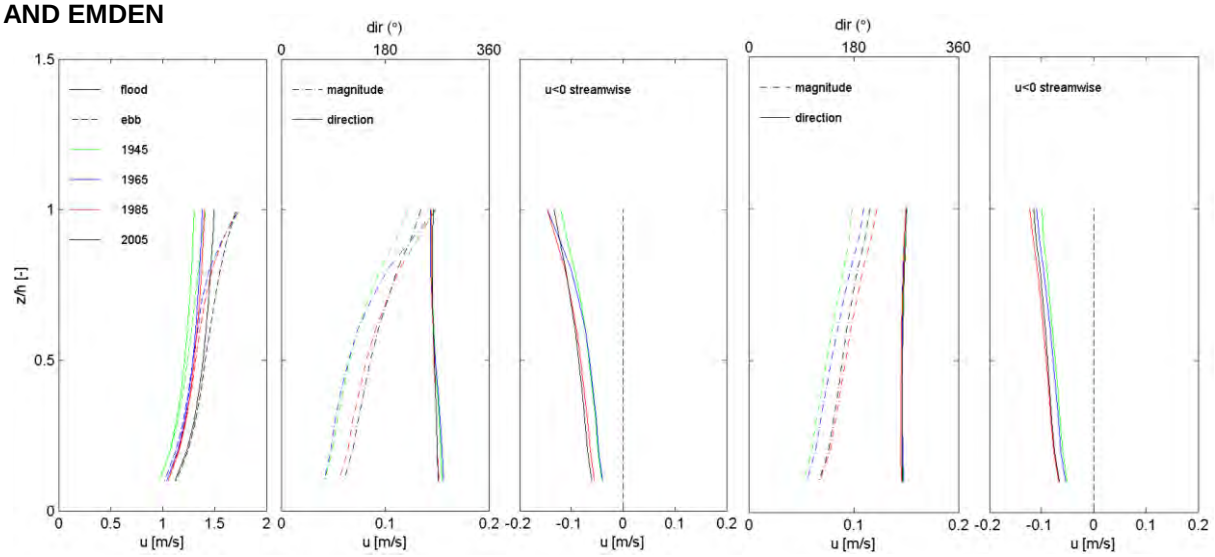

Salinity, high Q (spring-neap cycle):

Salinity, high Q (1 day):

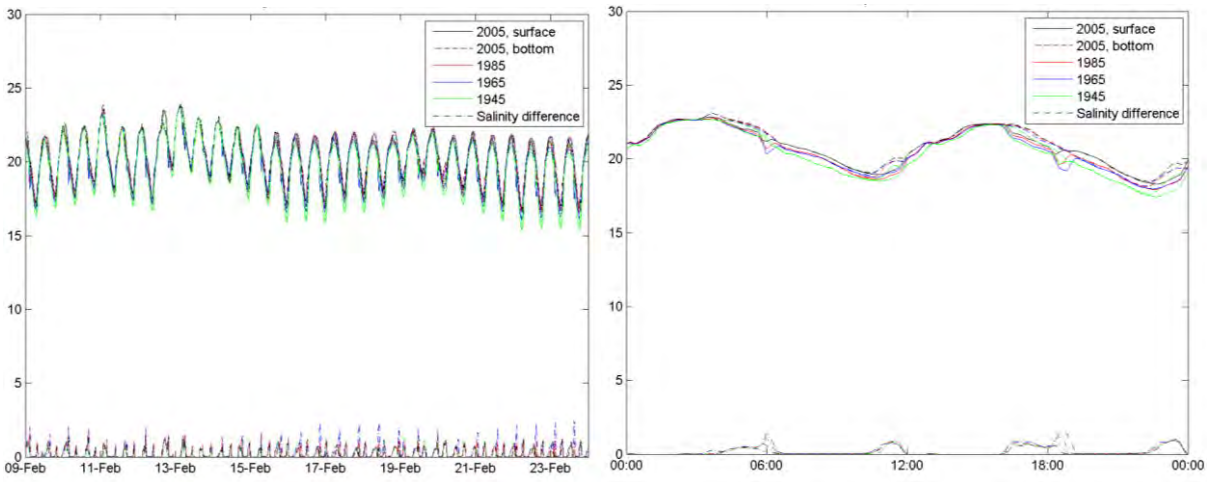

Salinity, low Q (spring-neap cycle):

Salinity, low Q (1 day):

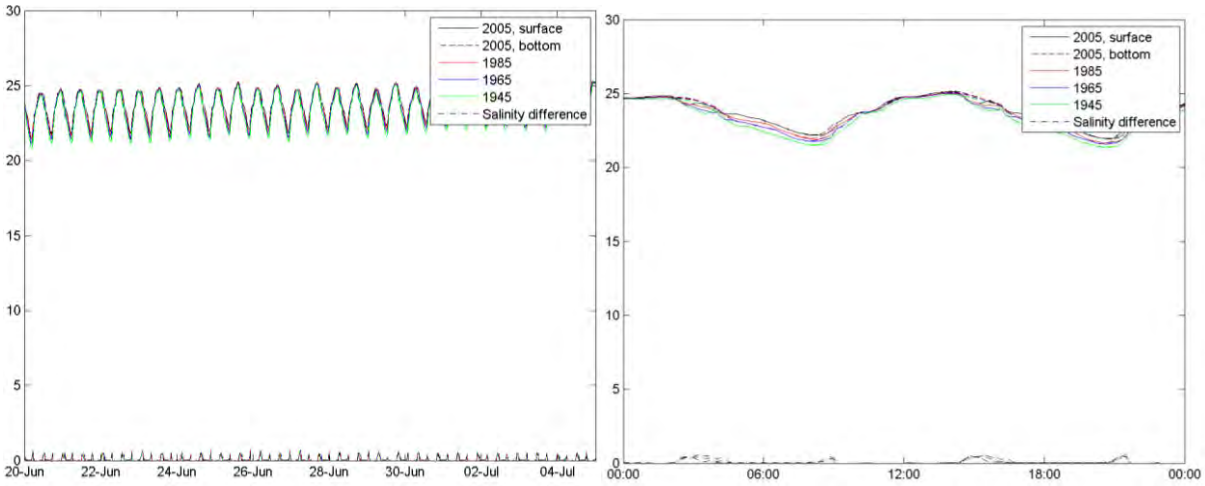

Residual current, high Q (spring-neap cycle):

Residual current, low Q (spring-neap cycle):

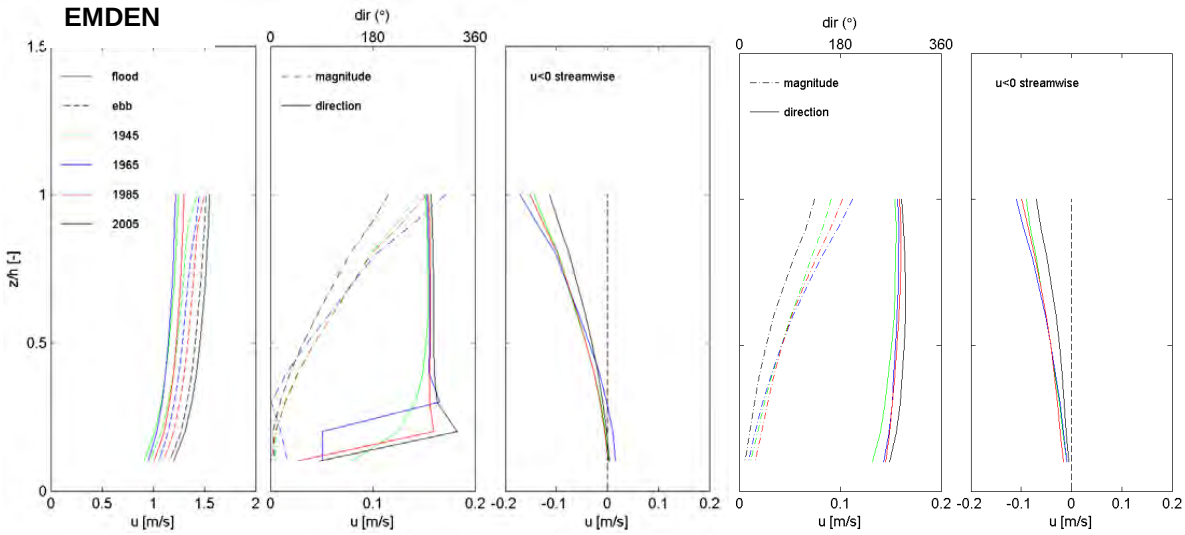

Salinity, high Q (spring-neap cycle):

Salinity, high Q (1 day):

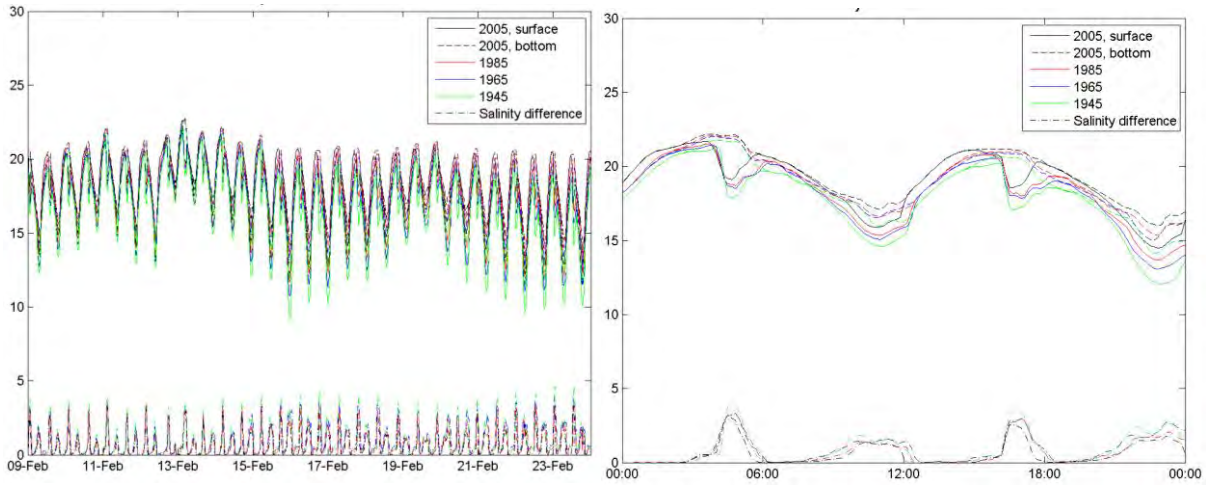

Salinity, low Q (spring-neap cycle):

Salinity, low Q (1 day):

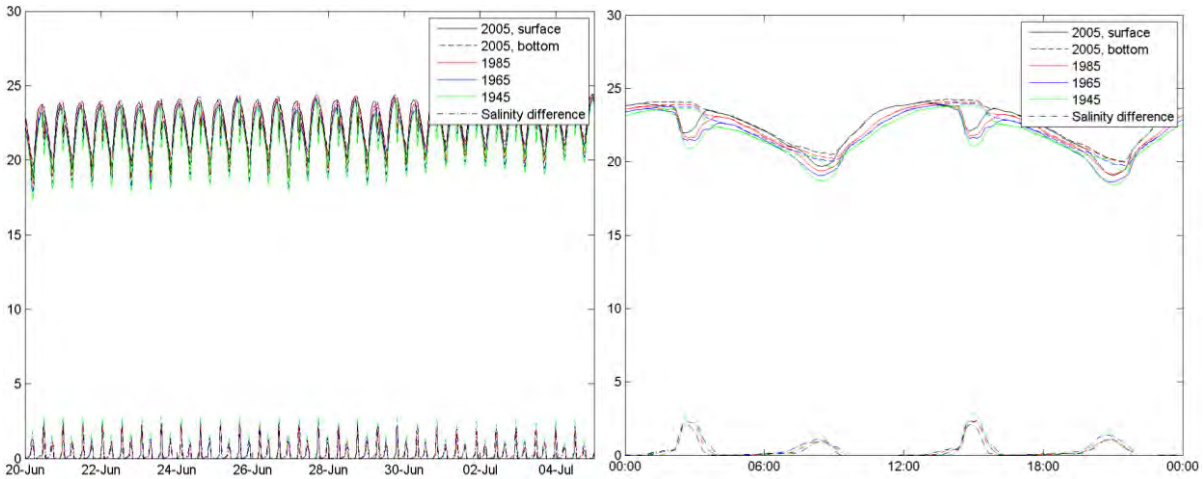

BETWEEN EMDEN AND POGUM

Residual current, high Q (spring-neap cycle):

Residual current, low Q (spring-neap cycle):

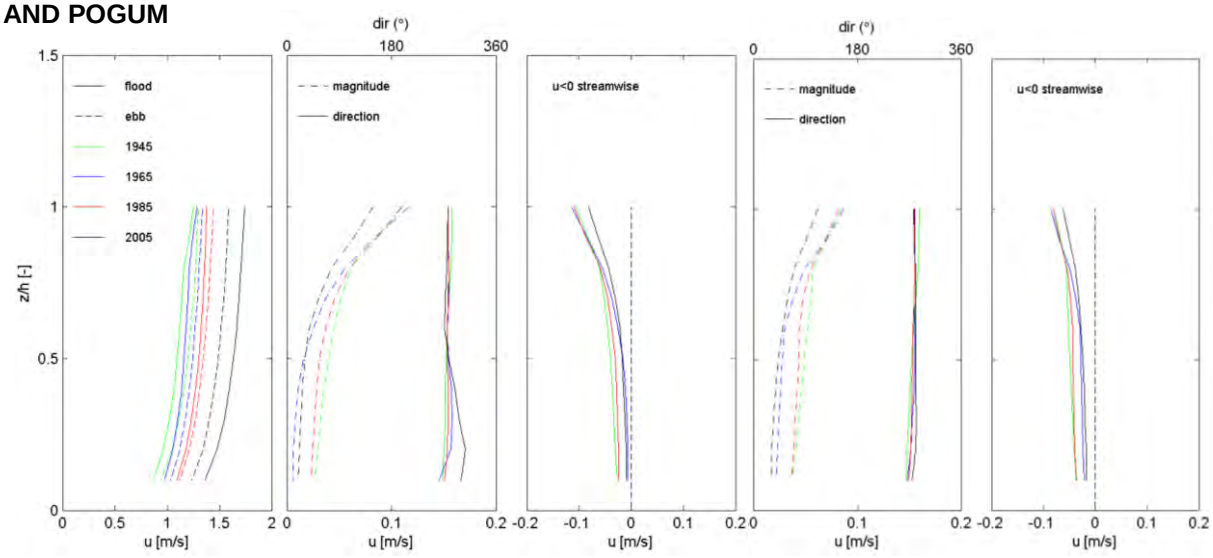

Salinity, high Q (spring-neap cycle):

Salinity, high Q (1 day):

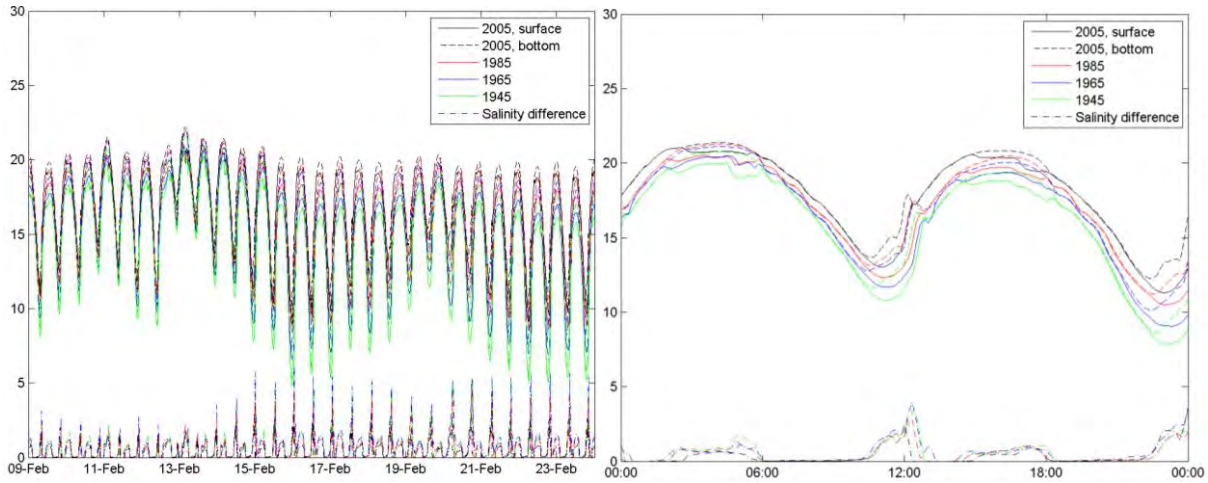

Salinity, low Q (spring-neap cycle):

Salinity, low Q (1 day):

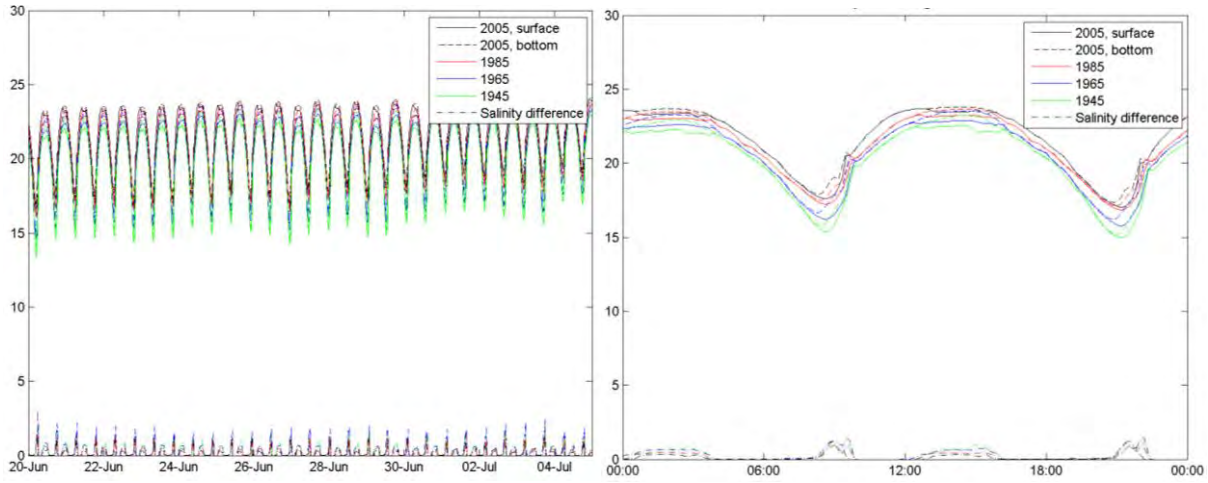

Residual current, high Q (spring-neap cycle):

Residual current, low Q (spring-neap cycle):

POGUM

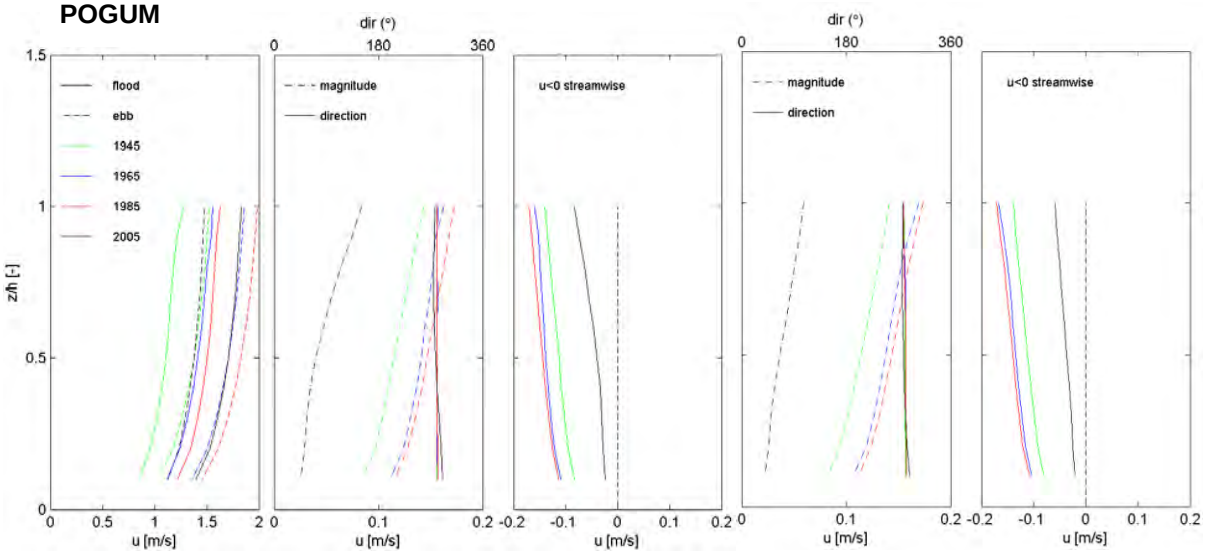

Salinity, high Q (spring-neap cycle):

Salinity, high Q (1 day):

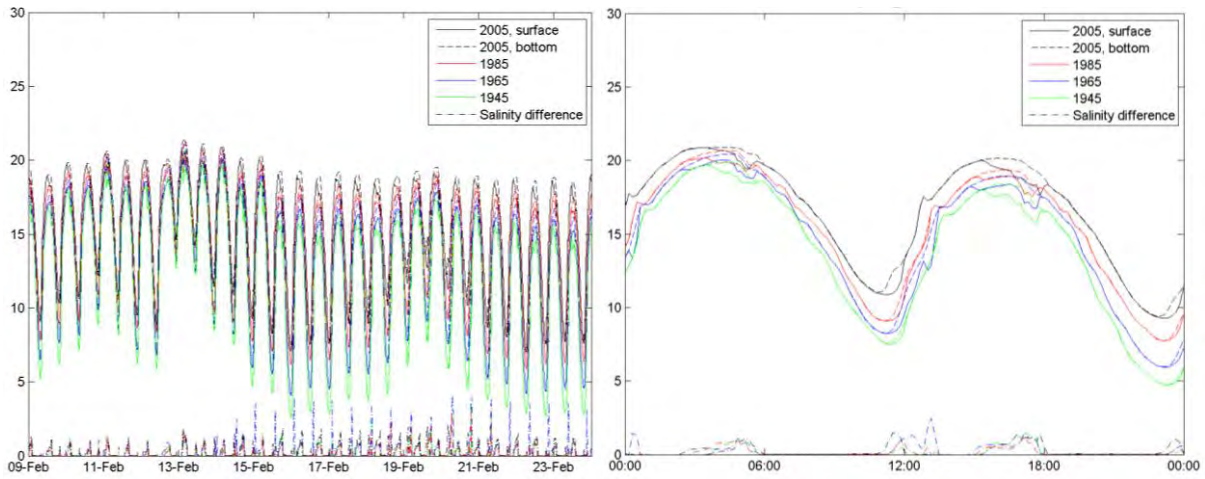

Salinity, low Q (spring-neap cycle):

Salinity, low Q (1 day):

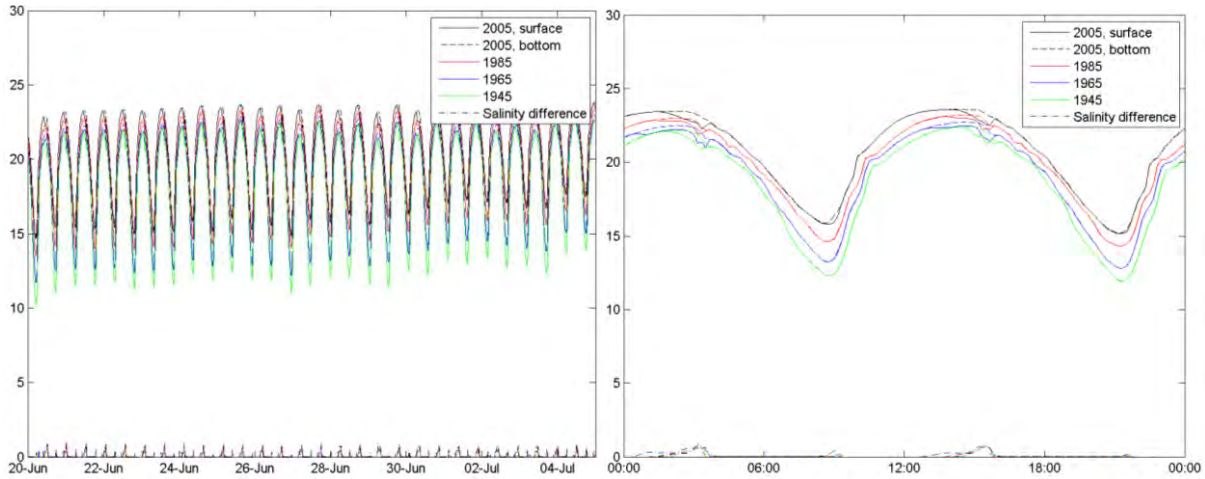

Residual current, high Q (spring-neap cycle):

Residual current, low Q (spring-neap cycle):

EMSSPERRWERK

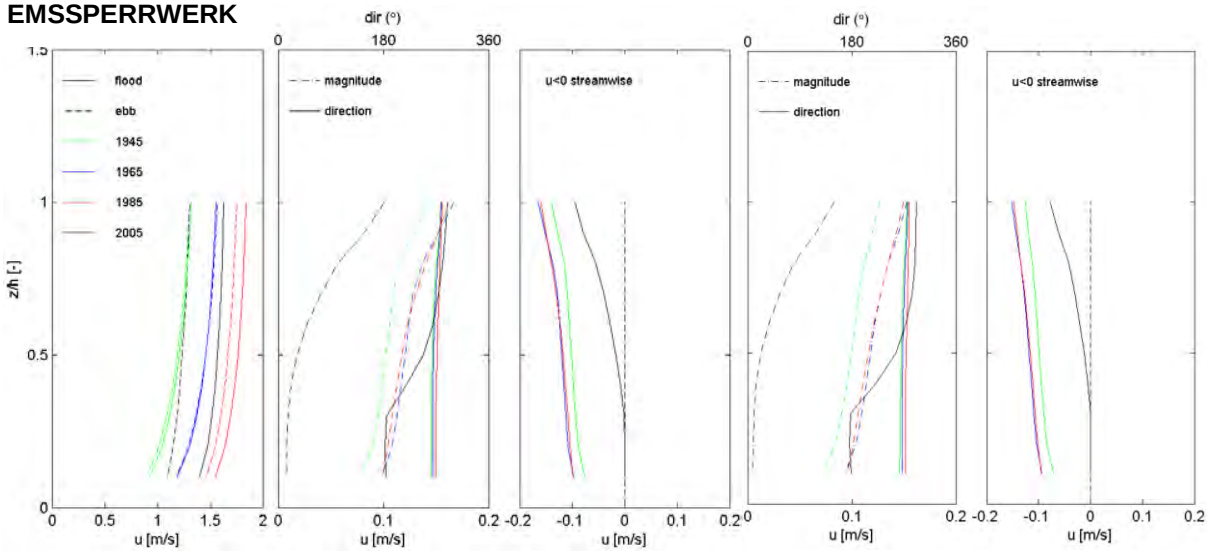

Salinity, high Q (spring-neap cycle):

Salinity, high Q (1 day):

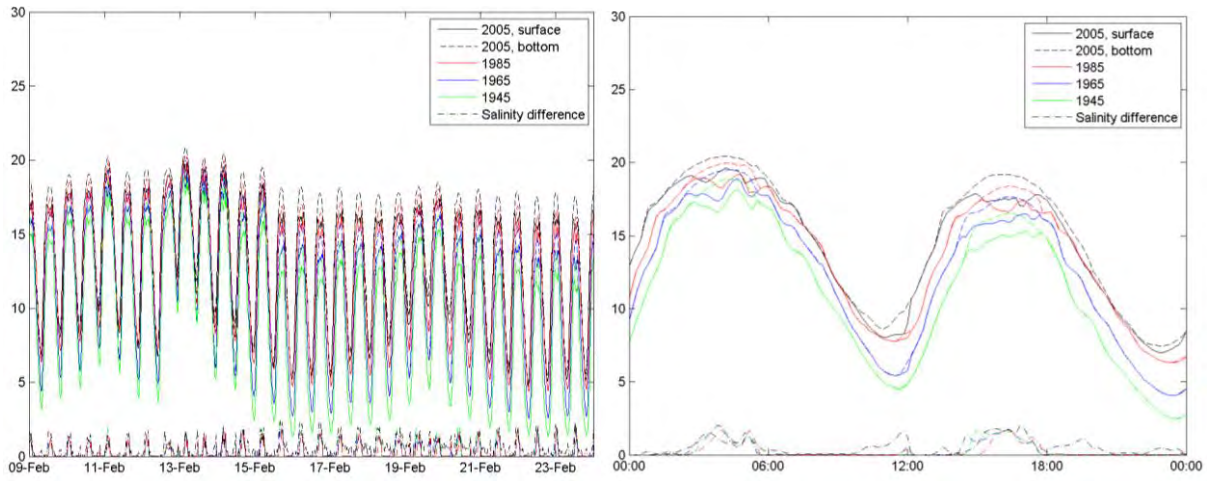

Salinity, low Q (spring-neap cycle):

Salinity, low Q (1 day):

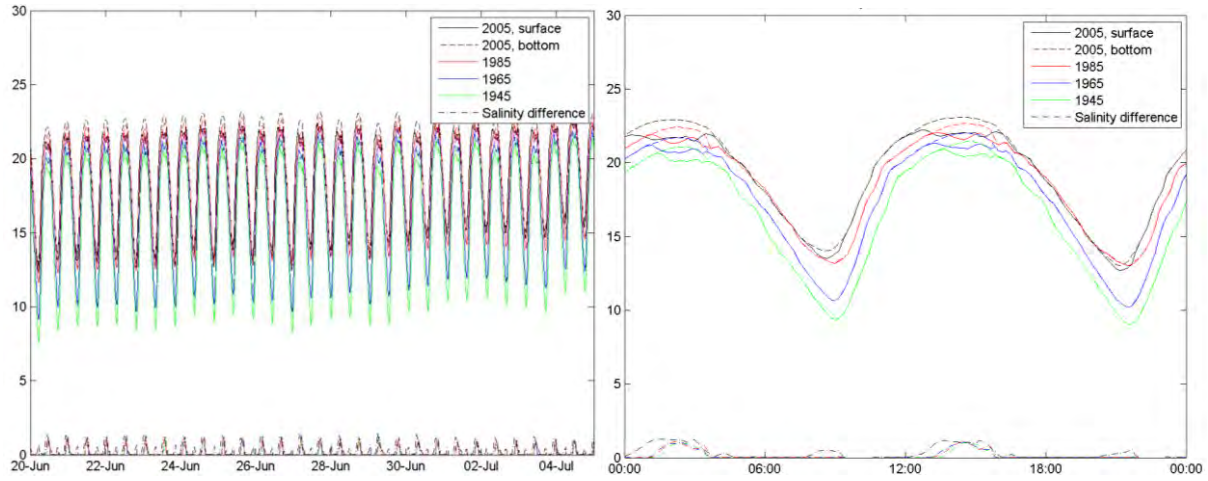

Residual current, high Q (spring-neap cycle):

Residual current, low Q (spring-neap cycle):

TERBORG

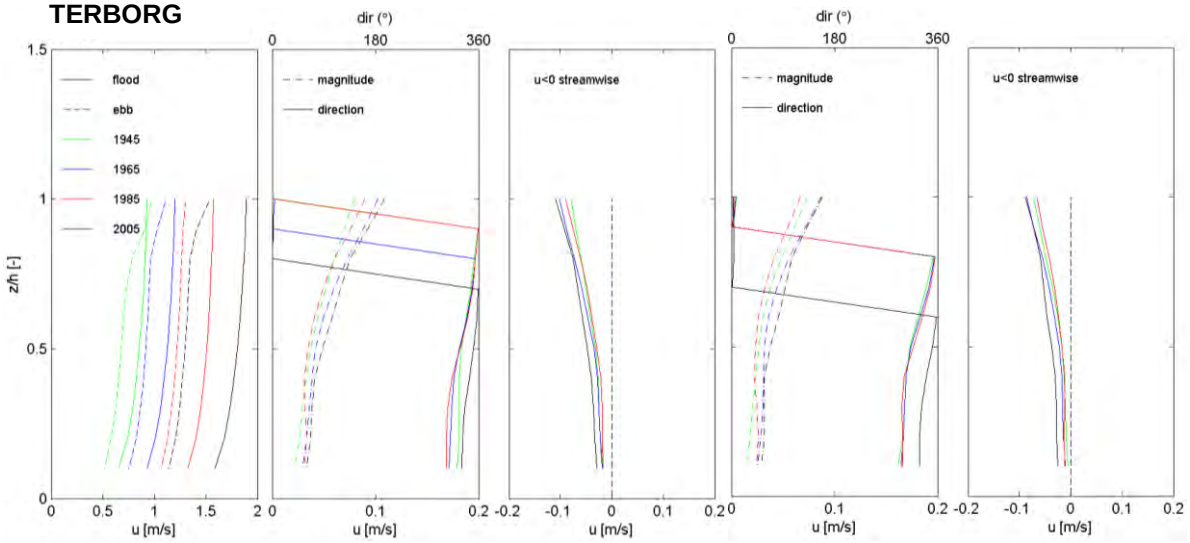

Salinity, high Q (spring-neap cycle):

Salinity, high Q (1 day):

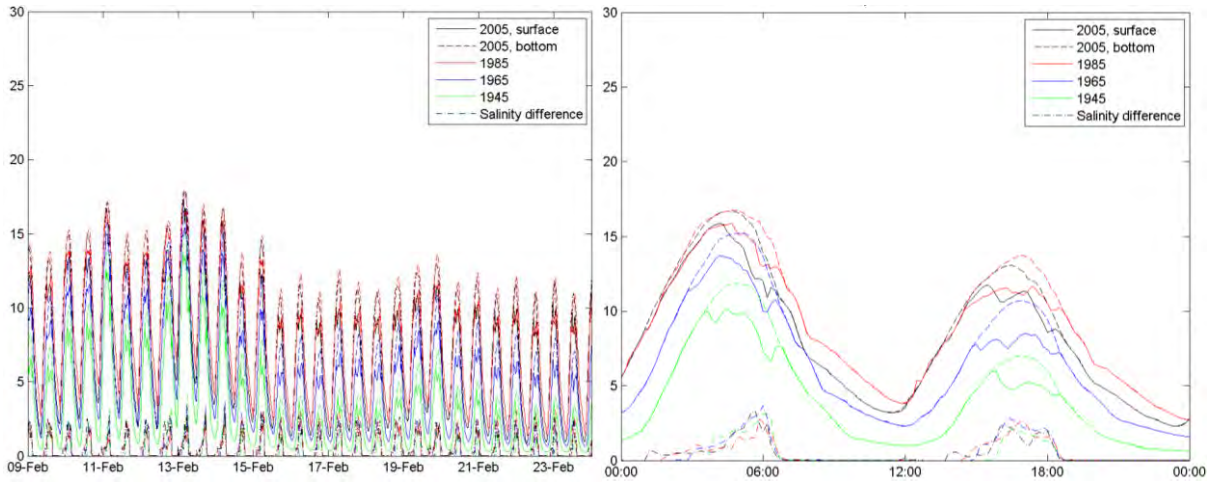

Salinity, low Q (spring-neap cycle):

Salinity, low Q (1 day):

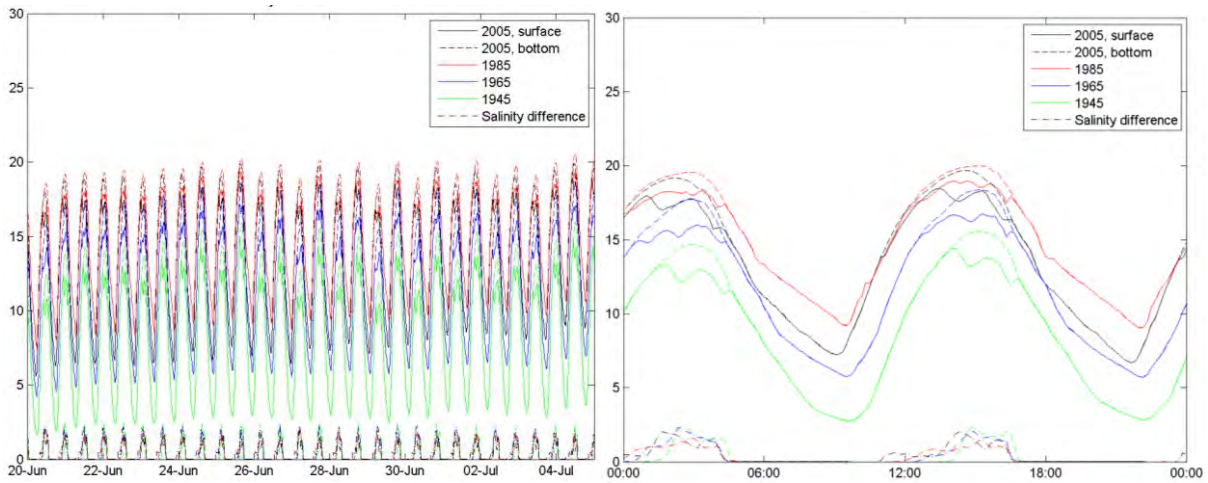

BETWEEN TERBORG AND LEERORT

Residual current, high Q (spring-neap cycle):

Residual current, low Q (spring-neap cycle):

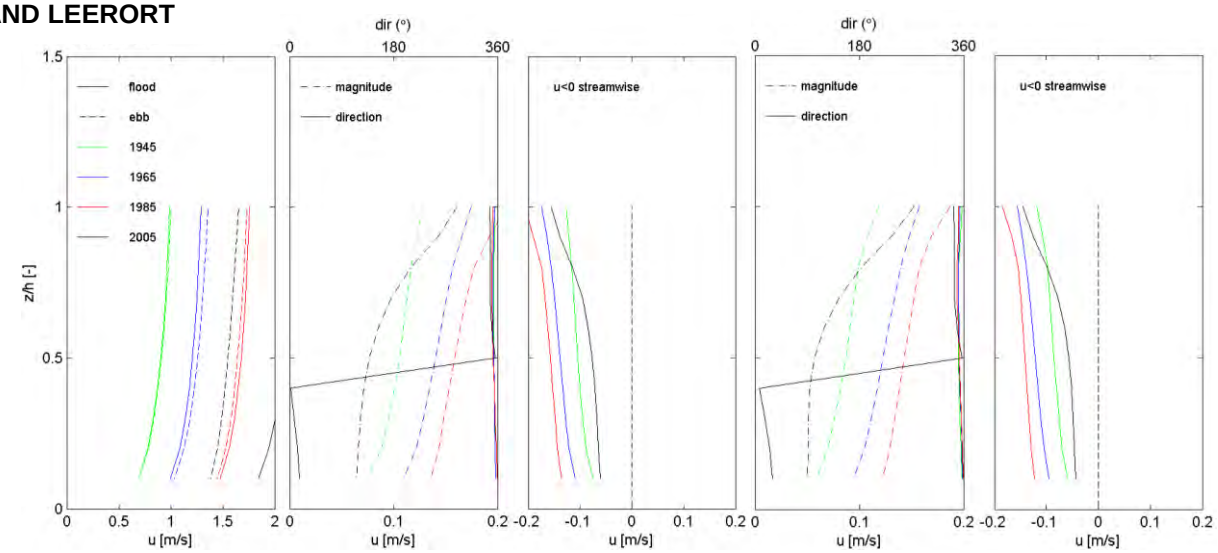

Salinity, high Q (spring-neap cycle):

Salinity, high Q (1 day):

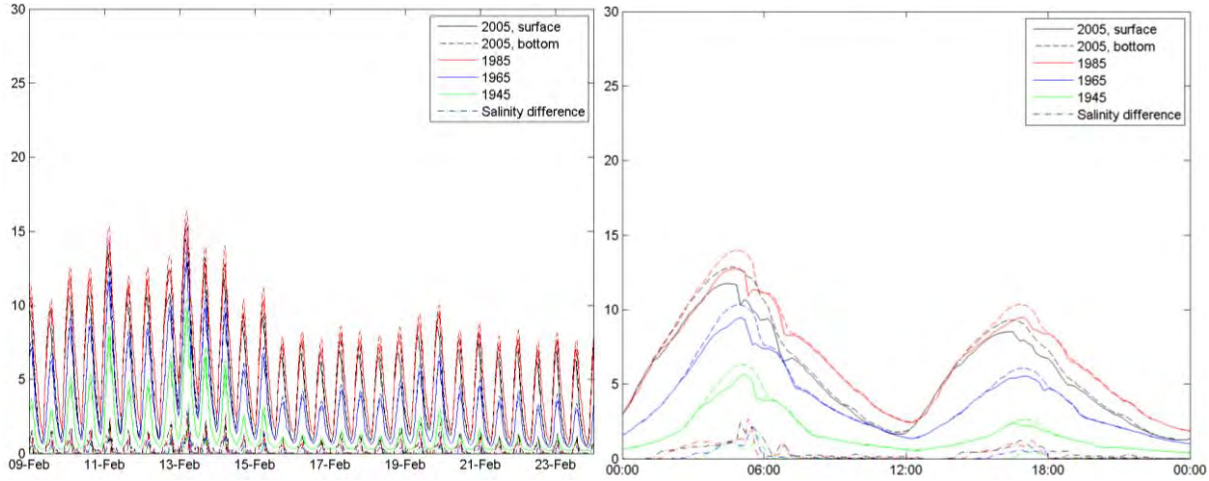

Salinity, low Q (spring-neap cycle):

Salinity, low Q (1 day):

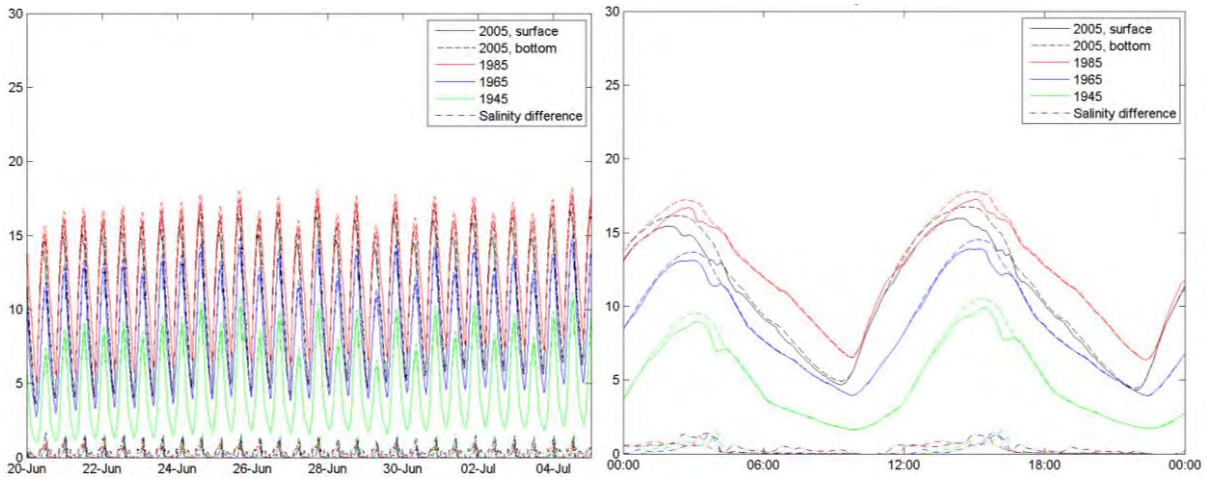

Residual current, high Q (spring-neap cycle):

Residual current, low Q (spring-neap cycle):

LEERORT

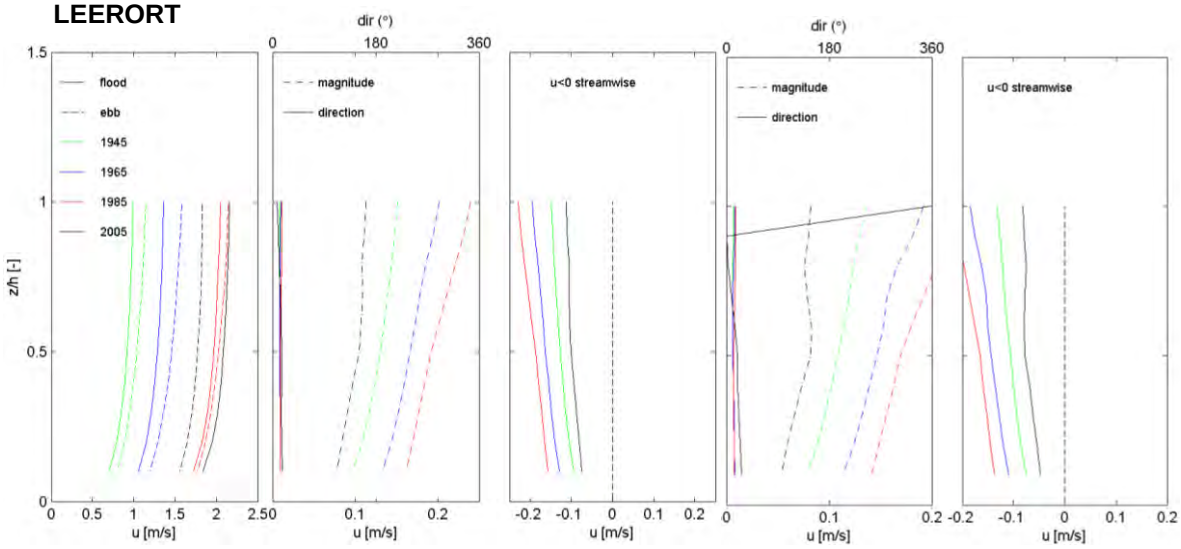

Salinity, high Q (spring-neap cycle):

Salinity, high Q (1 day):

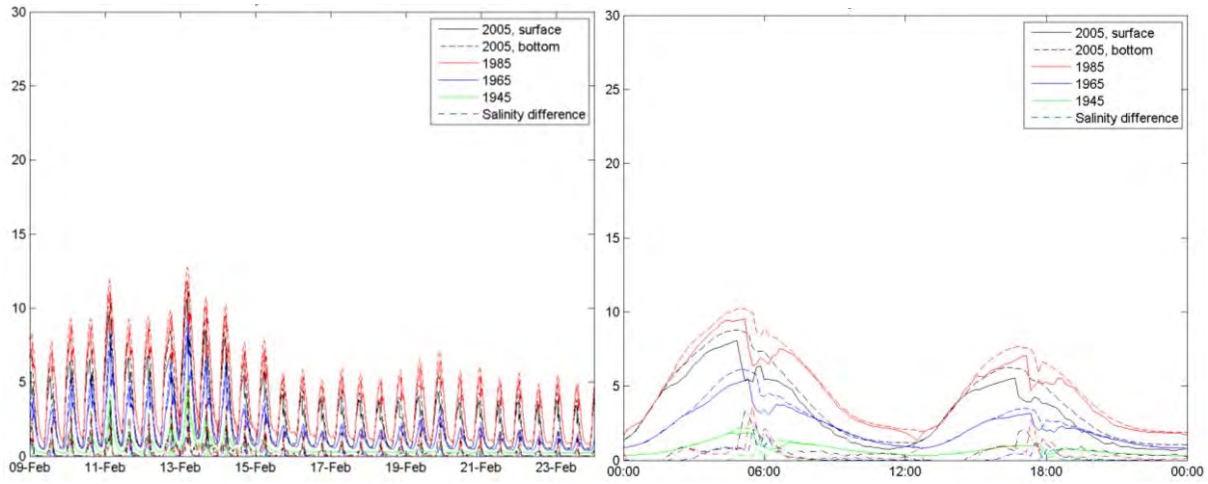

Salinity, low Q (spring-neap cycle):

Salinity, low Q (1 day):

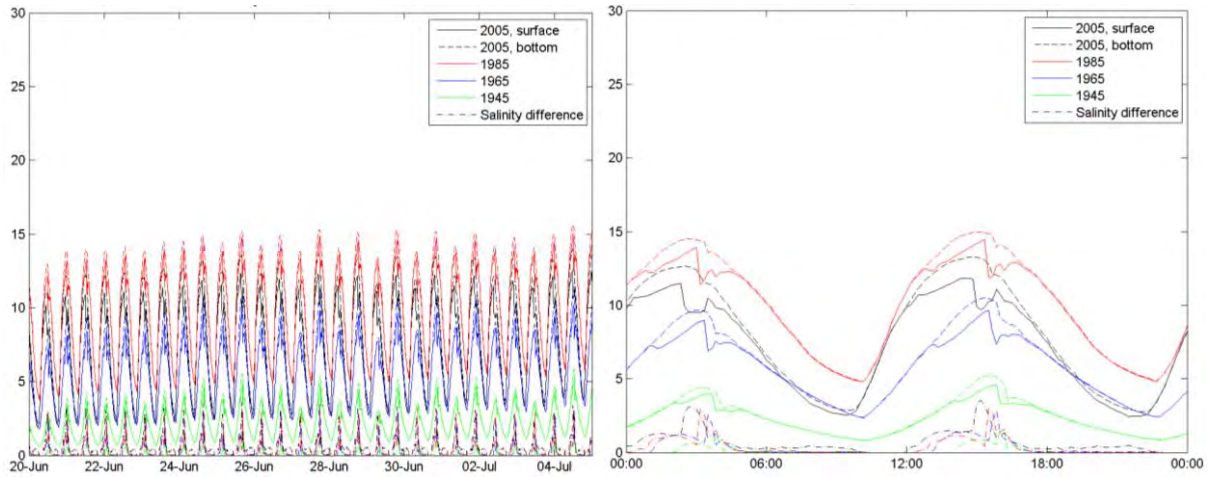

Residual current, high Q (spring-neap cycle):

Residual current, low Q (spring-neap cycle):

WEENER

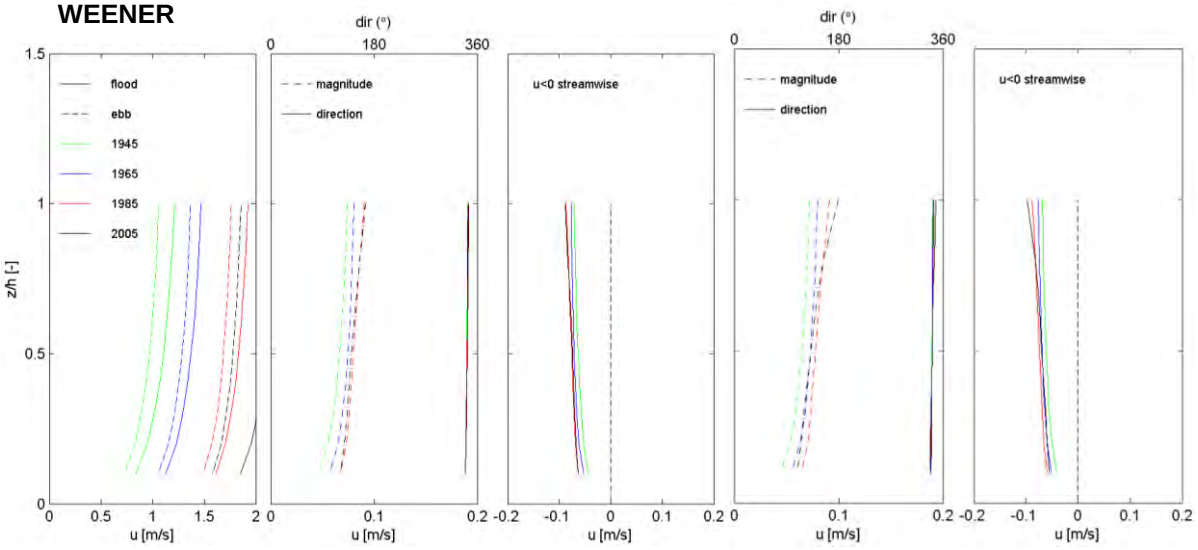

Salinity, high Q (spring-neap cycle):

Salinity, high Q (1 day):

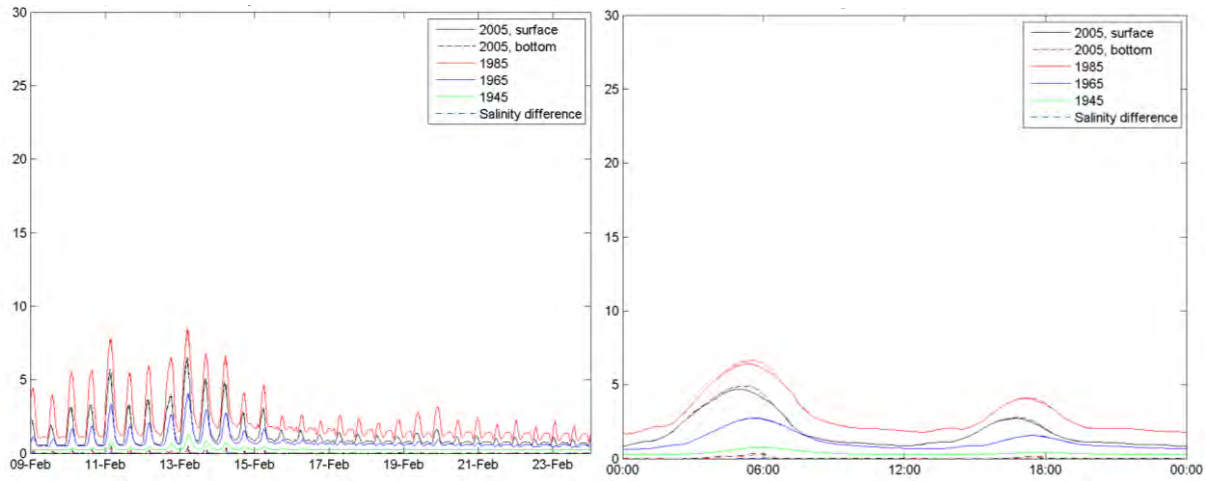

Salinity, low Q (spring-neap cycle):

Salinity, low Q (1 day):

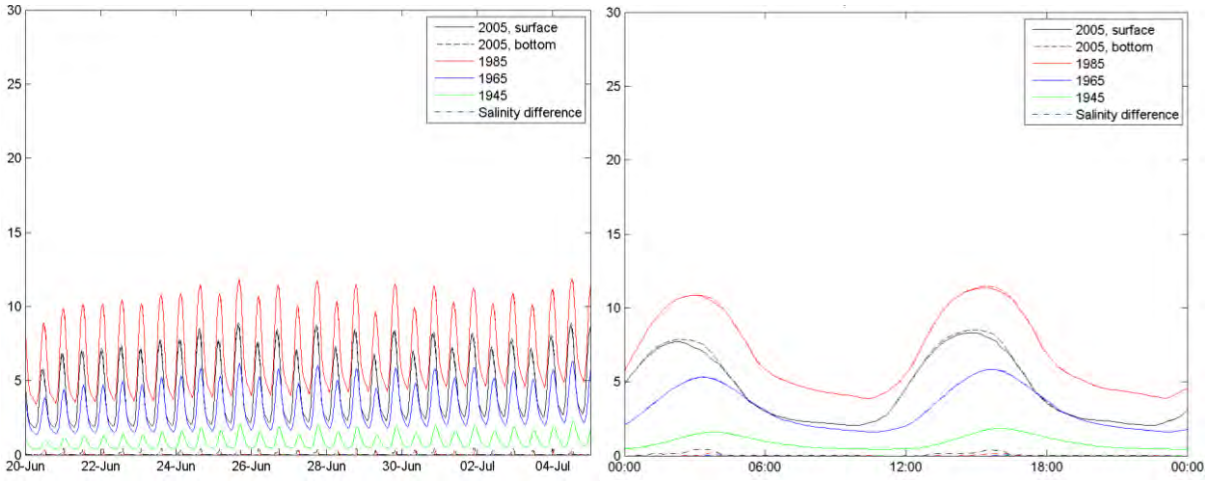

Residual current, high Q (spring-neap cycle):

Residual current, low Q (spring-neap cycle):

PAPENBURG

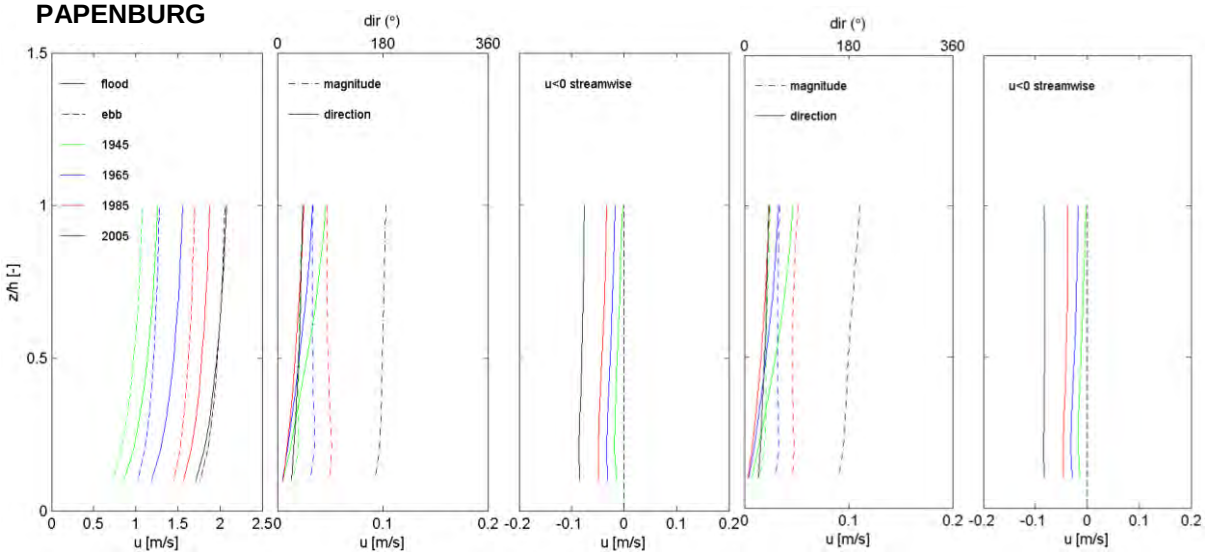

Salinity, high Q (spring-neap cycle):

Salinity, high Q (1 day):

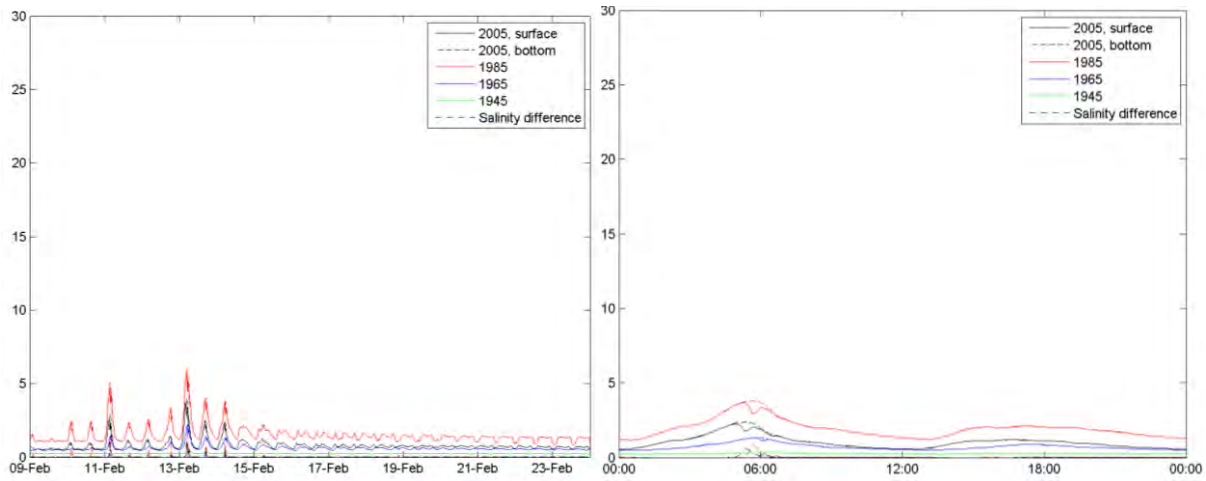

Salinity, low Q (spring-neap cycle):

Salinity, low Q (1 day):